The Structure and Properties of Soluble Phosphate Based Glasses

Thesis submitted by
Katrin Franks
For the degree of
DOCTOR OF PHILOSOPHY
In the
Faculty of Dentistry
University of London

Department of Biomaterials,
Eastman Dental Institute
For Oral Healthcare Sciences,
University College London,
256 Gray's Inn Road,
London WC1X 8LD

-2000-

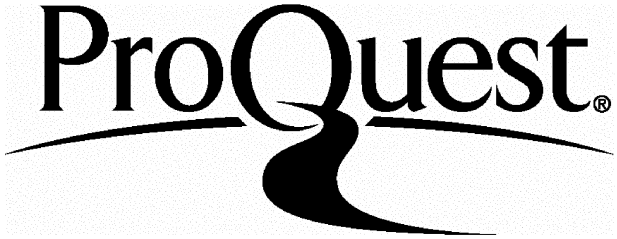

Unser Kopf ist rund, damit das Denken die Richtung wechseln kann.

...our head is round to allow our thoughts to change directions.

Antoine de Saint-Exupéry

Phantasie ist wichtiger als Wissen, denn Wissen ist begrenzt.

...imagination is more important than knowledge because knowledge is limited.

Albert Einstein

Für meine Eltern

For my parents

Abstract

The recent discipline of tissue engineering has developed innovative degradable and non-degradable (dependant upon application) materials in combination with low toxicity and good biocompatibility. The major focus of these new technologies is to guide the regenerative process. The aim of this project was to take the regenerative tissue healing process a step further by developing a material which not only guides the tissue regeneration process, but also enhances it and has a degradation profile that is tailored to the tissue and on degradation, leaves no toxic or irritating debris behind to cause any tissue reaction. The chosen material was a soluble phosphate based glass, modified with CaO, Na_2O, MgO, K_2O and/or CaF_2. Materials have been developed in order to work as closely as possible to the natural phase of bone, within the limitations imposed by the glass forming process.

5 different glass systems have been synthesised via conventional glass making procedures and the solubility process has been investigated via weight loss experiments and ion and pH measurements. All materials were soluble with different degradation processes, depending on the composition of the glass. Glasses with low CaO content showed a linear relationship between weight loss per unit area and time. Glasses with higher CaO content show an increasing non-linearity in their weight loss behaviour. The pH showed a significant increase in the first stages of degradation, which was explained by cation-exchange processes taking place from the material to the solution and vice versa. The ion concentration in solution was found to increase with time as expected and it mirrored the weight loss curves.

Preliminary cell culture tests (MTT tests) using the MG63 human osteoblast cell line were established to test the biocompatibility of the soluble extracts from the different glasses. The tests revealed that glasses with low CaO content, i.e. high solubility, showed

reduced proliferation below the control line of tissue culture plastic. Proliferation was however similar to the control line or above for glasses with CaO contents higher than 30 mol%, i.e. low solubility. The best test results, with enhanced proliferation was seen for glass with the highest CaO content. The MTT test results look very promising for materials with a high calcium oxide content, indicating biocompatibility with enhanced cell proliferation. There was also evidence that small amounts of K_2O and MgO affected cell proliferation.

Structural analysis was carried out using DTA and MAS-NMR spectroscopy. The results from the glasses were found to be in line with X-ray analysis of similar glass-ceramics, which had been analysed in earlier studies. Thermal analysis revealed multi-crystallisation events as evidenced by the presence of one or two crystallisation peaks with more than two or three corresponding melting points. The use of MAS-NMR spectroscopy showed that two species, Q^1 and Q^2 formed the basis of the glass structure and it was possible to identify the dominant Q^2 species as $Na_4Ca(PO_3)_6$. The Q^1 species is represented by ($Ca_3(PO_4)_2$ or $Na_2P_2O_7$). However, it was up to the present time not possible to identify the Q^1 species unambiguously.

The work has shown that it is possible to synthesise biodegradable glasses for hard tissue surgery, whose composition is close to the inorganic phase of bone. Biocompatibility studies have helped to define optimal compositions and it is therefore hoped that the results from this study will contribute towards future implant research utilising soluble glasses.

Acknowledgements

I would like to thank Dr. Jonathan Knowles and Dr. Isaac Abrahams for their supervision and support throughout the my Ph.D.

I very much enjoyed the work on the MAS-NMR Spectroscopy and would like to thank Dr. Geoff Hawkes at Queen Mary and Westfield College for his support for the analysis and Dr. Abil Aliev at University College London for his help and guidance.

I am extremely grateful for the MTT test on my material, carried out by Dr. Vehid Salih at the Eastman Dental Institute. I am indebted, many thanks.

Furthermore, I would like to thank Colebrand for the scholarship, without this the Ph.D. would not have been possible.

I also would like to thank Dr. Mike Braden and Dr. Showan Nazhat for the discussions regarding aspects of diffusion and also Jill Williams for the advice for the fluoride measurement, of which I am very grateful.

Finally, a huge thanks goes to all my friends in England and Germany.

List of Figures

List of Tables

Chapter 1

Introduction

1.1 Materials for hard tissue surgery

The quest for materials, which replace parts of the human skeleton, is not new. There is a general need for some type of bone replacement or regeneration for patients who have suffered from trauma or chronic degenerative diseases, which lead to bone loss or abnormalities.

There are many requirements that these materials must meet if they are to be implanted in the human body.

The main requirements are:

1.) Chemical and physical stability for the required lifetime of the device

2.) A wound healing tissue response with no toxic, allergic or chronic inflammatory reaction.

1.1.1 Host /Tissue Response

No implant material is completely inert. Many years of research have made it clear that any changes in a material, which is implanted into a living tissue, can be linked to the tissue response.

According to *Hench* (1) 4 types of response can occur:

1.) The implant material is toxic and the surrounding tissue dies

2.) The implant material is non-toxic and almost inert, fibrous tissue forms

3.) The implant material is non-toxic and biologically active and a tissue attachment is formed

4.) The implant material dissolves and the surrounding tissue replace it.

These response types are not discrete and do overlap, but clearly, responses type 1 and 2 are far from ideal and can lead to loss of the implant. Only responses 3 and 4 with either a direct stable attachment of tissue to the implant, or a complete replacement of the implant by natural bone will be useful and successful.

Figure 1 shows the general series of overlapping cellular events, which occurs during hard tissue wound healing.

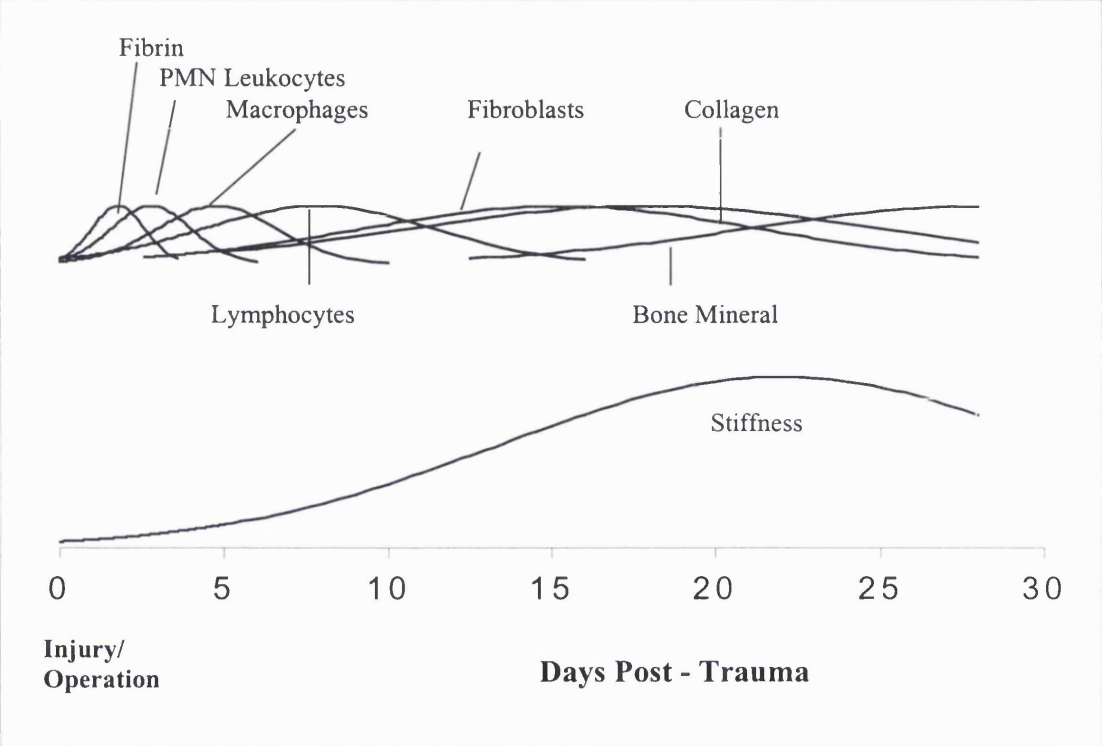

Figure 1. Shows the cellular progression after implantation.

Initial events are concerned with cleaning of debris from the wound side, followed by soft tissue formation, such as the laying down of collagen.

The bone formation usually starts around the 14th day. An ideal implant for bone regeneration will show low levels of fibrous capsule formation and support and enhance the bone matrix repair process. Recently, the discipline of Tissue Engineering has been established to develop degradable and non-degradable biomaterials, which support and guide the tissue healing process. One example of a biocompatible but stable polymer is a PTFE fibrous membrane, which is used for treating periodontal disease. An example of degradable polymers widely used for internally suturing of wounds would be a polymer or copolymer such as polyglycolic/polylactic acid and is sold under the tradename Vicryl® (2). These degradable polymers are now being used

in place of PTFE as they are degradable. The major aim of the technologies above is to guide the regenerative process in terms of reproducing new, fully functioning living tissue. This newly formed tissue will be formed on top of a polymer matrix or in a porous scaffold. Degradable polymers, as mentioned above, show the advantage of initiating and supporting new guided tissue formation, however their disadvantage is the unpredictable degradation process.

As one can see from Figure 1, the bone mineral matrix formation is generated after 14 days. An ideal material would be a scaffold material, which is stable up to 14 days and then slowly dissolves and is replaced by the newly developing bone matrix. An additional advantage would be a material, which dissolves in a way that it will release beneficial ions, which may be used by the cells to produce mineralised tissue.

There have been developments in the use of glasses for hard and soft tissue regeneration, which show evidence of at least a partial degradation mechanism. Developments and features of these materials will be reviewed in the following chapter.

1.1.2 Bioactive Glasses

In 1969, *Hench* (1) developed the well known and clinically used Bioglass® and it was the first synthetic material to bond with living bone. Bioglass® is a bioactive SiO_2 based glass. With compositional features such as SiO_2 content <60 mol.%, high CaO/P_2O_5 ratio and high CaO and Na_2O content, this distinguishes Bioglass® from any other "normal" soda-lime silica glass. Today bioactive glasses are clinically used in non-load bearing situations, and have been used for alveolar ridge augmentation, periodontal pocket obliteration and maxillofacial reconstruction.

Over several years many other bioactive silica glasses have been developed, however they are still based on the original 45S5 (Bioglass®) composition, which is today used as a baseline for many further developments, for example the glass with the composition SiO_2: 45mol%; P_2O_5: 6mol%; CaO: 24.5mol% and Na_2O: 24.5mol%

Bonding to bone in the compositional range of 45S5 glass was first demonstrated by *Boutin* in 1987 (3).

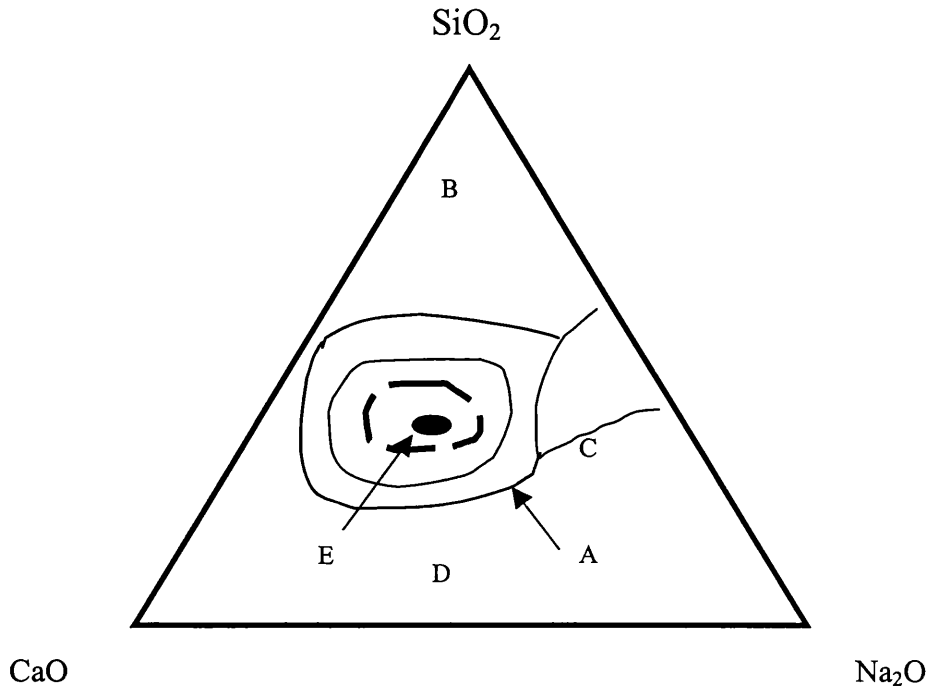

Figure 2. Compositional dependence (in weight percent) of bone bonding. All compositions in region A have a constant amount of 6 wt% P_2O_5. All compositions within this region bond to bone and the region is termed the bioactive-bone-bonding boundary. Region E (inside the dashed line) is the soft-tissue bonding region. Silica glasses in region B behave as nearly inert materials and will elicit fibrous capsule formation. Glasses in region C are resorbable, 10-30 days after implantation. Region D represents technical glasses with limited biological use.

Bioactive glasses show a common characteristic feature of a time dependent surface modification after placing in tissue. When implanted, the surface of the glass undergoes a transformation to form a biologically active hydroxyapatite layer (HCA). It forms the basis of a strong bond with bone. *Hench* (1) concluded that bioactivity only occurs if certain amounts and ratios of glass forming or modifying oxides are present. If the tissue forms a bond to the implant a layer of biologically active HCA must form. "This is perhaps the only common characteristic of all known bioactive implant materials" (1).

12 reaction steps are needed to successfully bond to bone and these are shown in the following figure (3).

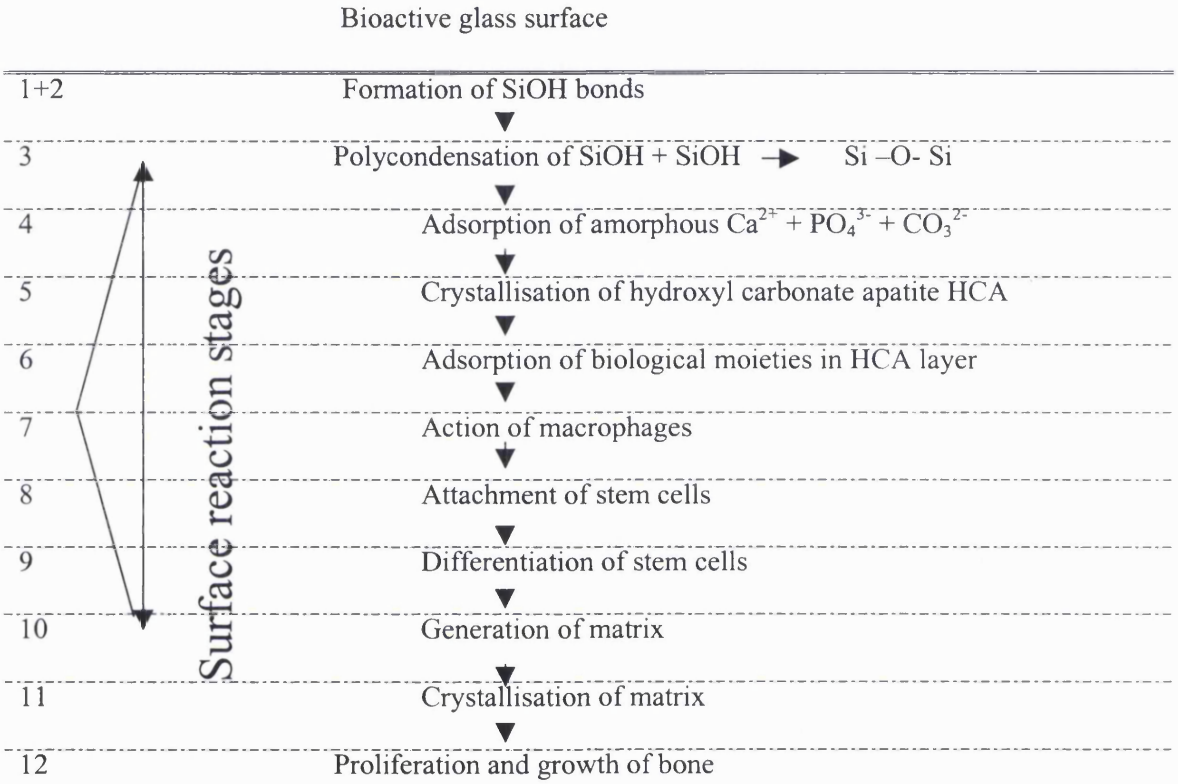

Figure 3. Surface reaction stages for Bioglass®

The alkali-ion-hydrogen-ion exchange is the first reaction process stage and occurs quite rapidly. After 20 min. all of the Si-O-Si bonds are broken and transformed to give Si-OH (silanols). The result is a silica gel-layer of polycondensated silanol groups. As early as 10 minutes after implantation a calcium phosphate layer appears due to migration of Ca^{2+} and PO_4^{3-} ions through the SiO_2 layer. This formed calcium phosphate layer will thicken with time by incorporation of further Ca^{2+} and PO_4^{3-} ions

from solution. With time, this amorphous calcium phosphate layer will transform into a hydroxy-carbonate-apatite layer (5), (6), (7).

Bioglass® has the advantage of being able to bond to hard tissue via the HA layer formed, however the disadvantage of this material is its brittleness. As a consequence, difficulties in shaping arise and so its use for load bearing applications is limited. Improvements have been made by incorporation of Bioglass® particles in a high-density polyethylene (HDPE) matrix. According to *Wang et al.* (8) microhardness increased with increased Bioglass® volume while tensile strength and fracture strain decreased. These composite materials still develop the same biological apatite layer like the bulk glass when placed in simulated body fluid.

A modification of Bioglass® by *Kim* (9) was developed. This was a fluoride containing glass, which might be beneficial for dental applications. With the use of fluoride it was hoped to form a fluoro-hydroxyapatite instead of a hydroxyapatite layer. A fluoro-hydroxyapatite can release fluoride, which may help to stabilise the mineral phase in teeth and prevent decay.

In this study 40mol% of the original CaO content was replaced by CaF_2. After soaking in Tris-Buffered Solution for several hours a crystalline fluoroapatite phase was formed on the surface of the glass.

Toxicology and biocompatibility studies of Bioglass® took place as early as 1981 by *Wilson et al.* (10) on Bioglass® and modified Bioglass®, where CaF2 substitutes CaO. This work studied the *in vitro* and *in vivo* response with different cell types. In comparison to quartz powders, which showed up to 50% toxicity, both Bioglass®

types proved to show only 2-5% toxic effects to cells. Similar test results were observed for the *in vivo* testing where after 2.5 years no toxic effect was seen.

In contrast, a paper on the toxic effect of silica-containing glasses was demonstrated by *Nagase et al.* in 1991 (11). This was an extension of a preliminary study published in 1987 (12) on a fine powder of silicate containing glass-ceramics, which showed toxic effects in mice. However the mechanism of toxicity and the exact composition of the silica-containing glass-ceramic, which evoked the toxicity remains unclear.

Suspensions of calcium phosphate glasses with various amounts of SiO_2 were injected into mice to determine the mortality rate. The mortality of the mice was directly proportional to the dissolved amount of released Si^{4+} ions. The conclusion was drawn that SiO_2 when dissolved in the body has a high toxic potential.

A less strong toxic effect for Bioglass was seen on human synoviocyte cultures. *Bendall et al* (13) described the effect of particulate Bioglass® in a concentration range of 1.0 –10 μg/ml as having low cytotoxicity. However these concentrations induced the secretion of tumour necrosis factor-α (TNFα), which is an inflammatory cytokine.

1.1.3 Controlled Released Glasses

Phosphate based glasses – a possible biomaterial?

What can be seen from the above discussion is that it is still not clear what effects the release of Si^{4+} ions has on human tissue.

Glasses, which consist only of biologically related phosphorus, calcium and sodium ions, offer great potential as a biomaterial. They show characteristics making them potentially useful as a temporary device such as predictable solubility, controllable chemical composition and therefore controllable solubility, biodegradability without toxic residues and most importantly it might be possible to reproduce the stoichiometric phase of natural bone within the glass matrix.

Vogel and Höland (14) developed in 1987 silicon free phosphate based glasses and glass ceramics of various compositions for biomedical applications. $CaO\text{-}Al_2O_3\text{-}P_2O_5$ formed the basic system and gradually this system has been extended to $Na_2O\text{-}CaO\text{-}Al_2O_3\text{-}P_2O_5$ and $Na_2O\text{-}CaO\text{-}Al_2O_3\text{-}P_2O_5\text{-}F$. Na_2O was used to break down chains within the structure in order to enhance the possibility of apatite formation when heat-treated to convert the glasses to glass-ceramics.

Preliminary *in vivo* tests showed in general very promising results. However, the idea of avoiding silicon in bioactive glasses or glass-ceramics for biomedical use is relatively new and therefore no precise and systematic toxicity studies are available, as this is the case with silicon based glass materials. Work carried out in this thesis will show that by avoiding silicon an enhanced biocompatibility may be achieved.

Soluble phosphate glasses can be used not only for guided tissue regeneration, they can also be used for localised release of specific ions, for example platinum for cancer treatment or silver in order to treat bacterially infected tissue.

In the sixties phosphate based glasses were originally investigated for their electrical properties for communication use. From the late seventies onwards many pesticides commonly used were banned because they were considered to be too hazardous. At the Standard Telecommunication Laboratories, Essex, UK, *Drake and Graham* (15-17) developed slowly releasing biocidal glasses, doped with biocidal ions such as copper, silver or boron to be considered as a substitute for the banned pesticides or fungicides. As the glass dissolves, biocidal ions constantly leach out until the glass completely dissolves leaving no residue behind. A decade later *Allen et al* (18-22) was involved in another investigation field to cure trace element deficiencies in cattle and sheep. Classic metabolic diseases such as milk fever, fatty liver syndrome and ketosis are caused by nutritional deficiency of either major or trace elements. To prevent for example milk fever, it is important to ensure an adequate intake of magnesium for the lactating animal. With the use of slow release phosphate glasses, which are doped with essential ions, they hoped to cure such diseases and indeed showed that a significant improvement can be made.

Chapter 2

Aims of This Work.

This project was mainly aimed at the development of novel soluble glasses for periodontology treatment (Periodontitis). The before mentioned use of a GoreTex® PTFE fibrous membrane which act as a scaffold to promote hard and soft tissue re-growth is up to day the best choice for patients who suffer from reduced jaw lines caused by chronic degenerative diseases which lead to bone loss. The use of this membrane is proven to rebuild tissue matrix however there is a major drawback. Once the membrane is set in place by a surgical procedure the tissue starts to regenerate. This membrane has to be removed, hence this is on the one hand very inconvenient for the patient and it will on the other hand remove parts of the newly formed tissue. It seems obvious that improvements are necessary. A possible alternative would be a system which promotes bone re-growth in the same way the membrane functions but with the difference that the material itself degrades after the bone healing process starts.

One aspect of this project is to develop a soluble scaffold matrix, which acts in a similar way to the GoreTex® membrane in terms of its biocompatibility but also degrades slowly in an appropriate time. An additional consideration is the careful choice of the material. When the implant is placed and it starts to degrade and release structural units, one should bear in mind the toxic or allergic effect this might cause to the surrounding tissue. The question which will be related to this consideration is: Is there a material, which not only avoids any toxic and/or allergic reaction, furthermore, is there a material which can be beneficial for the tissue?

A potential alternative to a GoreTex® membrane might be a soluble phosphate based glass modified by chemical elements, found in the natural inorganic phase of bone. It is well known in the literature that phosphate salts are soluble, however the solubility of a phosphate based glass matrix has not been fully investigated. Therefore some questions surfaced here:

1 Is it possible to develop a soluble glass which lasts for the duration of the bone healing process and

2 is it possible to incorporate beneficial elements such as calcium, magnesium and sodium into the phosphate glass matrix in order to enhance biocompatibility? In addition,

3 how do these elements affect the solubility of these phosphates glasses and is one able to calculate and predict their solubility,

4 how will the solubility change by adding different alkaline and alkaline earth oxides? Most important of all,

5 how will cells react towards a basic phosphate glass and how will they react towards modified phosphate glass systems? Therefore preliminary cell tests such as the MTT test has been set up to determine how cells will react towards a system *in vitro.*

MTT tests are of great importance; the results help us to understand how cells respond and to predict if a material is biocompatible or not. Furthermore they can be of great help to decide if additions of ions are beneficial or even enhance cellular activity.

There is also a more theoretical approach of the project. Up to today the structure of glasses in general and especially phosphate glasses are not fully understood.

Structural investigation with the use of Solid State Nuclear Magnetic Resonance Spectroscopy (SS-NMR), Differential Thermal Analysis (DTA), X-ray Diffraction and Infrared Spectroscopy (IR) helped at least to understand parts of the structural arrangements. However, more work needs to be carried out to understand this completely. With further knowledge of the structure it might be possible to relate the structure of the glasses with their solubility.

Further questions arise, such as (1) how are structural units arranged in a phosphate based glass matrix, (2) what kind of analytical tool is best to analyse it (3) how will additional modifiers intervene and (4) is there a noticeable trend by systematically incorporating different modifiers to the glass network?

If there is a trend in structural changes, can the same trend be found for the solubility changes of the glass? Is there a relationship between these two?

Chapter 3

Glass

This chapter was drawn up in order to provide information regarding glass science, including a survey of the literature of glass-structure theories investigated using X-ray Photoelectron Spectroscopy (XPS), ^{31}P MAS-NMR spectroscopy and Differential Thermal Analysis (DTA).

MAS-NMR is a relatively new technique allowing close observation of the local environment around a particular element and will therefore provide new insights to the glass structure theories. Differential Thermal Analysis (DTA) can be utilised for two things:

(1) It may be used for measurement of classical polymer characteristics such as glass transition temperature (T_g), melting temperature (T_m) and crystallisation temperature (T_c) which are vital for the process of glass making.

(2) On the other hand, phenomena such as phase separation in the glass are still not fully understood and to a certain extent DTA can help to investigate this effect.

The following pages will start with a simple glass forming oxide, explaining important terminology and parameters in glass science. The complexity of the system will be increased and binary systems will be considered. It will also be at this stage that the glass structure theory with a literature survey will be found. As was mentioned above, no clear structural theory is today available. However, with the use of MAS-NMR in conjunction with XPS, a better picture of the glass structure may be elucidated. XPS and MAS-NMR will be explained at this place followed by literature survey.

Finally, DTA and the significance of parameters such as T_g, T_m and T_c will be explained as well as the glass forming process. The DTA was extensively used for the observation of these parameters but also the phenomena of phase separation will be considered.

3.1 Glass in general

Man-made glasses appeared around 4000 BC in Egypt but were merely decorative. Around 1500 BC there were significant developments in both the art and the technology of glasses and this was followed by further technological developments in glass science by Faraday, Zeiss, Abbe and Scott to name but a few. Their primary interest was in glasses for optical use. Nowadays, glasses are widely used both for everyday applications such as containers, automobiles and windows, but also for special applications, such as fibre optics. However, the idea of using a soluble glass as a biomaterial is a relatively new one.

A glass is in general an amorphous supercooled molten mass, which has not undergone crystallisation. This supercooled liquid softens very slowly on heating and its structure shows only short-range order. The "non-crystalline elastic solid" typically has a maximum ordering range of 2.0 nm with a viscosity $>10^{13.5}$ poise ($10^{12.5}$ Ncm^{-1}) (23). Glasses based on oxides such as M_2O_3 (e.g. B_2O_3, Al_2O_3), MO_2 (e.g. SiO_2, GeO_2) and M_2O_5 (e.g. P_2O_5, As_2O_5), where M is an element of the third, fourth or fifth chemical group of the periodic table have extremely low crystal formation velocities. The rates of crystallisation are lowest for substances easily cooled to glasses, such as silica and germania, whereas they are higher for glasses incorporating alkali and

alkaline earth compounds which must be cooled more rapidly to avoid crystallisation (24).

3.1.1 Single Oxide Glass System

Vitreous oxides:

Due to their relative abundance in nature (silicon and oxygen are very common on earth (24)), silicates have been extensively studied. Historically, silica (SiO_2) has been treated as a classic network-forming oxide in both crystals and glasses. This is due to the fact that silicon has a high affinity to oxygen and secondly The structural unit of silica is tetrahedral in which silicon is four-fold co-ordinated by oxygen. This tetrahedron is the basic unit and one mono silicate is cross linked with its neighbours over corners to form a whole network.

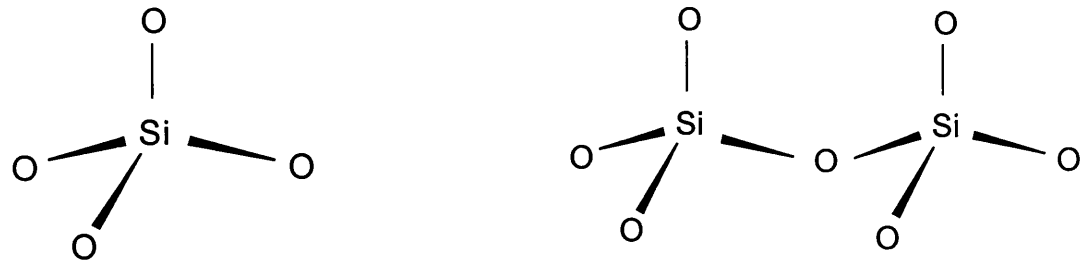

Figure 4: (a) Monosilicate structure [SiO_4^{4-}] and (b) two linked (condensed) monosilicate [$Si_2O_7^{6-}$]

The ability of SiO_4 to cross-link is a well-known principle, which is confirmed by the existence of many known crystals. An example of a crystal is the mineral Beryl $Be_3Al_2Si_6O_{18}$. This cross-link principle forms not only the basis for crystals, it can also be found in glasses (24).

Vitreous silica can be made, but from an industrial point is not routinely used due to the very high temperatures involved to form such a glass. Modifying oxides are able to break down the structure and significantly reduce the melting temperature. This is a major benefit for the production process.

But silicon in conjunction with oxygen atoms is not the only element, which forms crystals or glasses. Phosphorus is another example of a chemical element which can be found in both crystals and glasses with a similar structural relationship.

Phosphorus is an element of the fifth group of the Periodic Table and has an electron configuration of $3s^2p^3$, showing that it has one extra electron in comparison to Si ($3s^2p^2$). In consequence, phosphorus tends to form a P-O double bond but will still be co-ordinated tetrahedrally as found in silica (24).

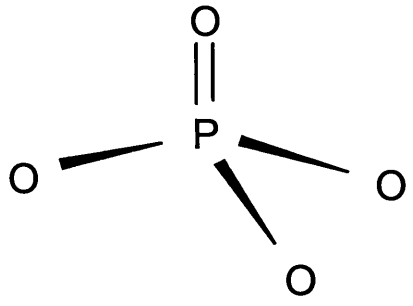

Figure 5: Phosphate mono unit

Biscore et al (25) have shown that the unit formation in all P_2O_5 based glasses is the $[PO_4]$- tetrahedron which is linked to form a three-dimensional network similar to mica glasses. The incorporation of alkali ions into a three-dimensional network leads to chain structures.

In comparison to SiO_2 in its vitreous state, P_2O_5 is very difficult to obtain in a glassy form. This is due to the fact that P_2O_5 is very hygroscopic and volatile and hence the number of papers investigating the structure of this state is rather limited. *DeDecker* (26) observed in 1942 that for a crystalline P_2O_5(c-P_2O_5) system 2 crystalline structures exist.

A rhombohedral polymorph will change at high temperature at around 260^0C into a orthorhombic system. He claimed that the volatile, low temperature modification is built of P_4O_{10} molecules, whereas the high temperature modification consists of two-dimensional planes, which have a more network-like nature. This latter form is easily supercooled to form a glass. At this stage no infrared or no detailed MAS-NMR spectroscopy observations on vitreous P_2O_5 have been reported.

3.1.2 Binary glass systems:

Oxides, which readily form glasses are SiO_2, GeO_2, B_2O_3, P_2O_5 and As_2O_3. However, most glasses are made from a mixture of oxides including network modifiers and network intermediates.

Network modifying oxides

Technical glasses consist of additional compounds. These additions are called modifying oxides, as they modify the glass structure, and are in general alkali- and alkali earth metal oxides, which break down parts of the network.

To clarify this process:

Using a Na_2O modifier:

$R_3Si - O - SiR_3 + Na_2O \rightarrow 2\ R_3Si - ONa$

Using a CaO modifier:

$R_3Si - O - SiR_3 + CaO \rightarrow R_3Si - O - Ca - O - SiR_3$

R = oxygen linkage

Na_2O as well as CaO are able to break down the strong Si - O - Si bonds and therefore change the structure and characteristics of the glass. If Na_2O is used as a modifier the corresponding Na^+ ion has only one positive charge and will terminate the network at a certain point. Ca^{2+} however can cross-link the network as it is a "species with two arms" (2 positive charges) hence it can re-stabilise the glass network. This may manifest itself in a significant increase in T_g with CaO addition.

Intermediate oxides

Other groups are oxides such as Al_2O_3, Fe_2O_3, MgO and BeO, to name but a few, which cannot form glasses on their own but they can to a certain extent substitute for the SiO_2. Colour changes or conductivity changes are examples of the properties modified by these oxides.

The addition of modifiers will, with respect to silicate based glasses, reduce production costs. Lime for instance is extremely cheap to manufacture and thus is a very cost effective network modifier. In terms of P_2O_5 based glasses, the addition of

modifiers will make this glass less hygroscopic, hence structural information may be more easily obtained. The hygroscopic nature of phosphate glasses remains a problem when the modifying oxide is below 30 mol% (27).

When adding alkali oxides to P_2O_5, 3 main reactions can occur which are shown in figure 6 (28).

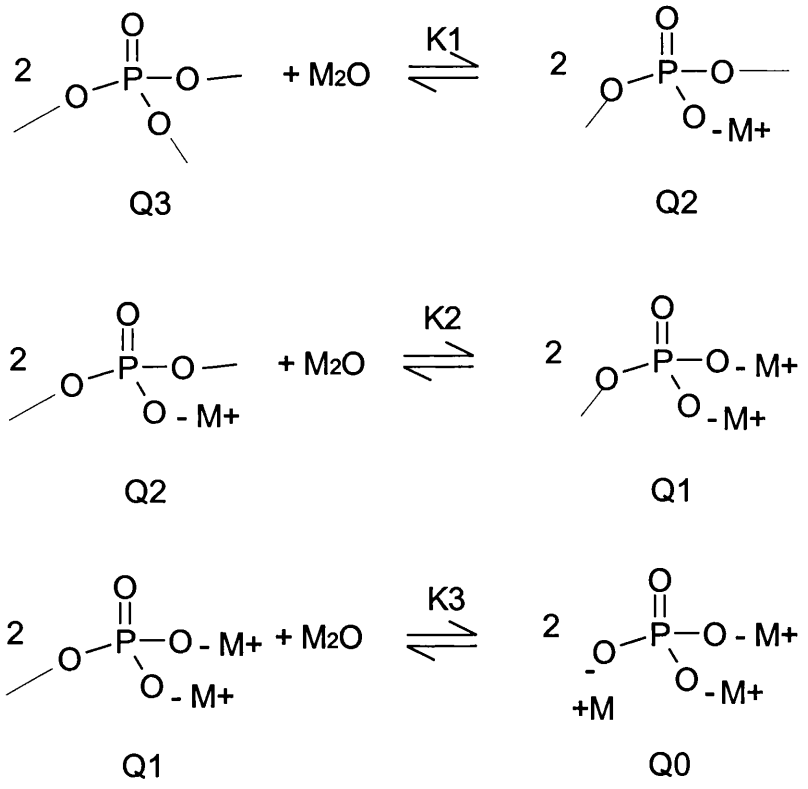

Figure 6: Structural changes by adding alkaline oxides to P_2O_5 with Q-nomenclature for appropriate species

According to these equations, structural changes continue to occur with increasing addition of alkali oxides to the system. Starting with ultra phosphates, which are found in chain or linear arrangements of PO_4 (Q^3) units. By further addition of alkaline

oxides the structure changes to linear, pyro- and ortho phosphates and finally to ortho phosphate as single ionised PO_4 groups (Q^0).

3.2 Glass Structure Theories

Glasses may be regarded as polymeric oxides with varying degrees of three-dimensional cross-linked network structures. It is therefore possible to regard oxide glasses as polymers of oxygen. In contrast to organic polymers which are formed from chains of adjacent carbon atoms, oxygen polymers contain networks of alternating oxygen atoms and intermediate, multivalent atoms, such as silicon, boron and/or phosphorus. Since the early decades of this century many workers have been studying the structure of glasses, unfortunately no definitive structure is yet apparent. Two major structure theories exist and over the years they have been reviewed and refined. In 1926 *Goldschmidt* (29) formed a hypothesis that any oxide A_mO_n with a radius ratio of R_A/R_O is in the range 0.2-0.4 will form a glass (R= radius, A= metal or non-metal and O= oxygen). This work showed that oxides were tetrahedrally co-ordinated and that this special co-ordination was necessary to form a glass. However, a vitreous BeO has not been made, although the radius ratio is 0.3, this should according to *Goldschmidt's* theory form a glass. In 1932 *Zachariasen* (30) published work on the glass structure concerning simple glass systems such as SiO_2. This work considered glasses as continuous, irregular networks where oxygen polyhedra were linked together over their corners. Addition of modifiers such as alkaline or earth alkaline ions were placed in the hollow space of the network without forming any special chemical phases within the glass.

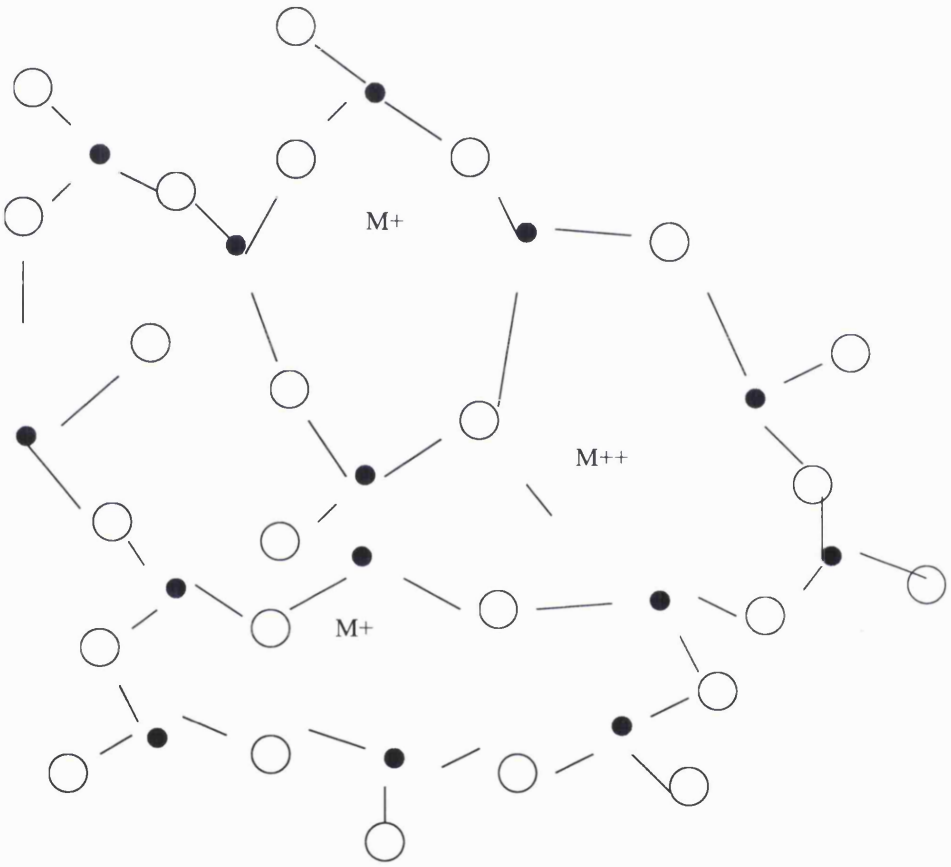

Figure 7: Structure of glass with modifying ions. Black circles: metal or non-metal, white circles: oxygen atoms, M^+ or M^{2+}: modifying oxides (30)

According to this theory, any metal or non-metal oxide should form a glass. The non-existence of a glass form of TiO_2 or Al_2O_3 could not have been explained with this theory. A further theory about glass structure and the possibility of glass formation

was presented one year later in 1933 by *Warren* (31) who regarded glasses as micro-heterogens with the existence of defined chemical phases which are linked together and it was these that therefore built up the glass structure. However, again this theory could not explain the non-existence of TiO_2 in a glassy form.

A refinement of *Warren's* glass structure interpretation took place one year later in 1935 when Hägg (32) focused on the glass forming process from the point of the cooling process. He believed that glasses consist of chains or two-dimensional nets and it was this that was the main difference to the interpretation of *Zachariasen.* With this theory he was able to explain why species like SiO_2 form a glass and TiO_2 do not. He believed that the symmetry and the bulkiness of the glass forming units above the melting temperature are responsible for the glass forming capacity. He supported his theory with the example of KNO_3. Above the melting point the ions K^+ and NO_3^- are small and mobile enough that they can easily come together and form KNO_3 and if that molten mass cools down rapidly enough it will freeze-in as a glass. Only materials which will have one-dimensional or two-dimensional unlimited cross-linked units in the corresponding crystals will be able to form a glass. For example, SiO_2 exists in crystalline form as chain and ring silicates (Beryl $Be_3Al_2Si_6O_{18}$), which has unlimited cross-linking. TiO_2 however exists "only" in the form of 3 defined crystal modifications, where oxygen atoms co-ordinate Ti in an octahedral form. There are no long chains or ring structures known.

Still, there is no precise structural model, which covers all glass types. The development of modern analytical techniques such as solid state NMR-spectroscopy (SS-NMR), X-ray Powder Diffraction, X-ray Photoelectron Spectroscopy (XPS) and

Differential Thermal analysis (DTA) has helped to produce a more coherent model for glass structures.

3.3 Solid State NMR Spectroscopy (MAS-NMR)

Nuclear magnetic Resonance (NMR) spectroscopy is one of the most powerful methods for structural analysis of inorganic and organic compounds and especially of disordered materials such as glasses. This technique gives very detailed information about the very nearest environment around the nucleus under investigation. Even different surrounding atoms with different charges such as Na^{+} or Ca^{2+} can be detected. Only magnetically active nuclei such as isotopes of H, C, N, F, and P, which have a nuclear spin different from zero, can be observed using this technique. NMR spectroscopy has recently been revolutionised by improved electronics and design, which have dramatically improved sensitivity and chemical shift separations. With the development of magic-angle spinning NMR technique (MAS-NMR) chemists no longer have to rely on liquid NMR spectroscopy techniques to investigate structures. If normal NMR methods were applied to solids broad peaks would be the result, hiding the desired information. This is due to chemical shift anisotropy, which leads to a simultaneous absorption for all possible random orientations for a powder sample. With magic angle spinning NMR however, the sample is spun at high velocity around an axis inclined at an angle of $54^{0}44'$ to the magnetic field. This effect leads to a modification of the shift anisotropy to give isotropic chemical shift with sharp lines.

3.3.1 Beginning of MAS-NMR Spectroscopy with Commercial Phosphates

In the early eighties *Grimmer and Haubenreisser* (33) reported their work on polycrystalline P_4O_{10} and binary phosphates in the compositional range of $P_2O_5.\times K_2O$ ($0 \leq \times \leq 3$). Samples included phosphates of P_4O_{10}, K_3PO_4, $K_4P_2O_7$, $K_5P_3O_{10}$, $K_3P_3O_9$ and $(KPO_3)_x$ and were measured at 109.3 MHz. ^{31}P shielding values gave isotropic chemical shifts for K_3PO_4 isolated groups of PO_4 at –11.7 ppm and $K_4P_2O_7$ show end groups at 0.3, 2.2, 2.4 and 4.9 ppm. $K_5P_3O_{10}$ consisted of end and middle groups at 1.2, 4.2 and 19.4 ppm and $K_3P_3O_9$ showed a cyclic structure with middle groups at 18.2, 19.9 and 21.2 ppm. The polymer $(KPO_3)_x$ consisted of middle groups in a chain at 18.5 and 20.7 ppm.

In the same year as *Grimmer and Haubenreisser* published their results, another publication by *Duncan and Douglas* (34) dealt with the structural investigation of condensed potassium phosphates such as $K_4P_2O_7$, $Na_4P_4O_7$, $K_5P_3O_{10}$, $(NaPO_3)_x$ and pure P_4O_{10}, using MAS-NMR spectroscopy. The samples were commercial chemical products and were measured on a CXP-200 Bruker spectrometer using around 4-4.6 kHz rotation frequency. Experimental results for $K_4P_2O_7$ and $Na_4P_2O_7$ showed a centre band at 2.7 and –1.6 ppm, respectively. $K_5P_3O_{10}$ showed a different pattern with three different species, having isotropic shifts of 1.2, 4.0 (end units) and 19.5 ppm (middle group). The chain polyphosphate $(NaPO_3)_x$ gave a centre band at 19 ppm (middle group) with minor species at –2 ppm (end units). The cage phosphate P_2O_{10} was centred at 33 ppm. Unfortunately, the authors did not mention exactly the nature of this species.

In 1986 *Mudrakovskii et al* (35) used MAS-NMR to analyse a series of commercial phosphates such as $AlPO_4$, $Al(PO_3)_3$, $Zr(HPO_4)_2x2H_2O$, $Be_3(PO_4)_2$ x $6H_2O$ and $Mg_2P_2O_7$ etc. They recorded on a Bruker CXP-300 spectrometer at 121.46 MHz (magnetic field 7.05 T) and the spinning frequency was 3.5-4 kHz. The anisotropy $\Delta\sigma$ is negative or positive depending on the individual sample, and the isotropic chemical shifts ranged from –13 to 52 ppm. They found that both anisotropy $\Delta\sigma$ and the asymmetry parameter η equal 0, except for the $Mg_3(PO_4)_2$ sample. This indicated the equivalence of four P-O bonds for each PO_4 group. With the help of crystallographic data, they interpreted that the P-O bonds are close to a regular tetrahedron. Additionally, they also mentioned that the lack of anisotropy in spectra of $AlPO_4$ x $2H_2O$ and $Be_3(PO_4)_2$ x $6H_2O$ is an indication of high symmetry. The nearest oxygen atoms, which are surrounding the phosphorus atom, are arranged symmetrically. Distortion in the phosphorus environment with the appearance of anisotropy appeared in the spectra of $Zr(HPO_4)_2$ x $2H_2O$, $Mg_3(PO_4)_2$ and KH_2PO_4. According to the chemical shift values observed for $Mg(HPO_4)$ x $3H_2O$, $CaHPO_4$ and $Ca(H_2PO_4)$ x H_2O there was evidence for two crystallographically non-equivalent phosphorus atoms present.

3.3.2 Structural Investigation by MAS-NMR Spectroscopy for Binary Glass Systems

Villa et al (36) were the first to use MAS-NMR for structural investigations of alkali boron phosphate and silver boron phosphate glasses. They examined glasses prepared in a range of $0.45 \leq xAg_2O \leq 0.59$ and $0.39 \leq xLi_2O \leq 0.59$ and observed that by

increasing the alkaline content the polymerisation of the phosphate units was reduced. In this same work, it was mentioned that binary phosphate glasses of the type M_2O-P_2O_5, consist of

(1) branching units $O=P-O_3$ which have 3 bridging oxygen's and are neutral in their charge,

(2) middle units with 2 bridging oxides and 1 negative charge and

(3) end units with 1 bridging unit and 2 negative charges.

Furthermore binary phosphate glasses consist of monomeric units, which can be found in orthophosphates M_3PO_4.

On the basis of a binary silver phosphate glass, MAS-NMR revealed that these glasses consisted of middle units at -10- (-20) ppm and end phosphate units at + 10ppm which gave curves fitted by nearly two Gaussian lines. More complicated glass systems were prepared by doping this binary silver phosphate glass with B_2O_3. Here, monomeric units appear at +30ppm and units at +10ppm, middle units connected to one boron at around 0 ppm and another middle unit at -10 to -20 ppm connected to one boron atom and one phosphorus atom.

In 1987 ^{31}P-MAS-NMR investigations of glassy inorganic phosphates were carried out by *Parbhakar et al.* (37). Glasses were prepared using $(NH_4)_2HPO_4$ as a starting reagent, heating to 920 K for several hours and the melt was quenched by pressing it onto a stainless steel plate. The ^{31}P -NMR spectra, recorded at 300 MHz show ortho-pyro and meta phosphates.

More modern ^{31}P MAS-NMR studies have dealt with the identification of the relative amount of Q^n phosphorus species present, $PO_{4-n}(PO)_n$ where n denotes the number of bridging oxygen's, since each of these species can be resolved in a MAS-NMR experiment.

A series of $x(Na_2O + H_2O)$ x (1-x) P_2O_5 glasses were characterised by *Brow et al* (38) in 1990 using ^{31}P MAS-NMR experiments. Spectra were collected at 145.7 MHz at a magnetic field strength of 8.45T. All samples showed a central peak in the range of –18 to –28 ppm.

^{31}P MAS-NMR studies of calcium phosphate glasses were presented by *Flechter et al.* (39) in 1993. They prepared several calcium phosphate glasses with compositional molar ratios between ($CaO:P_2O_5$ = 1) and ($CaO:P_2O_5$ =1.49) using chemicals such as CaO and $Ca(H_2PO_4)_2$ x H_2O and heating them in a platinum crucible at 1300^0C for one hour. The melt was poured into a graphite mould and the ^{31}P NMR spectra were obtained under MAS conditions using 145.7 MHz with MAS frequencies of 8.0-8.9 kHz. The resulting spectra showed peaks with chemical shifts at -8 to -10ppm and -25 to -28 ppm. They assigned these peaks to phosphorus in tetrahedral co-ordination, with polymerisation of Q^1 (-8 to -10ppm) and Q^2 (-24.9 to -28.0 ppm) and also they observed a small peak at -44 ppm, which they interpreted as Q^3. With increasing Ca content the Q^3 peak disappeared and the intensity of the Q^1 peak increased. In general, the authors pointed out a systematic variation of the relative peak areas for the different P polymerisation because of varying composition. They also mentioned an important fact based on their earlier studies with sodium phosphate glasses that in a

metaphosphate composition of sodium phosphate glass only Q^2 species occurred, whereas the calcium phosphate glasses show detectable species of Q^1 and Q^3.

Brow et al. (40) examined a series of various meta phosphates such as $Mg(PO_3)_2$, $Ba(PO_3)_2$, $LiPO_3$ and $NaPO_3$ with MAS-NMR spectroscopy preparing glasses by melting the appropriate crystalline chemical at 800°C for 1h, quenching and annealing afterwards. The ^{31}P MAS-NMR spectra were collected at 145 MHz and a magnetic field strength of 8.45 T. Spinning speeds varied between 6.5 and 9.2 kHz. All spectra showed typical peak positions between -20 and -30 ppm depending on the counter ion. The isotropic chemical shift reflected a Q^2 co-ordination for P -bonding over two bridging oxygen atoms and two non bridging oxygen atoms which represented the meta phosphate region and tied in accordingly with the findings of *Flechter et al.*

In 1995 *Kirkpatrick and Bow* (41) published results on ^{31}P MAS-NMR measurements of various alkaline and alkaline earth phosphate glasses and alumino-, boro-, and fluoro phosphate glasses in conjunction with other NMR measurements probing the appropriate element such as ^{7}Li and^{23}Na.

They also discussed the bond length (measured in Å) of the phosphorus – oxygen double bond, which became longer with decreasing polymerisation. This reflected a reduction in double bond character with an increase of non-bridging oxygen atoms per tetrahedron.

Binary sodium phosphate glasses in the ultraphosphate region with < 20mol% Na_2O are dominated by Q^3 species. If the Na_2O content approaches the metaphosphate region at around 50 mol% Na_2O Q^2 peaks become dominant. Q^1 prevails if the Na_2O content gets even higher. They mentioned that the ^{31}P chemical shift varies

systematically with composition. This is due to the fact that changes of bonding arrangements are occurring due to composition. The resulting consequences should be clarified in a picture:

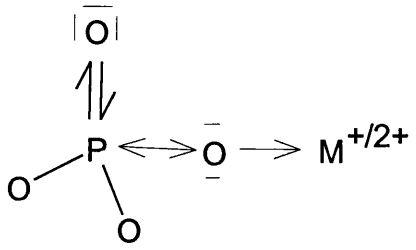

Figure 8: Schematic representation of electron transfer from oxygen to phosphorus within the double bond and single bond caused by modifying cation.

Increasing polymerisation will caused by increasing shielding effect at the phosphorus atom caused by shifted electrons of the oxygen at the double bond. That effect will shorten the bond length of the double bond and causes an increasing covalency of the bridging oxygen bond. Adding cations M^{+} or M^{2+} will then decrease the degree of polymerisation and the oxygen atom of the single bond will undergo an electron pull caused by the modifying cation. This will influence the double bonding by increase its length. All these effects can be seen in a MAS-NMR experiment by changed chemical shifts. For example in binary alkaline and alkaline earth ultraphosphate glasses the positions for Q^2 and Q^3 (high degree of polymerisation) become less shielded as the composition changes from P_2O_5 to the metaphosphate. And for metaphosphate, the Q^2 chemical shifts become more shielded (more negative) with increasing cation potential (charge/ionic radius) of the modifying cation. Therefore the nature of the cation will have an influential effect.

In work by Martin (28) simple binary alkali metal oxide-doped phosphate glasses were prepared and investigated via solid state NMR spectroscopy. It was observed that a systematic shift towards positive chemical shift values was seen by adding more non-bridging oxygen atoms.

In 1997 *Feike et al* (42) probed the local structure of phosphate glasses with 35 mol% Na_2O, and showed it contained a three-dimensional network of $Q^{(1)}$ and $Q^{(3)}$ groups and a glass with 58 mol% Na_2O contained two-dimensional chains of $Q^{(1)}$ and $Q^{(2)}$ species. All experiments were performed on a Bruker ASX 500 spectrometer using resonance frequency of 202 MHz. The rotation frequency was 12.5 kHz. Glasses were prepared by melting Na_3PO_4 and P_2O_5 at 1100^0C for 5h. Spectra showed for $Q^{(1)}$, $Q^{(2)}$ and $Q^{(3)}$ species, chemical shifts of 0, -20 and –40 ppm, respectively.

A significant study by Wenslow and Mueller (43) carried out ^1H and ^{31}P -MAS-NMR experiments on simple binary phosphate glasses to monitor the water attack on the structure forming P-OH groups. NaH_2PO_4 was used to give glasses near the meta phosphate region by standard melt/quench technique. Once the glasses were obtained water was added and investigated by NMR using a Chemagnetics CMX-300 spectrometer with a magnetic field of 7.05T. ^1H resonance was observed at 11.2 and 15.7 ppm assumed to be due to strong hydrogen bonds. ^{31}P resonance's showed 3 different chemical shifts at 1.9 (Q^1 species), -6.3 and –18.9 (Q^2 species). The resonance at –6.3, however, lay outside the value for 3 species commonly found in phosphate glasses. The only reported Q^1 species in this region was assigned by *Hartman and co-workers* (44). However, another possible source could be the intramolecular hydrogen bonding as shown below.

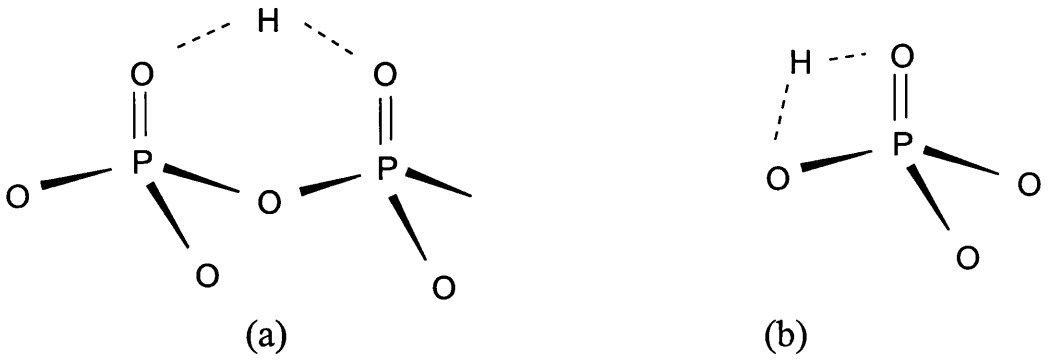

Figure 9: Proposed structure for inter (a) and intra (b) -molecular hydrogen bonding

They drew possible pathways for water attack to the glass network structure which left either only Q^1 or Q^0 + Q^1 species behind which can be detected via ^1H MAS-NMR and ^{31}P MAS-NMR spectroscopy. Using both techniques and with the additional interpretation of intra – and intermolecular hydrogen bonding they concluded out of their results that five distinguishable phosphate units occurred, revealing a more complex chemistry by water attack than originally thought. Results for isotropic chemical shifts are:

Q^1 phosphate side with only sodium next nearest-neighbours at 1.9ppm, Q^2 phosphate unit with only sodium next-nearest-neighbours at –18.9 ppm, Q^0 unit with strong intramolecular hydrogen bonding at –2.4 ppm. Furthermore, the Q^1 unit where the hydrogen is involved in a weaker intermolecular hydrogen bonding at –5.8 ppm and at –18.4 ppm they assumed that to be a Q^2 unit which is attached to a weaker intermolecular hydrogen bonging.

3.3.3 Structural Investigation by MAS-NMR Spectroscopy of Ternary and Quaternary Glass Systems

In 1987 *Haubenreisser et al* (45) were one of the first groups who used the relatively new MAS-NMR method for complex ternary or multiple glass systems. Originally they wanted to design glass-ceramics which would result in apatite formation by heat treating the corresponding glass system. Therefore, glasses such as $CaO\text{-}P_2O_5\text{-}Al_2O_3$, $CaO\text{-}P_2O_5\text{-}Al_2O_3\text{-}Na_2O$ or even more complex $CaO\text{-}P_2O_5\text{-}Al_2O_3\text{-}AlF_3\text{-}Na_2O$ were prepared and investigated by MAS-NMR with magnetic fields of 6.35 T and spinning speeds of 1kHz. For the ternary glass system, Q^2 species dominated the spectra. Increasing the CaO content resulted in Q^1 units as the dominant species. They also mentioned the high value for anisotropy $\Delta\sigma$ and the asymmetry parameter η, which was due to the fact, that phosphate units were bonded with AlO_4.

The author of this thesis carried out work on complex quaternary-based phosphate glasses within the system $P_2O_5\text{-}Na_2O\text{-}CaO\text{-}Al_2O_3$. ^{23}Na, ^{27}Al and ^{31}P NMR and X-ray powder diffraction studies on these glasses have been published in a paper by *Abrahams et al.* (46). ^{31}P-MAS-NMR were carried out on a Bruker MSL-300 spectrometer operating at 121.5 MHz and the magic angle spinning frequency was 10-11 kHz. Spectra of these glasses consisted principally, of two bands at –5 to –9ppm (Q^1) and at –21 ppm (Q^2), which falls in the range quoted by *Haubenreisser et al.* (45) and fits accordingly with their findings.

3.4 X-ray Photoelectron Spectroscopy (XPS)

Photoelectrons, which have been ejected caused by the X-ray bombardment of the specimen, can be analysed by the correlation of the expended X-ray radiation and their kinetic energy E_k. The correlation is given by:

$$h\nu = E_K + E_B$$

Where E_B = binding energy, $h\nu$ = energy of X-ray radiation and E_K = kinetic energy of ejected photoelectrons

This equation reveals that the kinetic energy (E_K) of the emitted electron is dependant on the energy of the incident photon ($h\nu$) and its binding energy (E_B). The measured kinetic energy and therefore the binding energy will give information about the atom and its orbital state, which is in the end a characteristic for the material. Commonly, photons are used in the soft X-ray region ($h\nu_{(AlK\alpha)}$ = 1486.6 eV; $h\nu_{(MgK\alpha)}$ = 1253.6 eV). According to different chemical environment, a difference in binding energy of 1-20 eV for the inner shell atoms can be detected and used for structural investigations. For example, by comparison of the integrated areas under the peaks, it is possible to estimate the stoichiometry.

3.4.1 Structural Investigation of Glasses using XPS

Graham's salt, which corresponds to $Na_2OxP_2O_5$, is a well studied salt used as a structural reference for binary phosphate glasses. Over the years, other types of polyphosphate have been discovered and today these glasses have found industrial applications. For example, they show the ability to complex alkaline earth metals (used as a water softener Calgon® (24).

As early as 1933 *Graham* (47) believed that polyphosphates had the basic structure, consisting of ortho-, pyro-, and meta-phosphoric acid. From these considerations, it is not surprising that phosphate glasses have been described in these terms. In 1939 *Kordes et al* (48) considered the formation of non-bridging oxygens in phosphate glasses. This work assumed that the P-O double bond remained and that the number of added alkaline oxides was in accordance with the number of formed non-bridging oxygens. A decade later *Van Wazer* (27) looked at different glasses based on Na_2O-P_2O_5 in different ratios. This work tried to separate these glasses into two groups. Case I was a balanced ratio of Na_2O and P_2O_5; this was also the case for Graham's salt, and case II for a range between pure P_2O_5 and Na_2O-P_2O_5. *Van Wazer* pointed out that in case I there are no termination points and hence PO_4 groups must be linked to give chains or rings. At Na_2O:P_2O_5 there were only rings or infinite chains and at $2Na_2O$:P_2O_5 there were only two-membered chains (pyrophosphate ions).

Gresch et al. (49) appeared to be the first to investigate a series of binary sodium phosphate glasses with XPS. The authors prepared glasses in the composition of Na_2O/P_2O_5 0.17, 0.28, 0.35, 0.56, 0.79, and 1.13 via standard solid state techniques. This work described the transformation as being from one compound to another due to

an alteration of oxygen atom binding state. By starting at $PO_{2.5}$ as the unit of P_4O_{10}, through PO_3^- ($NaPO_3$) and $PO_{3.5}^{2-}$ ($Na_4P_2O_7$) to PO_4^{3-} of Na_3PO_4 one of the binding oxygen atoms was successively replaced by non-bridging oxygen atoms. Therefore the binding energies of the oxygen atoms changed accordingly. Furthermore, it was observed that the XPS spectra of nearly pure P_4O_{10} (lowest alkali) glasses resembled that of pure P_2O_5. If the alkali content increased, the spectra become more metaphosphate like.

Brueckner (50) carried out some complementary studies in 1980, which led to different models in respect of oxygen double bonding. *Gresch* only saw evidence of P-O double bonding in very low alkaline glasses. *Brueckner* however, was able to assign low energy peaks for the double bonding in higher alkaline containing glasses ratio Na_2O/ P2O5: 0.61.

This led to the need for more thorough XPS studies especially for low alkaline phosphate glasses.

3.5 Glass Formation Process

Prior to discussing the theory of DTA, the process of glass formation will be discussed in order to understand the parameters measured via DTA. In addition the phenomenon of glass phase separation, currently not fully understood, was another subject, which hopefully can be explained by DTA.

Glass formation usually takes place by cooling the molten mass rapidly past the crystallisation point with solidification at the glass transition temperature T_g. For a successful transformation into a glass the crystallisation temperature range must be passed quickly. Figure 10 illustrates this process

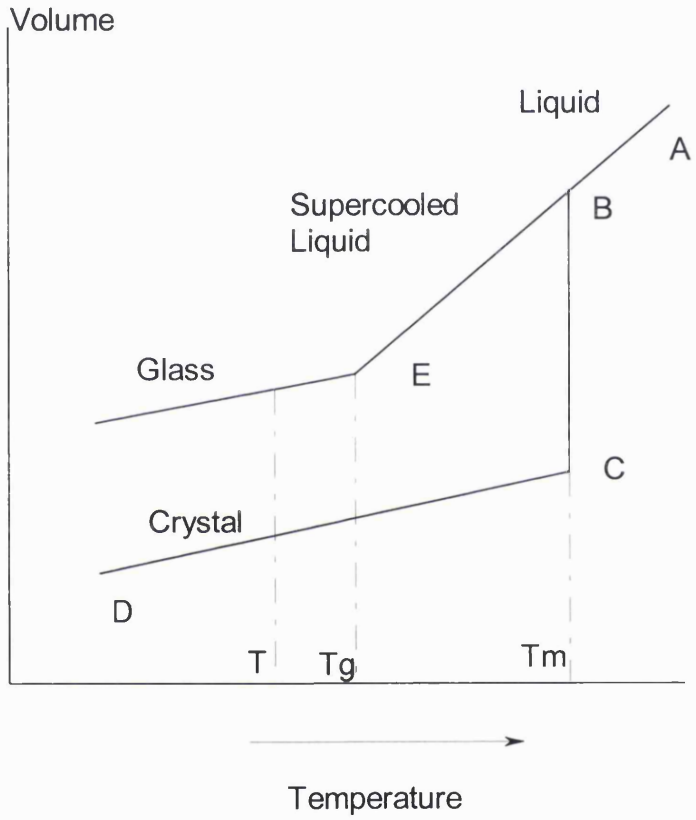

Figure 10: Glass formation process

Considering the liquid molten mass (state A), a continuous decrease in temperature will decrease the volume along line AB. If the decrease in temperature is carried out slowly enough, crystallisation at the melting point T_m will occur and a crystal product will form along line CD. However, if the temperature is reduced fast enough, the

crystallisation process will not occur at T_m and the volume change follows along line BE until it reaches room temperature, which would result in a glass.

3.5.1 Glass Transition Temperature

Phosphate glasses show unique features such as large thermal expansion coefficients, low optical dispersion and low glass transition temperatures T_g (41). T_g is defined as the temperature at which a polymeric, amorphous material is converted from the elastic-plastic state to the glassy state (24). Amorphous materials change when heated from a hard, glassy state to a soft, plastic state over a temperature interval. Considering polymeric oxide glasses as elastic solids at low temperatures, the degree of mobility increases within the transformation range as the temperature rises. This can only take place by bond switching or transfer of covalent bonds between oxygen atoms. The number of network bonds which become mobile at the glass transition temperature depends in the first place on the cross-link density of the network. The strength of the single bonds however, plays only a secondary role. For example, comparing the bond strength of several oxide glasses (such as oxides of arsenic, boron and phosphorus) this rises from 70 up to 110 kcal/mol (24) but all three networks have the same cross-link density resulting in similar glass transition temperatures. The glass transition temperature of an oxide network also depends upon the tightness of packing. If the network is less densely packed and more open, for example as a result of large cation incorporation, the transition temperature Tg will decrease.

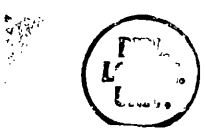

3.6 Differential Thermal Analysis (DTA)

Differential thermal analysis is a technique, which can detect exothermic and endothermic phase changes. Here, the temperature of a sample is continuously monitored with a thermocouple against an inert material as a reference sample. The temperature as a function of time is linear until an exothermic or endothermic event happens. Sample and reference are placed side by side in a heating block, which are connected to thermocouples.

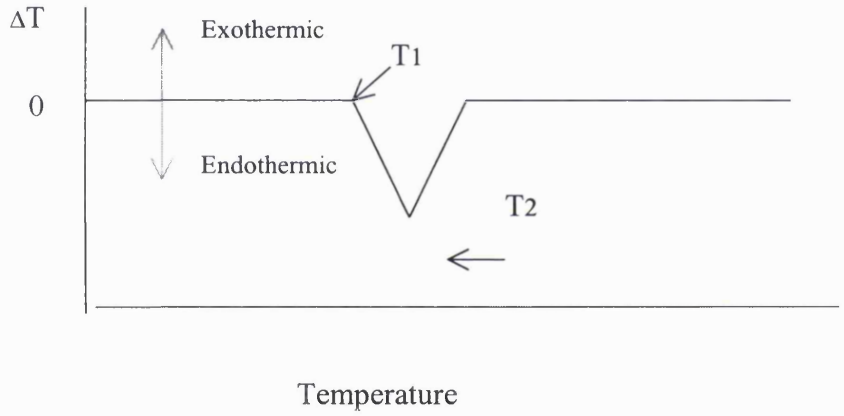

Figure 11: Typical DTA trace with two temperature events for a polymer

When sample and reference are at the same temperature, then the net output is zero. A thermal event in the sample will result in a temperature difference ΔT, which is detected by the net voltage of the thermocouples. A third thermocouple is used to monitor the temperature of the heating block and the results are presented in ΔT against temperature. It should be noticed that the temperature of the peak is taken as

the onset of the derivative from the baseline T_1 or as the peak temperature T_2 (see figure 11).

This analysis methodology is important to use in glass making. It can on the one hand be used to determine important parameters such as the melting point T_m of the glass and the glass transition temperature T_g. Another important not fully understood phenomenon is that of glass phase separation. The following literature review is conceived in two parts. One part discusses the general observation of T_g determination and trends. The second part discusses the literature review on phase separation.

The first paper to investigate T_g of phosphate glasses was published in 1966 by *Eisenberg et al* (51). This work wanted to obtain a complete picture of the effect on Tg of counter ions in pure homopolymers of HPO_3. They determined the T_g for pure HPO_3 doped with ions such as Li, Na, Ca, Sr, Ba, Zn and Cd and showed no linear correlation when q/a^2 was increased, where q = charge of the cation and a^2 = cation radius + oxygen anion radius.

The same authors also carried out another study on the effect on the T_g by using a neutralising effect of counter ions like Na^+ or Ca^{2+} on PO_3^-. Therefore, samples of either $NaPO_3$-HPO_3 or $NaPO_3$-$Ca(PO_3)_2$ were prepared by standard melting techniques and the T_g was measured. Within the $NaPO_3$-HPO_3 system, the T_g decreased with increasing Na^+ ions. By contrast, in the second system, with increasing Ca^{2+} ion concentration the T_g almost linearly increased.

Sahar and Kamaruddin (52) published a paper on the phase equilibrium of binary MgO and CaO phosphate glasses. Glasses were prepared from P_2O_5, $CaCO_3$ and MgO using standard melting techniques. Glasses in the system (1-x) MO x P_2O_5 (M = Ca,

Mg) were studied, ranging from $0.4 \leq x \leq 0.8$ for the MgO glass and $0.4 \leq x \leq 0.7$ for the CaO based glass. The authors plotted their data as $T_c - T_g$ against mol% CaO/MgO and it revealed two effects:

1. For the CaO based system a systematic increasing stability effect occurred and
2. the MgO glasses show a sudden stability rise for glass compositions above x = 0.46.

The authors speculated that this might be due to the glass structure changes from metaphosphate MgP_2O_6 (less stable) to pyrophosphate $Mg_2P_2O_7$ (more stable). They backed up their findings with phase analysis of corresponding crystallised glasses via X-ray powder diffraction.

Hudgens and Martin (53) prepared a series of glasses in the system Li_2O - P_2O_5 and investigated this system with FT-IR spectroscopy and DSC. By adding Li_2O to pure P_2O_5 initially decreased the T_g followed by an increase in the T_g as the metaphosphate composition was reached. Since the T_g was sensitive to the type and nature of the atomic bonding in the liquid they pointed out that the network degradation and intermediate order started at a compositional range of 20-25 mol% Li_2O. Beyond 33 mol% alkali long chains and ring structures occurred. Towards the metaphosphate composition $P\text{-}O^- - Li^+$ chains became theoretically infinite in length.

Another important factor is the charge density effect. If the alkaline cation is replaced by the alkaline earth cation of the same radius but double the charge, the T_g will increase

Another interesting study was published by *Suzuya et al.* (54). Glasses were prepared in the region of $(Na_2O)_x(P_2O_5)_{100-x}$ with x = 0, 10, and 20 mol%. The T_g reached a minimum at ~ 20mol% Na_2O and increases towards higher Na_2O content. This is in accordance with *Hudgens and Martin* who worked on Lithium based phosphate glasses (see above). However, these findings are not valid for larger cations. Here, T_g only decreased with increasing size of the cation. In addition, they mentioned that the alkaline earth phosphate glasses showed in general higher T_g's than alkali metaphosphate glasses. This was due to the higher charge density.

Studies of phosphate based glasses have mainly focussed on their use in optical roles, metal seals, nuclear waste and conductivity, but were limited by their very low durability. With the increase in activity of modern biomedical science, this very low durability may be useful. However, very few papers have been published including glasses, which have glass compositions that relate to inorganic phase of bone.

In 1993 *Uo et al.* (55) published a paper with the combination of structural investigation using DTA and solubility determination of phosphate glasses. They prepared binary glasses of Na_2O-P_2O_5 or CaO-P_2O_5 and a ternary phosphate glass system of Na_2O-CaO-P_2O_5 by standard melting techniques and the T_g and T_c were measured on a DTA. The authors found that the T_g and T_c decreased with increasing P_2O_5 content as the CaO content was more and more substituted by Na_2O. The same was true for the Na_2O-P_2O_5 and CaO-P_2O_5 binary glass compositions, T_g and T_c were found to increase with increasing Na_2O and CaO content, respectively.

Chapter 4

4.1 Soluble Glasses

The handling of glasses based on phosphorus pentoxide is difficult because of their poor chemical durability and their hygroscopic nature. In general this confines phosphate glasses to specialised applications such as optical and conducting glasses, glasses for heat protection or for nuclear waste vitrification (23). Recently however, phosphate glasses have been investigated for biomedical applications. As was mentioned in the introduction, advances have been made to treat periodontal diseases with the use of degradable polymers based on polyglycolic and polylactic acid (56-58). However, laboratory and clinical studies indicate a non-linear and very unpredictable degradation process for these materials. With the use of soluble phosphate glasses it is envisaged that the more predictable degradation will be of benefit in biomedical use. Prior to clinical use, basic laboratory studies of the solubility behaviour are imperative because of two reasons.

(1) To understand the material and predict their degradation process and

(2) To give a better understanding of their degradation process which will help to optimise the materials by tailoring the solubility according to the desired application.

Furthermore, as will be discussed in detail in the glass structure chapter, no precise structural information is currently available. The degradation process will release structural units from the glass, which can be detected by a combination of modern

analytical methods. It is hoped that with this additional information contributions to the structure analysis can be made.

Currently, the number of publications regarding the solubility of phosphate glasses is rather limited. The literature survey has been divided into two parts. First, related glass systems such as silicon based glasses were reviewed. This was carried out in order to give preliminary information about the degradation process in the glasses. Secondly, the survey was focussed on phosphate salts, such as Graham's salt or very basic binary phosphate based glass system. There were a limited number of studies, but further information where possible, discussed more complex ternary phosphate based systems for biomedical use.

4.1.2 Solubility of silicate glasses

Many familiar glass articles show high durability; for example commercial silica based glasses such as window glass. This is also clearly the case for vitreous silica. In 1962 *Morey et al* (59) showed that by rotating vitreous silica or quartz grains in water only 1 ppm soluble silica was detected after one year. But silica based glasses with different ratio's of network modifiers can have a range of durability in aqueous solutions. *Enss* (60) produced one of the very first publications regarding this subject in 1928. The paper considered the durability of a soda-lime-silica glass, where SiO_2 forms the network and soda ash or potash is necessary to flux the mixture at a more readily attainable temperature. Lime (CaO or CaO + MgO) increases the chemical durability of the final product. The extraction of material was measured by water

attack on crushed grains of glasses with varying SiO_2 and metal oxides contents. The SiO_2 glass was only stabilised up to a certain point depending on the content of metal oxides.

Charles published a more detailed study in 1958 (61). The corrosion process of alkali-silicate and alkali-lime-silicate glasses was examined in aqueous solutions and it was shown that alkali ions were first extracted and an alkali-deficient layer was formed on the surface of the glass. This layer acted as a barrier limiting further alkali ion diffusion, thus rapidly increasing the durability of the glass.

There are 2 equations to describe the corrosion process:

(1) $R_3 - Si - OR + H_2O <=> R_3 - Si - OH + R^+ + OH^-$

The formed hydroxyl- ion in equation (1) can now react with another siloxane bond in the glass:

(2) $R_3 - Si - O - Si - R_3 + OH^- <=> R_3 - Si - OH + R_3 - O^-$

Douglas and Isard (62) presented another study on the durability of ordinary glasses in 1949. The extraction of alkali ions from a commercial silicate based glass by distilled water was the subject of this study. The rate of sodium removed from the surface of the glass was found to be a function of the square root of time. The conclusion from this study indicated that this process was diffusion driven and that the rate of extraction of the sodium ions could be related to electrical conductivity of the

glass. During the diffusion of Na^+ ions to the surface of the glass the overall electrical neutrality must be maintained and that can only occur by counter-diffusion of other ions such as H_3O^+. If this were not the case, an electric double layer would occur, preventing further sodium ions from leaching out.

Dubrovo and Shimdt (63) published a more systematic study of a binary sodium/silicate glass where they studied the effect of water and hydrochloric acid solutions on a whole series of Na_2O-SiO_2 glasses. The interaction of sodium silicate with water can be divided into two stages:

1. Exchange of sodium ions in the glass for hydrogen ions in the solution. This process leads to a residual layer of silicic acid on the surface of the glass.

2. This formed layer can further react with the alkaline solution resulting in silicic acid.

Additionally, it was shown that if the Na_2O content is high (SiO_2 low), dissolution of the glass takes place and a kinetic equilibrium is established between stage 1 and 2. If the silica content is high (Na_2O low), the main process that occurred was the leaching of Na_2O from the glass.

Work by *Rana and Douglas* (64) indicated that rate of alkali extraction varies linearly with the square root of time for short measuring periods developing into a linear relationship for longer measuring time.

In 1963 *Hlavàc et al* (65) developed a mathematical model to describe the whole course of decomposition of a soda-silicate glass. A study on how the sodium ions leaching out of this glass and it's dependence on the temperature of the aqueous solutions. For all temperatures ranging from 60 – 100^0C the following 2 process were found:

Process I: exchange of cations from the glass for H_3O^+ ions. This is a diffusion driven process, which ends up forming a destroyed (leached) layer. Process II: dissolution of the leached layer, which is controlled by surface reactions.

In terms of a mathematical description, this means that there is a linear short-term relationship with a function of time $(min)^{-1/2}$ is followed by a long-term linear relationship for measurement times of greater than 30 hours. These findings are in accordance with the previous authors.

Dimbleby and Turner (66) carried out a study on a ternary Na_2O - MgO - SiO_2 glass where they questioned whether the surface area of the glass has any influence on the dissolution process. The weight loss was increased by a factor of 2 if the amount of the initial material was increased four times. Another study was carried out in 1966 by *Shamy* (67) on a binary K_2O – SiO_2 glass where the volume of the solution was kept constant at 100 ml while the weight of the glass grains was increased systematically. The amount of extracted silica per gram glass increased as the ratio of the surface area of the glass to the volume of the leaching solution increased.

Phosphate glasses differ from silicate glasses, in that they are usually completely soluble. Every possible ion will leach out into solution until the glass is completely degraded. The following passage will review the literature on the degradation process of soluble phosphate glasses in an aqueous environment. This review will start, like the review on silicate based glasses, with simple binary phosphate glasses or even phosphate salts and will then consider more complex phosphate glass systems. At this point the survey will also include a consideration of what occurs to the out-leached ions immediately on release from the glass and also at longer term. This is an important consideration as it is hoped that the phosphate-based glasses will form a precursor phase, which transforms into hydroxyapatite, the natural inorganic phase of bone, similar to the mechanism seen with Bioglass®. This way the implant can form a bond to bone.

4.1.2 Solubility of Phosphate Glasses

Over 100 papers have been published on the rate of hydrolysis of phosphates salts but only a handful considered the degradation process of phosphate based glasses.

One of the first phosphate based materials, where studies have been made on their solubility characteristics, is Graham's salt. A paper published by *Strauss et al.* (68) showed that a freshly prepared solution of Graham's salt decreases its pH and viscosity for several hours before it attains stability. This effect was ascribed to the degradation of weak P-O bonds at branch points in the polymeric chain. Van Wazer (27), who discussed the results of water attack on sodium phosphate glasses, published similar findings. The structure of Na_2O-P_2O_5 glasses consists of a three dimensional

network, which will be destroyed when placed in water. Findings were verified by *Westerman and Crowther* (69) in 1954 and by *Stevels and Trap* (70) in the same year.

One year later Schulz and Hinz (71) examined the solubility of phosphate glasses and their structure. The question was raised whether the water insoluble fractions of phosphate glasses have the same chemical structure as the solid itself. An investigation via chromatography was carried out by preparing several water soluble binary phosphate glasses based on the system P_2O_5 / MO (where MO= ZnO, CdO, PbO, MgO and CaO). In the case of an existing PO_4-tetrahedra, the P-O-P linkage were broken down in the solubility process whereas any other P-O-P linkage in the structure, such as di-, tri-or tetraphosphates or other long PO_3- chains were not broken down. These results gave evidence for the existence of meta phosphates and long PO_3-chains, rather than PO_4-tetrahedra, which are linked together, over a 3 dimensional network.

Kanazawa et al. (72) examined the solubility and physical properties of some alkaline earth binary and ternary phosphate glasses. The composition range studied was with RO:P_2O_5 ratio varied from 0.7 to 1.7 in molar ratio. The corrosion behaviour in different acidic and basic solutions was examined. The solubility increased as the RO/P_2O_5 ratio increased in acidic solution whereas the reverse occurred in basic solutions.

Bunker and co-workers (73) did the first more systematic study on a series of ternary CaO-Na_2O-P_2O_5 glasses where the solubility was reported in a systematic and mathematical way, plotted in weight loss per unit area per unit time ($g.cm^{-2}.min^{-1}$).

Glasses were prepared via a classic glass synthesis route. The glasses obtained were polished and pulverised with a mortar and pestle to give particle size ranges of 45-75 μm and 75-100μm. Surface areas were determined by BET N_2 or Kr adsorption isotherms. Weight loss experiments were carried out in deionised water. Solubility rates were obtained for the following glasses:

Composition (mol%)	Leach rate ($g.cm^{-2}.min^{-1}$)
$40Na_2O$-$10CaO$-$50P_2O_5$	5×10^{-5}
$30Na_2O$-$20CaO$-$50P_2O_5$	3×10^{-6}
$40Li_2O$-$10CaO$-$50P_2O_5$	6×10^{-6}
$30Li_2O$-$10CaO$-$50P_2O_5$	3×10^{-7}

The rate of dissolution was found to be sensitive to glass composition; the higher the alkali content, the higher the solubility. They observed the same mathematical function to describe the leaching process as other authors previously mentioned. Again there was evidence of it being a 2-stage dissolution process, where for the first stage, weight loss is a function of $t^{1/2}$ and the second stage can be described as linear weight loss with time.

Shih et al. (74) studied the corrosion behaviour of ternary phosphate glasses with the following compositions: $P_2O_5 \geq 40$, $CuO \leq 50$ and $Na_2O \leq 60$ mol%. The chemical durability was measured via weight loss experiments in deionised water for 4-24h at 30^0C. Each sample was measured in duplicate and the solubility was measured in ($g.cm^{-2}.min^{-1}$). Glasses with 60 mol% P_2O_5 have solubilities in the range of $1x10^{-4}$ – $8x10^{-7}$, glasses with 50 mol% P_2O_5 range from $2x10^{-3}$ to $9x10^{-6}$ and glasses with 40 mol% P_2O_5 are reported to have solubilities ranging from $5x10^{-3}$ to $2x10^{-7}$ ($g.cm^{-2}.min^{-1}$), depending on composition. Glasses were more stable when the CuO content increased. Unfortunately the author did not assign any mathematical function to the dissolution process.

An interesting study of the ternary system, which was also examined in this thesis, was published by *Uo et al* (55). Solubility of the ternary system Na_2O-CaO-P_2O_5 was measured in distilled water and SBF and showed similar trends for both mediums. P_2O_5 content ranged from 30-80mol%; CaO and Na_2O varied respectively. In addition, Almar Blue Assay estimated preliminary cytotoxicity *in vitro* using on human pulp cells. 1.00g of granules pieces was placed in 100ml of fluid at 37^0C and after certain time intervals weight loss measurements were carried out. Solubilities were obtained in $g.cm^{-2}.min^{-1}$. Depending on the P_2O_5 content, solubility rates ranged from $1.7x10^{-7}$ for the very high containing P_2O_5 glasses to $2.8x10^{-8}$ for low P_2O_5 containing glasses. Results are similar for tests in SBF, however dissolution in SBF (Simulated Body Fluid) was suppressed. Only glasses with P_2O_5 content of 50 mol% showed cytotoxicity. The findings were in accordance with that of *Bunker* (75), however the measurement temperatures were different. According to *Uo,* the addition of CaO has a

major effect on the solubility. Only 5 or 10 mol% will lower the solubility by a factor of 10. The reason for this is the cross-linking ability of Ca^{2+} ions. This fact has been discussed structurally by *Van Wazer* and other authors (see glass structure chapter).

Dissolution processes for sodium-calcium phosphate glasses were examined by *Delahaye et al* (76). This more recent study carried out the corrosion process in two different aqueous solutions on metaphosphate glasses in the compositional range of $(50\text{-}x)Na_2O\text{-}xCaO\text{-}50P_2O_5$.

Dissolution rates in ($mg.cm^{-2}.min^{-1}$) in distilled water ranged from 10^{-2} to 10^{-4} where the lowest rates were found for the highest CaO containing glasses. The $34Na_2O\text{-}16CaO\text{-}50P_2O_5$ glass was found to have a linear relationship in neutral solution. At pH 3 however a non-linearity was observed, especially for measurement times greater than 100 min. They could not explain the suppressed dissolution rate towards the end of measurement time in acid solution with the theory of an ion-exchange process. This would have resulted in a $t^{1/2}$ behaviour, which was not observed. They assumed that the increased ion strength of the solution was an influence on the dissolution rate. Therefore a further experiment was carried out, where the medium was replaced by fresh medium after certain time intervals. Under these conditions, the ionic strength of the solution was nearly kept constant. Dissolution rates were increased. Therefore, it was assumed that the solution influences the leaching process.

At this point having considered the dissolution process, the fate of the ions in the aqueous media will now be considered.

Materials, which are close to the inorganic phase of bone with a Ca/P ratio of 2 and 1.5 like tetracalcium phosphate, hydroxyapatite and β-whitlockite have different degradation properties, as shown by *Klein et al.* (77). The solubility and the chemical changes of hydroxyapatite and β-whitlockite when they were placed in different buffers at 37^0C was examined. They also had considered the formation or re-precipitation of HA from Ca^{2+} - and PO_4^{3-} ions in the solution. Ionic concentrations were measured by atomic absorption spectroscopy. The buffers used were lactate, citrate, Michaelis and Gomoris buffer which were freshly prepared with pH of 6.2 and of 7.2. The dissolving of phosphate and calcium ion concentration was highest in the citrate buffer. Overall they found that the dissolution process was higher for pH medium of 6.2 compared to 7.2. Only three thermodynamically stable calcium phosphates are known, all of them are most stable at different pH's. They discussed the possibility of hydroxyapatite formation from these:

1. Monocalcium phosphate is stable at pH < 2.5,

2. brushite at 1.5 < pH < 4.2 and

3. hydroxyapatite at pH > 4.2.

They concluded that at a sufficiently high concentration of calcium and phosphate ions, precipitation of hydroxyapatite should occur for all the buffers used.

Kokubo et al. (78) examined the chemical reaction of bioactive glass and glass-ceramics in simulated body fluids. Glasses and glass-ceramics in the $MgO\text{-}CaO\text{-}SiO_2$ system were prepared with different chemical compositions, pulverised to grain sizes

below 500μm and 4.0g of these powders were immersed in 50ml SBF. Temperatures were kept at 36.5^{0}C and after certain times aliquots of the fluids were taken and analysed with inductively coupled plasma (ICP) to measure the ion concentration changes. Depending very much on the individual material, pH and ion concentration curves were almost exponential for most of the glasses and glass-ceramics. However, only one material, the apatite-wollastonite glass-ceramic showed linearity.

Knowles et al. (79) measured the out-leaching ions of soluble phosphate glasses when the glasses were placed in simulated body fluid SBF. The interaction of the ions from the dissolving glass and the ions in the fluid were responsible for forming a crystalline layer on the glass. This layer was detected and analysed by FT-Raman spectroscopy and thin film x-ray diffraction. Quaternary glasses P_2O_5-Na_2O-CaO-Al_2O_3 were prepared via traditional glass preparation methods. Discs of glasses were placed in SBF, which was prepared from a method of *Kukubo et al.* (80). After certain time intervals samples were taken out of solution and analysed. FT Raman spectroscopy and this showed changes occurring at very early time points, with evidence for a carbonate containing compound forming on the glass surface, which may act as a precursor on which bone can attach. However, due to the soluble nature of these materials this layer appeared to be short lived.

A very recent paper by *Kumar* (81) described the transformation of brushite and modified brushite in Hank's Buffered Saline solution (HBSS). Brushite, a calcium phosphate, is relatively soluble in physiological type solutions. When used as an implant, the calcium and phosphate ion concentrations can increase at the

implant/tissue interface. This study was carried out to prove the transformation of brushite to hydroxyapatite using SEM, XRD and FTIR spectroscopy. The overall transformation rate was assumed to be altered if calcium was partially substituted for potassium (modified brushite).

Transformation studies were carried out by placing samples of brushite and modified brushite in 50 ml of HBSS and stored at RT without agitation for 24h. XRD and FTIR spectroscopy results confirm for both types of brushite, transformation into hydroxyapatite occurred with a signature peak in the FTIR spectrum at 960 cm^{-2}. The main difference however is that for the modified brushite type, an FTIR band occurred at 1112 cm^{-1} which was assigned to a poorly crystalline HA. This peak was not observed for the non-modified brushite. An important difference in transformation rate was observed for modified brushite, which transformed to HA much faster than non-modified brushite. The findings were the result of x-ray diffraction studies, where reflections for normal brushite remained after 48h whereas for modified brushite no such reflections were present.

Chapter 5

5.1 Materials and Methods

The experimental part contains four sections:

1.) *Glass preparation for 5 glass systems*

2.) *Solubility testing for 5 glass systems*

3.) *Ion release measurements for 5 glass systems*

4.) *Detailed structural analysis for 2 systems*

5.1 General Remarks

In total five different glass-systems have been prepared. The first system was from the ternary phase diagram of Na_2O-CaO-P_2O_5 and was carried out as the other glasses investigated were modifications of this basic system. A wide compositional range of glasses with varying CaO, Na_2O and P_2O_5 content was undertaken for the Na_2O-CaO-P_2O_5 system. Preliminary cell culture tests were carried out to determine the best compositional range for optimal cell response. Once established, this *in vitro* data was used to select glasses for further modification. In addition, it was hoped that with the simplicity of the first ternary system, interpretable results would be achieved which can answer some of the questions regarding structural inaccuracies seen in the literature (discussed in the glass structure chapter). The second ternary system, a K_2O-CaO-P_2O_5 system, was produced to determine the effect of substituting Na_2O with

K_2O, in terms of structural changes, solubility effects, biocompatibility and bioactivity.

Two quaternary system Na_2O-K_2O-CaO-P_2O_5 and Na_2O-CaO-MgO-P_2O_5 were prepared. The first system is seen as an extension of the studies on the Na_2O-CaO-P_2O_5 and the K_2O-CaO-P_2O_5 systems and the second is to investigate the possibility of producing glasses with compositions more closely related to the composition of natural dentition. Attempts to work as close as possible to the composition of natural dentition failed because of glass manufacturing limitations. However, it was tried to work as closely as possible to natural hard tissue composition. Again, a whole spectrum of glass compositions was produced and *in vitro* studies were carried out to optimise the cellular response.

In order to limit variables, the valence of substituted cations has been kept constant. Oxides like Na_2O with sodium having one positive valence have been substituted by potassium having the same valence. The same logic was used for the other quaternary system where the cation calcium with a valence of two has been replaced by magnesium with the same valence.

The final glass system investigated, based on Na_2O-CaO-CaF_2-P_2O_5 was carried out to investigate whether fluoride may structurally affect this system. In this system, oxygen was partially replaced by fluoride. It should be noted that the use of fluoride is difficult because of the relative ease with which F^- will bond to H^+ to give HF. HF is a very volatile substance which may be easily lost at the elevated temperatures used during glass making. Incorporation of fluoride in a glass system was found to be difficult but was achieved by the use of a different precursor compound (see

preparation of this glass system) to limit fluoride loss. Preliminary solubility testing and structural analyses have been carried out.

5.1.1 Selection of Glass Composition

As it was mentioned in the aim chapter, glasses were prepared in order to synthesise implant materials, which are closely related to natural hard tissue phases. As it was discussed before, the inorganic part of hard tissue like bone and teeth consist of mainly hydroxyapatite. Calcium and phosphate are present at high levels in hydroxyapatite, hence it was tried to incorporate as much calcium as possible. A quantitative analysis of enamel revealed additional magnesium,- carbonate,- fluoride,- sodium and potassium ions as minor representatives (82).

Not all compositions could make the same range of glasses and so glasses within a system have been selected according to this.

5.2 Preliminary Glass Making Studies for the ternary System

5.2.1 Establishment of glass production methodology.

Preliminary studies were carried out in order to determine the optimal chemical precursors for adequate glass production.

The major problem encountered was with the use of raw P_2O_5. This chemical is extremely hygroscopic and very volatile at elevated temperatures. This lead to two problems (1) water absorption can affect the batch weights and (2) loss of P_2O_5 during melting. Both of these will ultimately alter the final glass composition.

Chemicals of NaH_2PO_4 and $CaHPO_4$ were initially tested as precursors in an attempt to limit the use of P_2O_5. With these precursors, it was possible to make glasses with up to 16 mol% CaO. Over this limit, crystallisation of the glass readily occurred. This was likely to be due to the presence of water in the glass, which is known to readily nucleate crystallisation in glasses.

It was found that using $CaCO_3$ to deliver CaO, in combination with fresh and dry P_2O_5 and NaH_2PO_4 gave optimal results. With this choice of chemicals a whole range of varying Na_2O-CaO-P_2O_5 glasses could be readily achieved. To avoid excess loss of P_2O_5, a layering technique for the chemicals before the melting process was established. The appropriate amount of NaH_2PO_4 and $CaCO_3$ were weighed out, mixed together and put aside. P_2O_5 was weighed out and placed into the bottom of the platinum crucible. The NaH_2PO_4 and $CaCO_3$ mixture was then placed on top of P_2O_5. That way two things were achieved. During the mixing time of $CaCO_3$ and NaH_2PO_4, P_2O_5 was kept sealed in the bottle without having extended contact with moisture.

After use, the bottle was additionally sealed with Parafilm (Solmedia Ltd, England) to avoid contact with moisture. During the melting process H_2O and CO_2 was evolved, helping the molten mass to flux. However if P_2O_5 was within the mixture, it would contact the evolved H_2O more easily and bind the water into the glass structure with the associated problems described above. When the P_2O_5 is placed at the bottom of the crucible, the surface area was minimised to avoid contact with the gas evolution process. All the glasses, which have been used for further testing, have been produced in this way.

5.3 Chemical Equations and Compositional Calculations

The following pages detail the chemical reactions and how the glass compositions were calculated:

Using NaH_2PO_4

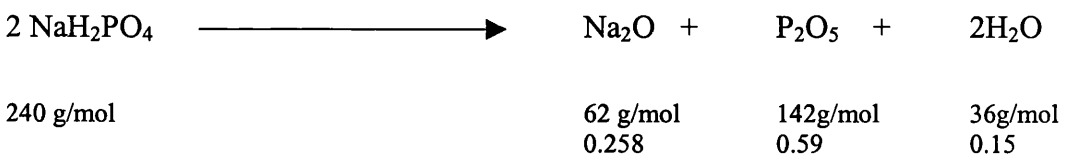

Using $CaCO_3$

Example:

if 20 mol % CaO is needed:

(0.20 mol x 56 g/mol) / 0.56 = 20 g $CaCO_3$

Using KH_2PO_4

$2\ KH_2PO_4 \longrightarrow K_2O + P_2O_5 + 2H_2O$

272.24 g/mol

94.2 g/mol 142 g/mol 36g/mol
0.346 0.521 0.13

Using $MgCO_3$

$MgCO_3 \longrightarrow MgO + CO_2$

84.31 g/mol

40 g/mol 44 g/mol
0.474 0.52

Using $(NaPO_3)_x$

$2\ (NaPO_3)_x \longrightarrow Na_2O + P_2O_5$

236.35 g/mol

62 g/mol 142 g/mol
0.30 0.69

The final glass composition was calculated according to the above mentioned equations, following rules for stoichiometric calculations, for example, if 39 mol% Na_2O is required in the final glass, the amount of NaH_2PO_4 required would be calculated as followed:

Example:

(0.39 mol x 62 g/mol) / 0.2 = 120.9 g of NaH_2PO_4

This also means that by using 120.9 g NaH_2PO_4, 55.614g P_2O_5 will be processed at the same time. This total P_2O_5 content has to be offset by this amount when considering the total amount of P_2O_5 required.

P_2O_5 and CaF_2 amounts were calculated from the mol percentages needed.

5.4 Glass Preparation

5.4.1 Standard Glass Preparation

General procedure

All chemicals, apart from phosphorus pentoxide and sodium polyphosphate (Aldrich), were of analytical purity, manufactured by BDH, England.

The precursors were weighed out on analytical balance (Precisa, England) and placed as described above in a Pt/10%Rh crucible (Type 71040, Johnson Matthey, Herts, UK). Immediately after the chemicals had been layered in the crucible, it was placed in a pre-heated furnace at between 1000-1200^{0}C dependent on the final glass composition (for appropriate temperatures see Table 3). In general a batch of glass comprised of around 60g of glass product, which means that around 120g of precursor chemicals were required. The starting materials were divided into three smaller batches. The separate amounts were melted consecutively and after each melting cycle the glass was set aside. After having produced the three batches they were combined and re-melted for 3 hours at the appropriate temperature. This re-melting process had two additional benefits, (1) it helped to entirely homogenise the melt, as inhomogeneities may occur with the layering method, and (2) it would help to reduce the possibility of phase separation.

When the final melt was ready for pouring, another furnace was used for the annealing process. This was important to ensure stress free glasses for any further testing. The furnace and graphite mould was kept at temperatures between 300-400°C depending on the glass (see table 3). Upon removal of the melted glass, the melt was poured very

rapidly into the graphite mould. This split mould was cut out of a graphite block, which had 2 separate holes (6cm long, 1,5 cm wide) hollowed out. The graphite mould was then placed in the second furnace and kept at temperature for one hour. The furnace was then switched off and allowed to cool down over night.

5.4.2 Glass Cutting and Storage

Having obtained glass rods, these were cut into 15mm diameter and 2mm thickness discs, using a Testbourne diamond saw. The optimal cutting liquid was found to be a 50:50 mixture of H_2O and methanol (BDH, Poole, UK). The final discs were thoroughly dried with cotton tissue. Using heat guns to dry the specimens rapidly were found to create extra stress in the glass surface.

Any glass rods remaining were stored in sterile test tubes (Sterilin, England). The method of storage was found to be sufficient to overcome the problem with phosphate based glasses, which are known to absorb moisture from the atmosphere. Assurance that this method was adequate was obtained by carrying out a simple weight change experiment. A glass rod was weighed over the course of a year to check any weight change, which would be the case with moisture absorbency. Note, a high solubility glass was used, i.e. with high Na_2O and low CaO content.

Initial weight for glass $Ca_{20}Na_{23}P_{45}$ On date 3/02/1998	Final weight for glass $Ca_{20}Na_{23}P_{45}$ On date 17/02/1999
20,1831 g	20,1836 g

Table 1: Weight gain check

The weight gain was 0.0005g (0.024%), or 2.77 x 10^{-5} mol H_2O have been absorbed. It should be noted that this level of absorbed water is negligible compared to the levels of water absorption after placing in water. Furthermore, the solubility testing was carried out very soon after glass production. Also for any glasses to be used for spectroscopic analyses, the measurements were carried out as soon as possible after glass preparation.

Solubility tests

All measurements for this test were performed in triplicate to ensure accuracy.

Surface area of the glass discs was calculated from measurements of the disc thickness and diameter measured with vernier calipers (Mitutoyo, Tokyo, Japan). The samples were weighed and then the discs were placed in 75ml volume plastic containers, which were sealed with plastic lids. The liquid in which the test was carried out was double distilled water. For the ternary system, an additional test in Hank's Buffered Saline Solution (HBSS) (Gibco BRL, Scotland) was also carried out. The test protocol used was based around protocols drawn up for toxicity testing of biomaterials from the British Standards Institute (BSI). The standards did not precisely specify any volume to surface area relationship. Therefore, after preliminary volume to surface area relationship tests, 25ml volume to 1.5 cm^2 of specimen surface area were used. The containers were kept for the entire test period in an incubator maintained at 37±1^{0}C. At various time points, the samples were removed and dried with cotton tissue until no excess surface moisture was visible. Specimens were weighed on an analytical balance (Precisa 120A, European Instruments) and then placed back in the solution. The

weight loss M_t at a certain time t point was subtracted from the initial weight M_o and divided by the surface area A to give weight loss per unit area:

$$\text{Weight loss: } (M_o - M_t)/A$$

$$\text{Where A = surface area } (cm^2)$$

The data was then plotted as weight loss per unit area against time. From the resultant graph, a slope was determined with the slope giving solubilities in $g.cm^{-2}.hr^{-1}$. All measurements were carried out to a maximum of 8 weeks.

5.4.3 pH Measurements

Over the solubility test period, pH measurements have been carried out on a Jenway 3045 Ion Analyser with an Orion pH electrode. The electrode was calibrated with standard solutions (BDH, pH colourkey buffered solution, pH 4,7 and 10) before the measurements. The electrode was placed in the solution in which the specimen had been immersed and then the reading was allowed to stabilise for three minutes prior to noting the value. Again, triplicate measurements were performed.

5.4.4 Ion Measurements

During solubility tests the out leaching ion process was followed for the following ions: Ca^{2+}, Na^+, K^+ and F^-.

Ion measurements have been carried out on a Jenway 2240 Ion Meter at certain time points. ELIT mono solid state ion selective electrodes with appropriate reference electrodes were used obtained from BDH, England.

The following ion selective electrode/reference electrode systems have been used Ca^{2+}/AgCl, Na^{+}/LiAc, K^{+}/NaCl and F^{-}/AgCl.

Standard solutions for calibration of each electrode were prepared in 1000, 100, 10 and 1 ppm concentrations. Sodium and fluoride volumetric standards were obtained from Aldrich, calcium volumetric standard from Russell (Russell pH Limited, Scotland) and the potassium volumetric standard solution was obtained from Fluka, UK. Examples of the calibration curves are as follows:

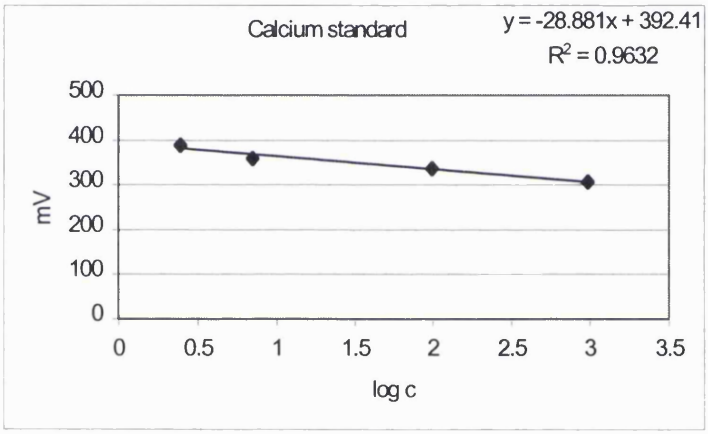

Figure 12: Calibration curve for calcium standard

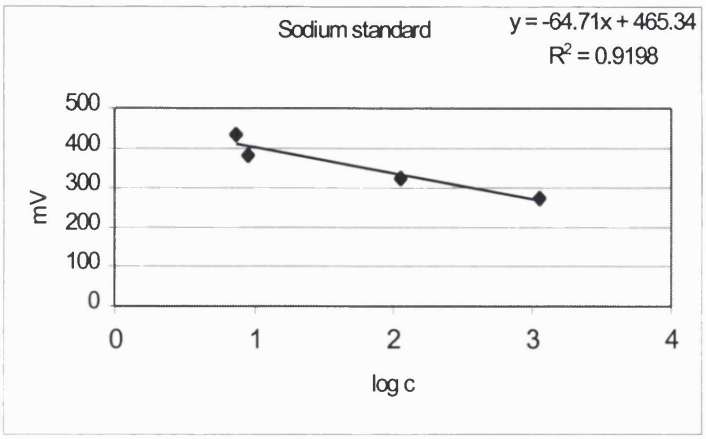

Figure 13: Calibration curve for sodium standard

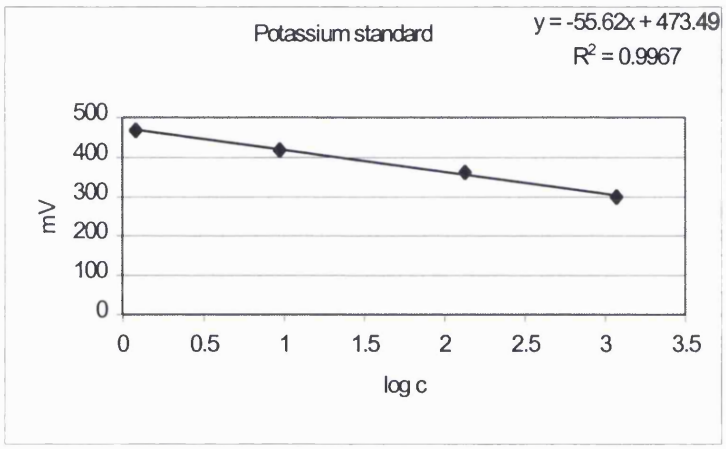

Figure 14: Calibration curve for potassium standard

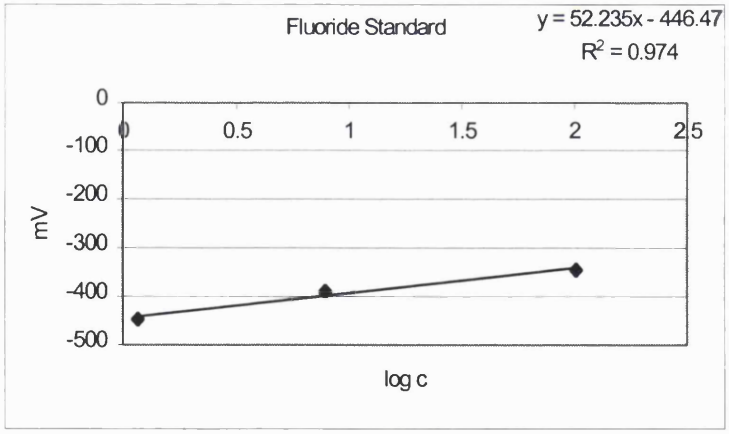

Figure 15: Calibration curve for fluoride standard

Calibration curves have been plotted of log concentration (ppm) against the mV reading (according to manufacturer).

For this type of measurement it was found best to calibrate the appropriate ion selective electrode every day to ensure regular performance, even when no measurement took place that day. For measuring times greater than 3 weeks, calibration took place once a week. If this was not performed, difficulties occurred to obtain comprehensive values especially for the extended measuring times.

However, it should be noted here that the accuracy of ion measurement was difficult to maintain if the measurement time exceeded 8 weeks. This was thought to be due to overlong storage of the calibration solution.

Chapter 6

Ternary system $CaO-Na_2O-P_2O_5$

6.1 Special Procedures for the Ternary System $CaO-Na_2O-P_2O_5$

NaH_2PO_4, P_2O_5 and $CaCO_3$ have been used to form this glass system. P_2O_5 has been kept constant, with CaO and Na_2O content varying. All of these glasses have been synthesised to form the sodium based ternary system. Compositions have been calculated based on equations mentioned previously.

Note that the used glass code represent the mol% of each oxide.

Glass code	CaO content (mol%)	Na_2O content (mol%)	P_2O_5 content (mol%)
$Ca_8Na_{47}P_{45}$	8	47	45
$Ca_{10}Na_{45}P_{45}$	10	45	45
$Ca_{12}Na_{43}P_{45}$	12	43	45
$Ca_{16}Na_{39}P_{45}$	16	39	45
$Ca_{20}Na_{35}P_{45}$	20	35	45
$Ca_{24}Na_{31}P_{45}$	24	31	45
$Ca_{28}Na_{27}P_{45}$	28	27	45
$Ca_{32}Na_{23}P_{45}$	32	23	45
$Ca_{36}Na_{19}P_{45}$	36	19	45
$Ca_{40}Na_{15}P_{45}$	40	15	45

Table 2: Glass codes and oxide composition in mol%

Glasses with CaO content greater than 40 mol% have been prepared but were found to crystallise on casting, hence they have been rejected for any further testing. Thus, 40 mol% CaO can be regarded as the upper limit for CaO content.

Glass code	Melting temperatures and time (^{0}C/hours)	Casting temperature (^{0}C) and time (hours)	result
$Ca_8Na_{47}P_{45}$	1050/3	300/1	Glass, stress free
$Ca_{10}Na_{45}P_{45}$	1050/3	300/1	Glass, stress free
$Ca_{12}Na_{43}P_{45}$	1050/3	300/1	Glass, stress free
$Ca_{16}Na_{39}P_{45}$	1050/3	300/1	Glass, stress free
$Ca_{20}Na_{35}P_{45}$	1050/3	300/1	Glass, stress free
$Ca_{24}Na_{31}P_{45}$	1050/3	380/1	Glass, stress free
$Ca_{28}Na_{27}P_{45}$	1150/3	380/1	Glass, stress free
$Ca_{32}Na_{23}P_{45}$	1150/3	380/1	Glass, stress free
$Ca_{36}Na_{19}P_{45}$	1150/3	380/1	Glass, stress free
$Ca_{40}Na_{15}P_{45}$	1200/3	400/1	Glass, stress free

Table 3: Melting and casting temperatures

The processing temperatures were originally established by trial and error, until the glass was formed. Afterwards the glass has been analysed by DTA to obtain thermal characteristics for the glasses. Once established, precise temperatures (see table) were used in order to avoid crystallisation and also to avoid residual stress on casting. The methodology was used for all glass systems.

6.1.1 Solubility Tests in Distilled Water. Preliminary Experiments

In these preliminary experiments, glasses $Ca_8Na_{47}P_{45}$ and $Ca_{10}Na_{45}P_{45}$ were completely dissolved within 2-3 hours which was not the case for the remaining members of this system. It was not possible to measure the solubility for these two glasses. However, in some additional experiments, detailed later, it was possible to measure the solubility accurately by decreasing the interval between measurement times.

As a first approximation weight loss results were plotted in $g.cm^{-2}$ against time and using the curve fit in Excel, a line was fitted, forcing through zero and with a minimal R^2 value. The slope of the lines gave the solubility in $g.cm^{-2}.h^{-1}$. It was found to be very unrealistic to line fit members of this system with CaO content higher than 28 mol%. The slope was more of an exponential nature; this needed further mathematical analysis. However, in this preliminary study a line was fitted, even for the glasses with high CaO content (see dotted line fittings). This was carried out in order to rank glasses within the same glass system. It should be emphasised that this is not correct and subsequently a more precise study was carried out, where measurements were carried out approximately every 10 minutes. In this way more precise weight loss

results were achieved even for glasses with lower CaO content than 12 mol%. Log 10 weight losses were plotted against log 10 time [min] and the straight lines were observed.

6.1.2 Preliminary Studies on the Solubility of the Na_2O-CaO-P_2O_5 System.

All measurements were carried out in distilled water

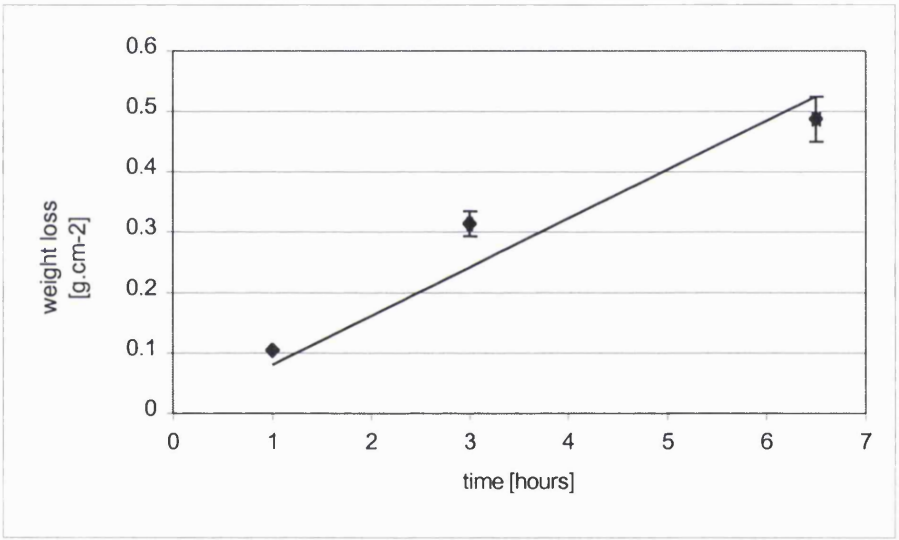

Figure 16: Weight loss curve for $Ca_{12}Na_{43}P_{45}$

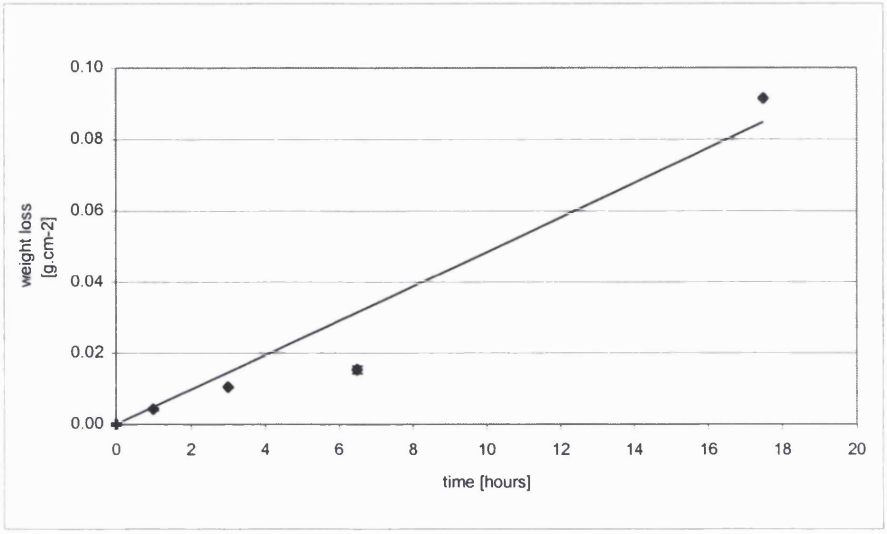

Figure 17: Weight loss curve for $Ca_{16}Na_{39}P_{45}$

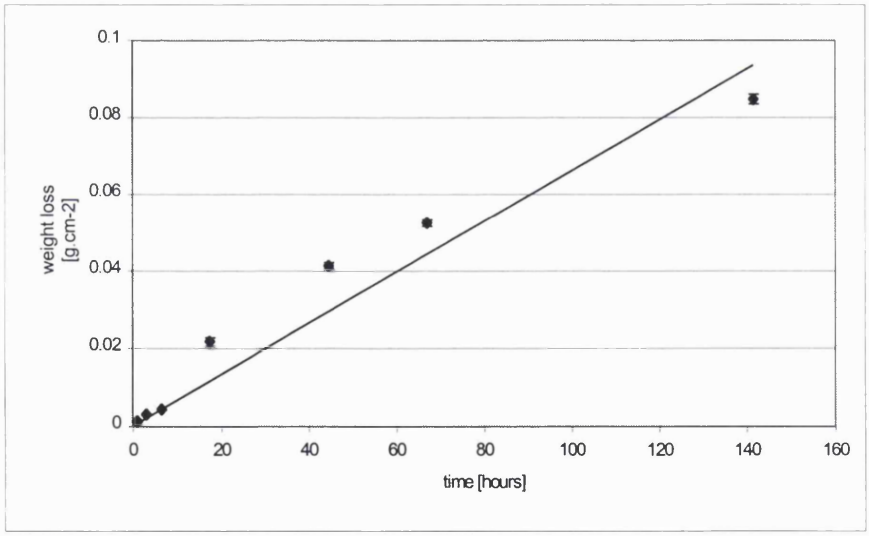

Figure 18: Weight loss curve for $Ca_{20}Na_{35}P_{45}$

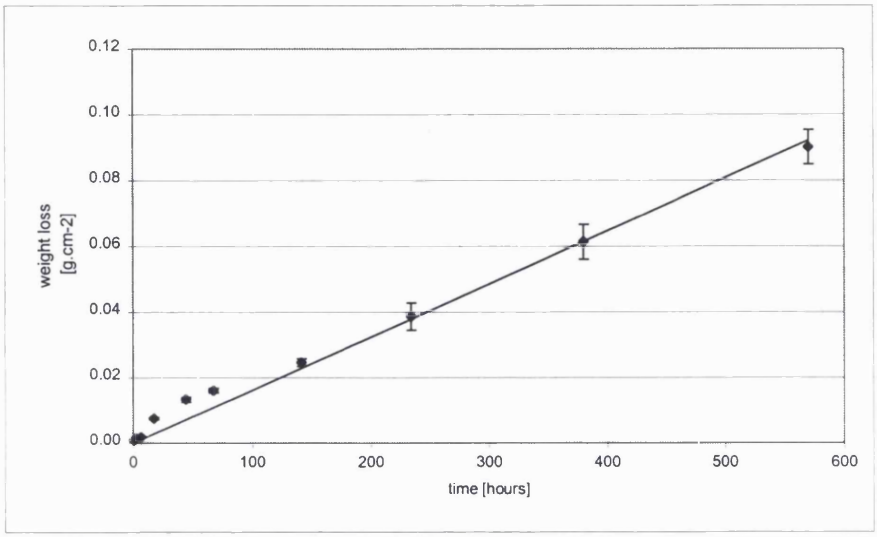

Figure 19: Weight loss curve for $Ca_{24}Na_{31}P_{45}$

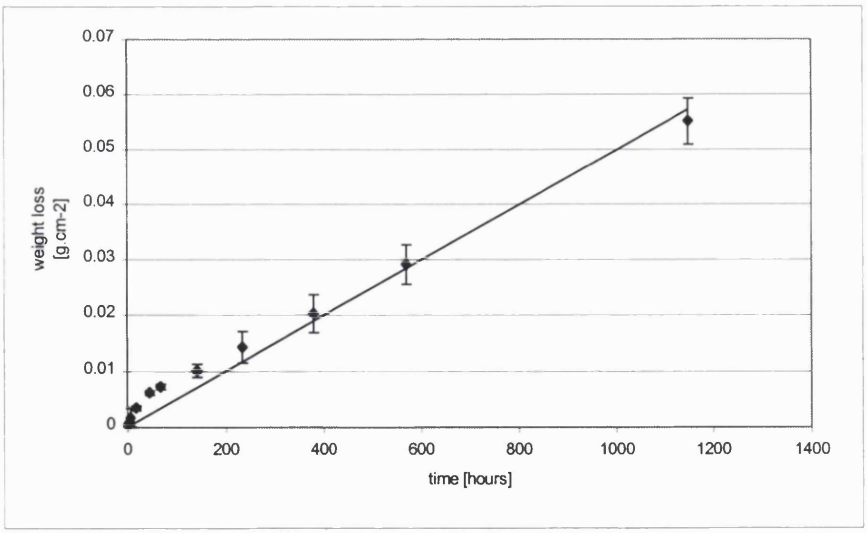

Figure 20: Weight loss curve for $Ca_{28}Na_{27}P_{45}$

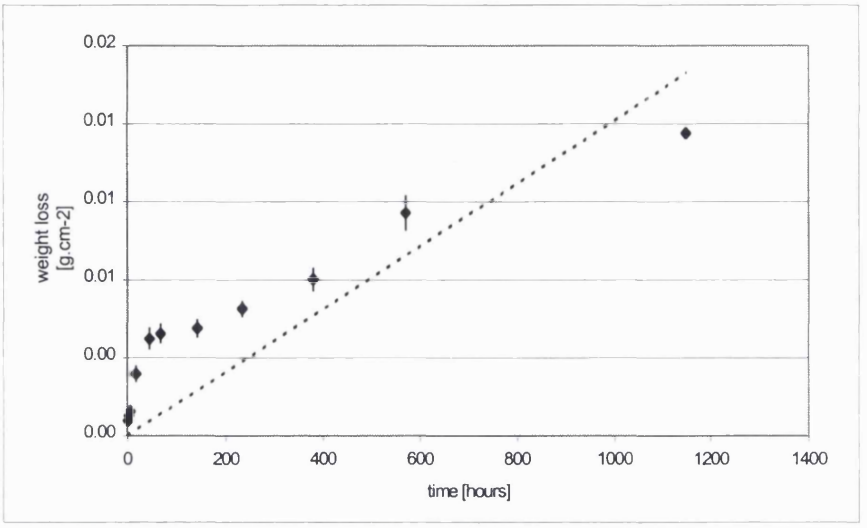

Figure 21: Weight loss curve for $Ca_{32}Na_{23}P_{45}$

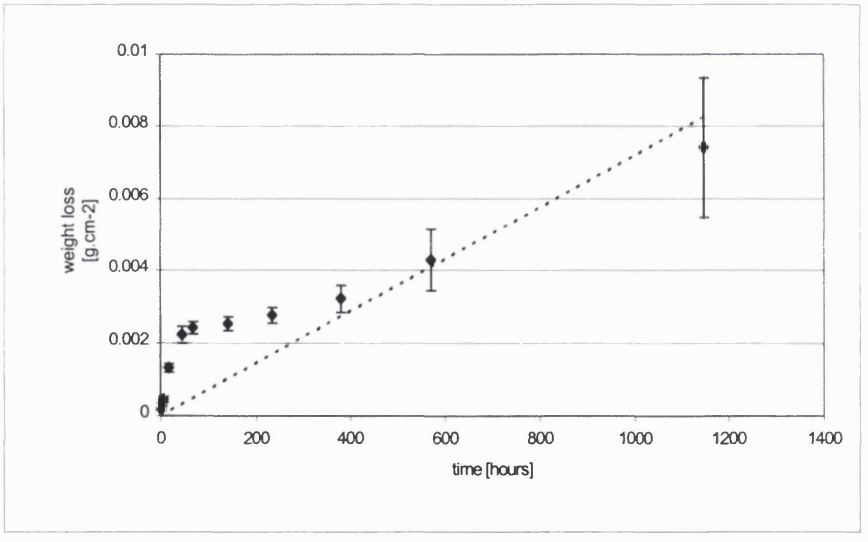

Figure 22: Weight loss curve for $Ca_{36}Na_{19}P_{45}$

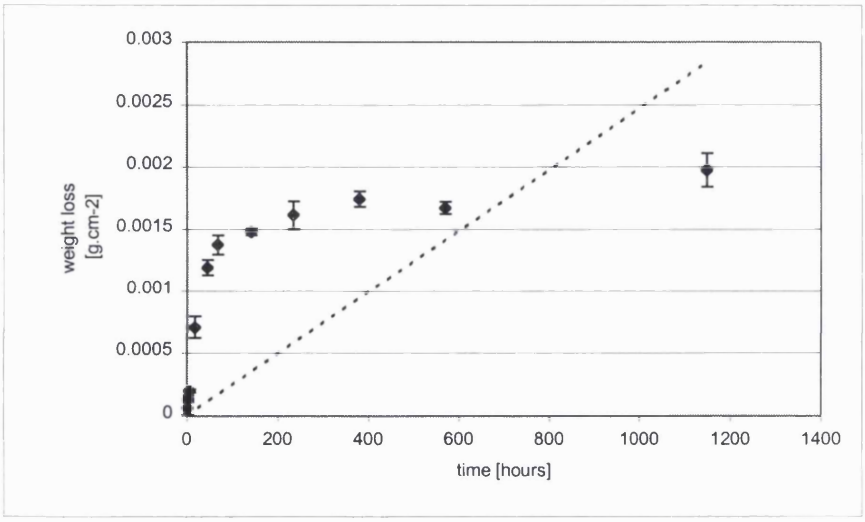

Figure 23: Weight loss curve for $Ca_{40}Na_{15}P_{45}$

Glass code	Solubility [$g.cm^{-2}.h^{-1}$]
$Ca_8Na_{47}P_{45}$	Too fast to measure
$Ca_{10}Na_{45}P_{45}$	Too fast to measure
$Ca_{12}Na_{43}P_{45}$	2.36×10^{-2}
$Ca_{16}Na_{39}P_{45}$	5.40×10^{-3}
$Ca_{20}Na_{35}P_{45}$	6.00×10^{-4}
$Ca_{24}Na_{31}P_{45}$	2.00×10^{-4}
$Ca_{28}Na_{27}P_{45}$	5.00×10^{-5}
$Ca_{32}Na_{23}P_{45}$	1.00×10^{-6}
$Ca_{36}Na_{19}P_{45}$	6.00×10^{-6}
$Ca_{40}Na_{15}P_{45}$	3.00×10^{-6}

Table 4: Overview of measured solubilities for the ternary Na_2O-CaO-P_2O_5 system.

The first major feature of these graphs that can be seen is that as the CaO content is increased, the solubility decreases. The second feature seen in the graphs, is that the curves become non-linear with increasing CaO content.

6.1.3 pH Measurements

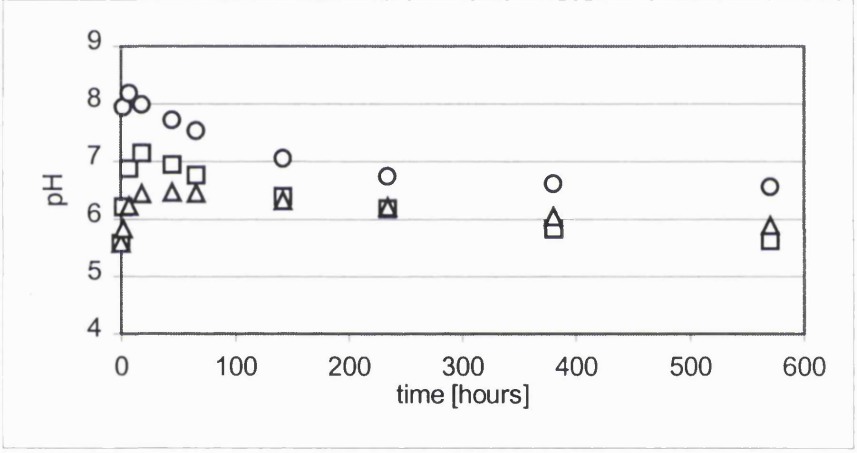

Figure 24: pH progress with time for the ternary $CaO\text{-}Na_2O\text{-}P_2O_5$ system
O $Ca_{12}Na_{43}P_{45}$ ▫ $Ca_{24}Na_{31}P_{45}$ Δ $Ca_{36}Na_{19}P_{45}$

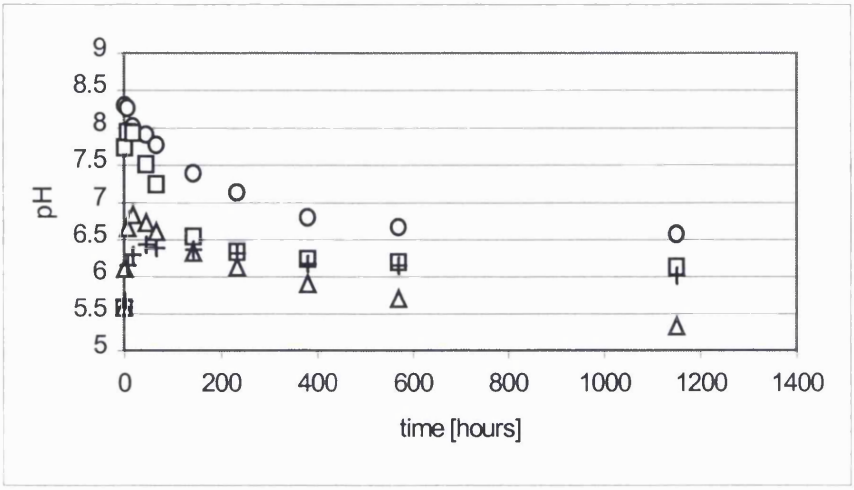

Figure 25: pH progress with time for the ternary $CaO\text{-}Na_2O\text{-}P_2O_5$ system
O $Ca_8Na_{47}P_{45}$ ▫ $Ca_{16}Na_{39}P_{45}$ Δ $Ca_{28}Na_{27}P_{45}$ + $Ca_{40}Na_{15}P_{45}$

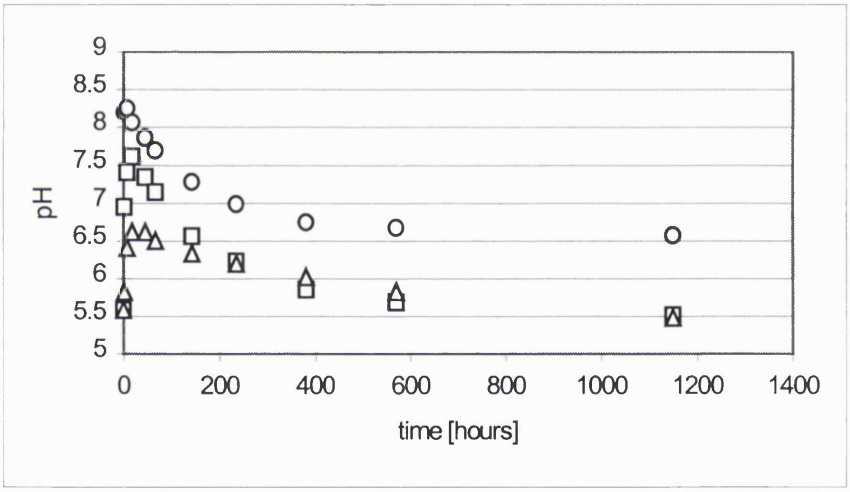

Figure 26: pH progress with time for the ternary $CaO\text{-}Na_2O\text{-}P_2O_5$ system
O $Ca_{10}Na_{45}P_{45}$ ▫ $Ca_{20}Na_{35}P_{45}$ Δ $Ca_{32}Na_{23}P_{45}$

It can be seen from figure 24 to figure 26 that the pH of the solution can have different patterns of change with time, depending on the CaO content of the glass. Glasses with lower CaO content show the highest initial increase in pH from 5.5 (distilled water) to

8.5, whereas glasses with higher CaO content show only an increase of one pH unit, from 5.5 to 6.5.

6.2 Ion Measurements

6.2.1 Calcium Measurements

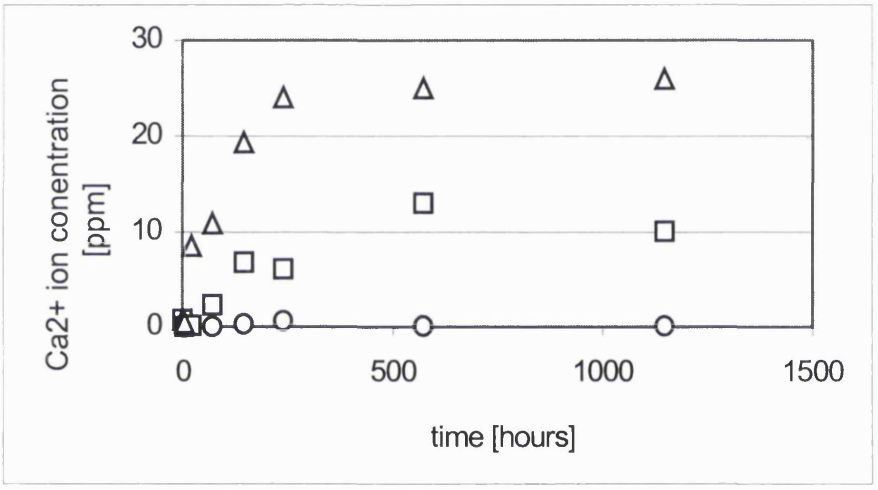

Figure 27: Ca^{2+} ion measurement for ternary system $CaO\text{-}Na_2O\text{-}P_2O_5$
O $Ca_{12}Na_{43}P_{45}$ ▫ $Ca_{24}Na_{31}P_{45}$ Δ $Ca_{36}Na_{19}P_{45}$

It can bee seen from figure 27 that glasses with low CaO content show lowest Ca^{2+} ion concentration change with time, even though these glasses have the highest solubility compared to their counterparts with higher CaO levels. Glasses with higher CaO content show highest Ca^{2+} ion release against time. It can also be seen that the curve shape is similar to the weight loss curves (see solubility test No 1).

Figure 28 and figure 29 show the ion release for the other members of this glass system and these were found to be similar to glasses discussed for figure 27.

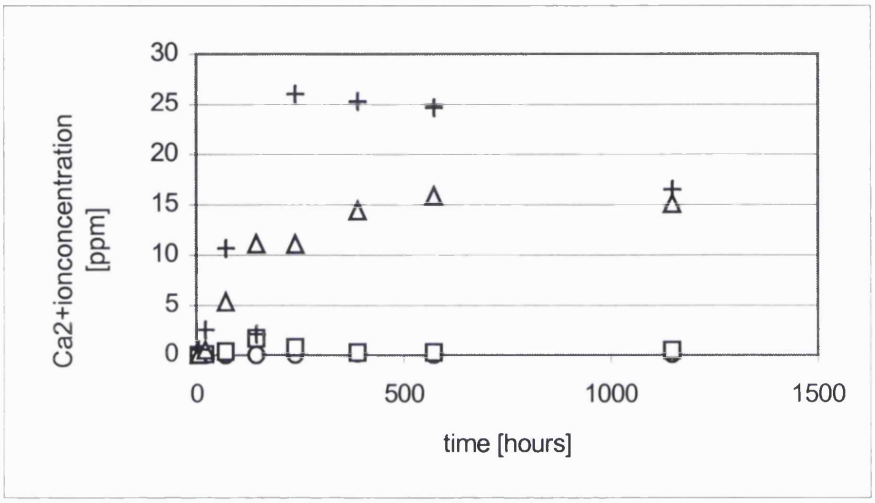

Figure 28: Ca^{2+} ion measurement for ternary system $CaO\text{-}Na_2O\text{-}P_2O_5$
O $Ca_8Na_{47}P_{45}$ ▫ $Ca_{16}Na_{39}P_{45}$ Δ $Ca_{28}Na_{27}P_{45}$ + $Ca_{40}Na_{15}P_{45}$

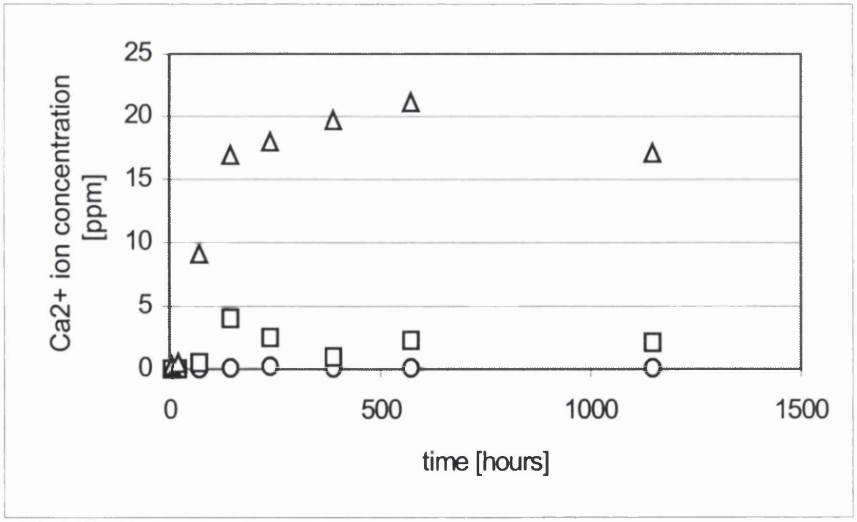

Figure 29: Ca^{2+} ion measurement for ternary system $CaO\text{-}Na_2O\text{-}P_2O_5$
O $Ca_{10}Na_{45}P_{45}$ ▫ $Ca_{20}Na_{35}P_{45}$ Δ $Ca_{32}Na_{23}P_{45}$

6.2.2 Sodium Measurements

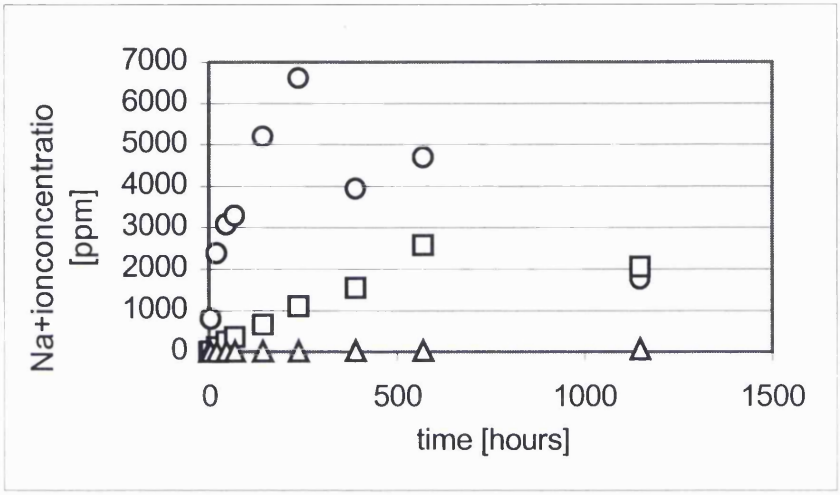

Figure 30: Na^+ ion measurement for ternary system $CaO\text{-}Na_2O\text{-}P_2O_5$
O $Ca_{12}Na_{43}P_{45}$ ▫ $Ca_{24}Na_{31}P_{45}$ Δ $Ca_{36}Na_{19}P_{45}$

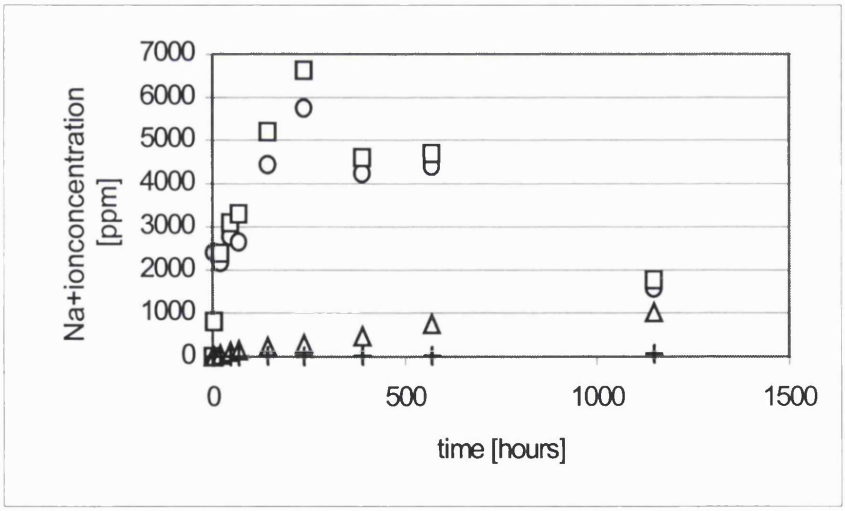

Figure 31: Na^+ ion measurement for ternary system $CaO\text{-}Na_2O\text{-}P_2O_5$
O $Ca_8Na_{47}P_{45}$ ▫ $Ca_{16}Na_{39}P_{45}$ Δ $Ca_{28}Na_{27}P_{45}$ + $Ca_{40}Na_{15}P_{45}$

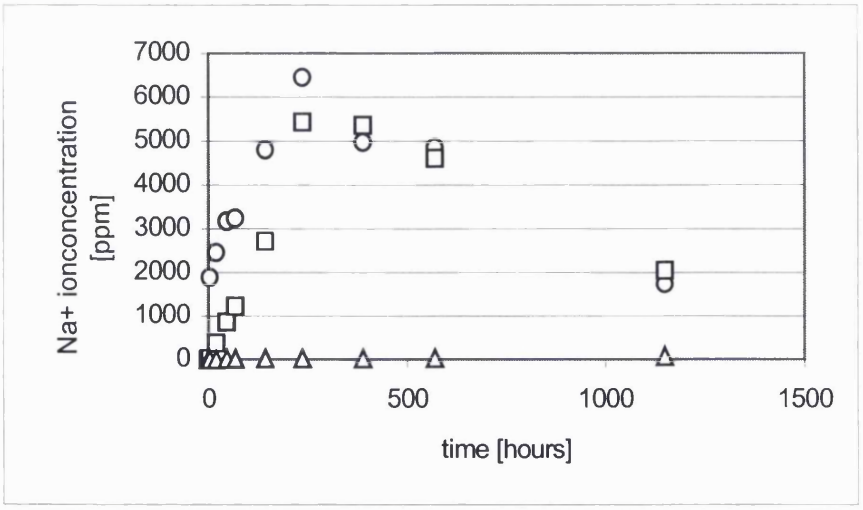

Figure 32: Na^+ ion measurement for ternary system $CaO\text{-}Na_2O\text{-}P_2O_5$
O $Ca_{10}Na_{45}P_{45}$ ▫ $Ca_{20}Na_{35}P_{45}$ Δ $Ca_{32}Na_{23}P_{45}$

The Na^+ ion measurements seem to show a similar trend to the Ca^{2+} ion measurement results, however, the values in ppm are much higher than for calcium measurements and the curves appear slightly more linear.

The decrease in ion concentration was assumed to be due to precipitation after measuring times greater than 400 hours. Therefore sodium ions are no longer detectable in solution. However, precipitate analysis should be carried out in order to verify this.

6.2.3 Solubility Test in HBSS

A second series of dissolution testing was performed in HBSS. Only 3 selected glasses are shown here because of the similarity to the solubility test carried out in distilled water.

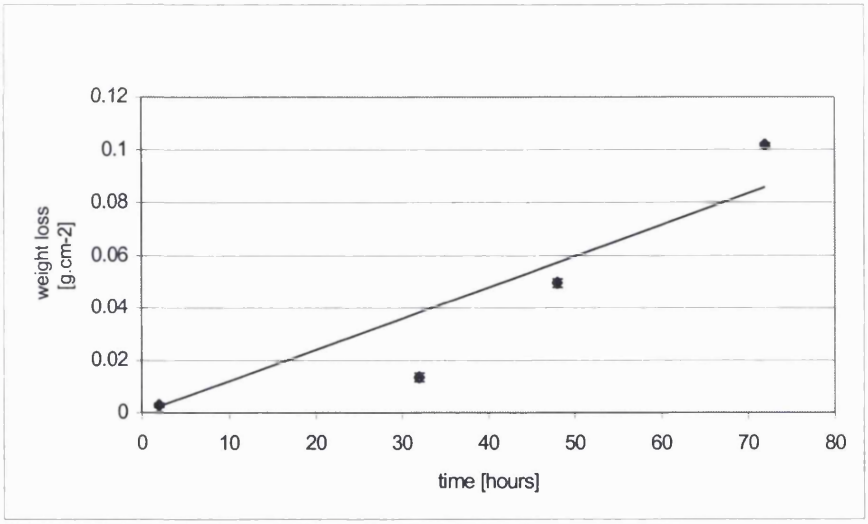

Figure 33: Weight loss plot for $Ca_{20}Na_{35}P_{45}$

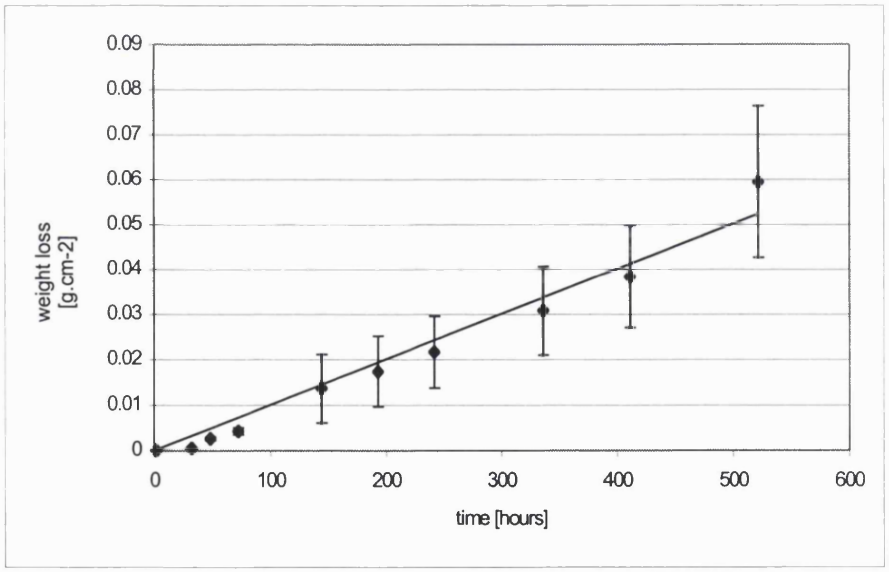

Figure 34: Weight loss plot for $Ca_{28}Na_{27}P_{45}$

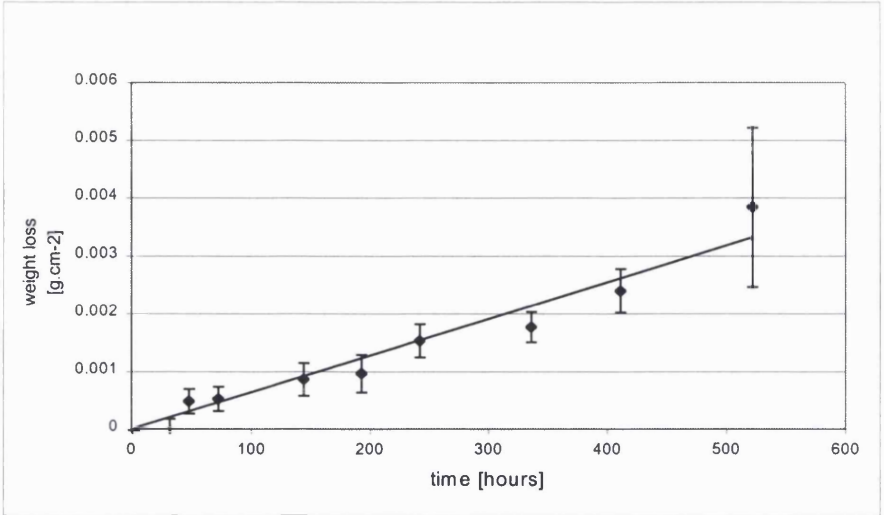

Figure 35: Weight loss plot for $Ca_{40}Na_{15}P_{45}$

Glass code	Solubility [$g.cm^{-2}.h^{-1}$]
$Ca_8Na_{47}P_{45}$	Too fast to measure
$Ca_{10}Na_{45}P_{45}$	Too fast to measure
$Ca_{12}Na_{43}P_{45}$	15.99
$Ca_{16}Na_{39}P_{45}$	1.20×10^{-3}
$Ca_{20}Na_{35}P_{45}$	3.00×10^{-4}
$Ca_{24}Na_{31}P_{45}$	1.00×10^{-4}
$Ca_{28}Na_{27}P_{45}$	4.00×10^{-5}
$Ca_{32}Na_{23}P_{45}$	1.00×10^{-6}
$Ca_{36}Na_{19}P_{45}$	8.00×10^{-6}
$Ca_{40}Na_{15}P_{45}$	6.00×10^{-6}

Table 5: Solubility overview for ternary system in HBSS

The solubility values determined from experiments using HBSS compared to distilled water seem to be similar. The main difference discerned from the experiments using HBSS is that the curves for the test in HBSS are found not to become more and more exponential when the CaO content of the glasses is increased. Solubilities in HBSS were found to be higher for lower CaO containing glasses compared to distilled water and slightly suppressed for the higher CaO containing glasses.

For the pH, the changes were found to be very similar in HBSS compared to distilled water, however since HBSS is a buffered solution, the effects are not as strong as those seen for distilled water.

Ion measurements were carried out but were found to be unsatisfactory. This was due to the type of ions being measured in the HBSS. HBSS is a buffered cell culture solution, including the following inorganic salt in g/L.:

$CaCl_2$ x 2 H_2O (0.185);

KCl (0.40);

KH_2PO_4 (0.06);

$MgCl_2$ x 6 H_2O (0.10);

$MgSO_4$ x 10 H_2O;

NaCl (8.00)

$NaHCO_3$ (0.35);

Na_2HPO_4 (0.048) and D-glucose (1.00).

Thus the relatively low levels of ions released from the glass was masked by the ions already in solution.

6.3 Discussion of the Ternary System Na_2O-CaO-P_2O_5

The solubility test in distilled water showed that the ternary Na_2O-CaO-P_2O_5 glass system has basically two different dissolution processes. For the glasses with CaO contents up to 20 mol% there seemed to be only one process responsible for the more or less linear dissolution process. This is in accordance with findings of other workers (17,83). At around 20 mol% CaO content, a slight exponential curve appears which increases in non-linearity right to the end of the ternary glass spectrum studied. It should be mentioned that ion-exchange processes are occurring where alkaline ions (in this case Na^+ ions) are exchanged by H_3O^+ ions (1,84,85). This is one part of the dissolution process. Glasses with higher sodium content (lower CaO content) show a more linear curve because one sodium ion is gradually replaced by H_3O^+ ions and logically, this exchange is most severe for glasses with highest Na_2O content. The proof that this exchange really takes place is reflected by the sharp pH increase for high sodium containing glasses. If H_2O is the starting solution, obviously the glass must consume H_3O^+ ions. This will release OH^- ions, which will then increase the pH. Glasses with higher CaO content and less Na_2O content do not show such extreme changes in pH because of the reduced Na_2O content, which decreases the ion exchange process. For these glasses the weight loss curve is more of an exponential nature. This is particularly clearly seen for glasses containing high levels of CaO. It is clear that the Ca^{2+} ion release measurements are more closely mirroring the weight

loss compared to the Na^+ ion curves. This might lead to the conclusion that the overall degradation process is mainly driven by the nature of the CaO interaction with the P_2O_5 in the glass structure, which slowly breaks down. For glasses containing higher sodium levels, this process is covered by the ion-exchange process, which will lead to more linear overall release characteristics.

For the test results of the solubility measurements in HBSS, it can be seen that for glasses with high sodium content, glasses dissolve at a faster rate in HBSS compared to distilled water. This can be explained by the fact that HBSS contains other cations, which can contribute to a faster ion exchange process. HBSS also contains nucleophilic ions, such as Cl^- ions, which can attack the glass structure more easily than water on its own. This might account for the fact that even for high CaO containing glasses, which show exponential weight loss behaviour in distilled water, the weight loss curve is more a markedly linear.

6.4 Detailed Study of the Non-Linear Behaviour of the CaO-Na_2O-P_2O_5 System

When the weight loss of the glass is plotted against time, two basic curves can be obtained for the ternary system. For glasses with a low CaO content a straight line is observed out of which the slope can be calculated to give the solubility. If the CaO content is high, curves are more exponential in their nature and it is no longer correct to fit these curves with a straight line. Other functions should be considered for these cases.

One possible approximation is to use an exponential plot in which the weight loss C can be described by

$$C = k\,t^{n}$$

Where C = weight loss

k = constant

t = time

n = exponential term

In order to obtain a straight line function from this equation, applying $\log_{10}$ would give:

$$\log_{10} C = \log_{10} k + n \log_{10} t$$

$$y = c + mx$$

It can be seen from this equation that n is described by the slope if $\log_{10} C$ is plotted against $\log_{10} t$.

If n is ½ the dissolution is described by Fick's law. If the slope is 1, case II diffusion is present occurring (86).

On the following pages the above mentioned approximation has been used in order to describe the dissolution process.

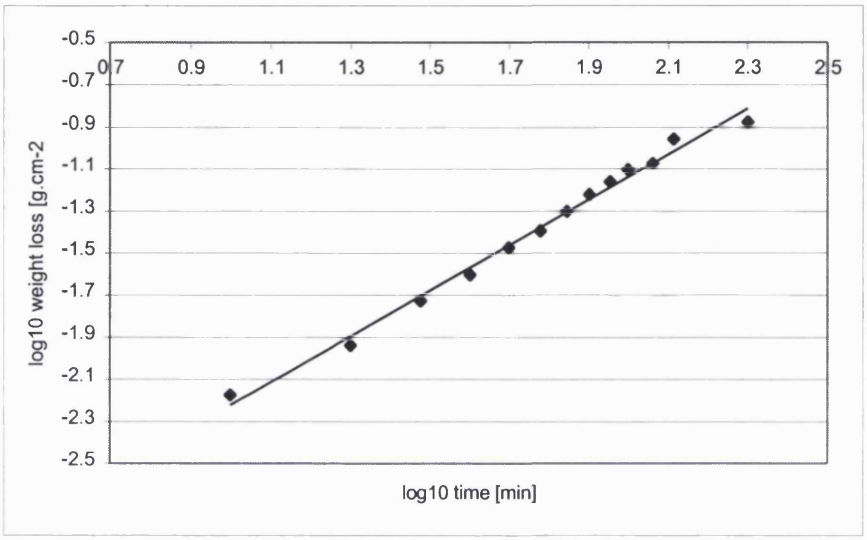

Figure 36: Solubility plot for $Ca_8 Na_{47}P_{45}$

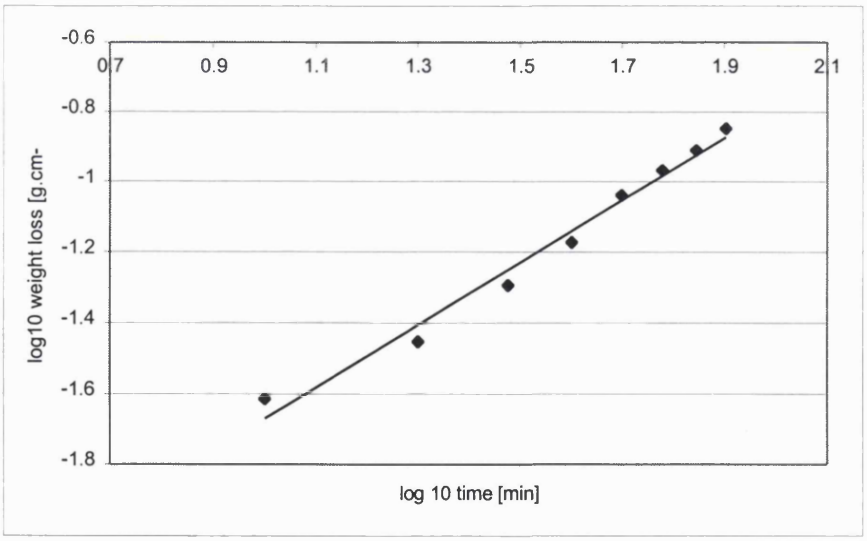

Figure 37: Solubility plot for $Ca_{10}Na_{45}P_{45}$

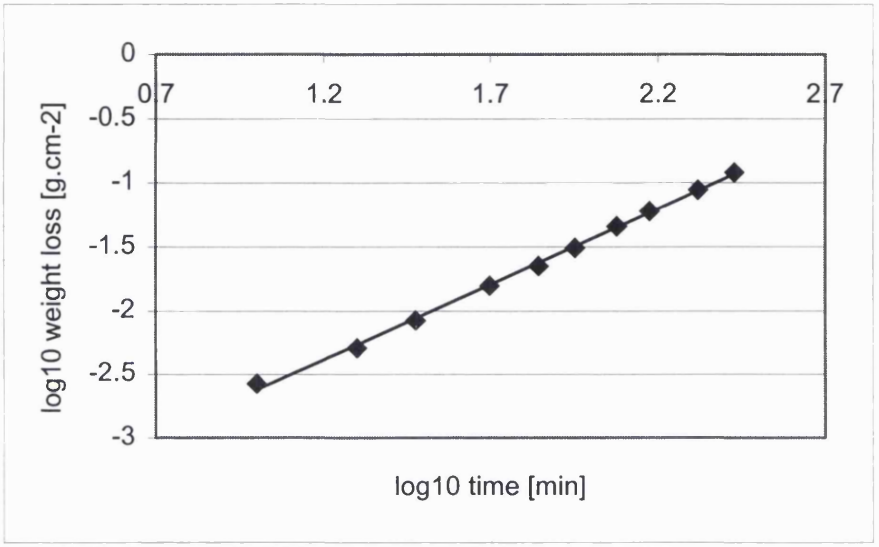

Figure 38: Solubility plot for $Ca_{12}Na_{43}P_{45}$

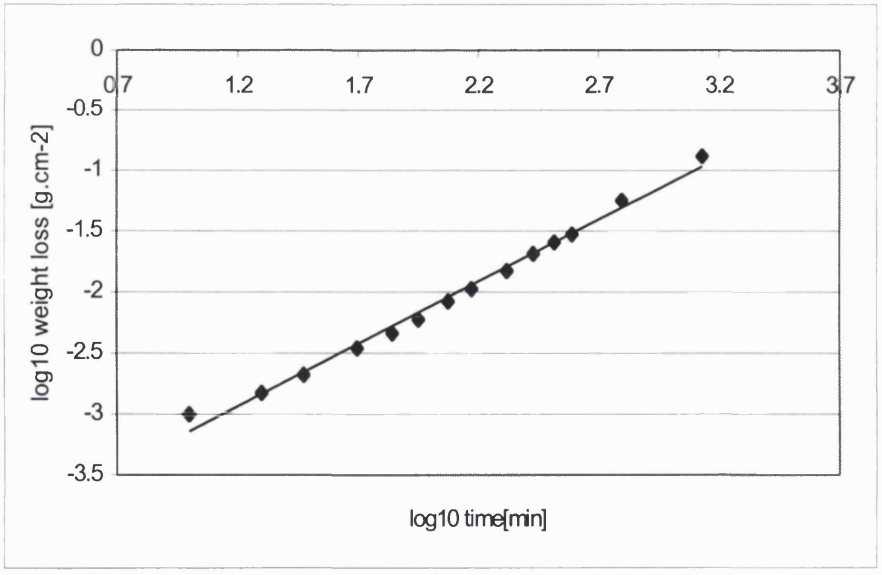

Figure 39: Solubility plot for $Ca_{16}Na_{39}P_{45}$

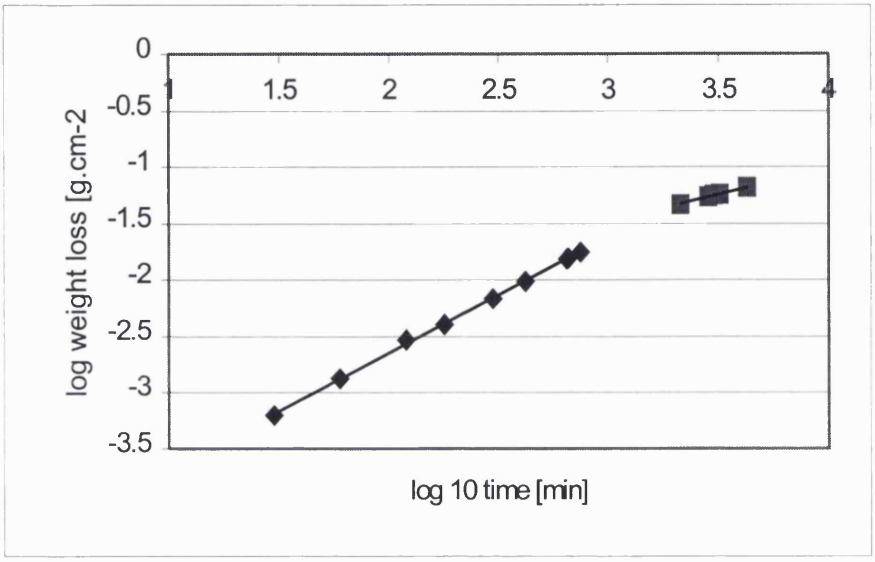

Figure 40: Solubility plot for $Ca_{20}Na_{35}P_{45}$

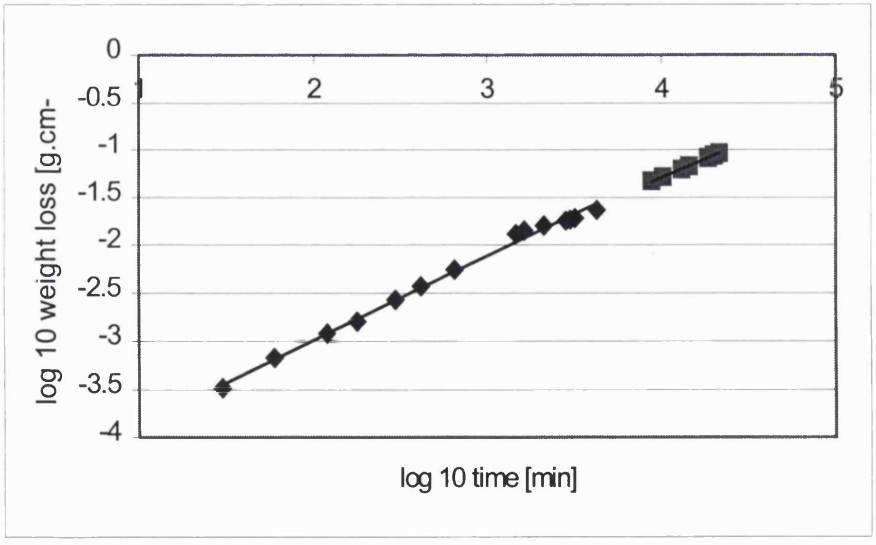

Figure 41: Solubility plot for $Ca_{24}Na_{31}P_{45}$

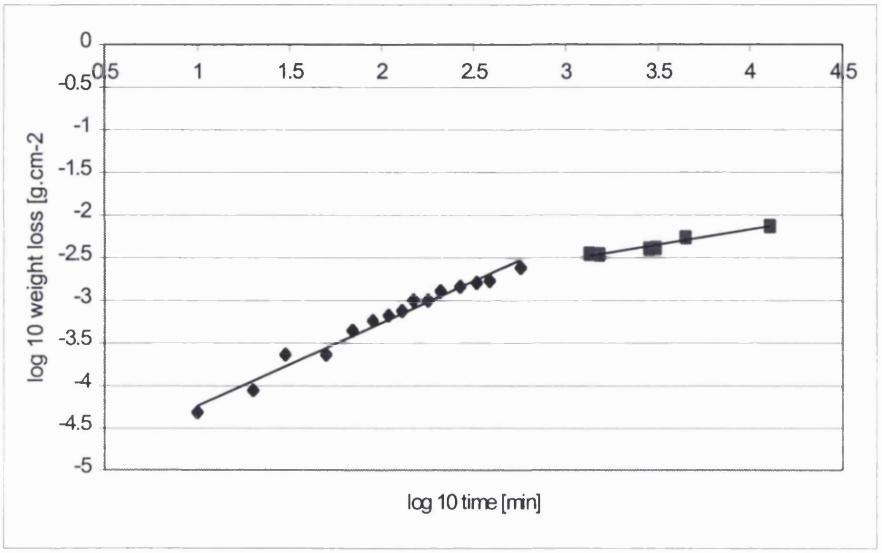

Figure 42: Solubility plot for $Ca_{28}Na_{27}P_{45}$

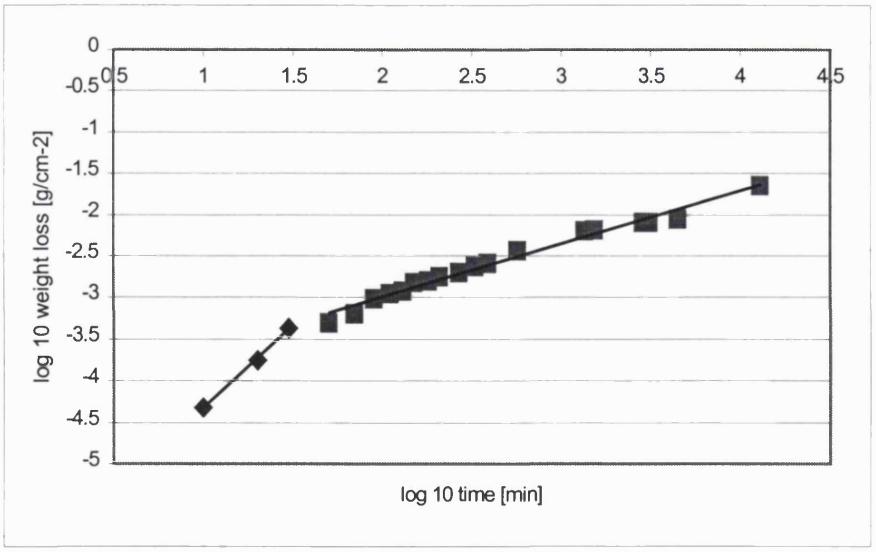

Figure 43: Solubility plot for $Ca_{32}N_{23}P_{45}$

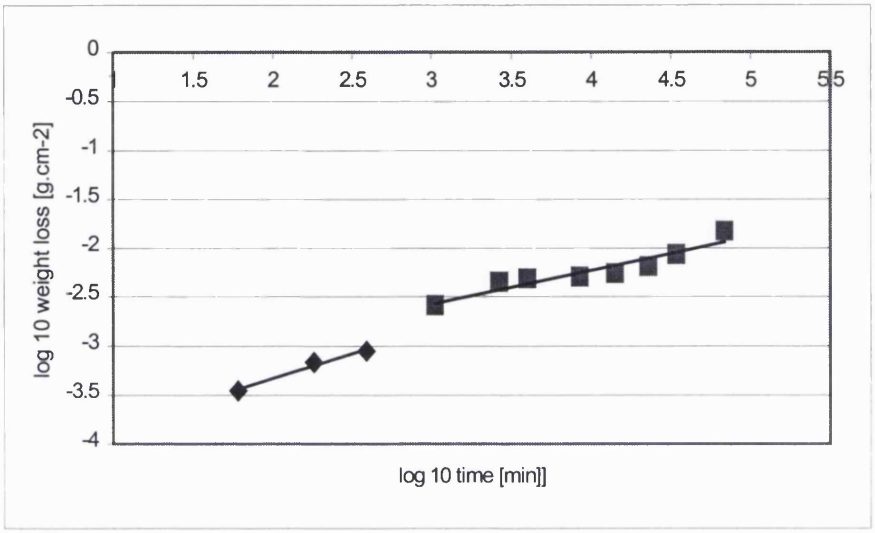

Figure 44: Solubility plot for $Ca_{36}Na_{19}P_{45}$

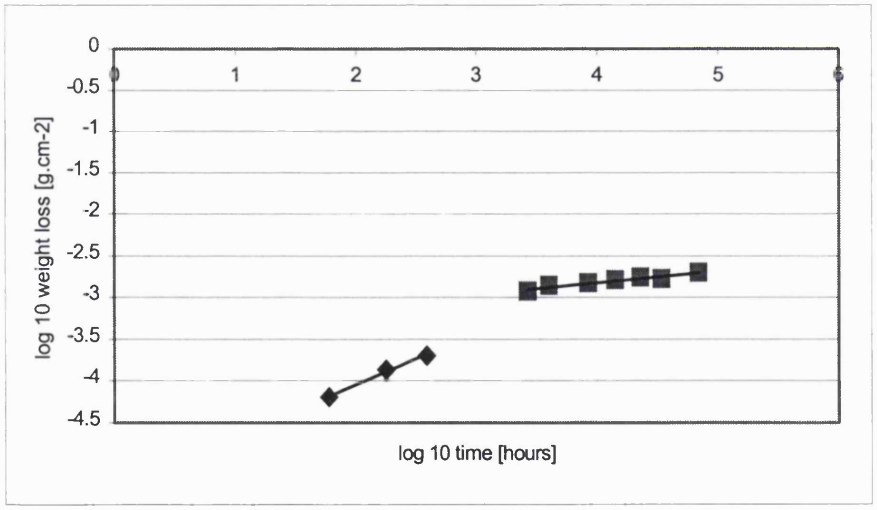

Figure 45: Solubility plot for $Ca_{40}Na_{15}P_{45}$

Glass code	n 1	n 2
$Ca_8Na_{47}P_{45}$	0.8845	
$Ca_{10}Na_{45}P_{45}$	1.085	
$Ca_{12}Na_{43}P_{45}$	1.179	
$Ca_{16}Na_{39}P_{45}$	1.021	
$Ca_{20}Na_{35}P_{45}$	1.0277	0.4937
$Ca_{24}Na_{31}P_{45}$	0.8744	0.7738
$Ca_{28}Na_{27}P_{45}$	0.977	0.3497
$Ca_{32}Na_{23}P_{45}$	1.9702	0.6419
$Ca_{36}Na_{19}P_{45}$	0.5069	0.341
$Ca_{40}Na_{15}P_{45}$	0.6152	0.1392

Table 6: Overview of Fickian/case II diffusion portion

6.4.1 Discussion

It can be seen from this way of analysing the solubilities that at 20 mol% CaO a clear change in slope occurs. A second line can be fitted, linking values obtained from later measuring times (grey line).

Two different processes occur, the first curve is represented by the ion-exchange and this curve decreases as a function of the decrease in Na_2O content. The second curve represents the gradual breakdown of the remaining glass-structure.

The first curve is of case II diffusion in nature, which is the main driving force for the dissolution process for glasses with CaO contents up to 16 – 20 mol%. With CaO contents above this level, an additional Fickian process takes place, which would represent the gradual breakdown of the remaining glass structure.

6.5 Comparison with findings of other authors

6.5.1 Solubility values

4 different authors (55,65,73,76) tested solubilities of phosphate based glasses and plotted them in $g.cm^{-2}.min^{-1}$. In this study solubilities were measured in $g.cm^{-2}.h^{-1}$ in order to give values that are within a reasonable number range. If the values in this thesis were re-calculated in $g.cm^{-2}.min^{-1}$ than comparison could be made more easily with this other work.

Glass code	Solubility $g.cm^{-2}.h^{-1}$	Solubility $g.cm^{-2}.min^{-1}$
$Ca_8Na_{47}P_{45}$	Too fast to measure	/
$Ca_{10}Na_{45}P_{45}$	Too fast to measure	/
$Ca_{12}Na_{43}P_{45}$	2.36 x 10-2	3.93×10^{-4}
$Ca_{16}Na_{39}P_{45}$	5.40 x 10-3	9.0×10^{-5}
$Ca_{20}Na_{35}P_{45}$	6.00 x 10-4	1.0×10^{-5}
$Ca_{24}Na_{31}P_{45}$	2.00 x 10-4	3.33×10^{-6}
$Ca_{28}Na_{27}P_{45}$	5.00 x 10-5	8.33×10^{-7}
$Ca_{32}Na_{23}P_{45}$	1.00 x 10-6	1.66×10^{-8}
$Ca_{36}Na_{19}P_{45}$	6.00 x 10-6	1.0×10^{-7}
$Ca_{40}Na_{15}P_{45}$	3.00 x 10-6	5.0×10^{-9}

Table 7: Solubility values

Bunker et al. carried out solubility measurements for 2 ternary Na_2O-CaO-P_2O_5 systems with CaO/P_2O_5 ratios of 0.2 and 0.4, which would be represented in this thesis by $Ca_{12}Na_{43}P_{45}$ and $Ca_{20}Na_{35}P_{45}$. *Bunker et al.* found leaching rates (for the glass with CaO/P_2O_5 ratios of 0.2) $5x10^{-5}$ and (for the glass with CaO/P_2O_5 ratios of 0.4) $3x10^{-6}$ $g.cm^{-2}.min^{-1}$. These values are slightly lower than those found in this thesis. However this difference may be accounted for by the study being performed at a different pH (2-6) and at a lower temperature of 20^0C, which influences the dissolution process.

The dissolution values in this thesis, for this system, were also compared with the work of Delahaye *et al.*

The glasses had comparable compositions, with P_2O_5 content of 49 mol% and CaO and Na_2O content ranging from 10-40 mol%. Glasses with CaO contents up to 20 mol% show very similar solubility rates. With CaO contents above 20mol.% however, the glasses showed a higher dissolution rate. This might be due to the fact that the pH was kept constant by the addition of HCl during measurement period.

Uo et al. carried out a dissolution study in both distilled water and simulated body fluid; however, glass compositions were different in that they had a much higher P_2O_5 content. In addition the measuring time was much shorter, hence weight loss curves are straight lines which is not the case for all glasses used in this thesis. However, they found similarities for solubility rates for both liquids.

Hlavac et al. developed a mathematical model to explain the whole course of the decomposition of silicate based glasses. They plotted weight loss (or cation increase in solution) against time^{½}, which results in a linear plot for short time measurements. For longer measuring times, plots become linear. A major point to emphasise is that the authors stated that there are two major processes occurring: the first will be a diffusion driven process where cations (Na^+ and Ca^{2+}) exchange for H_3O^+ ions from the solution forming a destroyed leached layer. The second step will be the dissolution of this leached layer. However, this process cannot be directly applied to the phosphate based glasses in this thesis. In the case of phosphate glasses, calcium and sodium ions are not leaching out in the same way as was mentioned by *Hlavac et al.* If that is the case, a glass which has similar levels of Na^+ and Ca^{2+} in the glass, for example $Ca_{28}Na_{27}P_{45}$,

then the levels of measured Na^+ and Ca^{2+} should be the same at different time points and this is not the case. Calcium levels are much lower than sodium ion levels.

In addition, both ion curves should give a straight line, plotting ion concentration against time^{½} to represent the first stage of a two step dissolution process. This is not the case as seen below.

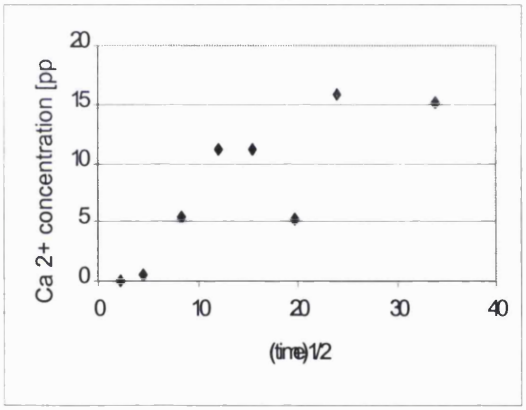

Figure 46: Ca^{2+} concentration plot for $Ca_{28}Na_{27}P_{45}$

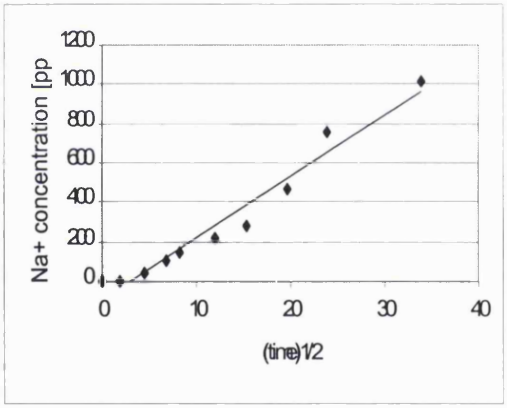

Figure 47: Na^+ concentration plot for $Ca_{28}Na_{27}P_{45}$

Only the plot for the sodium ion dissolution process gives an approximately straight line. Therefore these two ions are leaching out in different ways.

Chapter 7

7.1 Ternary system K_2O-CaO-P_2O_5

Glass preparation for this system was undertaken with the general glass making procedure. The precursor chemical used were KH_2PO_4, P_2O_5 and $CaCO_3$ to form this glass system and chemical compositions have been calculated using the methodology detailed previously.

This system was originally prepared for structural analysis to see if any differences occurred if sodium was exchanged for potassium. Therefore a more thorough study for this system was carried out with the DTA and NMR investigation (see structural part). However in addition, 3 glasses have been selected for solubility testing, including pH and ion measurements.

Glass code	CaO content (mol%)	K_2O content (mol%)	P_2O_5 content (mol%)
$Ca_{16}K_{39}P_{45}$	16	39	45
$Ca_{20}K_{35}P_{45}$	20	35	45
$Ca_{24}K_{31}P_{45}$	24	31	45
$Ca_{28}K_{27}P_{45}$	28	27	45
$Ca_{32}K_{23}P_{45}$	32	23	45

Table 8: Glass codes and oxide composition in mol%

Glass code	Melting temperatur time (^{0}C/hours)	Casting temperature time (^{0}C /hours)	result
$Ca_{16}K_{39}P_{45}$	1000/3	311/1	Glass, stress free
$Ca_{20}K_{35}P_{45}$	1000/3	330/1	Glass, stress free
$Ca_{24}K_{31}P_{45}$	1050/3	330/1	Glass, stress free
$Ca_{28}K_{27}P_{45}$	1150/3	370/1	Glass, stress free
$Ca_{32}K_{23}P_{45}$	1200/3	400/1	Glass, stress free

Table 9: Melting and casting temperature overview

Attempts at making glasses with CaO content lower than 16 mol% or higher than 32 mol% were unsuccessful due to crystallisation on casting. Therefore, materials outside these limits have been rejected for further testing and are not listed here because they represent the borders of glass forming region of the phase diagram. Casting temperatures have been chosen according to DTA results.

7.1.1 Solubility test results for ternary K_2O-CaO-P_2O_5 glass system

All tests have been carried out in distilled water. It should be noted that the rate of dissolution is different depending on composition, similar to the Na_2O-CaO-P_2O_5 ternary system. Therefore, tests have different measuring time end-points in relation to the loss of material.

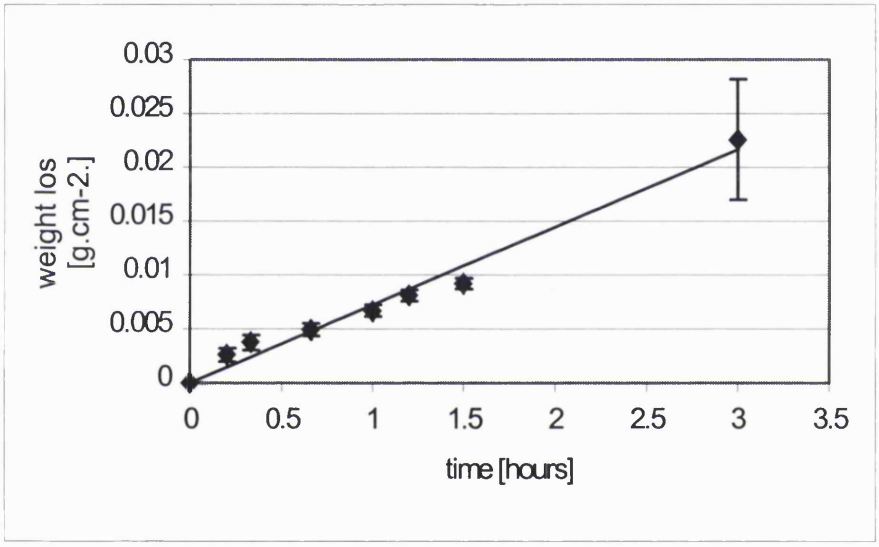

Figure 48: Solubility plot for $Ca_{16}K_{39}P_{45}$

The solubility curve is very similar to the corresponding glass of the Na_2O-CaO-P_2O_5 ternary system. The weight loss is still linear and a straight line can be fitted.

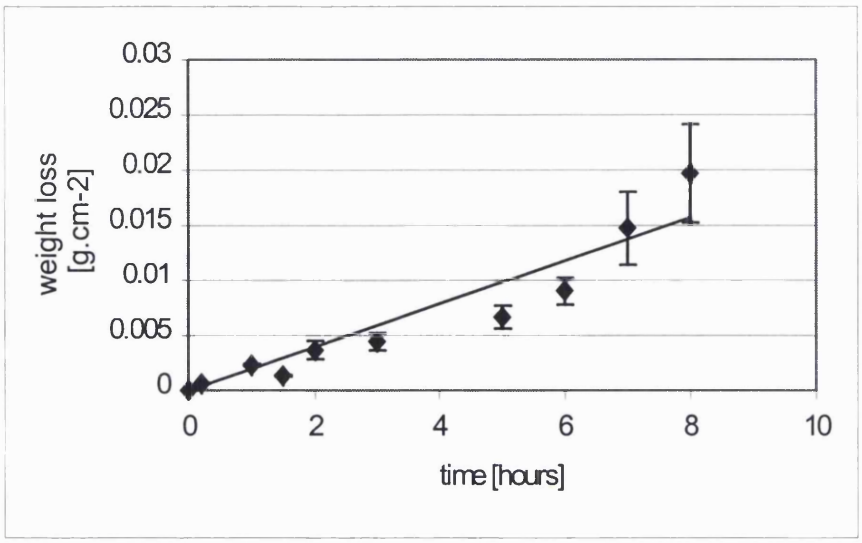

Figure 49: Solubility plot for $Ca_{24}K_{31}P_{45}$

The weight loss curve seems to be similar to the corresponding Na_2O-CaO-P_2O_5 ternary glass system; the weight loss curve is almost linear and a straight line is fitted. However, little changes in the first few hours of the weight loss experiment can be seen because this curve appears more linear than the corresponding $Ca_{24}Na_{31}P_{45}$ glass.

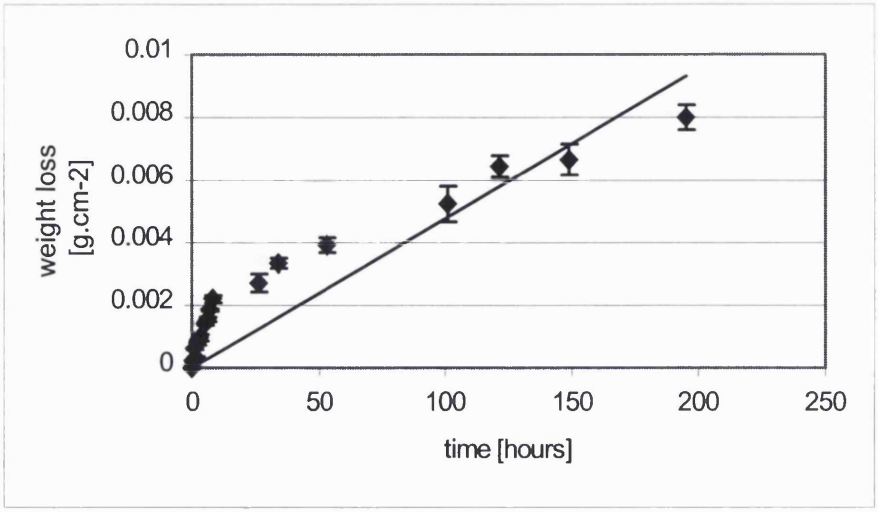

Figure 50: Solubility plot for $Ca_{32}K_{23}P_{45}$

Here, the exponential nature of the weight loss curve is obvious and similar to findings of the sodium based ternary glass system.

Glass code	Solubility [$g.cm^{-2}.h^{-1}$]
$Ca_{16}K_{39}P_{45}$	7.2×10^{-3}
$Ca_{24}K_{31}P_{45}$	2.0×10^{-3}
$Ca_{32}K_{23}P_{45}$	5.0×10^{-5}

Table 10: Solubility overview for ternary $CaO\text{-}K_2O\text{-}P_2O_5$

7.1.2 pH measurements

pH and ion measurements have been carried out as described before.

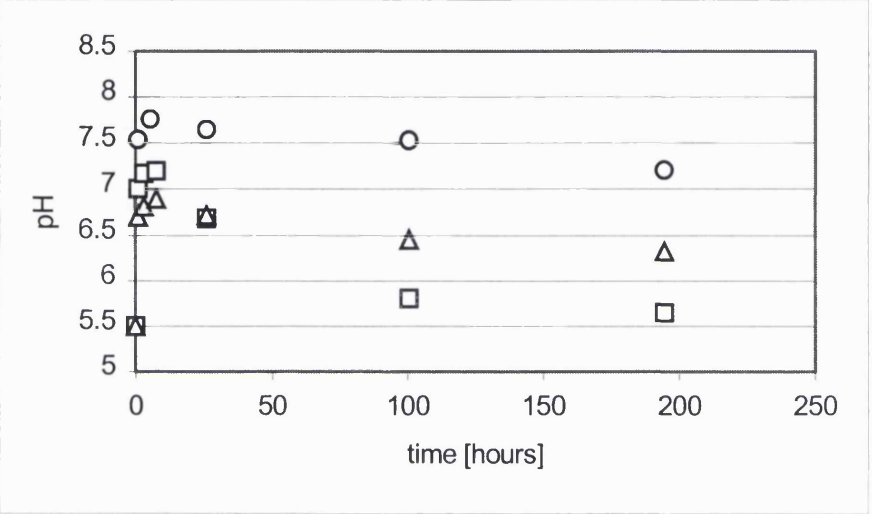

Figure 51: pH measurement for o $Ca_{16}K_{39}P_{45}$ ▫ $Ca_{24}K_{31}P_{45}$ Δ $Ca_{32}K_{23}P_{45}$

pH measurements were found to be identical for both ternary systems and therefore plots are not shown here. The similarity for both systems reveals that ion-exchange process takes place in the same way for both systems.

7.1.3 Ion measurements

Ca^{2+} ion measurements

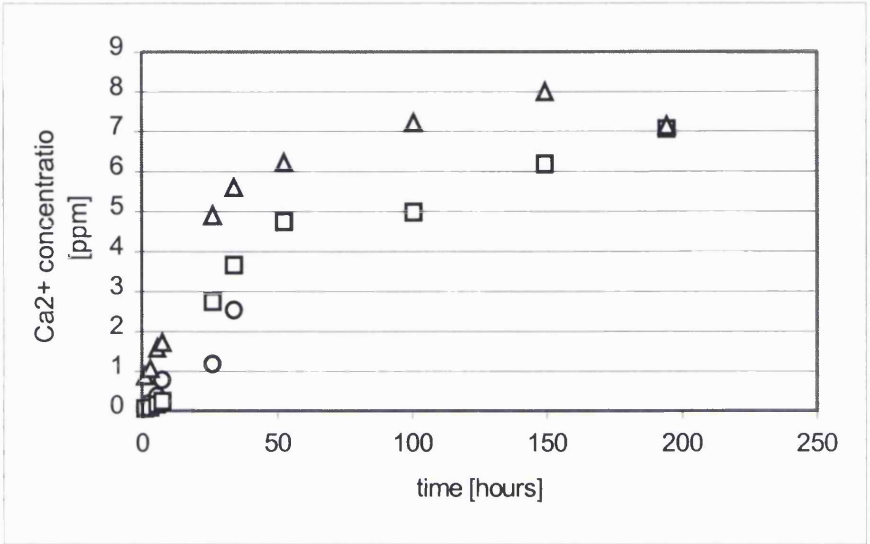

Figure 52: Ca^{2+} ion measurements for o $Ca_{16}K_{39}P_{45}$ ▫ $Ca_{24}K_{31}P_{45}$ Δ $Ca_{32}K_{23}P_{45}$

The Ca^{2+} ion leaching process was found similar to the sodium based ternary glass system. The ions in all three cases having an exponential nature and mirroring the weight loss process.

K^+ ion measurements:

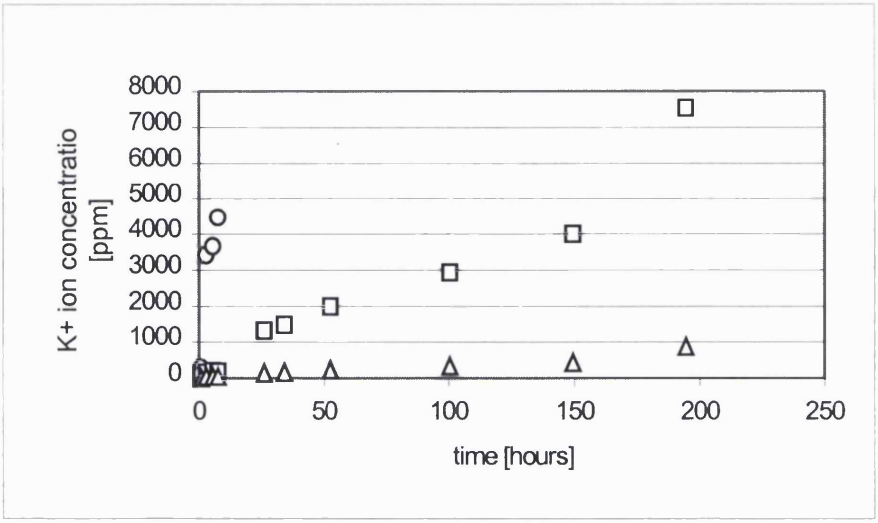

Figure 53: K^+ ion measurements for o $Ca_{16}K_{39}P_{45}$ ▫ $Ca_{24}K_{31}P_{45}$ Δ $Ca_{32}K_{23}P_{45}$

The potassium ion measurements were found to be similar to the sodium ternary system; sodium and potassium ions leaching out in an almost linear behaviour.

It was questioned if one or the other ion will influence each other in terms of their solubility behaviour. By completely replacing sodium oxide by potassium oxide, it can be seen that the Ca^{2+} ion release is not affected. For the weight loss, this process appears more exponential. In the same way, comparison of the K^+ ion release compared to the Na^+ release for the same glass showed no difference. Overall it can be said that no differences between the Na_2O-CaO-P_2O_5 and the K_2O-CaO-P_2O_5 were seen and it can be assumed that Ca^{2+} ions leaching out of the whole glass structure are independent from Na^+ or K^+ ions, otherwise differences would have been seen.

Ternary potassium oxide based glasses show similar trends in their solubility behaviour with identical pH changes and similar ion measurement studies. However, glasses were found to dissolve more quickly when Na_2O is completely substituted by K_2O.

Chapter 8

Quaternary system Na_2O-K_2O-CaO-P_2O_5

Glass preparation was carried out for all glasses using the general procedure. NaH_2PO_4, KH_2PO_4, $CaCO_3$ and P_2O_5 were used as precursors for this system and oxide contents were calculated as documented in the Materials and Methods section.

Glass code	CaO content (mol%)	Na_2O content (mol%)	K_2O content (mol%)	P_2O_5 content (mol%)
$Na_{20}K_{15}Ca_{20}P_{45}$	20	20	15	45
$Na_{15}K_{20}Ca_{20}P_{45}$	20	15	20	45
$Na_{10}K_{25}Ca_{20}P_{45}$	20	10	25	45
$Na_5K_{30}Ca_{20}P_{45}$	20	5	30	45
$Na_{26}K_5Ca_{24}P_{45}$	24	26	5	45
$Na_{21}K_{10}Ca_{24}P_{45}$	24	21	10	45
$Na_{16}K_{15}Ca_{24}P_{45}$	24	16	15	45
$Na_{11}K_{20}Ca_{24}P_{45}$	24	11	20	45
$Na_6K_{24}Ca_{24}P_{45}$	24	6	24	45
$Na_{22}K_5Ca_{28}P_{45}$	28	22	5	45
$Na_{17}K_{10}Ca_{28}P_{45}$	28	17	10	45
$Na_{12}K_{15}Ca_{28}P_{45}$	28	12	15	45
$Na_7K_{20}Ca_{28}P_{45}$	28	7	20	45
$Na_{20}K_3Ca_{32}P_{45}$	32	20	3	45
$Na_{15}K_8Ca_{32}P_{45}$	32	15	8	45
$Na_{10}K_{13}Ca_{32}P_{45}$	32	10	13	45
$Na_5K_{18}Ca_{32}P_{45}$	32	5	18	45

Table 11: Glass codes and oxide compositions in mol%

Glass code	Melting temperature and time (^{0}C/Hours)	Casting temperatures (^{0}C/Hours)	Result
$Na_{20}K_{15}Ca_{20}P_{45}$	1000/3	350/1	Glass, stress free
$Na_{15}K_{20}Ca_{20}P_{45}$	1000/3	350/1	Glass, stress free
$Na_{10}K_{25}Ca_{20}P_{45}$	1000/3	350/1	Glass, stress free
$Na_5K_{30}Ca_{20}P_{45}$	1000/3	320/1	Glass, stress free
$Na_{26}K_5Ca_{24}P_{45}$	1000/3	320/1	Glass, stress free
$Na_{21}K_{10}Ca_{24}P_{45}$	1000/3	320/1	Glass, stress free
$Na_{16}K_{15}Ca_{24}P_{45}$	1000/3	320/1	Glass, stress free
$Na_{11}K_{20}Ca_{24}P_{45}$	1000/3	320/1	Glass, stress free
$Na_6K_{24}Ca_{24}P_{45}$	1050/3	320/1	Glass, stress free
$Na_{22}K_5Ca_{28}P_{45}$	1050/3	350/1	Glass, stress free
$Na_{17}K_{10}Ca_{28}P_{45}$	1100/3	350/1	Glass, stress free
$Na_{12}K_{15}Ca_{28}P_{45}$	1100/3	350/1	Glass, stress free
$Na_7K_{20}Ca_{28}P_{45}$	1100/3	350/1	Glass, stress free
$Na_{20}K_3Ca_{32}P_{45}$	1100/3	350/1	Glass, stress free
$Na_{15}K_8Ca_{32}P_{45}$	1100/3	320/1	Glass, stress free
$Na_{10}K_{13}Ca_{32}P_{45}$	1100/3	350/1	Glass, stress free
$Na_5K_{18}Ca_{32}P_{45}$	1200/3	320/1	Glass, stress free

Table 12: Melting and casting temperatures

Temperatures for melting and annealing were chosen from experience with the other systems. However, this was confirmed with DTA results obtained later on. It should be noted that occasionally some of the glasses with CaO content of 32 mol% showed evidence for partial crystallisation (marked with *). This occurred at the very top of the rod when cast at 350°C. The casting temperature was altered to 320^0C (see table 12) to obtain glasses without any remaining crystallisation that were also still stress free. This onset of the crystallisation event reflects the glass making limitation for glasses with CaO content higher than 32mol%.

8.1 Solubility test for Quaternary Glass System Na_2O-K_2O-CaO-P_2O_5

The data that is presented here, is for glasses with fixed P_2O_5 content, CaO content of 20, 24, 28 or 32mol.% with varying Na_2O:K_2O ratio.

Glasses with fixed CaO content of 20mol%

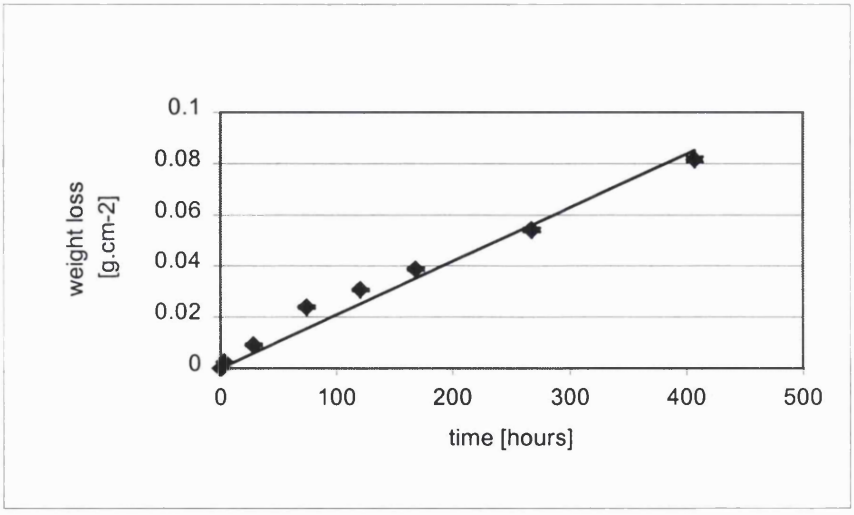

Figure 54: Solubility plot for $Na_{20}K_{15}Ca_{20}P_{45}$

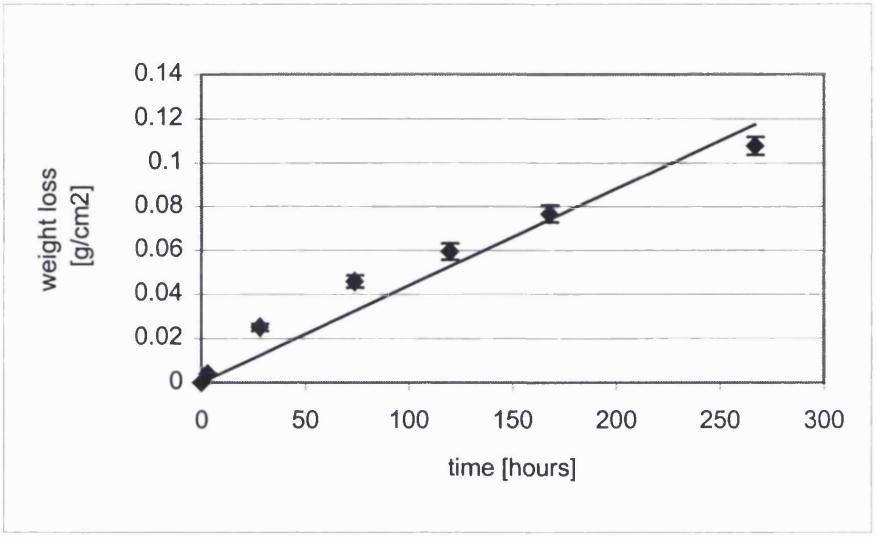

Figure 55: Solubility plot for $Na_{15}K_{20}Ca_{20}P_{45}$

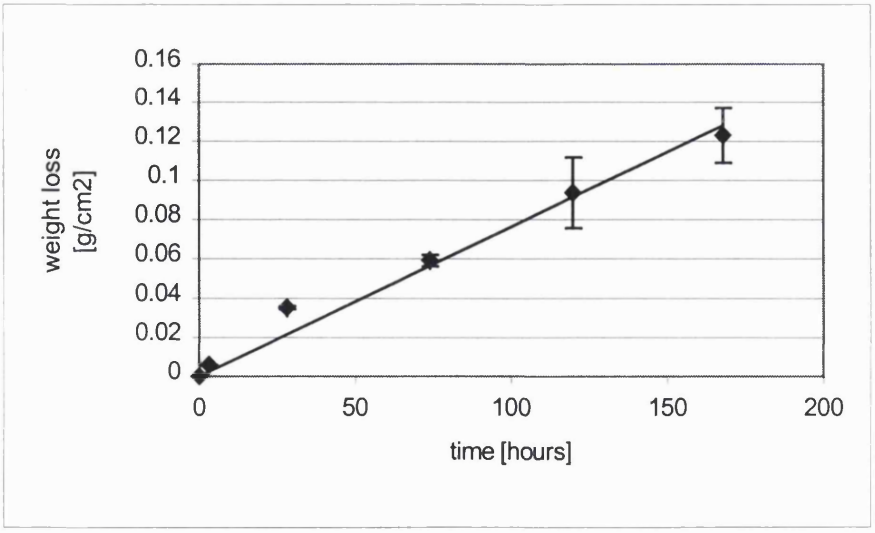

Figure 56: Solubility plot for $Na_{10}K_{25}Ca_{20}P_{45}$

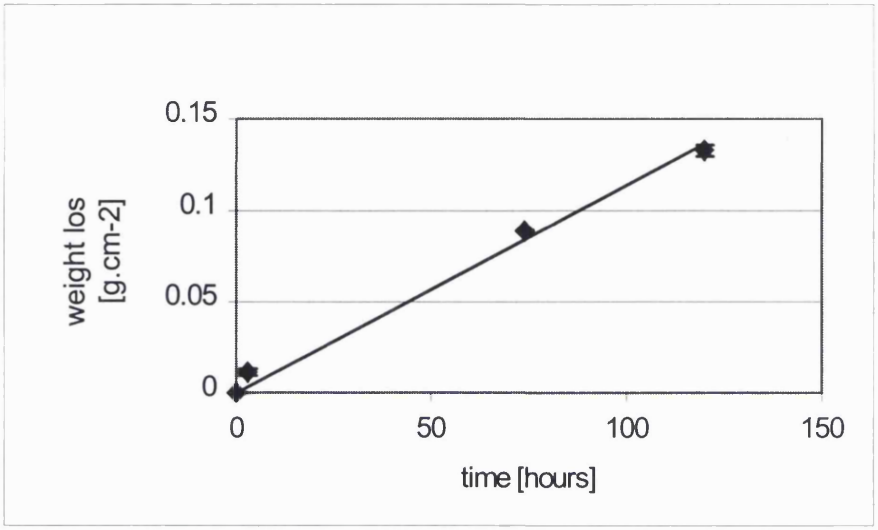

Figure 57: Solubility plot for $Na_5K_{30}Ca_{20}P_{45}$

Figure 54 to 57 show the solubility for a fixed CaO content of 20 mol% and Na_2O:K_2O ratios of 1.3, 0.8, 0.4 and 0.16. The solubilities are relatively linear; glasses with highest K_2O content dissolve quicker than glasses with lower K_2O content.

Glasses with fixed CaO content of 24 mol%.

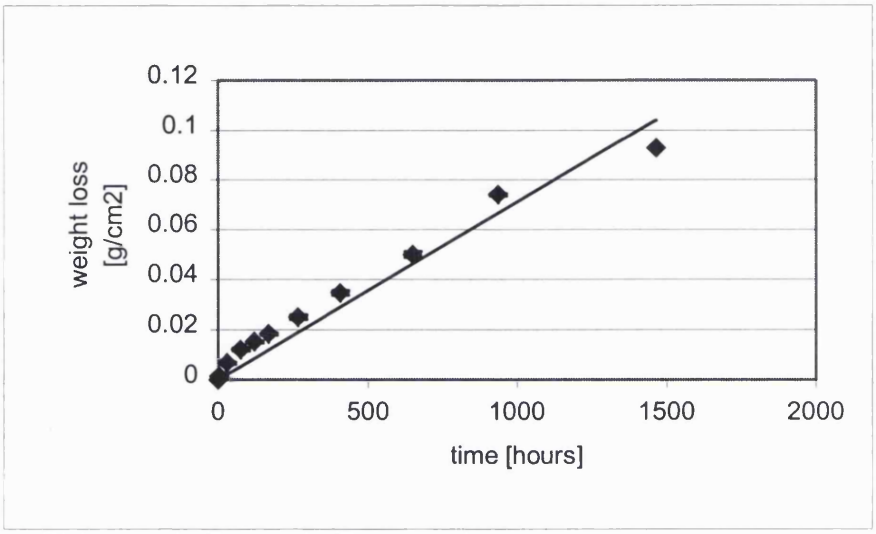

Figure 58: Solubility plot for $Na_{26}K_5Ca_{24}P_{45}$

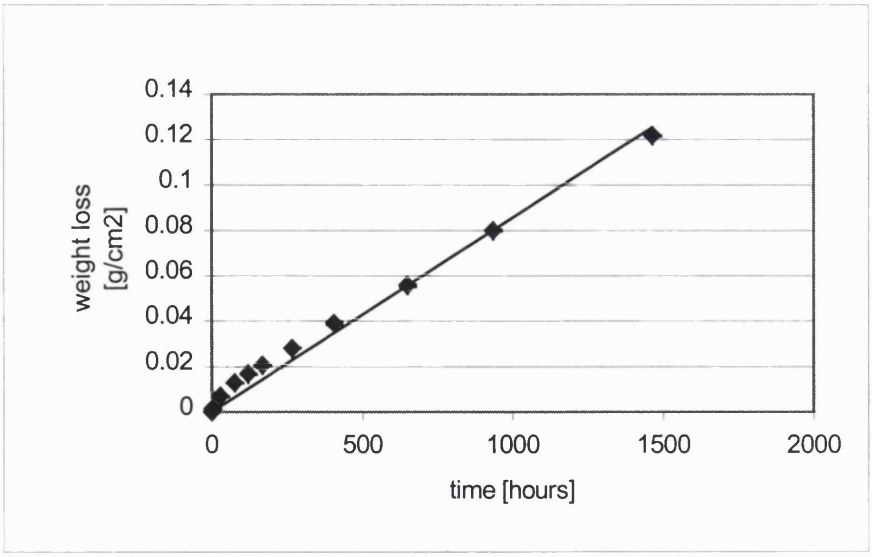

Figure 59: Solubility plot for $Na_{21}K_{10}Ca_{24}P_{45}$

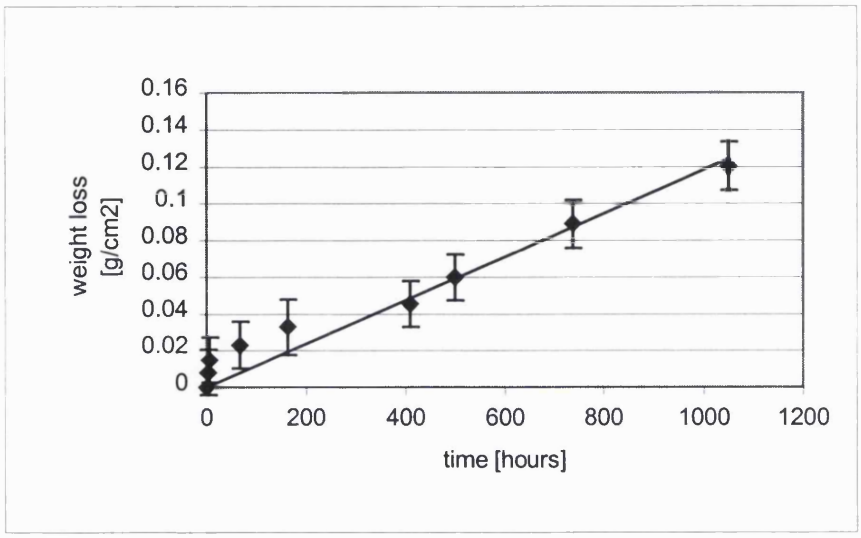

Figure 60: Solubility plot for $Na_{16}K_{15}Ca_{24}P_{45}$

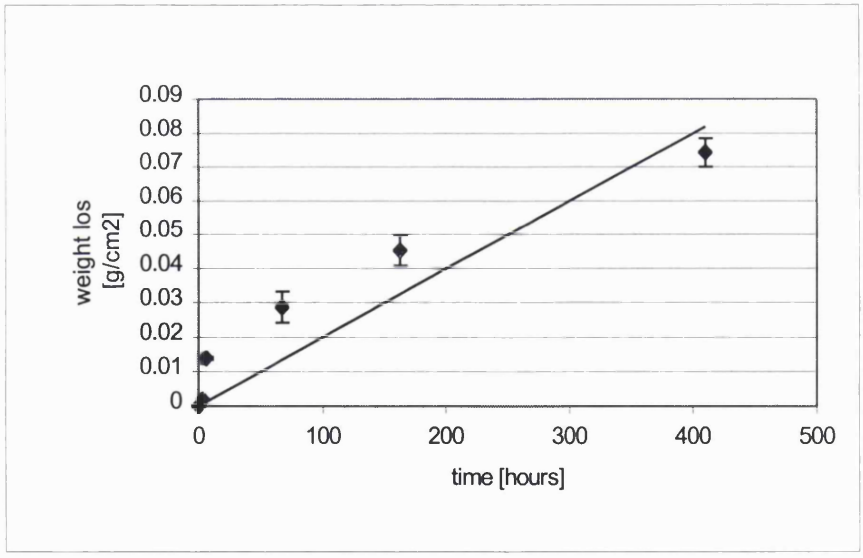

Figure 61: Solubility plot for $Na_{11}K_{20}Ca_{24}P_{45}$

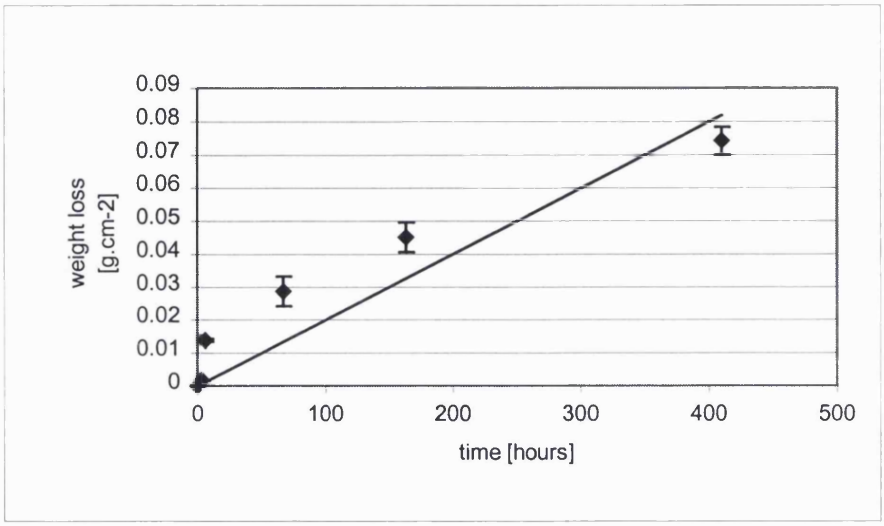

Figure 62: Solubility plot for $Na_6K_{25}Ca_{24}P_{45}$

Figure 58 to Figure 62 show the solubility for a fixed CaO content of 24mol.% and Na_2O:K_2O ratios of 5.2, 2.1, 1.1, 0.6 and 0.24 respectively. For the high ratio, the solubility appears relatively linear as it does for the low ratio.

Glasses with fixed CaO content of 28 mol%

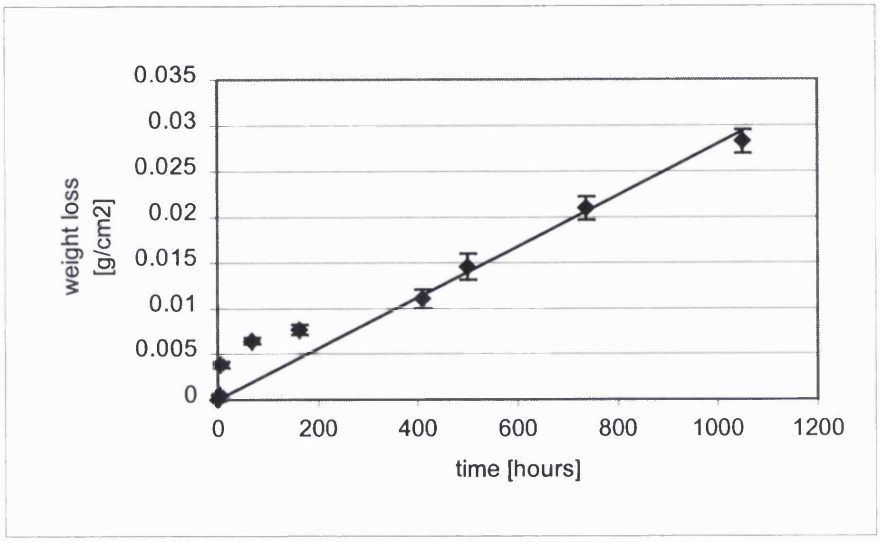

Figure 63: Solubility plot for $Na_{22}K_5Ca_{28}P_{45}$

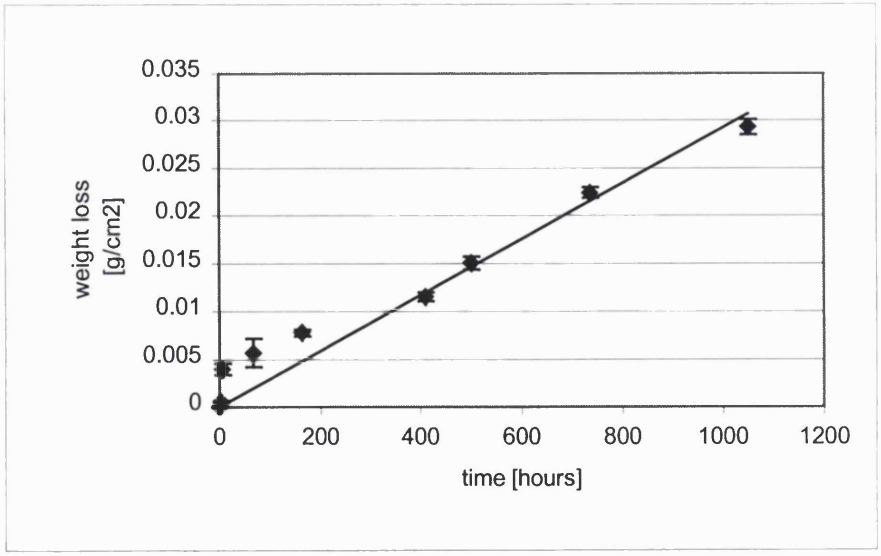

Figure 64: Solubility plot for $Na_{17}K_{10}Ca_{28}P_{45}$

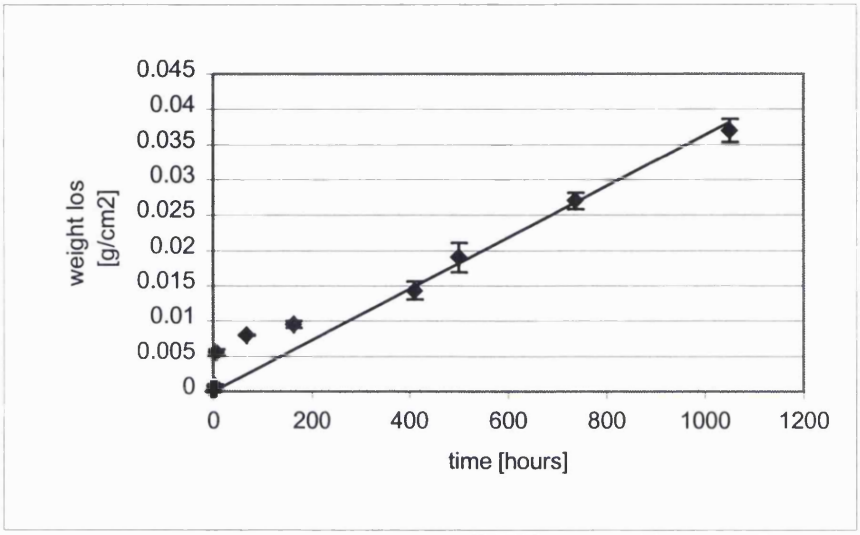

Figure 65: Solubility plot for $Na_{12}K_{15}Ca_{28}P_{45}$

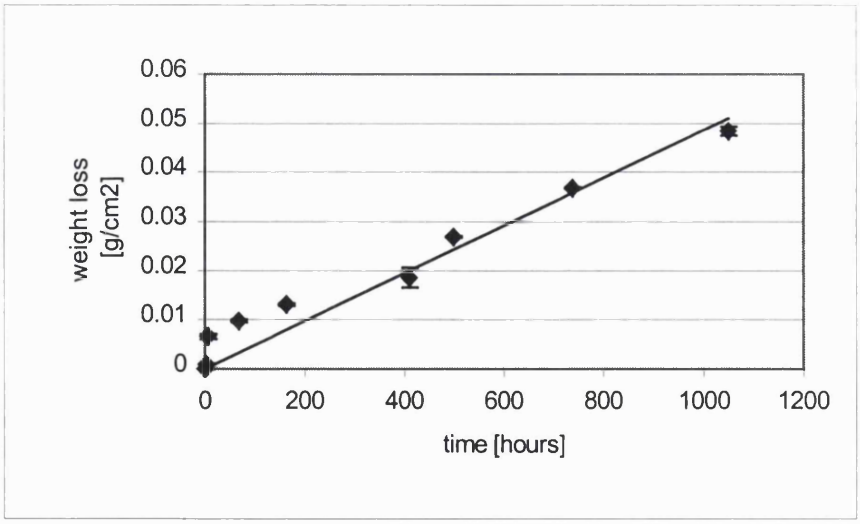

Figure 66: Solubility plot for $Na_7K_{20}Ca_{28}P_{45}$

For glasses with a CaO content of 28mol.% (Figure 63 to figure 66) similar trends are seen. They appear to have a relatively linear relationship but show some evidence of the exponential nature of the weight loss curve, similar to the ternary Na_2O-CaO-P_2O_5 system.

Glasses with fixed CaO content of 32 mol%

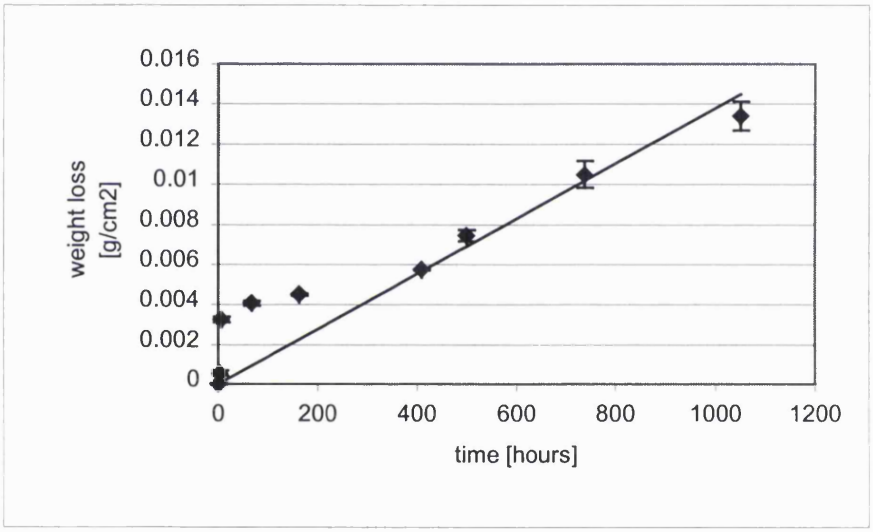

Figure 67: Solubility plot for $Na_{20}K_3Ca_{32}P_{45}$

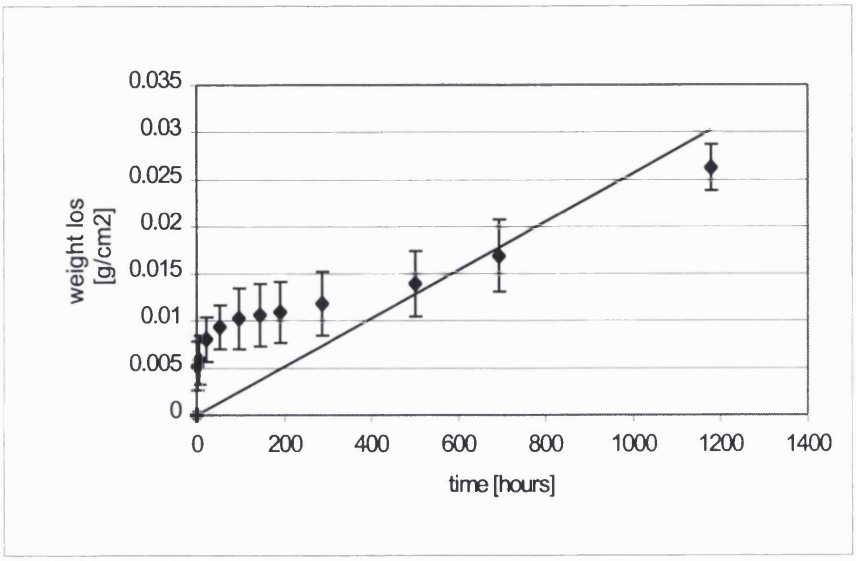

Figure 68: Solubility plot for $Na_{15}K_8Ca_{32}P_{45}$

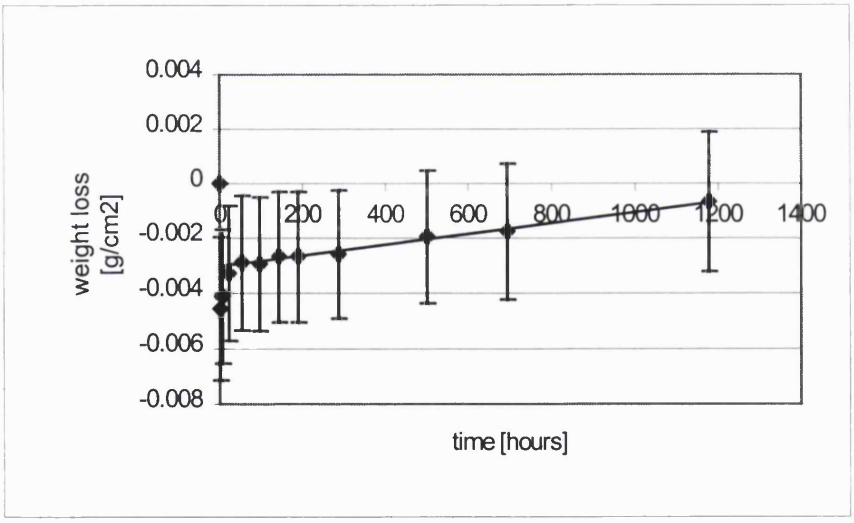

Figure 69: Solubility plot for $Na_{10}K_{13}Ca_{32}P_{45}$

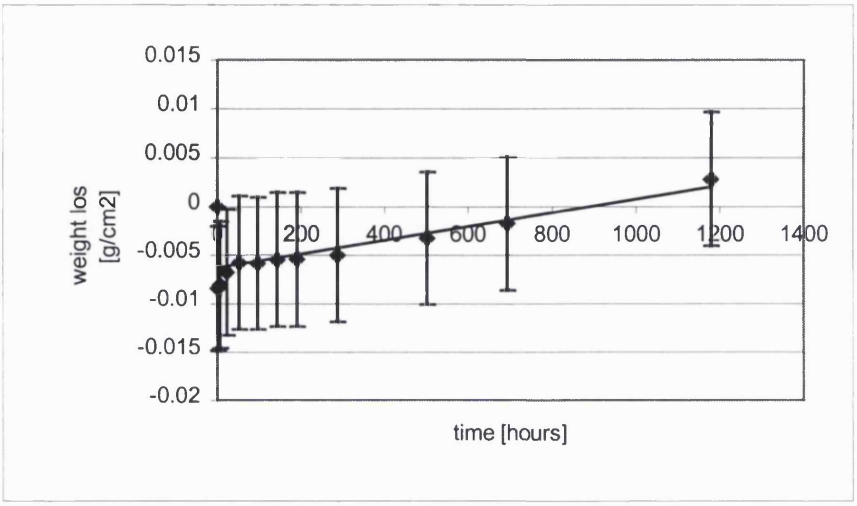

Figure 70: Solubility plot for $Na_5K_{18}Ca_{32}P_{45}$

As expected, for glasses with high CaO content and as seen in the ternary system, the glasses become more non-linear. Figure 69 and figure 70 show weight losses in the negative area, this was because the glasses gained weight after they have been placed in distilled water. This phenomenon was only found for glasses $Na_{10}K_{13}Ca_{32}P_{45}$ and $Na_5K_{18}Ca_{32}P_{45}$ and was seen in the same way when tests were repeated. It is assumed that the weight gain is due to water absorbance. Overall it can be said that there be some evidence for the K_2O content affecting this non-linearity.

Glass code	Solubility ($g.cm^{-2}.h^{-1}$)
$Na_{20}K_{15}Ca_{20}P_{45}$	2.0×10^{-4}
$Na_{15}K_{20}Ca_{20}P_{45}$	4.0×10^{-4}
$Na_{10}K_{25}Ca_{20}P_{45}$	8.0×10^{-4}
$Na_5K_{30}Ca_{20}P_{45}$	1.2×10^{-4}
$Na_{26}K_5Ca_{24}P_{45}$	7.0×10^{-5}
$Na_{21}K_{10}Ca_{24}P_{45}$	9.0×10^{-5}
$Na_{16}K_{15}Ca_{24}P_{45}$	1.0×10^{-4}
$Na_{11}K_{20}Ca_{24}P_{45}$	1.0×10^{-4}
$Na_6K_{24}Ca_{24}P_{45}$	2.0×10^{-4}
$Na_{22}K_5Ca_{28}P_{45}$	3.0×10^{-5}
$Na_{17}K_{10}Ca_{28}P_{45}$	3.0×10^{-5}
$Na_{12}K_{15}Ca_{28}P_{45}$	4.0×10^{-5}
$Na_7K_{20}Ca_{28}P_{45}$	5.0×10^{-5}
$Na_{20}K_3Ca_{32}P_{45}$	1.0×10^{-6}
$Na_{15}K_8Ca_{32}P_{45}$	2.0×10^{-6}
$Na_{10}K_{13}Ca_{32}P_{45}$	2.0×10^{-6}
$Na_5K_{18}Ca_{32}P_{45}$	7.0×10^{-6}

Table 13: Solubility overview for the quaternary Na_2O-K_2O-CaO-P_2O_5 system

As can clearly be seen, the measured solubility values show a systematic trend, with solubility values decreasing with increasing CaO content as seen with the ternary

Na_2O-CaO-P_2O_5 system. There is also a secondary effect in that as the Na_2O:K_2O ratio decreases, the solubility increases for a fixed CaO content.

8.1.1 pH Measurements

pH and ion measurements have been carried out as described previously.

pH measurements for glasses with fixed CaO content of 20 mol%

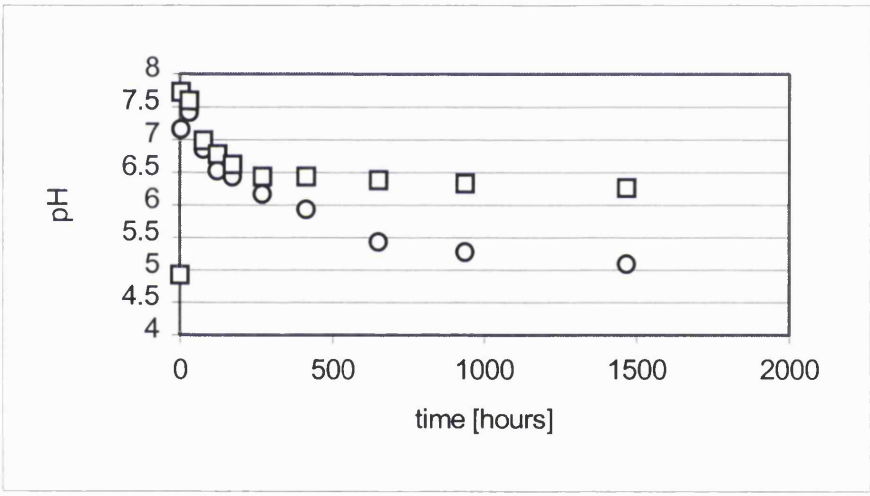

Figure 71: pH progress for o $Na_{20}K_{15}Ca_{20}$ P45 and ▫ $Na_5K_{30}Ca_{20}P_{45}$

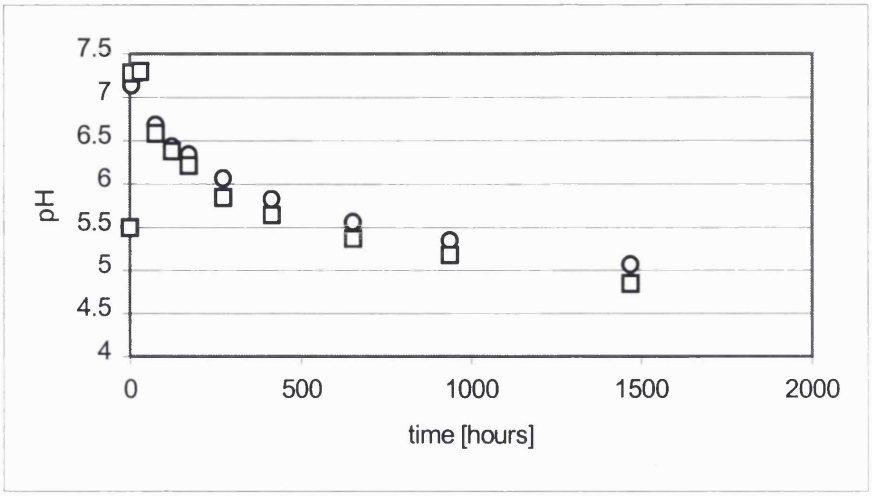

Figure 72: pH progress for o $Na_{15}K_{20}Ca_{20}$ P45 and ▫ $Na_{10}K_{25}Ca_{20}P_{45}$

The pH values for glasses with fixed CaO content of 20 mol% were found similar to the pH values and progress as for the corresponding glasses of the ternary Na_2O-CaO-P_2O_5 system.

pH measurement for glasses with fixed CaO content of 24 mol%

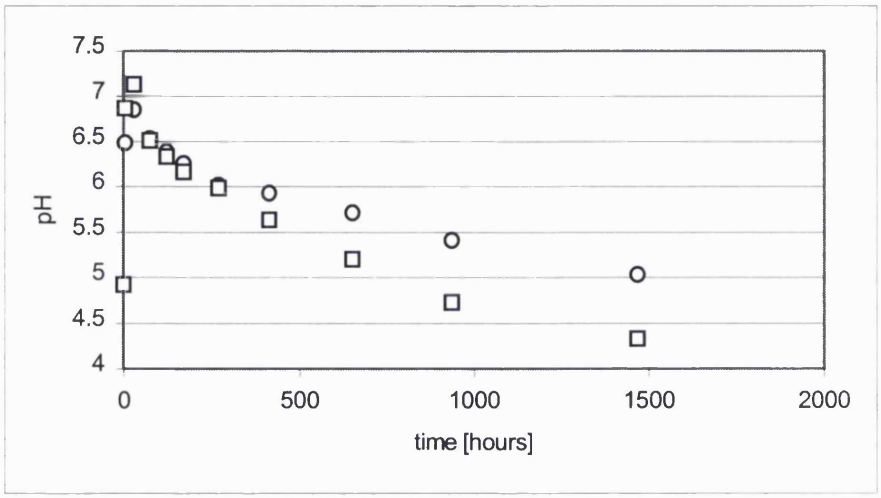

Figure 73: pH progress for o $Na_{21}K_{10}Ca_{24}P_{45}$ and ▫ $Na_6K_{24}Ca_{24}P_{45}$

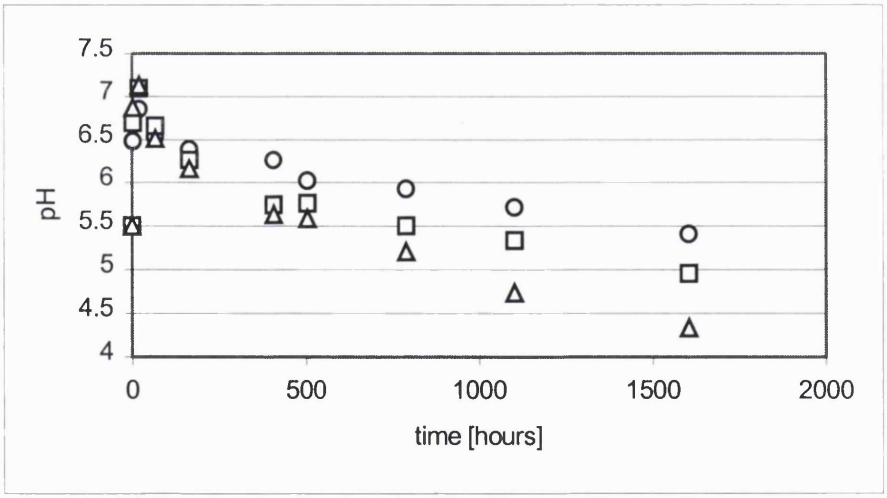

Figure 74: pH progress for o $Na_{26}K_5Ca_{24}P_{45}$ and ▫ $Na_{16}K_{15}Ca_{24}P_{45}$ Δ $Na_{11}K_{20}Ca_{24}P_{45}$

pH measurements for glasses with fixed CaO content of 28 mol%

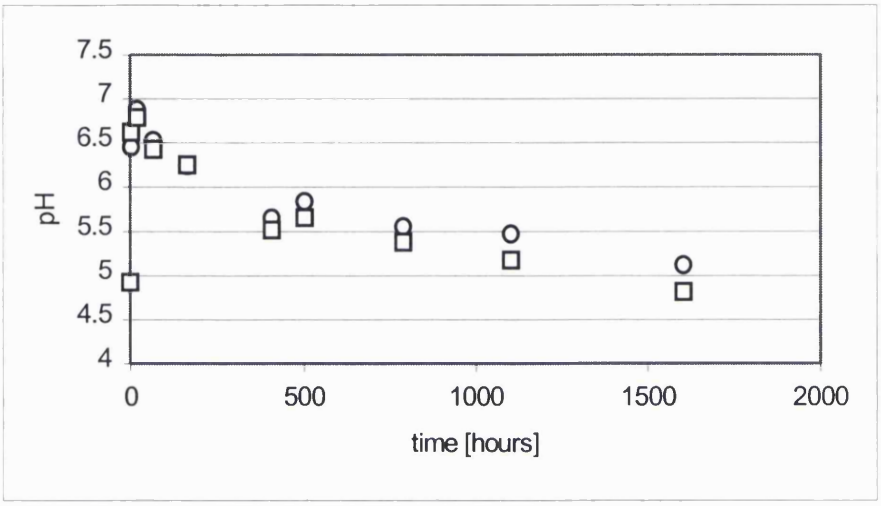

Figure 75: pH progress for o $Na_{22}K_5Ca_{28}P_{45}$ and ▫ $Na_7K_{20}Ca_{28}P_{45}$

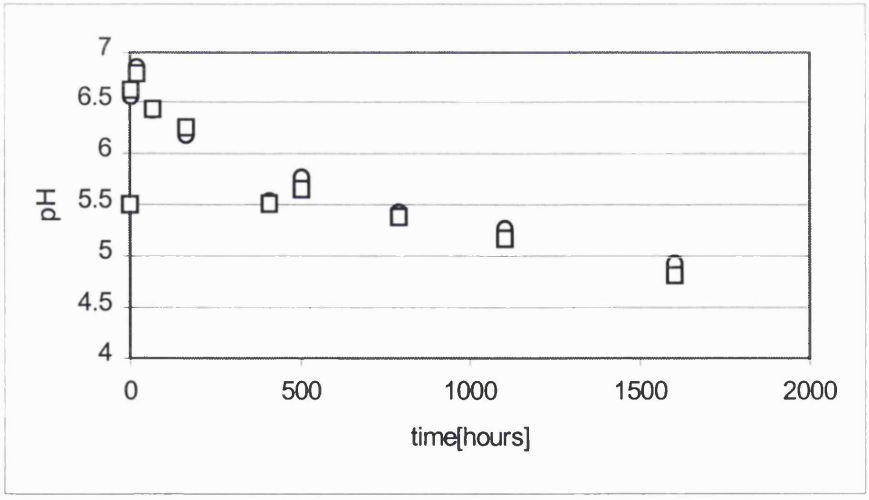

Figure 76: pH progress for o $Na_{17}K_{10}Ca_{28}P_{45}$ and ▫ $Na_{12}K_{15}Ca_{28}P_{45}$

pH measurement for glasses with fixed CaO content of 32 mol%

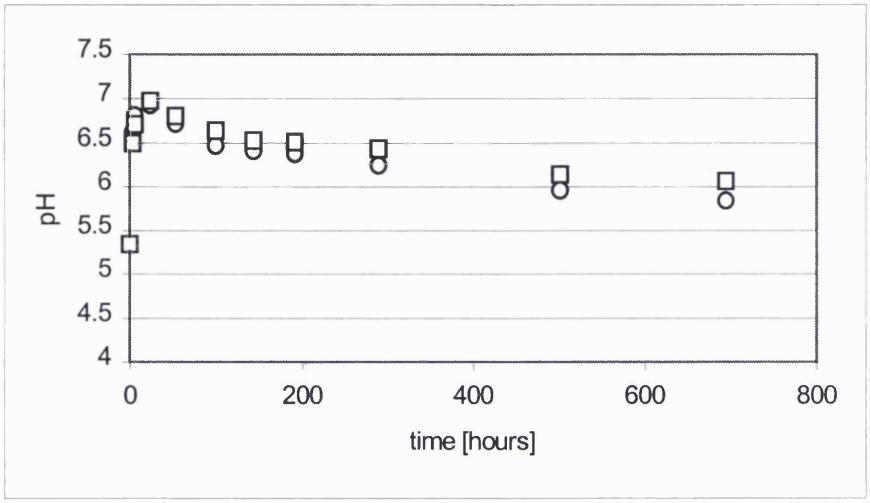

Figure 77: pH progress for o $Na_{20}K_3Ca_{32}P_{45}$ and ▫ $Na_5K_{18}Ca_{32}P_{45}$

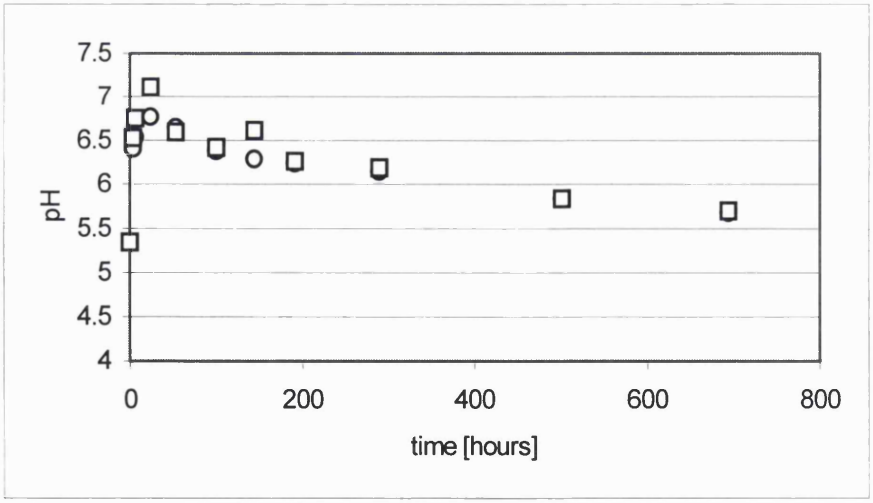

Figure 78: pH progress for o $Na_{15}K_8Ca_{32}P_{45}$ and ▫ $Na_{10}K_{13}Ca_{32}P_{45}$

pH values and progress for glasses with fixed CaO content of 24, 28 and 32 mol % were found similar to the ternary Na_2O-CaO-P_2O_5 glass system indicating an ion-exchange process, which was previously discussed for the Na_2O-CaO-P_2O_5 ternary system. Glasses with fixed CaO content of 20 mol% show the same trend with one abnormality of glass $Na_5K_{30}Ca_{20}P_{45}$. Here the pH is closer to neutral for extended measuring times.

8.1.2 Ion Measurements

Calcium measurements for glasses with fixed CaO content of 20 mol%

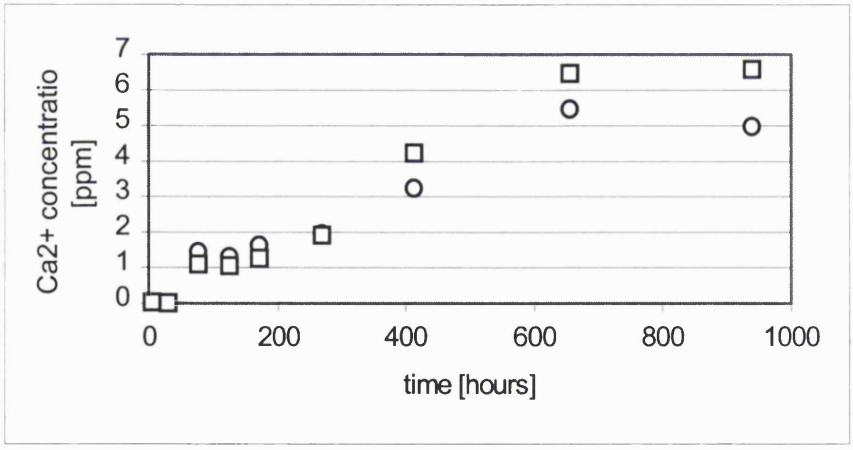

Figure 79: Ca^{2+} ion measurement for o $Na_{20}K_{15}Ca_{20}P_{45}$ and ▫ $Na_5K_{30}Ca_{20}P_{45}$

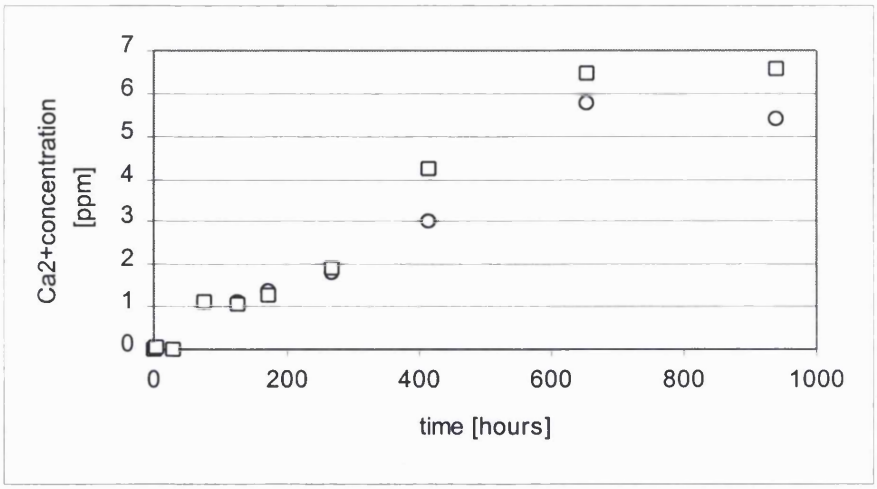

Figure 80: Ca^{2+} ion measurement for o $Na_{15}K_{20}Ca_{20}P_{45}$ and ▫ $Na_{10}K_{25}Ca_{20}P_{45}$

Ca^{2+} ion measurements for glasses with fixed CaO content of 24 mol%

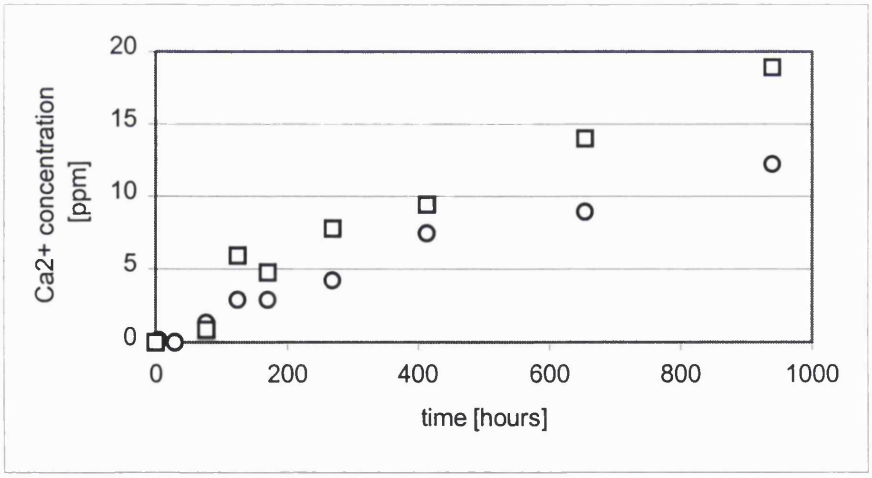

Figure 81: Ca^{2+} ion measurement for o $Na_{21}K_{10}Ca_{24}P_{45}$ and ▫ $Na_6K_{24}Ca_{24}P_{45}$

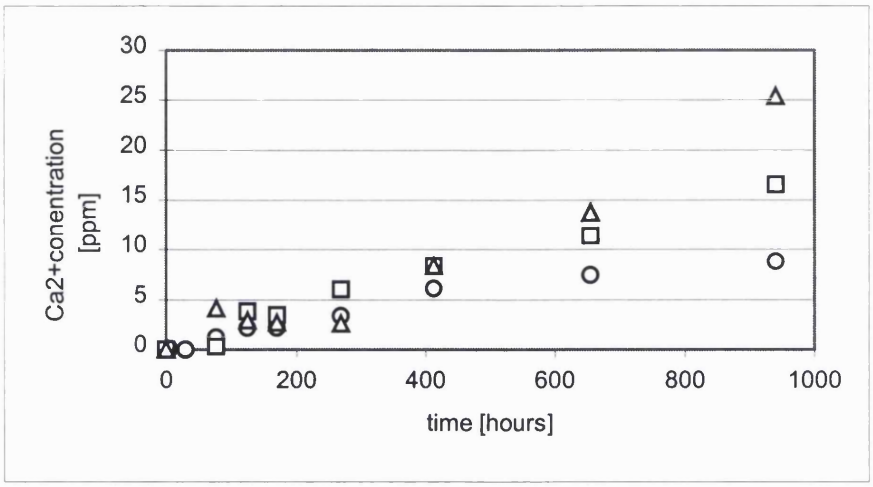

Figure 82: Ca^{2+} ion measurement for o $Na_{26}K_5Ca_{24}P_{45}$ ▫ $Na_{16}K_{15}Ca_{24}P_{45}$ and Δ $Na_{11}K_{20}Ca_{24}P_{45}$

The calcium ion releases for glasses with fixed CaO content of 20 and 24 mol% were found to be similar to the corresponding glasses of the ternary Na_2O-CaO-P_2O_5 glass system. The ion release curves mirror the weight loss curve, which is, for this level of CaO content (20 and 24 mol%), still linear.

Ca^{2+} ion measurements for glasses with fixed CaO content of 28 mol%

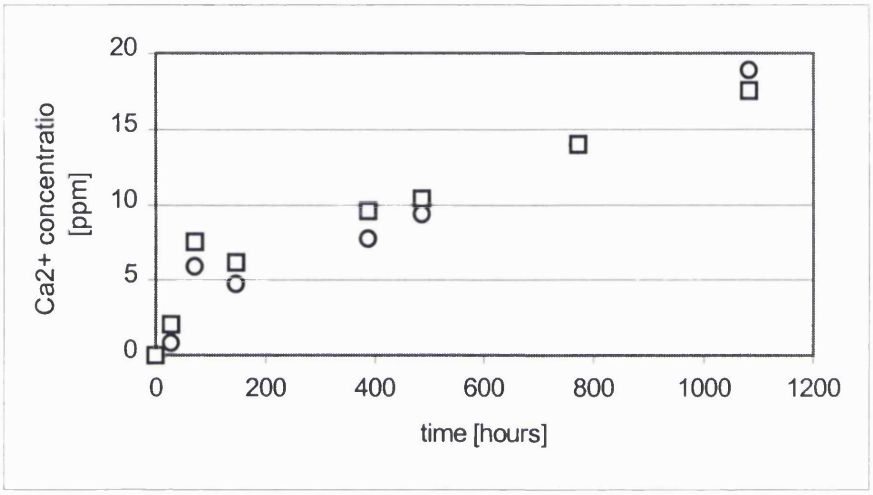

Figure 83: Ca^{2+} ion measurement for o $Na_{22}K_5a_{28}P_{45}$ and ▫ $Na_7K_{20}Ca_{28}P_{45}$

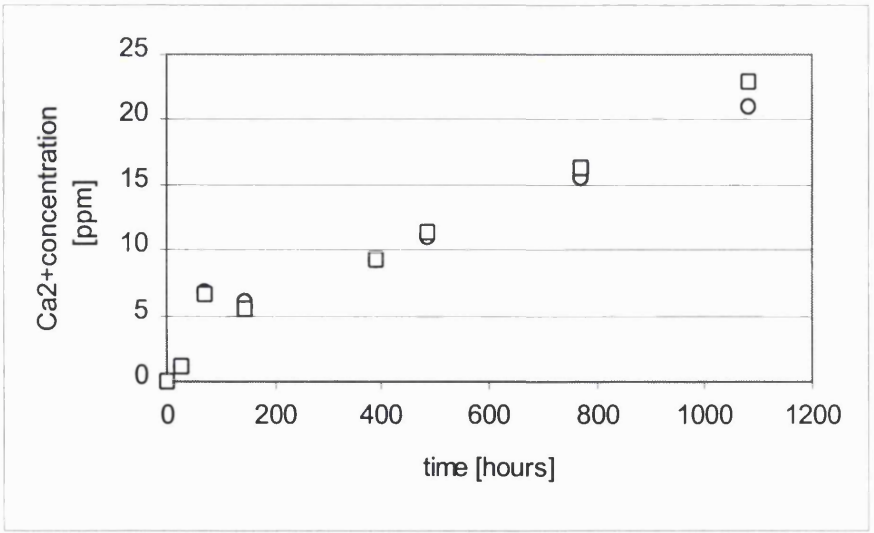

Figure 84: Ca^{2+} ion measurement for o $Na_{17}K_{10}Ca_{28}P_{45}$ and ▫ $Na_{12}K_{15}Ca_{28}P_{45}$

Figure 83 and figure 84 show calcium ion release, which represent an almost straight line for glasses with fixed CaO content of 28 mol%. This is not in accordance with glasses of the corresponding ternary Na_2O-CaO-P_2O_5 system. No apparent reason was found for this.

Ca^{2+}ion measurements for glasses with fixed CaO content of 32 mol%

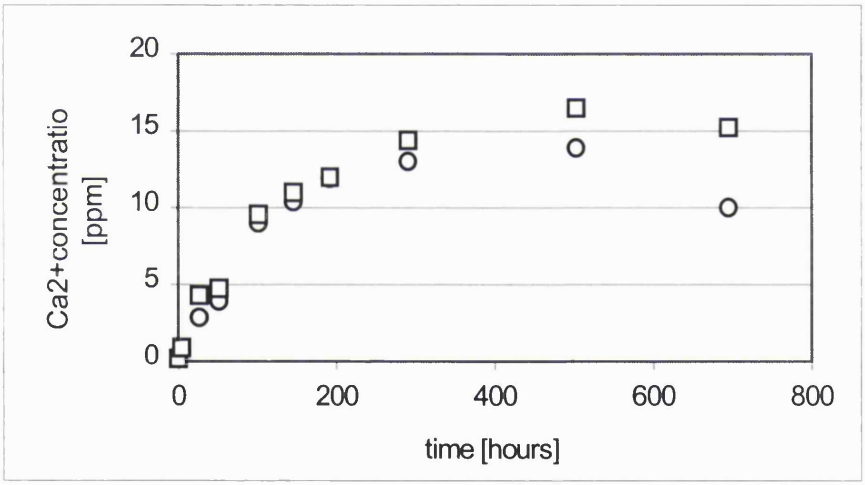

Figure 85: Ca^{2+} ion measurements for o $Na_{20}K_3Ca_{32}P_{45}$ and ▫ $Na_5K_{18}Ca_{32}P_{45}$

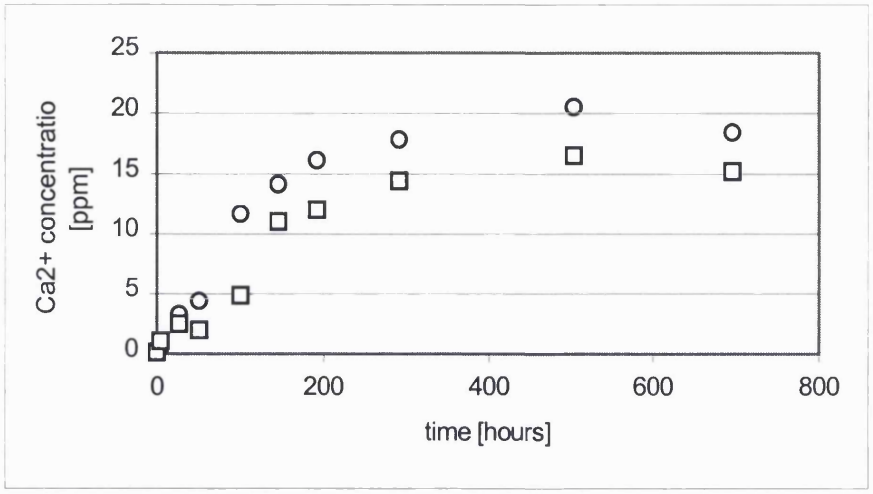

Figure 86: Ca^{2+} ion measurements for o $Na_{15}K_8Ca_{32}P_{45}$ and ▫ $Na_{10}K_{13}Ca_{32}P_{45}$

Figure 85 and figure 86 show Ca^{2+} ion release curves for glasses with fixed CaO content of 32 mol%, which are similar to counterpart glasses of the ternary Na_2O-CaO-P_2O_5 glass system. The ion release curve describes the exponential weight loss curve.

Na^+ ion measurements for glasses with fixed CaO content of 20 mol%

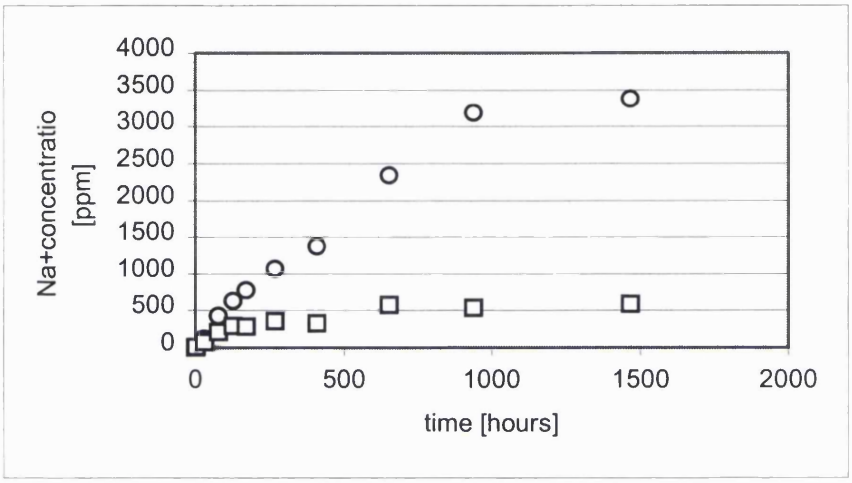

Figure 87: Na^+ measurement for o $Na_{20}K_{15}Ca_{20}P_{45}$ and ▫ $Na_5K_{30}Ca_{20}P_{45}$

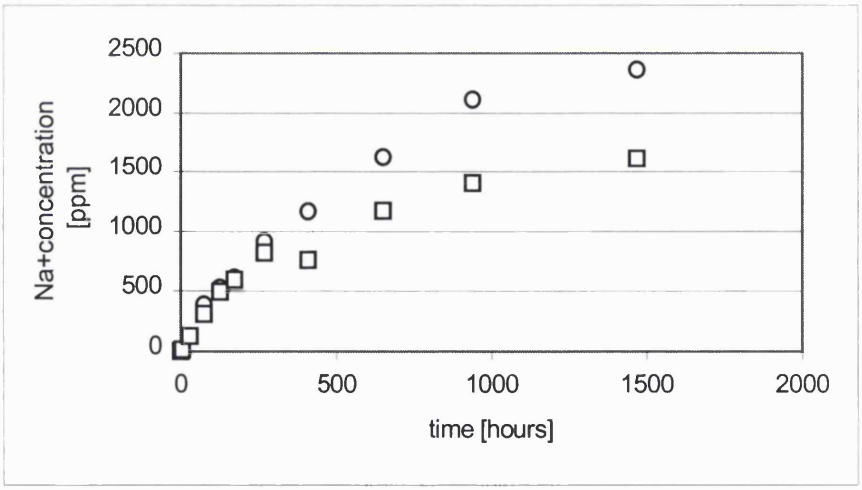

Figure 88: Na^+ ion measurement for o $Na_{15}K_{20}Ca_{20}P_{45}$ and ▫ $Na_{10}K_{25}Ca_{20}P_{45}$

Figure 87 and figure 88 show relatively linear sodium ion releases, similar to ion releases for the ternary counterpart glasses. However, total values for sodium ions are decreased because of the sodium substitution.

Na^+ ion measurement for glasses with fixed CaO content of 24 mol%

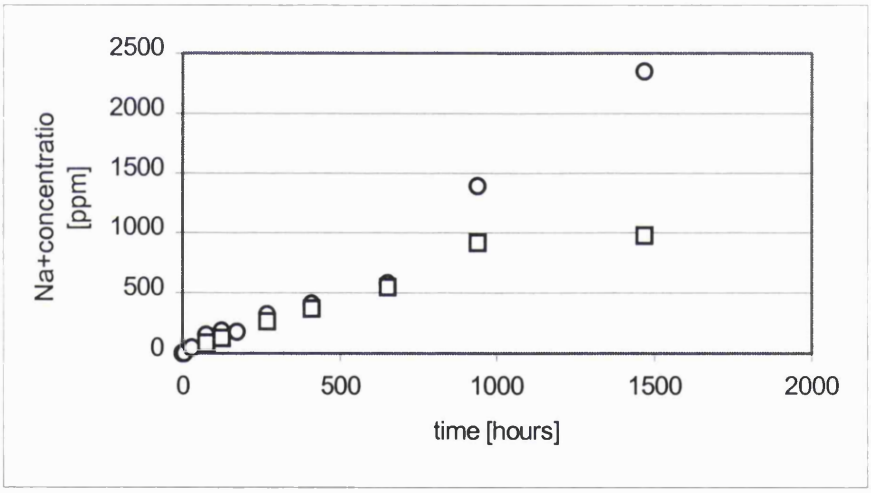

Figure 89: .Na^+ ion measurements for o $Na_{21}K_{10}Ca_{24}P_{45}$ and ▫ $Na_6K_{24}Ca_{24}P_{45}$

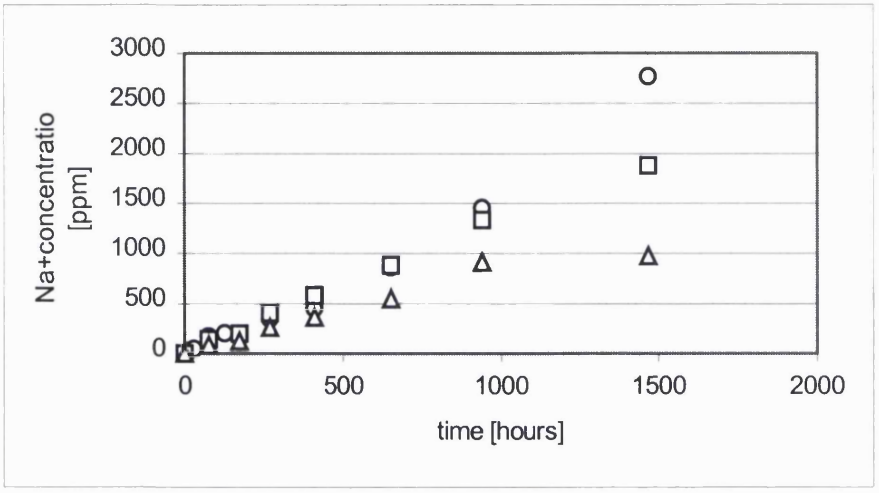

Figure 90: Na^+ ion measurement for o $Na_{26}K_5Ca_{24}P_{45}$, ▫ $Na_{16}K_{15}Ca_{24}P_{45}$ and Δ $Na_{11}K_{20}Ca_{24}P_{45}$

Na^+ ion measurement for glasses with fixed CaO content of 28 mol%

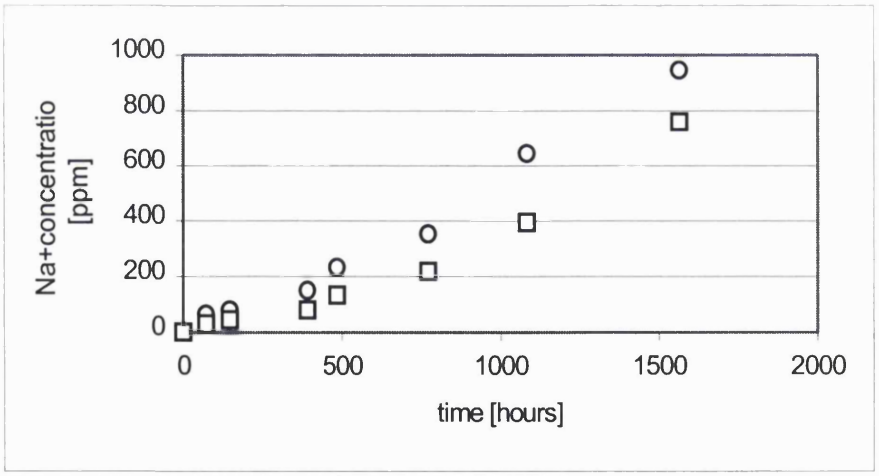

Figure 91: Na^+ ion measurements for o $Na_{22}K_5Ca_{28}P_{45}$ and ▫ $Na_7K_{20}Ca_{28}P_{45}$

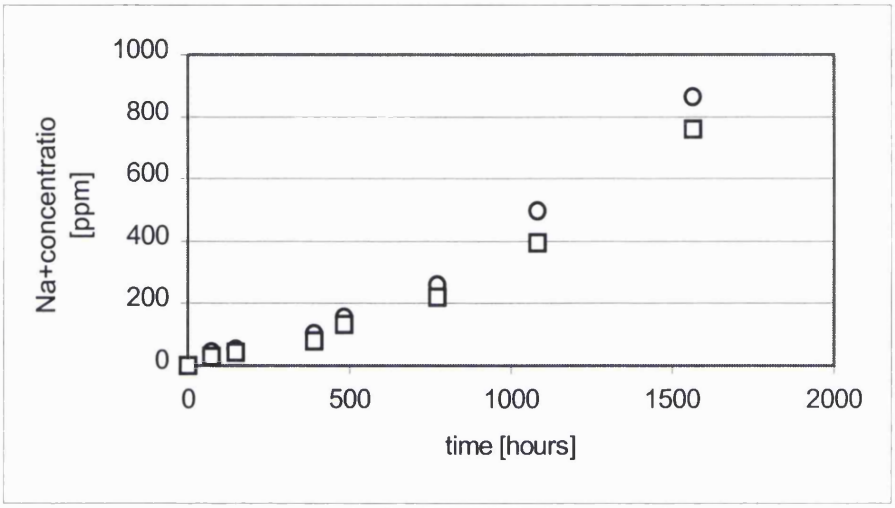

Figure 92: Na^+ ion measurement for o $Na_{17}K_{10}Ca_{28}P_{45}$ and ▫ $Na_{12}K_{15}Ca_{28}P_{45}$

Sodium ion release for glasses with fixed CaO content of 24 and 28 mol% were found to be similar to the counterpart glasses of the ternary Na_2O-CaO-P_2O_5 glass system and show a relatively linear release rate.

Na^+ ion measurement for glasses with fixed CaO content of 32 mol%

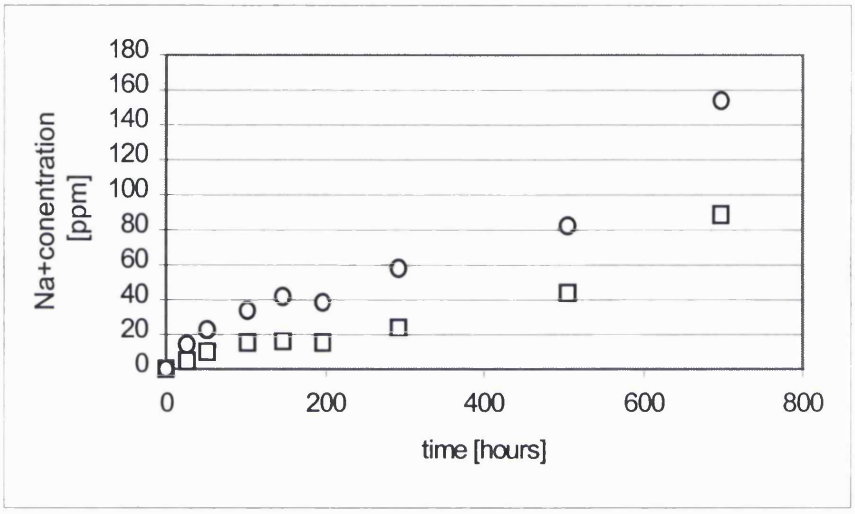

Figure 93: Na^+ ion measurement for o $Na_{20}K_3Ca_{32}P_{45}$ and ▫ $Na_5K_{18}Ca_{32}P_{45}$

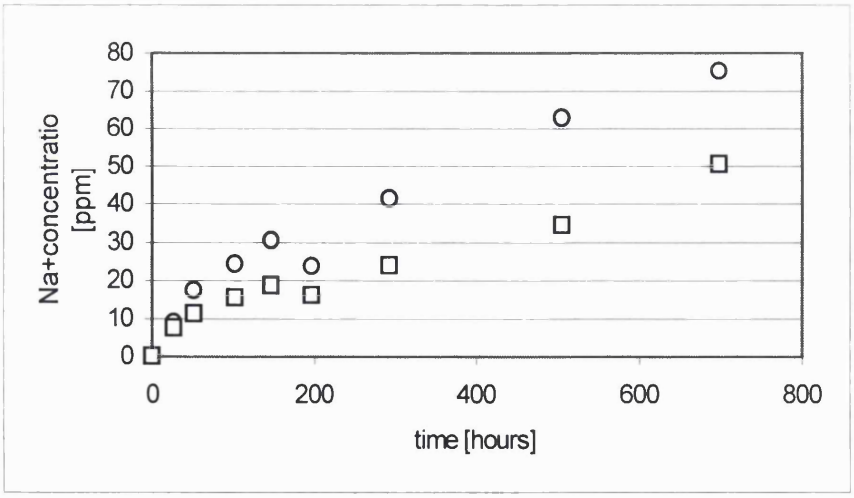

Figure 94: Na^+ ion measurement for o $Na_{15}K_8Ca_{32}P_{45}$ and ▫ $Na_{10}K_{13}Ca_{32}P_{45}$

Figure 93 and figure 94 show linear ion releases, which is similar to the counterpart glasses of the ternary Na_2O-CaO-P_2O_5 glass system.

8.2 Discussion

Solubility curves were found to be similar to the ternary Na_2O-CaO-P_2O_5 system. At around 20 mol% CaO curves starting to show a slight exponential weight loss behaviour which is similar to both ternary Na_2O-CaO-P_2O_5 and K_2O-CaO-P_2O_5 glass systems. This trend was found to be the same for the quaternary Na_2O-K_2O-CaO-P_2O_5 system.

Change in solubility with potassium oxide content

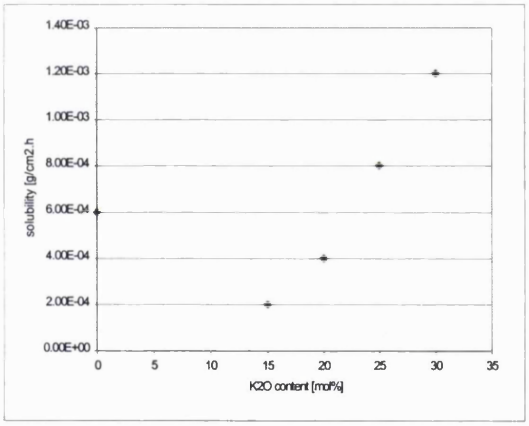

Figure 95: CaO content 20mol%

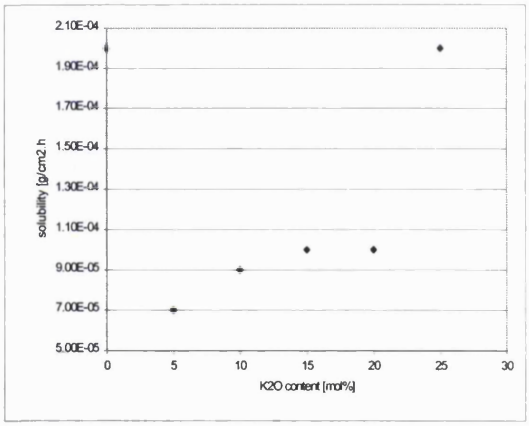

Figure 96: CaO content 24 mol%

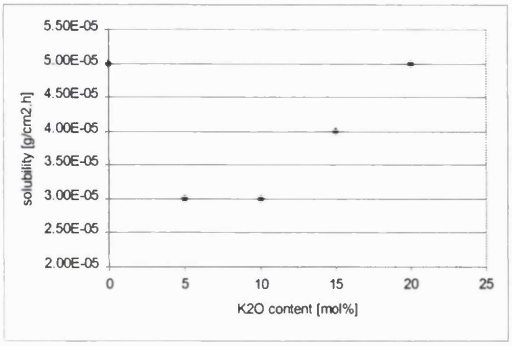

Figure 97: CaO content 28 mol%

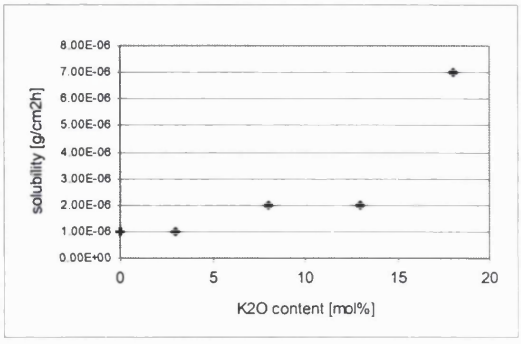

Figure 98: CaO content 32 mol%

Figure 95 to 98 plots the calculated solubility values against K_2O content for a fixed CaO content. With this way of plotting solubility it highlights that potassium can further affect the solubility. For the 20mol% CaO containing glasses, two trends can be seen here. (1) Small amounts of potassium will initially decrease the solubility, however, increasing the K_2O content then increases the solubility. For the glasses with 24 and 28 mol% CaO content this same trend can be observed. However, when the end point of potassium substitution is reached, the glasses do not show any difference in solubility values compared to the same glass with 0mol% Na_2O. The reason why this shift is seen is due to the effect of mixed alkaline ions, which diffuse at different rates through the glass structure. Potassium, being the larger ion will a.) be transported with a slower speed through and out of the glass network and b.) as the potassium ion (K 39.098 g/mol) is leaching completely out of the glass structure, the measured weight loss will be higher in comparison to the effect of the lighter sodium ion (Na 22.989 g/mol).

It should be noted that for the glasses with 20, 24 and 28 mol.% the levels of K_2O can equal and in some cases exceed the CaO content. However, for the glasses with 32 mol% CaO, compositional limits are reached and the upper limit for K_2O content is 18 mol%. Thus the major weight loss effect comes from the gradual breakdown of the glass structure and not from an ion exchange process.

pH values were again found to be similar to the ternary system. pH values show significant initial increases and decrease towards neutral for longer measuring times. This effect is strongest for glasses with the lowest CaO content. This feature reflects the ion exchange process (see ternary system Na_2O-CaO-P_2O_5). One event which can

be observed is that, in general, glasses with higher potassium oxide content have slightly higher pH decreases than glasses with less K_2O. One abnormality is glass $Ca_{20}Na_5K_{30}P_{45}$, which has the highest potassium content of all prepared glasses in this system. It showed a reduced change in pH and values are more neutral than found for any other glass. However, it is not clear if the highest potassium content is the reason for this finding.

As was performed for the ternary Na_2O-CaO-P_2O_5 system, the glasses with fixed CaO content of 28 mol.% and an Na_2O:K_2O ratio of 4.4 and 0.35, the Na+ and Ca^{2+} ion measurements have been plotted against $t^{1/2}$ to try and explain whether an ion-exchange process is taking place.

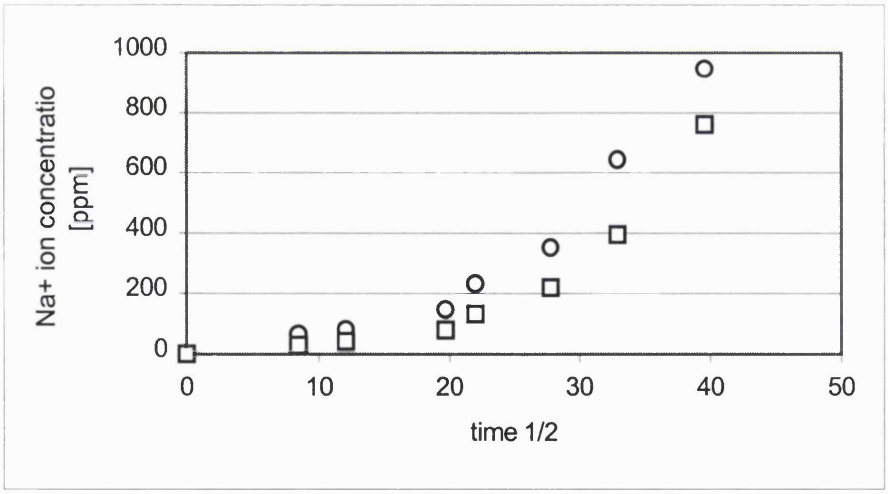

Figure 99: Ion concentration plotted against $t^{1/2}$ for o $Na_{22}K_5Ca_{28}P_{45}$ and ▫ $Na_7K_{20}Ca_{28}P_{45}$

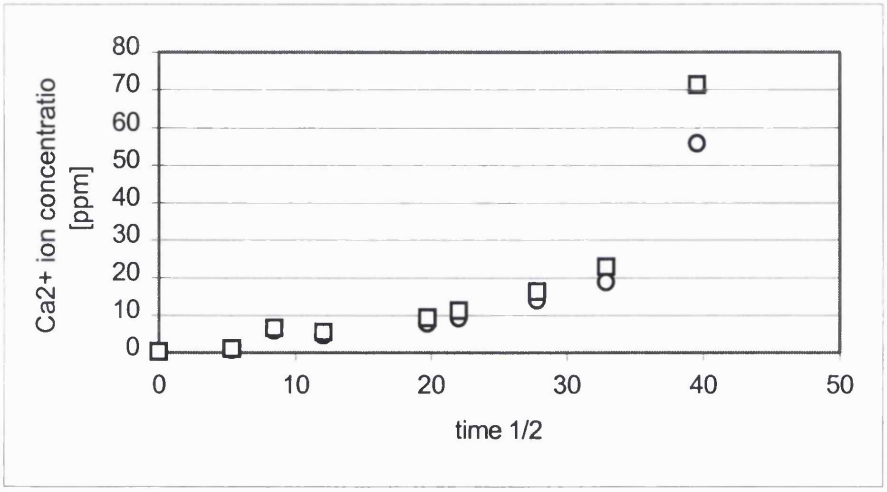

Figure 100: Ion concentration plotted against $t^{1/2}$ o $Na_{22}K_5Ca_{28}P_{45}$ and ▫ $Na_7K_{20}Ca_{28}P_{45}$

These plots reflect a difference compared to the ternary system. For the ternary system, only the plot for sodium ion measurement followed a rule of $t^{1/2}$ (see figure 47), this was not really observed for the calcium ion measurement (see figure 46). For this quaternary system however, the calcium measurement follows a similar trend as the sodium ion measurements and it might be possible to fit a line through some data points. This would indicate that there is an ion-exchange process for both ions.

Chapter 9

Quaternary system Na_2O-CaO-MgO-P_2O_5

NaH_2PO_4, $CaCO_3$, $MgCO_3$ and P_2O_5 precursors were used for this glass system. Chemical compositions were obtained via previous calculation methodology. Glasses were prepared using general glass making procedures detailed previously. The glass compositions were made such that the P_2O_5 content was kept fixed as was the Na_2O content and the CaO:MgO ratio was varied.

Glass code	CaO content (mol%)	MgO content (mol%)	Na_2O content (mol%)	P_2O_5 content (mol%)
$Ca_{30}Mg_2Na_{23}P_{45}$	30	2	23	45
$Ca_{25}Mg_7Na_{23}P_{45}$	25	7	23	45
$Ca_{20}Mg_{12}Na_{23}P_{45}$	20	12	23	45
$Ca_{15}Mg_{17}Na_{23}P_{45}$	15	17	23	45
$Ca_{10}Mg_{22}Na_{23}P_{45}$	10	22	23	45

Table 14: Glass composition with oxide contents

Glass code	Melting temperature and time (^{0}C/Hours)	Casting temperatures (^{0}C/Hours)	Result
$Ca_{30}Mg_2Na_{23}P_{45}$	1200/3	350/1	Glass, stress free
$Ca_{25}Mg_7Na_{23}P_{45}$	1200/3	350/1	Glass, stress free
$Ca_{20}Mg_{12}Na_{23}P_{45}$	1200/3	350/1	Glass, stress free
$Ca_{15}Mg_{17}Na_{23}P_{45}$	1200/3	350/1	Glass, stress free
$Ca_{10}Mg_{22}Na_{23}P_{45}$	1200/3	350/1	Glass, stress free

Table 15: Melting and casting temperatures

At either end of the CaO:MgO compositional ratio spectrum, attempts to increase CaO or MgO content were unsuccessful due to spontaneous crystallisation of the glass. Because of this consequence, only a very small compositional range in this Na_2O-CaO-MgO-P_2O_5 glass system is presented in this chapter.

Because of the relative ease with which crystallisation occurred, great care was taken in terms of casting temperatures. For this system, if the casting temperature was too close to the glass crystallisation temperature (T_c) crystallisation occurred. Thus to optimise the glass forming process, the T_g was measured for the glass and was found to be around 500°C and the casting temperature was chosen to be much lower than this. 350°C was chosen as this gave non-crystalline materials with little residual stress. This casting temperature was (relative to the T_g for these glasses) much lower than other systems.

9.1 Solubility Test Results

As the number of glasses made in this system is much reduced, all the data will be presented for all five glasses.

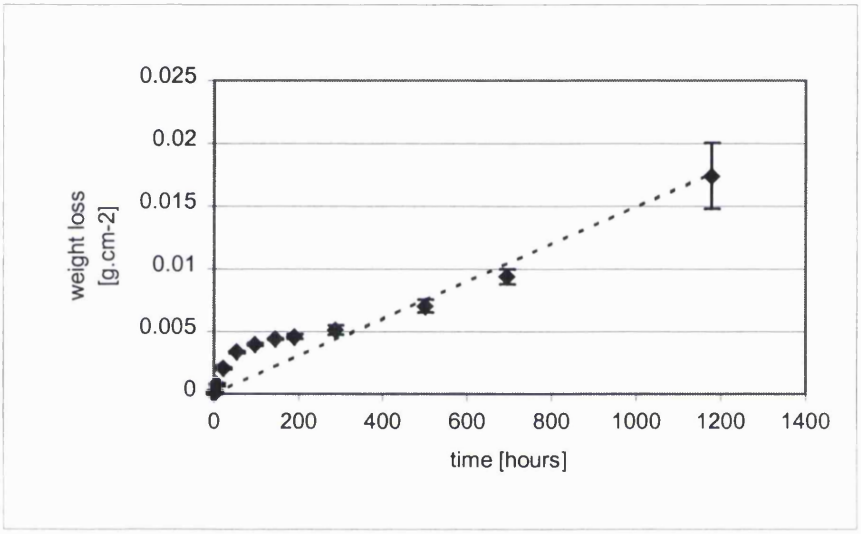

Figure 101: Solubility plot for $Ca_{30}Mg_2Na_{23}P_{45}$

The solubility figure is very much similar to the corresponding sodium based ternary system ($Ca_{32}Na_{23}P_{45}$). It shows the exponential nature of the weight loss.

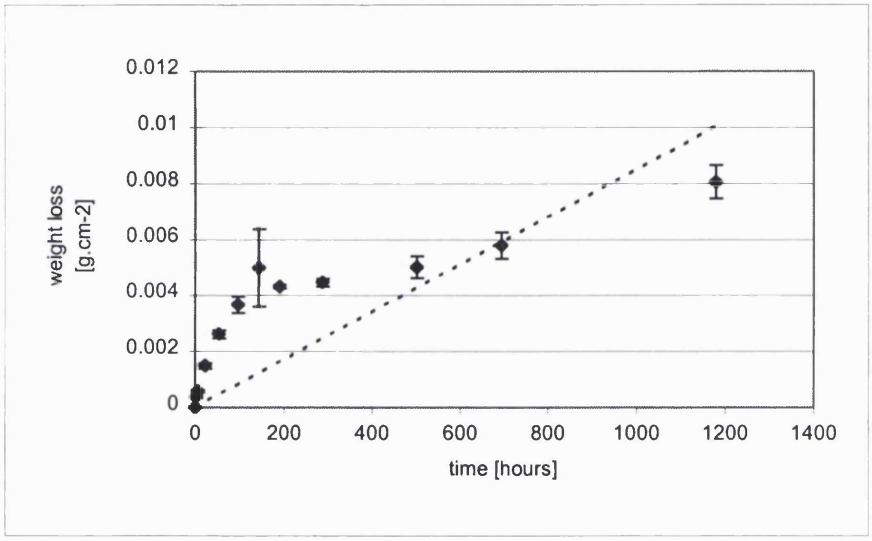

Figure 102: Solubility plot for $Ca_{25}Mg_7Na_{23}P_{45}$

Here again, the exponential nature of the weight loss is clearly seen.

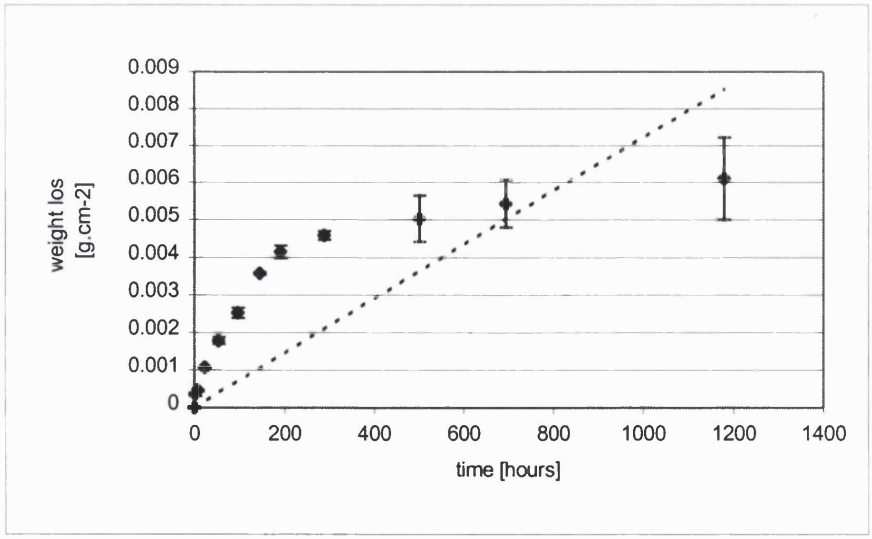

Figure 103: Solubility plot for $Ca_{20}Mg_{12}Na_{23}P_{45}$

The weight loss behaviour begins to change slightly for this glass composition. The curve starts to flatten and becomes less exponential.

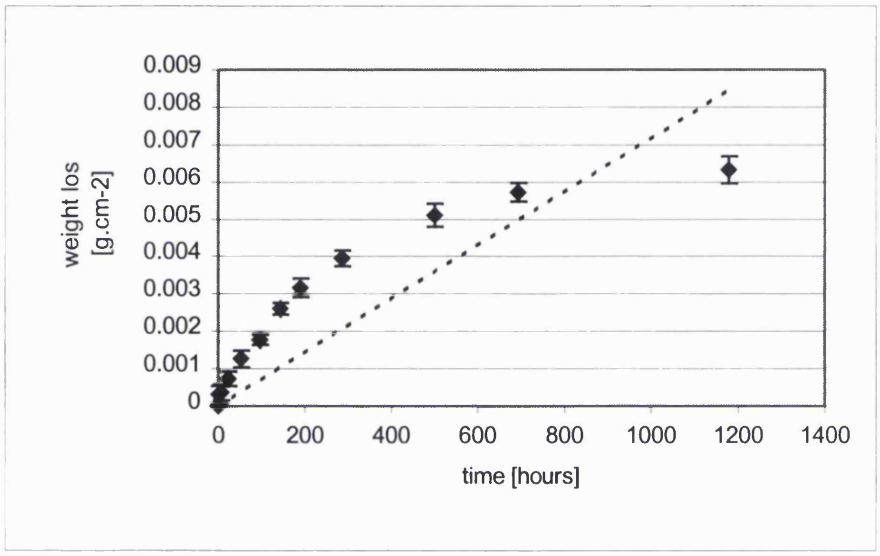

Figure 104: Solubility plot for $Ca_{15}Mg_{17}Na_{23}P_{45}$

For this glass composition (Figure 104) an even lesser exponential curve can be seen in this plot.

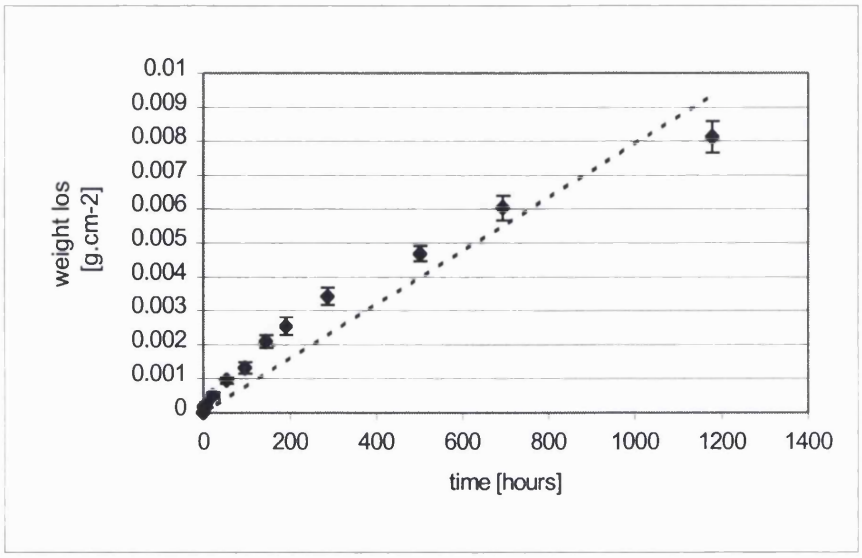

Figure 105: Solubility plot for $Ca_{10}Mg_{22}Na_{23}P_{45}$

At the end of the spectrum with only 10 mol% CaO and consequently the highest MgO content, the weight loss curve is almost linear and has lost its exponential nature.

Glass code	Solubility [$g.cm^{-2}.h^{-1}$]
$Ca_{30}Mg_2Na_{23}P_{45}$	2.0E-06
$Ca_{25}Mg_7Na_{23}P_{45}$	9.0E-06
$Ca_{20}Mg_{12}Na_{23}P_{45}$	7.0E-06
$Ca_{15}Mg_{17}Na_{23}P_{45}$	7.0E-06
$Ca_{10}Mg_{22}Na_{23}P_{45}$	8.0E-06

Table 16: Overview of solubilities for quaternary system CaO- MgO-Na_2O-P_2O_5

It can be seen from the plots that the non-linearity/linearity of the weight loss nature can change with increasing MgO content. The more CaO is replaced by MgO the more

linear the weight loss curve gets. This lead to the assumption that the calcium oxide places the major part and therefore has a greater impact on the weight loss process than for example magnesium oxide.

For the following pH and ion measurements, data will be presented for glasses with a fixed P_2O_5 and Na_2O content and varying CaO:MgO ratio. The first figure represents a glass with low and very high CaO:MgO ratio to highlight the difference, followed by glasses with all other ratios.

9.2 pH Measurements

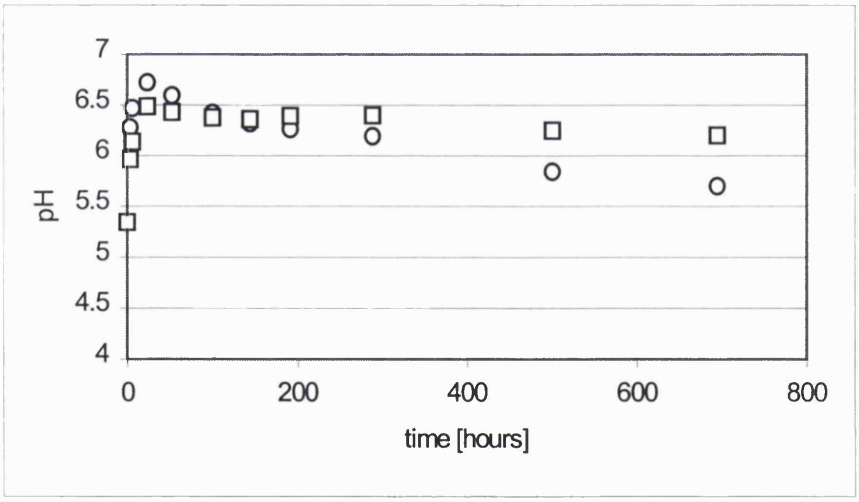

Figure 106: pH measurement for o $Ca_{30}Mg_2Na_{23}P_{45}$ and ▫ $Ca_{10}Mg_{22}Na_{23}P_{45}$

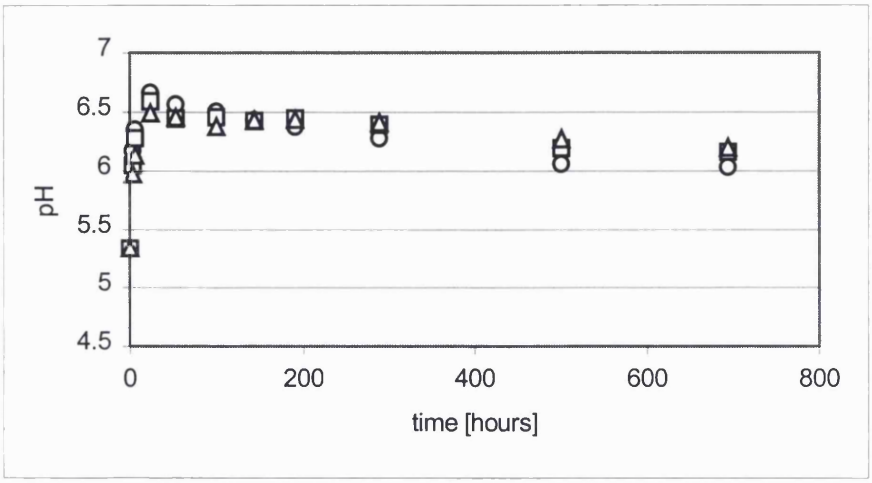

Figure 107: pH measurement for o $Ca_{25}Mg_7Na_{23}P_{45}$, ▫ $Ca_{20}Mg_{12}Na_{23}P_{45}$ and Δ $Ca_{15}Mg_{17}Na_{23}P_{45}$

9.3 Ion Measurements

Ca^{2+} ion measurements

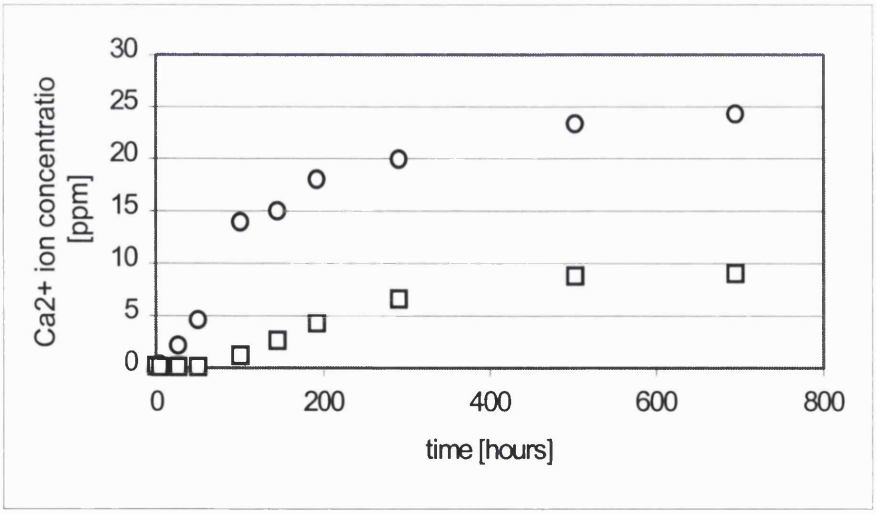

Figure 108: Ca^{2+} ion measurement for o $Ca_{30}Mg_2Na_{23}P_{45}$ and ▫ $Ca_{10}Mg_{22}Na_{23}P_{45}$

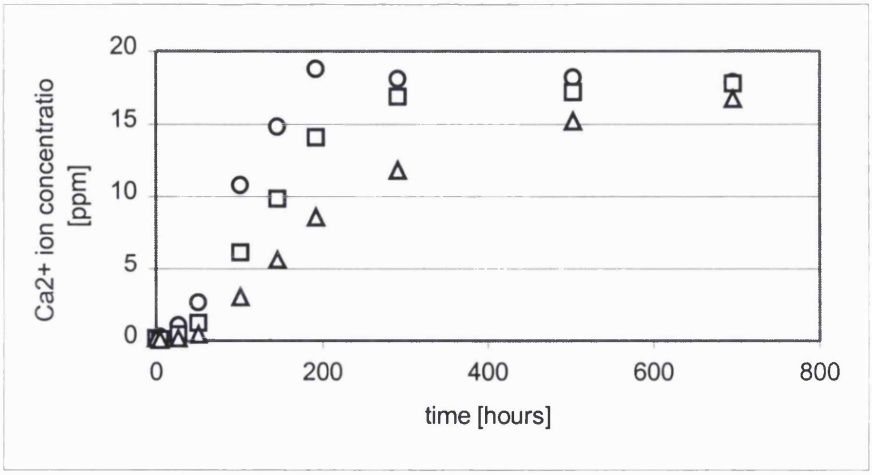

Figure 109: Ca^{2+} ion measurement for o $Ca_{25}Mg_7Na_{23}P_{45}$, ▫ $Ca_{20}Mg_{12}Na_{23}P_{45}$ and Δ $Ca_{15}Mg_{17}Na_{23}P_{45}$

The Ca^{2+} leaching process (figure 108 and 109) is similar to previous findings, the Ca^{2+} ions mirroring the weight loss process; the higher the CaO content the more the curve becomes exponential in nature.

Na^+ ion measurements

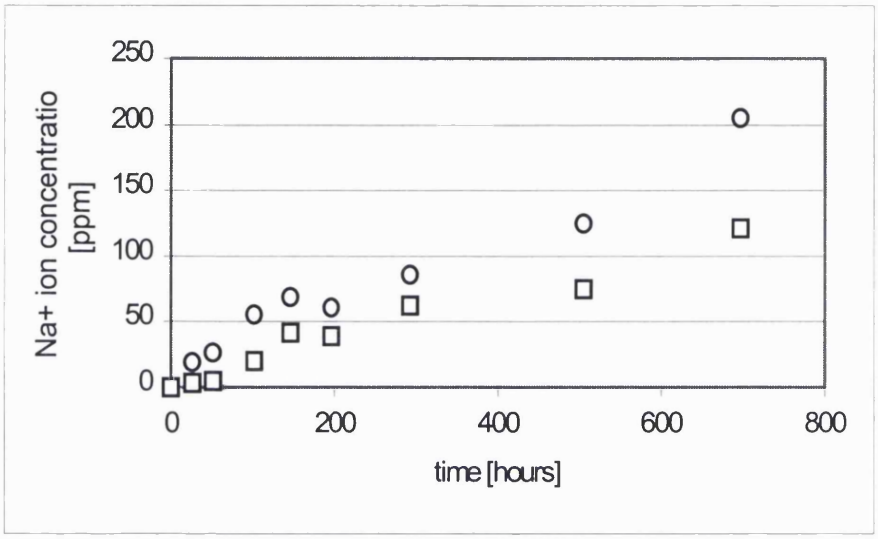

Figure 110: Na^+ ion measurement for o $Ca_{30}Mg_2Na_{23}P_{45}$ and ▫ $Ca_{10}Mg_{22}Na_{23}P_{45}$

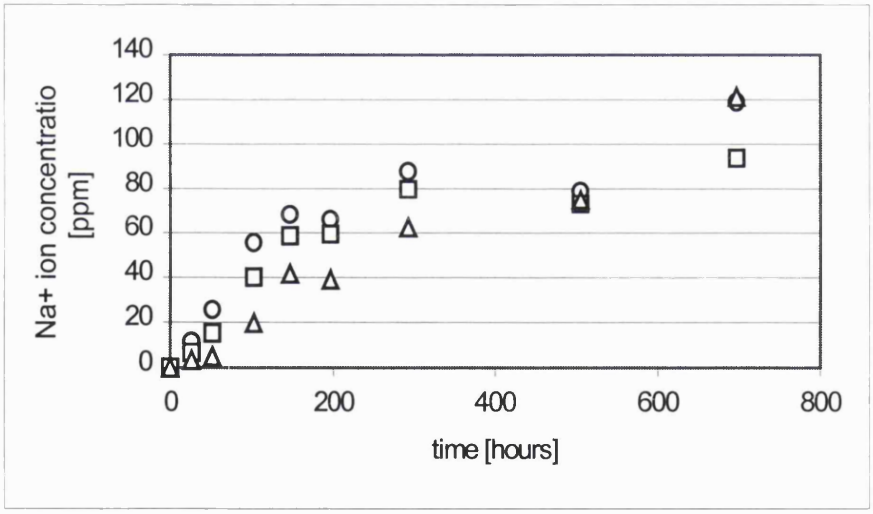

Figure 111: Na^+ ion measurement for o $Ca_{25}Mg_7Na_{23}P_{45}$, ▫ $Ca_{20}Mg_{12}Na_{23}P_{45}$ and Δ $Ca_{15}Mg_{17}Na_{23}P_{45}$

Similar findings are seen for these Na^+ ion measurement curves (figure 110 and 111), with ion concentration increasing almost linearly with time.

9.4 Discussion

This system study was carried out by systematically replacing calcium oxide with magnesium oxide to determine the effect of replacing an ion with one of the same valence, but with a differing ionic radius and to determine how this affects the solubility behaviour. It clearly demonstrates that the CaO content plays a major contribution in terms of solubility behaviour. It can be seen from the curves that by systematically replacing CaO with MgO, the solubility curves lose their exponential nature. This might be deduced as evidence that CaO makes a significant contribution to controlling the solubility process more than for example sodium oxide or potassium oxide. This system has been calculated as 32 mol% of 2^+ valence oxide in total. A $Ca_{32}Na_{23}P_{45}$ ternary glass has a solubility value of 1.00 x $10^{-}06$ $g.cm^{-2}.h^{-1}$, which is lower (dissolves less quickly) than the glasses of the corresponding magnesium quaternary system. This effect can not necessarily be explained by the fact of Mg^{2+} being the lighter ion (Ca 40.1g/mol Mg 24.3g/mol) (24). If that would be the case solubility values should be smaller. It might be the case that the magnesium ion is smaller and hence is able to leach through and out of the glass structure more easily and therefore account for the higher weight loss and higher number.

However, it was found to be unrealistic to just compare this system with the ternary system simply by comparing solubility values based on their divalent oxide content. For example within the ternary system values varying from "too fast to measure"

(CaO 10mol%) to 1.00 x 10^{-6} $g.cm^{-2}.h^{-1}$ (CaO 32mol%). Within the quaternary system this effect has not been observed.

pH

The pH progress with time was found to be similar to other systems. However, the glass with the highest MgO content shows the lesser decrease in pH even for longer time periods.

Ion measurements

Both ion measurements were found to be expected and are very similar to other glass systems. Again, lower CaO content show less exponential ion concentration curves, higher CaO containing glasses show a more exponential figure which then reflects the weight loss curves.

Chapter 10

10.1 Fluoride System $CaO-Na_2O-CaF_2-P_2O_5$

10.1.1 Preparation

Preliminary experiments were carried out to produce fluoride containing glasses.

Glass code	CaO Mol%	Na_2O Mol%	P_2O_5 Mol%	CaF_2 Mol%	NaF Mol%
1	35	15	45	5	/
2	30	15	45	10	/
3	25	15	45	15	/
4	20	15	45	20	/
5	/	35	50	/	15
6	/	35	50	15	/
7*	/	40	40	20	/
8*	/	30	30	40	/
9*	/	35	35	30	/

Table 17: Preliminary compositions attempted
*For this system the phosphate precursor was changed to $(NaPO_3)_x$.

For all glass with codes 1-6, incorporation of fluoride failed if the level of H^+ ions was too high. This was because during melting, H^+ will easily bond with F^- to give HF,

which is highly volatile. Therefore, P_2O_5 had to be avoided because of its hygroscopic nature. Also NaH_2PO_4 will release H_2O, which can react with fluoride to form HF.

Attempts with NaH_2PO_4 in combination with NaF and CaF_2 failed to incorporate fluoride. Quantitative F^- ion measurements with fluoride selective electrodes (Orion) have shown that for code No 5, a 10 ppm calculated solution of the dissolved glass had a reading of 0.056ppm, a 100 ppm calculated solution of the dissolved glass gave a 0.076 ppm reading. Codes 1-4 gave similar findings. Code 6 gave a 0.59 ppm reading for a 100 ppm calculated solution. These findings showed that no matter how high the amount of P_2O_5, CaF_2 or NaF were, the reading of fluoride never matched the calculated amount of fluoride. Also, no changes were seen whether fluoride precursors NaF or CaF_2 was used. In addition tests have been repeated with the use of EDTA as an ion-complex material to check if any ion interference is occurring. But no change was found.

Only the use of the polymer $(NaPO_3)_x$ was successful. Glasses with codes 7-9 gave readings around 80-90 ppm for 100ppm calculated solutions. The advantage of this material is that no decomposition and loss of H_2O or H_2 occurs during melting and thus, the only route for moisture absorption will be at the surface. Because of this, CaF_2 was placed at the bottom of the crucible and covered by the other precursor chemicals. It was found that by using this method, even small amounts of P_2O_5 could be used without too much fluoride loss.

Therefore, this system has been made from $(NaPO_3)_x$, P_2O_5, $CaCO_3$ and CaF_2.

Glass code	CaO content (mol %)	Na_2O content (mol%)	P_2O_5 content (mol%)	CaF_2 content (mol%)
1	0	35	35	30
2	0	40	40	20
3	0	45	45	10
4	30	27,5	37,5	5
5	25	27,5	37,5	10
6	25	32.5	37,5	5

Table 18: Glass codes and chemical compositions

Glass code	Melting temperature and time (^{0}C/Hours)	Casting temperatures (^{0}C/Hours)	Result
1	1050/3	320/1	Glass, stress free
2	800/3	320/1	Glass, stress free
3	800/3	370/1	Glass, stress free
4	1150/3	400/1	Glass, milky
5	1150/3	420/1	Glass, stress free
6	1150/3	400/1	Glass, brittle

Table 19: Melting and casting temperatures

10.1.2 Solubility Test for Fluoride Glasses

Having produced a range of glasses, a number of further problems were encountered. Glasses with codes 1,2 and 3 were tested, but were found to have a very high solubility. Glass code No 6 was found to be too brittle for further testing and this was attributed to the high levels of network modifying oxides. Re-melting and re-casting at different temperatures failed. These glasses have not been considered for further testing. Therefore only glasses with code 4 and 5 have been finally tested; tests have been carried out in distilled water as described previously.

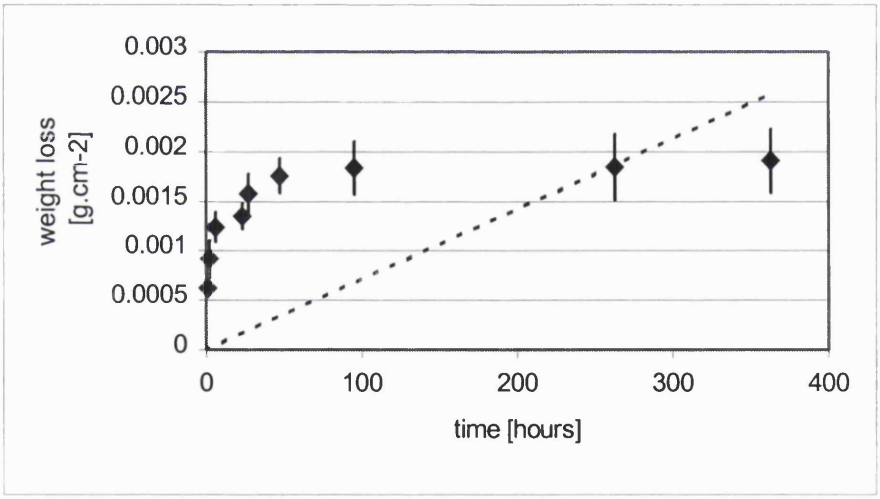

Figure 112: Solubility test for code 4

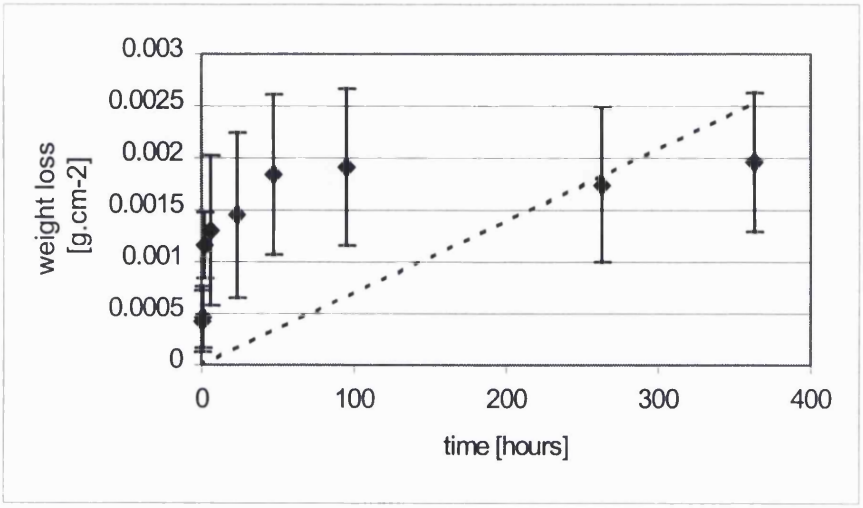

Figure 113: solubility plot for code 5

Glass code	Solubility [$g.cm^{-2}.h^{-1}$]
4	7.0×10^{-6}
5	7.0×10^{-6}

Table 20: Solubilities for code 4 and code 5

Glasses with codes 1,2 and 3 dissolved very rapidly which was similar to the rate seen for glasses in the ternary Na_2O-CaO-P_2O_5 glass system with CaO contents of 8 and 10 mol%. The reason why glasses 1, 2 and 3 dissolve too quickly might be the missing CaO content, however this was surprising as the reduced CaO content was balanced by the presence of CaF_2 in which fluoride delivers the negative charge instead of the oxygen. For the rest of the tested glasses it can be seen that both glasses show have

identical solubility values, which are, with respect to the CaO content of the glasses, slightly higher compared to previous systems.

It can be said from the preliminary study of this system that even if compositions are comparable to other systems with different precursors, the solubility values are altered. This might be explained by the use of a different precursor $(NaPO_3)_x$ instead of a combination of P_2O_5, NaH_2PO_4 and $CaCO_3$. The presence of the fluoride may also be significantly affecting the network connectivity.

More tests should be carried out to verify this unambiguously.

10.1.3 Ion Measurements

The fluoride ion measurement was done according to other already established ion measurement protocols.

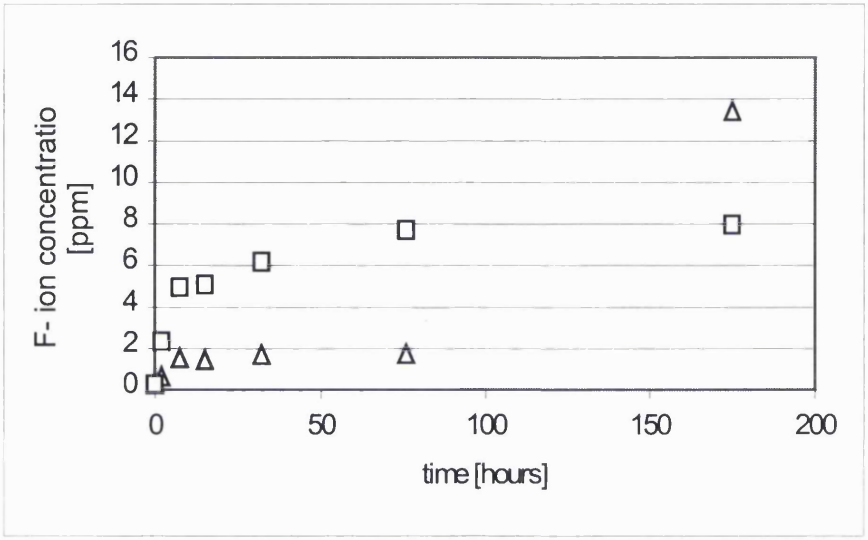

Figure 114: F^- ion measurements for Δ code 4 ▫ code 5

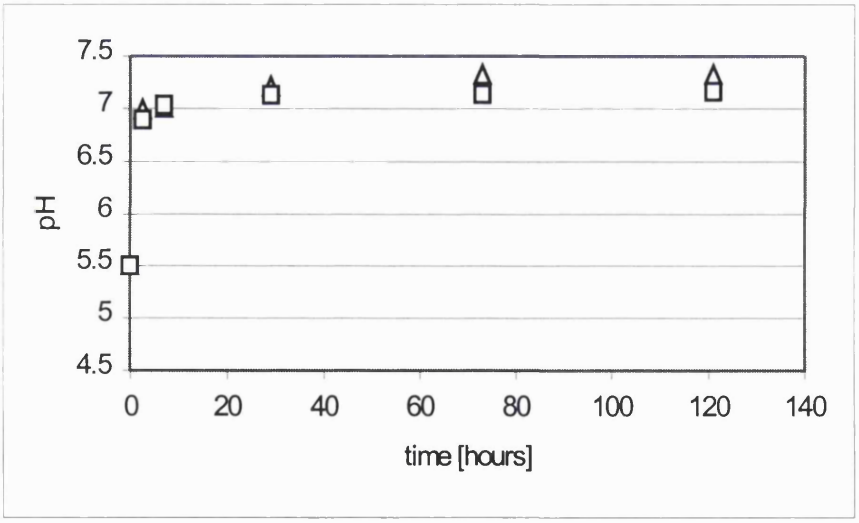

Figure 115: pH measurements for Δ code 4 ▫ code 5

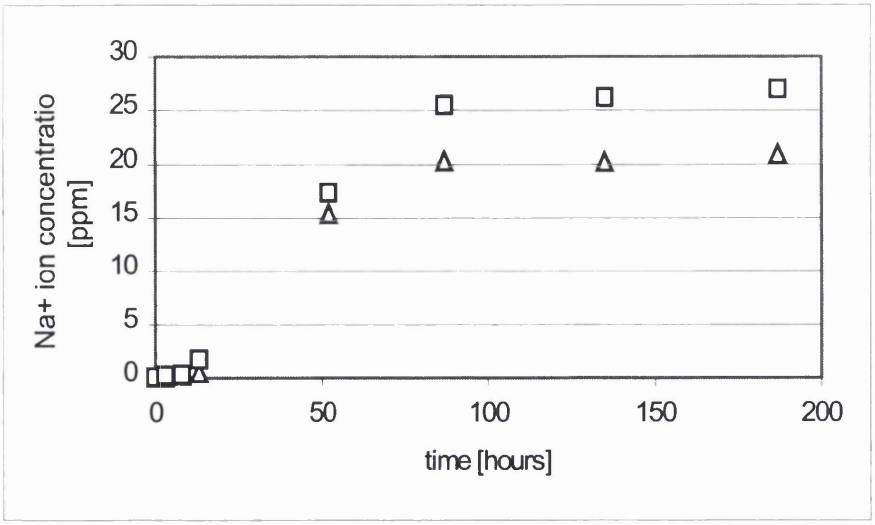

Figure 116: Ca^{2+} ion measurements for Δ code 4 ▫ code 5

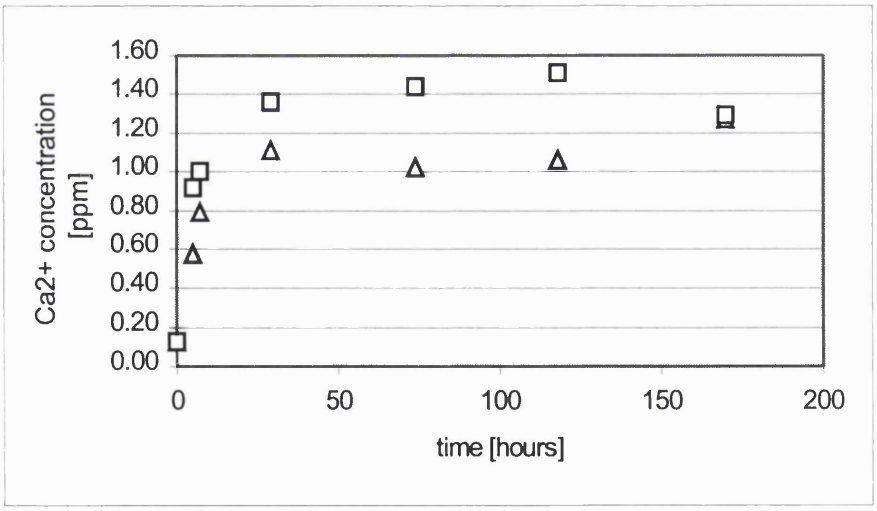

Figure 117: Na^{+} ion measurements for Δ code 4 ▫ code 5

10.1.4 Discussion

Solubility curves have been found to have similar trends to those previously seen. However the curves appear to be much more extreme. The fitting of a straight line for calculation of the solubility was found unrealistic and has been fitted as an approximation (grey line), similar to the ternary Na_2O-CaO-P_2O_5 (approximation study). Therefore other models have to be found to describe their solubilities more accurately. One point to note however is remarkable that the overall calcium ion content is around 35 mol% and solubility curves show similar shapes to for example the ternary CaO-Na_2O-P_2O_5 system with CaO contents greater than 30 mol%. With the use of $(NaPO_3)_x$ precursor, the overall amount of P_2O_5 was reduced and at the same time, the Ca^{2+} ion content in the glass system was increased. This is of significance since it was never possible to increase CaO content over 40 mol% in the ternary CaO-Na_2O-P_2O_5 system. With this way of producing biomedical glasses it may be possible to increase the Ca/P ratio and maybe it is possible to move towards a glass with a Ca/P ratio of 1.67 as seen in hydroxyapatite and this could have some very interesting properties.

This system delivers some information, which has not been seen in previous systems. The pH value increases in the same way as before, however it is not then followed by the expected decrease as seen in other systems. It stays more around the neutral level, without decreasing. Calcium ion measurements however show very similar trends as seen before but the values much lower, which is not surprising because these glasses have a much lower solubility. Sodium ion measurements are lower in their values as

well and show a more exponential curve, which has not seen before in such extreme shape. Fluoride measurements showed that fluoride is being released from the glasses similar to other ions and with similar values. The shape of the curve resembles sodium ion measurements of glass systems discussed previously. One reason for the lower values found for the ion measurements and the lack of change in pH might be the fact that the ion exchange process does not take place so strongly as in previous discussed systems. Fluoride and oxygen being the negative counterpart in the glass structure are holding positive charges firmly together. This effect is stronger for fluoride since fluoride has a higher electron negativity.

It can be said that the fluoride glass system is a promising system for biomedical application however more extensive work is required to investigate thoroughly.

Chapter 11

Structural Analysis

This chapter presents results of the structural analysis. DTA and SS-NMR spectroscopy were used in order to establish insights into the glass structure. As mentioned earlier, no precise glass structure exists and in this study the analytical methods were used to achieve two things. First, to analyse prepared glasses and secondly it might be possible to comment on the structural inconsistency seen in the literature, as far as this is possible.

As for the solubility tests, the ternary system Na_2O-CaO-P_2O_5 was used as a baseline and the materials and methods used are explained within this system. Abnormalities, which might have occurred for other systems will be discussed separately.

11.1Differential Thermal Analysis DTA

11.1.1 Materials and Methods

Three thermal parameters, glass transitions temperature T_g, crystallisation temperature T_c and the melting point T_m have been measured using a Setaram Differential Thermal Analyser (DTA). Measurements were carried out under an inert nitrogen atmosphere and a heating rate of 10^0C/min to a maximum of 1000^0C was used. Before samples were run, a blank run was done to establish a baseline, which is subtracted from the data. Around 60 mg of powdered sample was used for each measurement.

11.2 SS-NMR Spectroscopy

One-dimensional single-pulse ^{31}P spectra were recorded for the whole Na_2O-CaO-P_2O_5 ternary glass system and the K_2O-CaO-P_2O_5 ternary glass system, using a Bruker MSL-300 spectrometer operating at 121.5 MHz. The samples were contained in 4mm zirconia rotors and magic angle spinning rate was typically ca. 10-11kHz. 4 to 16 transients were accumulated for the ^{31}P spectra using a 60 s relaxation delay. Glasses were measured shortly after they had been synthesised to avoid any unnecessary contact with moisture.

11.3 Differential Thermal Analysis

11.3.1 DTA Results for Ternary System CaO-Na_2O-P_2O_5

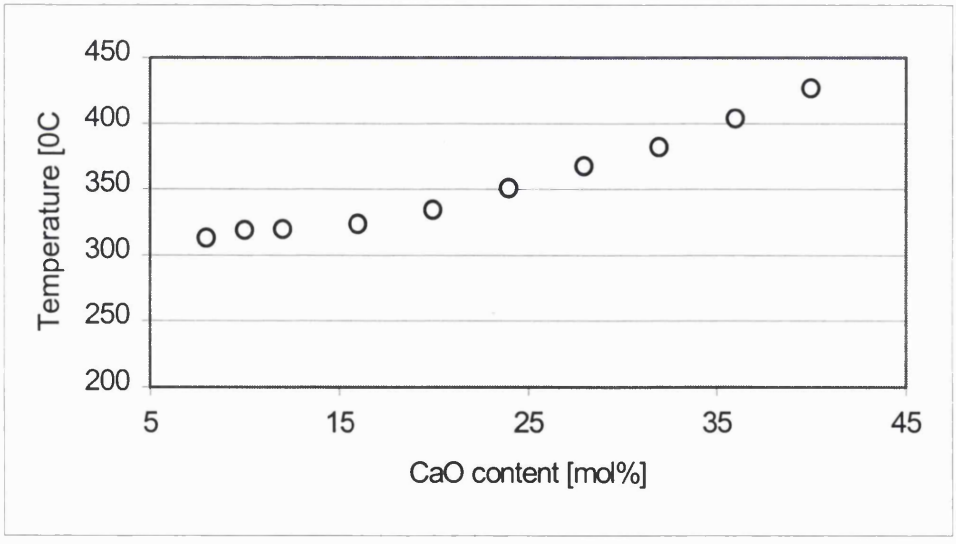

Figure 118: Shows the glass transition point Tg o plotted against the CaO content.

As can be seen from the graph the glass transition temperature increases almost linearly with the increasing CaO content.

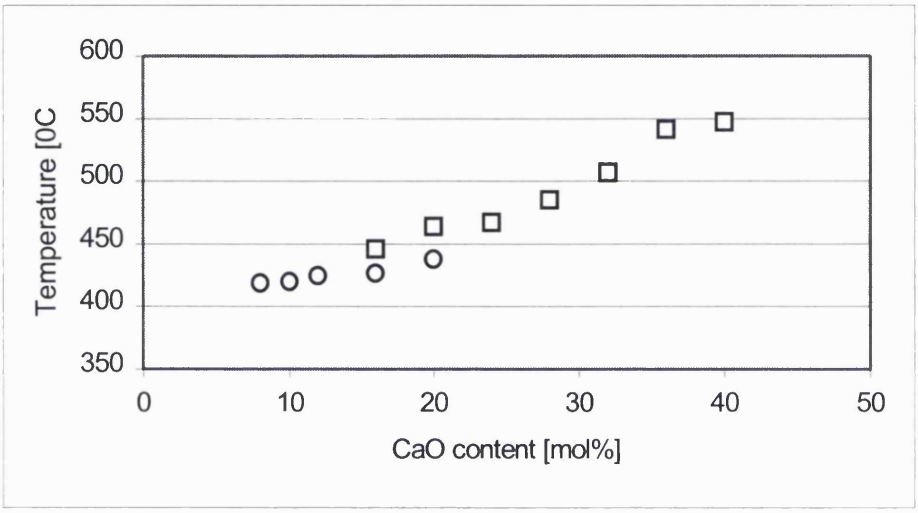

Figure 119: Shows the crystallisation temperatures T_c1 o and T_c2 ▫ plotted against the CaO content.

With increasing CaO content T_c increases. At either end of the compositional spectrum there are only single crystallisation events occurring, the mid regional composition shows two crystallisation points, one of which seems to decrease and disappear at higher CaO content.

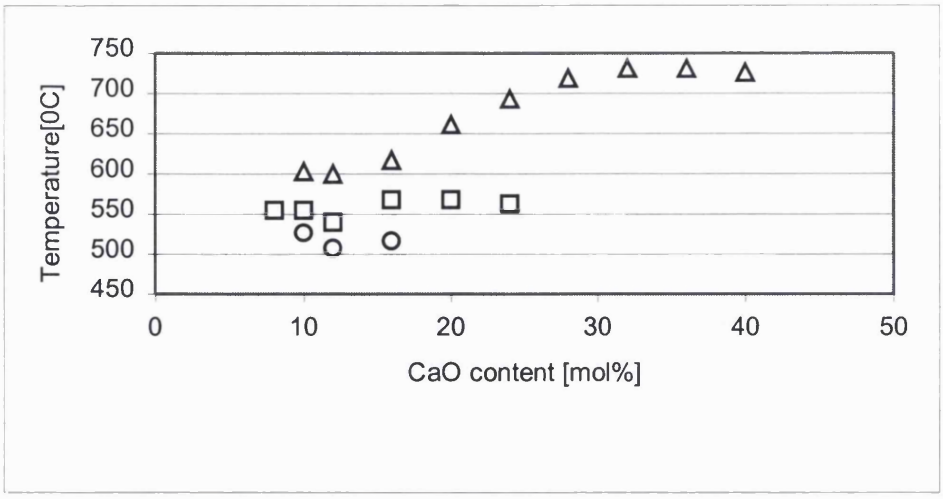

Figure 120: Shows melting points T_m1 o, T_m2 ▫ and T_m3 Δ plotted against CaO content.

As can be seen, there is more than one melting event taking place for most of the composition. No clear linear trends for either of the curves was seen, except for the T_m 3 melting point. This curve increases consistently up to a CaO content of 28 mol%, and then formed a plateau region.

11.3.2 Discussion

The glass transition temperature varies almost linearly with CaO content.

The glass transition temperature is the temperature at which a polymeric, amorphous material is converted from an elastic-plastic to a glassy state. That also means that below the glass transition temperature the molecular mobility is limited. Above this point, when heat is added, chain segments begin to move (87). Calcium is known to be a network re-stabilisor because of its 2 positive charges. An increasing Tg is therefore expected and is in accordance with findings of *Eisenberg et al.* (51) and *Uo et al.* (55).

T_c and T_m show some variation and this is related to a phenomenon called phase separation which is common in many silica based glasses (88-91). This very much depends on the glass making and cooling process (14). A theoretical and detailed study about the occurrence of glass separation was published by Vogel (92). Another publication by Vogel and W. Hoelland (14) dealt with the phenomena and the use of phase separation in silica based glasses. It was hoped that if phase separation can be controlled, beneficial apatite formation will occur when glasses are transformed to glass-ceramics. This was achieved by additions of CaO/P_2O_5 into the silicate glass. Another glasses system was investigated, based on P_2O_5-CaO-Na_2O-Al_2O_3. Similar to silicate based glasses, phosphate glasses showed phase separation as well and apatite formation was achieved by adding oxides like FeO/Fe_2O_3 and fluoride.

In this study, regarding Tc and Tm plots, it is obvious that there is more than one single event occurring. Glasses with CaO content above 10 mol% show either one or two crystallisation peaks corresponding to two or more melting events, respectively. Glasses with either very high or very low CaO content show no such phenomena; these plots showed one crystallisation peak corresponding to one melting event occurring. The middle region of 12-24 mol% CaO, however, phase separation occurs. Especially in the melting temperature plot for the lower CaO containing glasses two phases appear one of which disappears when the CaO content increases.

This complex behaviour can be explained by the phenomenon of phase separation in the glass (93). According to Dietzel (94) for binary glass systems, when a glass cools, three different phenomena can occur, which explain our findings. Dietzel ordered

cations according to their field strength. The field strength is defined as z e/r ^{2} where z = valence, e = elemental charge (constant) and r = radius of ion. Because of the constant factor e, to simplify the equation we will omit this constant factor. For further discussion, the field strength was altered to z/a^2, which means that the field strength is measured in terms of cation distance to anion (oxygen).

For a binary silicate glass, Dietzel discussed three simple conditions: if the difference in field strength of two cations ΔF is above $\Delta F = 0.3z/a^2$, crystallisation and compound formation occurs, whereas at $\Delta F = 0$ z/a^2 phase separation takes place. Glass formation occurs when $\Delta F > 1.33$ z/a^2. A similar consideration may be extended to the phosphate glasses in this work. According to Dietzel the element P has a field strength of 2.1, Na of 0.19 and Ca 0.33. In our case, we have a range of glasses with different CaO/Na_2O ratios and different phenomena occur. At one end, low CaO high Na_2O content no phase separation occurs. In the middle with balanced CaO/Na_2O ratio phase separation occurs. At the other extreme, with high CaO and low Na_2O content only a single phase is formed. To explain this phenomenon of separation in the middle region a binary P_2O_5 – Na_2O system should be considered, in which increasing levels of CaO are incorporated. In the case of the binary system, one phase will form which means that the relatively low field strength of Na_2O does not have a strong influence. Hence, the difference of two field strengths ΔF will not be 0 (the case for phase separation). If one incorporates a third component, such as CaO phase separation can occur but only if CaO is incorporated at a certain level that enough material is present to form a phase. In other words, the more CaO (Ca^{2+} has a higher field strength than Na^+) is incorporated the more ΔF tend towards zero. If the amount of CaO is further

increased, sodium content becomes extremely low and phase separation is not possible.

11.3.3 DTA Results for the Ternary Glass System K_2O-CaO-P_2O_5

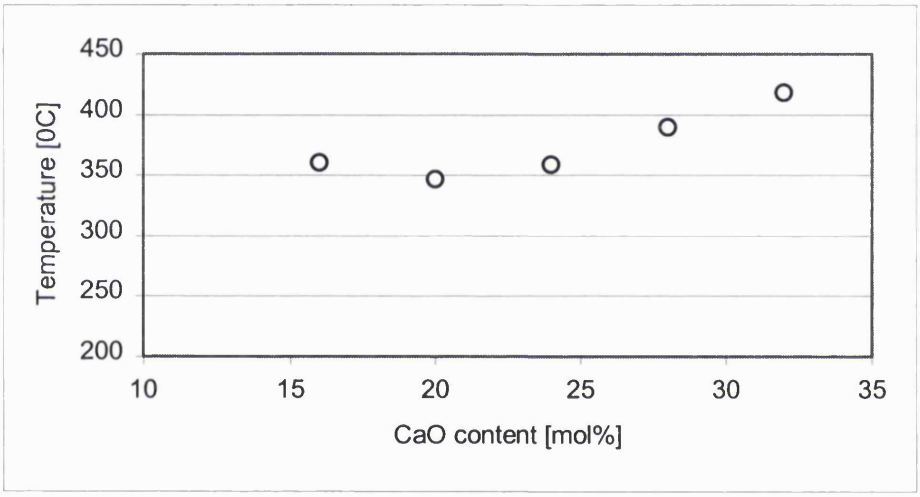

Figure 121: Tg plotted against CaO content

The values for Tg tend to show a slight drop followed by a linear increase with CaO content. It is not apparent if the initial drop is significant.

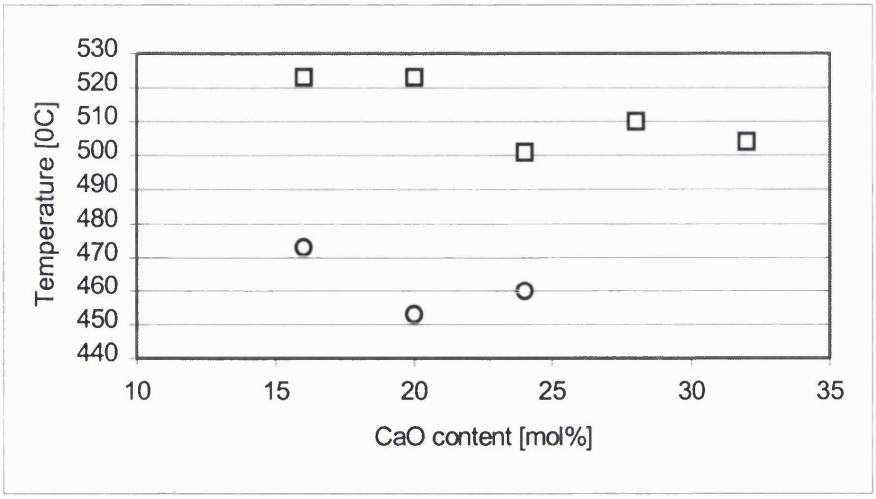

Figure 122: 2 crystallisation points T_c 1 o and T_c 2 ▫ plotted against CaO content.

Crystallisation slightly decreases with increasing CaO content.

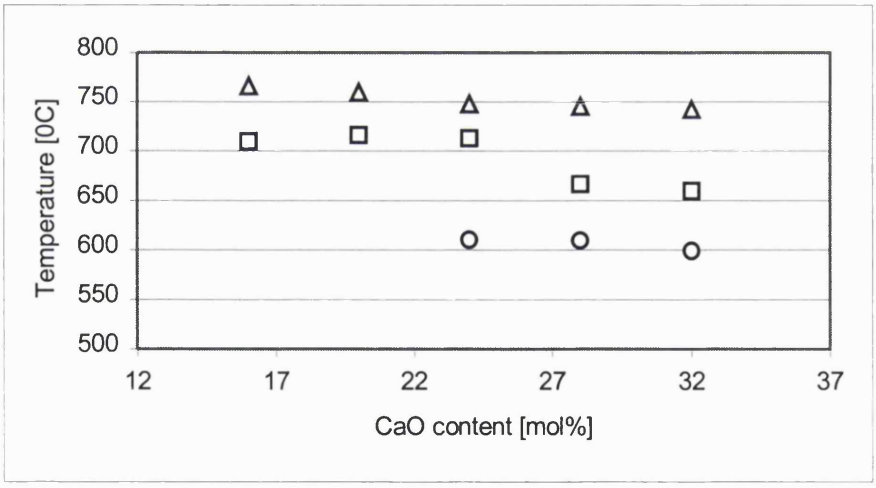

Figure 123: Shows melting points T_m 1 o, T_m 2 ▫ and T_m 3 Δ plotted against CaO content.

All melting events show a decreasing trend of temperature values with increasing CaO content.

For the second ternary glass system of K_2O-CaO-P_2O_5, phase separation is less favourable. It seems that the onset of this phenomenon is shifted towards higher CaO content in comparison to the Na_2O-CaO-P_2O_5 ternary glass. From 16 to 20 mol% CaO, two crystallisation effects occur with two corresponding melting events which is an indication of two distinct phases. However, phase separation does occur for glasses with CaO content higher than 24mol% CaO; this is in contrast to the other ternary system for which just a single phase and crystallisation event persisted at the higher CaO content.

In further comparison to the first ternary Na_2O-CaO-P_2O_5 glass system, all crystallisation and melting events show a different trend. Crystallisation and melting temperatures are decreasing with increasing CaO content, which is not the case for the other ternary glass system. The trend for the glass transition temperatures T_g is, however similar.

11.3.4 DTA results for the Quaternary Glass System CaO-Na_2O-K_2O-P_2O_5 System

The DTA results have been plotted in a slightly different way to demonstrate the influence of potassium. Therefore, plots have been made for 4 different quaternary glass types. Each glass type has a different, but fixed CaO content and varying K_2O content. It should be noticed here that for these glass systems phase separation is occurring. Note here that on the following plots, glass parameters for glasses with zero potassium content are used as reference points from the corresponding ternary Na_2O-CaO-P_2O_5 glass system.

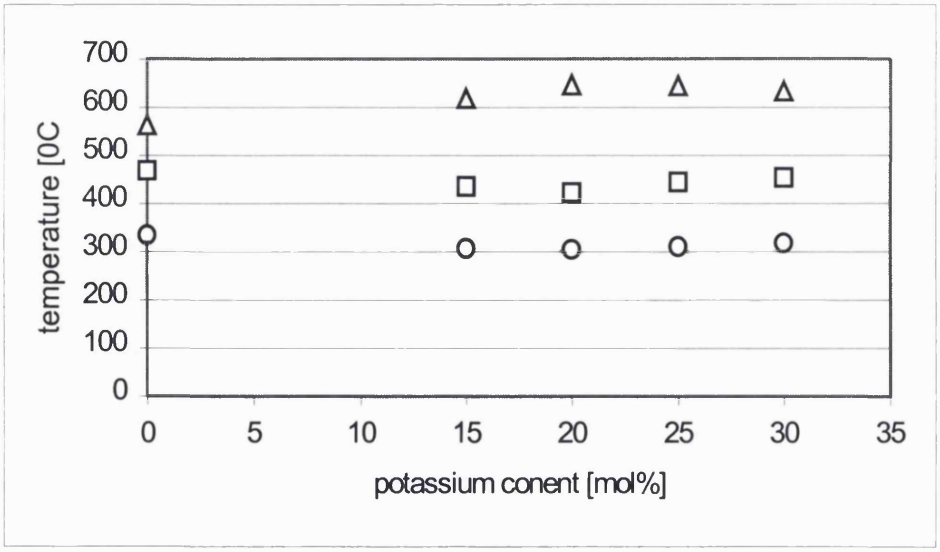

Figure 124: Thermal parameters for Na_2O-K_2O-CaO-P_2O_5 with fixed 20mol% CaO and varying K_2O
o T_g; ▫ T_c; Δ T_m

For this glass type, the effect of Na_2O substitution is almost insignificant.

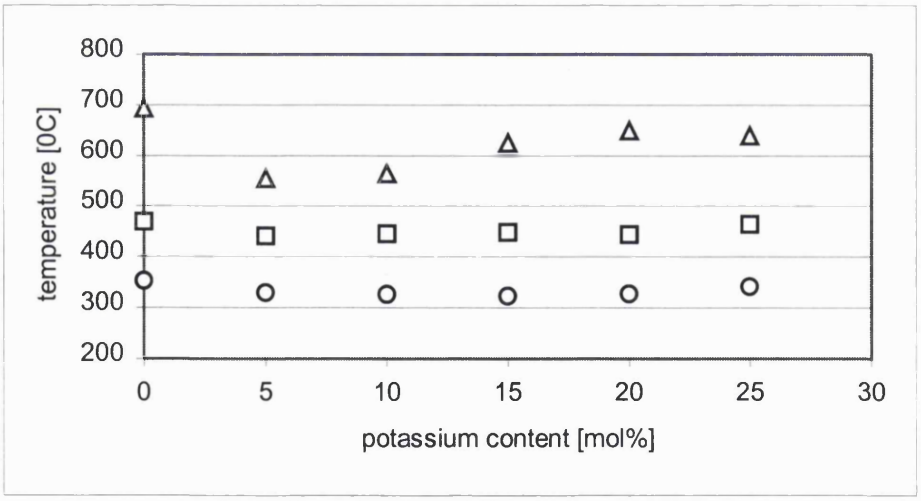

Figure 125: Thermal parameters for Na_2O-K_2O-CaO-P_2O_5 with fixed 24mol% CaO and varying K_2O
o T_g; ▫ T_c; Δ T_m

Here, compared to the previous glass type with 20mol% CaO, the effect of 5 mol% Na_2O substitution is the biggest, T_g, T_m and T_c decreased but slightly increased again towards higher substitution rate.

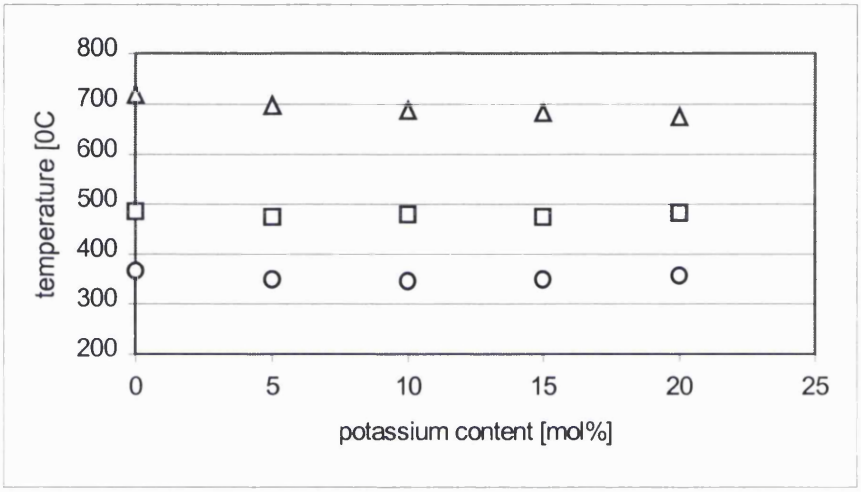

Figure 126: Thermal parameters for Na_2O-K_2O-CaO-P_2O_5 with fixed 28mol% CaO and varying K_2O
o T_g; ▫ T_c; ΔT_m

For this system only a slight decrease for all parameters were found.

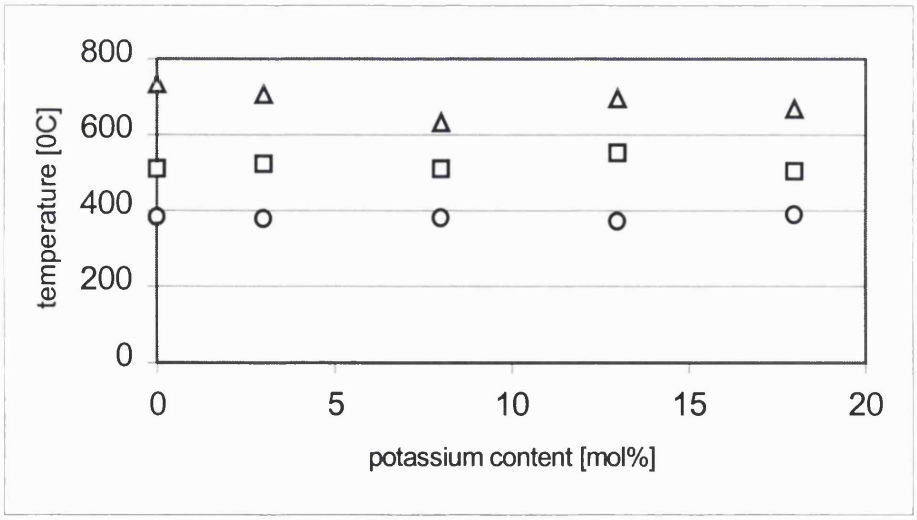

Figure 127: Thermal parameters for Na_2O-K_2O-CaO-P_2O_5 with fixed 32mol% CaO and varying K_2O
o T_g; ▫ T_c; ΔT_m

The effect of sodium substitution by potassium does not have a major influence, only a slight decreasing trend with increasing substitution can be seen. The effect is probably strongest for substitution by just 5 mol% K_2O.

11.3.5 DTA Results for Quaternary Glass System $CaO\text{-}Na_2O\text{-}MgO\text{-}P_2O_5$

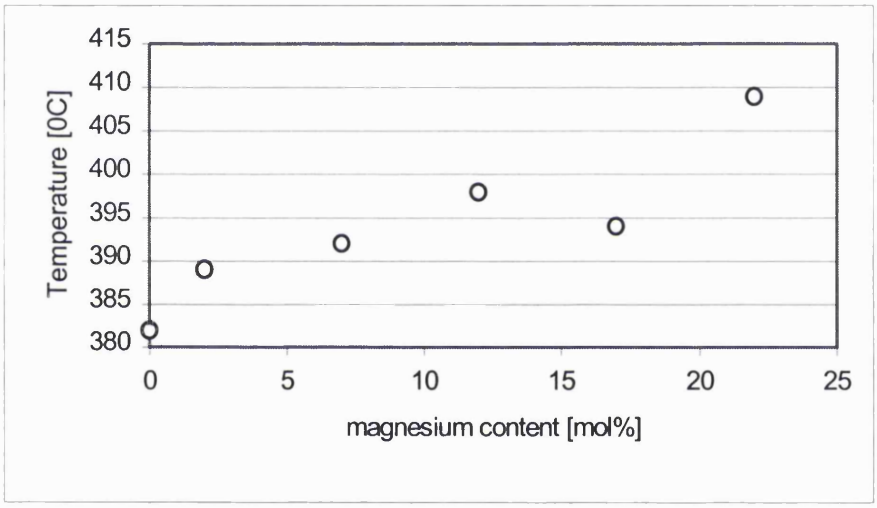

Figure 128: Shows increasing Tg o against increasing MgO content

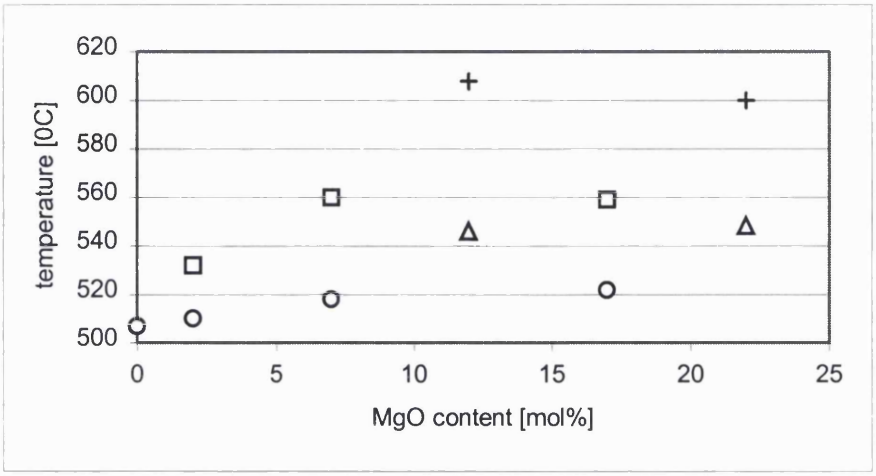

Figure 129: Crystallisation points against increasing MgO content
o T_{c1}; ▫ T_{c2}; Δ T_{c3}; +T_{c4}

The replacement of CaO with MgO has a strong effect on the T_g, even for very small substitutions and this stabilising effect is also described by Sahar and Kamaruddin (52). They assumed that for a binary MgO-P_2O_5 glass compositions change from metaphosphate (less stable) to pyrophosphate (more stable). The stability effect was seen for glasses with MgO/P_2O_5 ratio higher than 0.46. In this study however, the T_g increases linearly and is in general higher than the corresponding ternary Na_2O-CaO-P_2O_5 glass system.

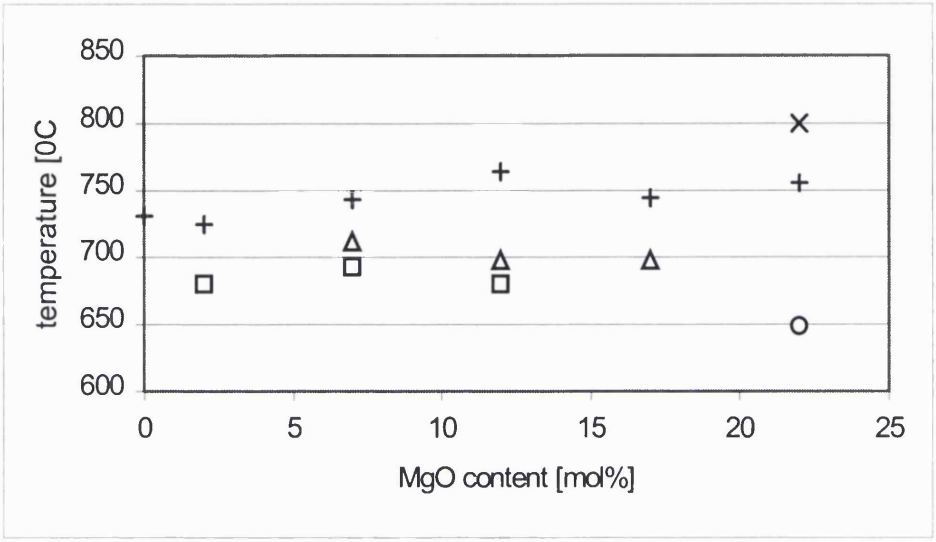

Figure 130: Melting points plotted against MgO content

o T_{m1}; ▫ T_{m2}; Δ T_{m3}; + T_{m4}; x T_{m5}

The complexity of this system seems to be greater in comparison with other systems. In almost every glass there are at least 2 crystallisation and 3 corresponding melting events occurring which is an indication of 1.) phase separation and 2.) greater complexity of the system verified by the multiphase appearance.

Glasses with MgO content of 12 mol% and 22 mol% show further crystallisation points, which are higher in temperature. This has not been seen in other members of the same system. For the same glasses, it appears that two crystallisation events at 560 and 520^{0}C collapse into a new crystallisation point at 540^{0}C which is not seen in other glasses. However, no corresponding events take place for the melting points. Here, only at very high MgO content, two new melting points appearing at 650 and 800^{0}C. All other glasses of the same system show relatively consistent melting trends.

11.4 ^{31}P-MAS-NMR Spectroscopy

The following figure is representative of all MAS-NMR spectra for two ternary Na_2O-CaO-P_2O_5 and K_2O-CaO-P_2O_5 glass systems. For all solid-state ^{31}P- MAS spectra please see Appendix.

All spectra show two main peaks Band A (~ - 20ppm) and Band B (~ 0ppm) with corresponding spinning side bands located on the left and right hand side of the main two peaks.

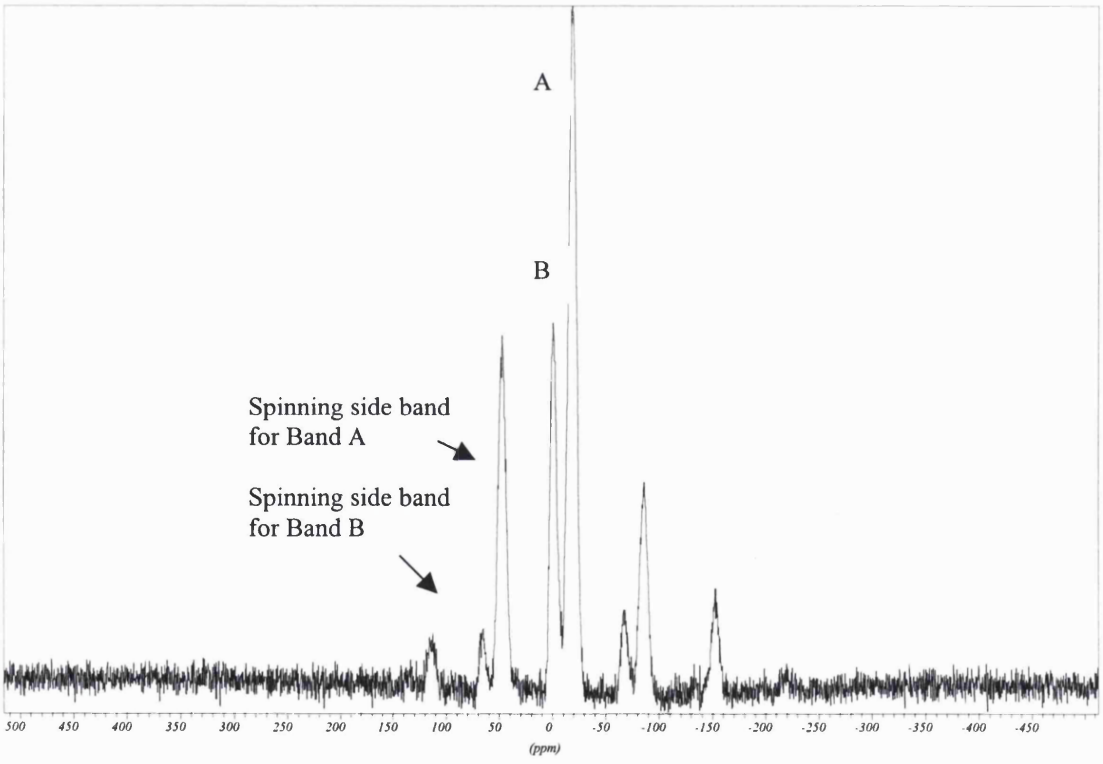

Figure 131: Show a typical ^{31}P-MAS-NMR spectrum for ternary glass system Na_2O-CaO-P_2O_5 with Band A and Band B and their corresponding side bands

11.4.1 Chemical Shift Assignment

The spectra of all glasses consists of basically 2 bands, one with a lower frequency, band A assigned to be Q^2 phosphates, and another band with a higher frequency, band B assigned to be Q^1 phosphates. The assignments of these bands was originally discussed by Hartman et al. (44) and the isotropic chemical shift falls within ranges quoted by Haubenreisser et al.(45) Therefore, polycrystalline phosphates are typical at 4 to –33δ (Q^1 units) and -18 to –53 δ for Q^2 units.

Brow et al. (40) assigned chemical shifts for binary sodium-phosphate glasses as follows: Q^1 ~ 0ppm, Q^2 ~ -20ppm and Q^3 ~ -40ppm which very much goes in accordance with the ternary $CaO\text{-}Na_2O\text{-}P_2O_5$ glass system. They reported the occurrence of Q^1 and Q^2 species and additionally Q^3 species occurred at higher P_2O_5 content.

Flechter et al. (39)assigned chemical shifts for Q^1 of –8 to –10δ, Q^2 –24.9 to –28δ and Q^3 around –44δ. They also mentioned an important fact about the occurrence of Q^3 species in binary calcium phosphate glasses, however they decreased and disappeared with increasing CaO content.

In contrast to *Flechter et al.* no such peak at ~ -44δ indicating Q^3 species was observed in any of the spectra reported here. The reason for that might be the sodium content of all glasses, which does not allow the formation of Q^3 species.

Overall both authors' assignments are comparable with the ternary glass system investigated here.

Earlier studies on similar glass system within the composition of Na_2O-CaO-P_2O_5-Al_2O_3 have shown aluminium free glasses having peaks falling in the same ppm range (46) as discussed above.

From this information, the peaks were assigned to be Q^1 for the B band and Q^2 for the A band.

11.5 Structural Investigations

11.5.1 Ternary CaO-Na_2O-P_2O_5 glass system

As one can see from the spectrum see Appendix 1, 2 bands, A and B, occur with corresponding spinning side bands. These bands have been deconvoluted separately using Bruker WIN-FIT software program. The sum of the intensities of band A together with all its sidebands was compared with the sum of the intensities of band B with its sidebands, to determine the Q^1/Q^2 ratio. The intensities of the spinning side bands were analysed by the method of Herzfeld and Berger (95) within the Bruker WIN-MAS program. This analysis yields the principle components (δ_{11}, δ_{22}, δ_{33}) of the chemical shift tensor, for which the isotropic chemical shift is given by

$$\delta_{iso} = (\delta_{11} + \delta_{22} + \delta_{33})/3$$

With the Haeberlen convention (96) $|\delta_{33} - \delta_{iso}| > |\delta_{11} - \delta_{iso}| > |\delta_{22} - \delta_{iso}|$ the chemical shift anisotropy ($\Delta\delta$) and asymmetry parameter (η) are given by:

$$\Delta\delta = \delta_{33} - (\delta_{11} + \delta_{22})/2$$

$$\eta = (\delta_{22} - \delta_{11})/(\delta_{33} - \delta_{iso})$$

The result of this deconvolution is shown in table 21

Glass Code	δ_{iso}	$\%Q^2$	δ_{11}	δ_{22}	δ_{33}	$\Delta\delta$	η
$Ca_8Na_{47}P_{45}$							
Band A	-19	72	75	28	-160	-212	0.3
Band B	-1		-66	-41	104	157	0.2
$Ca_{10}Na_{45}P_{45}$							
Band A	-20	69	81	20	-160	-211	0.4
Band B	-2		-76	-32	103	157	0.4
$Ca_{12}Na_{43}P_{45}$							
Band A	-19	70	80	21	-159	-209	0.4
Band B	-3		-66	-34	93	143	0.3
$Ca_{16}Na_{39}P_{45}$							
Band A	-20	72	82	20	-161	-212	0.4
Band B	-3		-66	-49	105	163	0.2
$Ca_{20}Na_{35}P_{45}$							
Band A	-21	66	92	5	-158	-206	0.6
Band B	-5		-95	-6	87	137	1.0
$Ca_{28}Na_{27}P_{45}$							
Band A	-22	65	83	9	-159	-205	0.5
Band B	-7		-73	-47	99	159	0.2
$Ca_{36}Na_{19}P_{45}$							
Band A	-23	70	75	15	-160	-206	0.4
Band B	-7		-68	-51	98	157	0.2

Table 21: Listed chemical shifts, % of Q^2 amount and anisotropic shift parameters with asymmetry parameter for the ternary Na_2O-CaO-P_2O_5 glass system

11.5.2 Ternary $CaO-K_2O-P_2O_5$ glass system

For measurements please see $CaO-Na_2O-P_2O_5$ glass system

Glass Code	δ_{iso}	$\%Q^2$	δ_{11}	δ_{22}	δ_{33}	$\Delta\delta$	η
$Ca_{16}K_{39}P_{45}$							
Band A	-20	70	80	20	-159	-209	0.4
Band B	-7		-91	-19	89	144	0.8
$Ca_{20}K_{35}P_{45}$							
Band A	-20	71	82	21	-164	-215	0.4
Band B	-6		-81	-29	91	146	0.5
$Ca_{24}K_{31}P_{45}$							
Band A	-22	74	73	26	-164	-213	0.3
Band B	-7		-74	-41	94	151	0.3
$Ca_{28}K_{27}P_{45}$							
Band A	-22	70	76	17	-158	-204	0.4
Band B	-7		-79	-36	92	150	0.4
$Ca_{32}K_{23}P_{45}$							
Band A	-22	60	74	16	-155	-200	0.4
Band B	-7		-83	-22	84	136	0.7

Table 22: Listed chemical shifts, % of Q^2 amount and anisotropic shift parameters with asymmetry parameter for ternary $K_2O-CaO-P_2O_5$ glass system

The isotropic chemical shifts are measured directly from the ^{31}P spectra and the error on the peak maxima will be about +/- 200Hz making an error on the δ_{iso} values ca. +/- 1.5 ppm. However the errors on the components (δ_{ii}) calculated from the spinning side band intensities are likely to be considerably larger (+/- 10ppm) with correspondingly large errors on $\Delta\delta$ and η.

In comparison with previous studies on calcium phosphate glasses, the values in the table are very similar. In earlier studies, CaO was substituted by Al_2O_3, which had a greater effect on the chemical shift anisotropy than the variation of Na_2O/CaO ration. In the following plots, the dependence of chemical shift parameters on the CaO content is demonstrated and compared with the results of other authors.

11.5.3 Discussion for Ternary Glass System Na_2O-CaO-P_2O_5

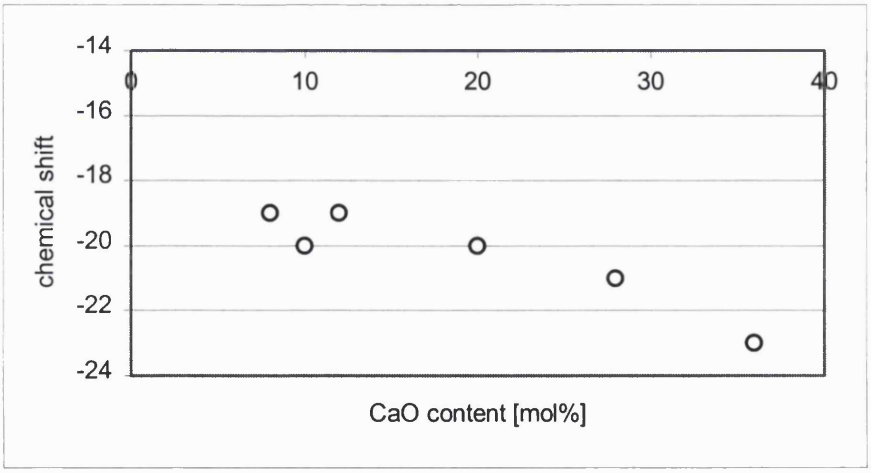

Figure 132: o Isotropic chemical shift δ_{iso} plotted against CaO content for the ternary glass system Na_2O-CaO-P_2O_5

Delahaye et al. (76) published similar findings about the variation in chemical shift in calcium-sodium phosphate glasses, where the chemical shift changes from ~ -21 ppm for lower CaO containing glasses to ~ -24ppm for higher CaO containing glasses. The chemical shift changes with CaO content for this system is just about significant according to previously mentioned errors.

Martin (28) observed a systematic positive chemical shift change when more non-bridging oxygens were added to binary alkali phosphates. In this study the opposite effect was found, chemical shifts for both species shifting towards more negative values.

11.5.4 Discussion for ternary glass system K_2O-CaO-P_2O_5

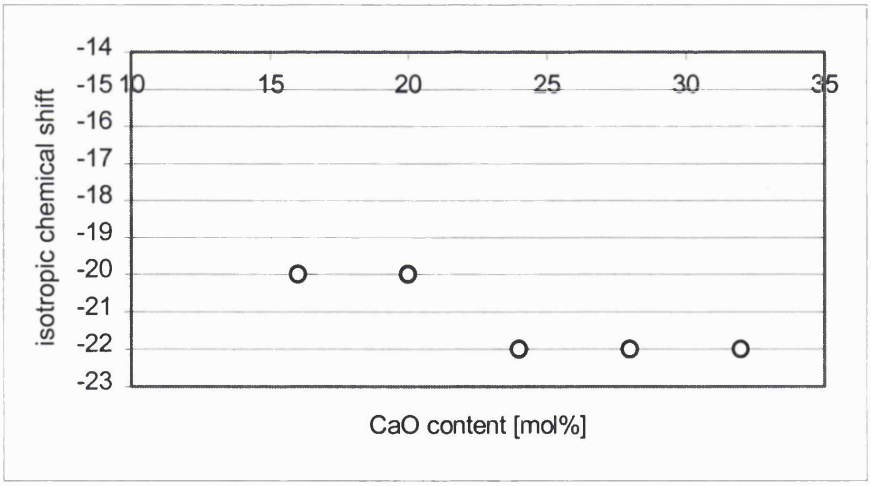

Figure 133: o isotropic shift δ_{iso} plotted against CaO content for ternary K_2O-CaO-P_2O_5 glass system

For this glass system no significant relationship between chemical shift variation and CaO content was found. The changes seen on the plot are within the error range, mentioned earlier.

11.6 Composition of the glass

11.6.1 Combined discussion of NMR and DTA results

It can be seen from the Table 20, spectra show the predominance of Q^2 species which is indicative of cyclic or long-chain meta phosphates

Chemical shift ranges for Q^0, Q^1 and Q^2 overlap, depending upon the cation. Therefore, isotropic δ value alone is not necessarily a definitive test of speciation. From previous studies of ternary glass and glass-ceramics within the Na_2O-CaO-P_2O_5 using X-ray Diffraction in combination with DTA, it is known that two species predominate, their relative amounts depending on the CaO content (46). Glasses with 8 mol% CaO show a very simple DTA spectrum with a crystal phase of only $NaPO_3$ (linear metaphosphate), confirmed by XRD. When the CaO content is increased, a second phase appears being $Na_4Ca(PO_3)_6$ (cyclic metaphosphate), which at the very highest CaO containing glasses is the main crystal phase. This is mirrored in the DTA traces, which show multiphase behaviour with more than one crystallisation and melting point with respect to single crystal and melting points at each end of the compositional range. However, it should be noticed here that not all multi crystallisation and melting points in the DTA traces can be explained by the presence of two different species in the glasses; the previously discussed phenomenon of phase separation should be considered here.

The structure of both two species are Q^2 and account for the fact that the percentage amount of this species does not alter much over the compositional range, because in any case, one Q^2 species will be transformed into another.

A structure has been suggested by *Griffith* (97)

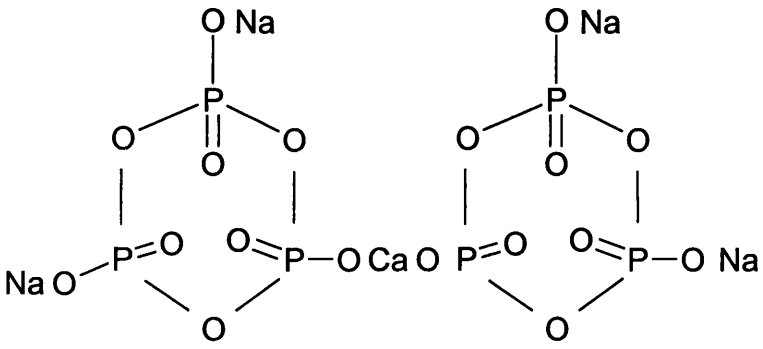

Figure 134: Suggested structure for $Na_4Ca(PO_3)_6$

As can be seen from the structure, phosphorus will be influenced by the sodium and calcium ions and that will account for the isotropic chemical shift values, changing from –19 to –23ppm. No such big shift is seen in the other ternary K_2O-CaO-P_2O_5 glass system. The effect is not as significant in the K_2O containing system because of the smaller compositional range.

The same effect is seen for the Q^1 species; isotropic chemical shift changes from –1 to –7ppm. This effect is in accord with the observation by Hartmann et al. (44). The isotropic chemical shift is consistent with calcium orthophosphate $[Ca_3(PO_4)_2]$ (37) or sodium pyrophosphate $Na_4P_2O_7$ (98). However, the chemical shift anisotropy $\Delta\delta$ for the band B is around 140-160, which is close to that reported for $Na_4P_2O_7$ ($\Delta\delta$ 127) (99) and very different to that for $Ca_3(PO_4)_2$ ($\Delta\delta$ 0) (35). Hence, it is likely that the Q^1 species is in fact a sodium pyrophosphate.

The results of the second ternary glass system K_2O-CaO-P_2O_5 were found to be similar and it is suspected that the compositional species of this glass is similar to the ternary Na_2O-CaO-P_2O_5 system, however more structural analysis needs to be carried out to verify this.

Chapter 12

12.1 The MTT Test- Cell Culture Testing

The MTT assay has been useful for examination of the effect of extracts from the glasses on the proliferation of a bone cell line. In this study the MTT assay was used to determine the cytotoxicity of selected soluble ternary and quaternary phosphate based glasses as a preliminary cell culture study and screening exercise.

12.2 Introduction

The MTT test was developed by Mosmann (1983) (100) for the study of cellular growth and survival of cells. This test is therefore sensitive to the number of living cells present and related to the mitochondrial activity of living cell. The MTT substrate is a (3-(4,5-dimethylthiazol-2-yl)-2,5-diphenyl tetra sodium bromide, which will be transformed to a dark blue formazan product due to activity of active mitochondria. This product can be colorimetrically analysed by measuring the absorbance at 570nm on an ELISA plate. Thus if cells are active and hence mitochondria are active, more of the dye will be converted to the formazan product and hence there will be an increased absorbance measured via the spectrometer.

We have already been able to deduce that the high solubility glasses will be unsuitable for testing as the release rate will be too high. However, with higher CaO content in the glass i.e. lower solubility, these glasses should be suitable for implant use. Hence, in general the glasses tested via the MTT assay had CaO contents of at least 24mol.%. The following glasses have been tested:

Ternary glass system $CaO\text{-}Na_2O\text{-}P_2O_5$

$Ca_{24}Na_{31}P_{45}$

$Ca_{28}Na_{27}P_{45}$

$Ca_{32}Na_{23}P_{45}$

$Ca_{36}Na_{19}P_{45}$

$Ca_{40}Na_{15}P_{45}$

Quaternary glass system $CaO\text{-}K_2O\text{-}Na_2O\text{-}P_2O_5$

$Ca_{28}Na_{22}K_5P_{45}$

$Ca_{28}Na_{17}K_{10}P_{45}$

$Ca_{28}Na_{12}K_{15}P_{45}$

$Ca_{28}Na_7K_{20}P_{45}$

Quaternary system $CaO\text{-}MgO\text{-}Na_2O\text{-}P_2O_5$

$Ca_{30}Mg_2Na_{23}P_{45}$

$Ca_{25}Mg_7Na_{23}P_{45}$

$Ca_{20}Mg_{12}Na_{23}P_{45}$

$Ca_{15}Mg_{17}Na_{23}P_{45}$

$Ca_{10}Mg_{22}Na_{23}P_{45}$

A Human osteoblast cell line (MG63) was incubated in culture medium containing increasing concentration of phosphate glass extracts for 2 days and the cell

proliferation was measured using MTT test (Chemicon, Temecula Ca., USA). Absorbance at 560nm was measured at a Titertek Multiskan Spectrometer.

Cells were plated at a density of 2000cells/well in replicate 96 well culture plates and allowed to attach overnight at 37^0C, after which the media were removed and replaced by the diluted/neat extracts. Cells maintained in normal culture medium were used as controls. The cells were incubated for 2 days and then the proliferation was measured. The results were expressed as the average absorbance of six replicate wells. The results were normalised with respect to the tissue culture plastic, by dividing the test values by the tissue culture control values. Hence a value of 1 indicates proliferation similar to the tissue culture plastic, below 1 indicates decreased and above 1 increased cellular activity.

12.3 Results

12.4 Ternary glass system $CaO\text{-}Na_2O\text{-}P_2O_5$

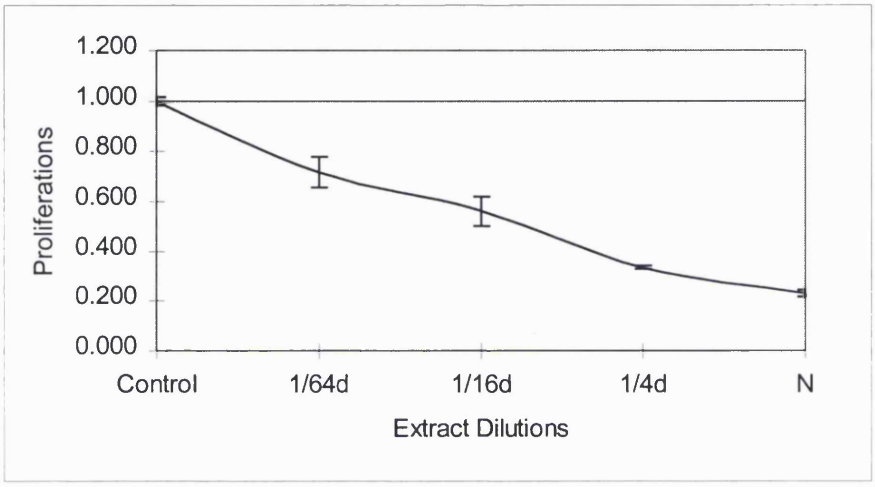

Figure 135: MTT test result for glass $Ca_{24}Na_{31}P_{45}$ (test result after 2 days of incubation)

This figure represent a typical plot of a glass extract incubated with MTT assay for 2 days. After this time the absorbance has been measured for dilutions in 1/64, 1/16, 1/4 and neat extracts as a proliferation indicator and has been plotted against the dilutions. The line at value 1.00 is the control line for cell tissue culture plastic. The tissue culture plastic is designed to promote cell attachment and proliferation. Thus the plastic represents a relatively high level of cellular activity. Values below this line indicate a down regulation or suppression of cellular activity in comparison to the tissue culture plastic material. Above this line indicates that enhanced cellular activity and proliferation in comparison to cell tissue plastic is occurring.

For this glass, the proliferation is down regulated for neat and all dilutions. However, it should be noted that as the extracts are diluted, the down regulation becomes less marked.

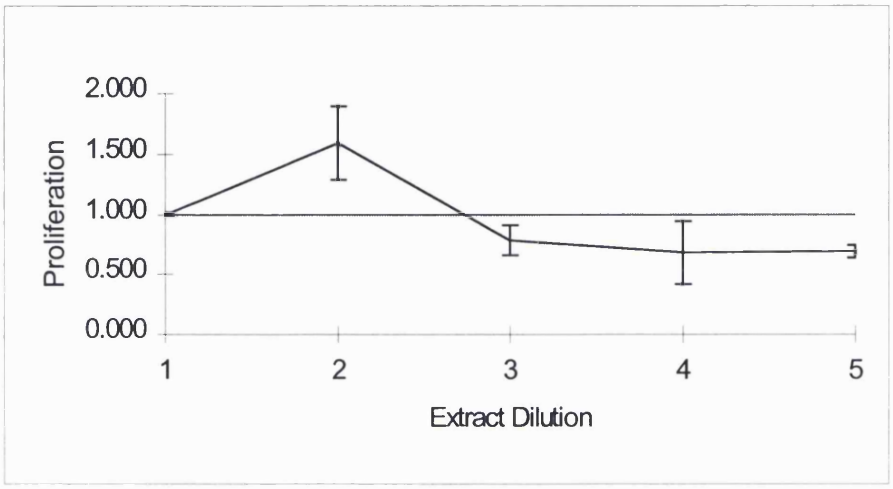

Figure 136: MTT test result for glass $Ca_{28}Na_{27}P_{45}$ (test result after 2days of incubation) With following dilution 1 = control; 2 = 1/64 d; 3 = 1/16 d; 3 = ¼ and 5 = neat

For this next glass, as the CaO content is higher, the solubility is lower. This can be seen in the MTT assay in that overall the cellular activity is not suppressed as much as the previous glass and furthermore, at the highest dilutions, cellular proliferation is enhanced relative to the tissue culture plastic.

Figure 137: MTT test result for glass $Ca_{32}Na_{23}P_{45}$ (test result after 2 days of incubation)

With increasing CaO content i.e. decreasing solubility, cellular activity is increasingly less suppressed. It appears that cellular activity in general was enhanced relative to the tissue culture plastic. However, at a dilution of 1 in 16 the values are suppressed. This appears to be a spurious result.

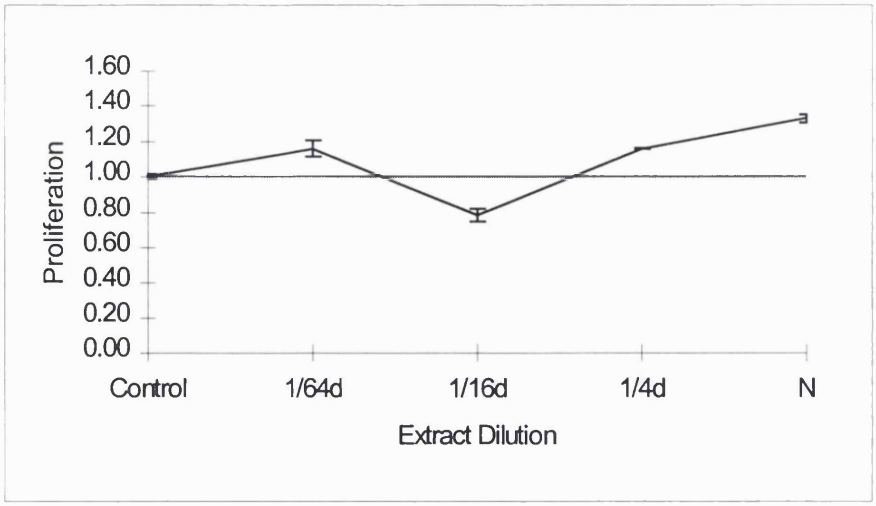

Figure 138: MTT test result for glass $Ca_{36}Na_{19}P_{45}$ (test result after 2 days of incubation)

Again the effect of this glass is very similar to the previous one. This glass showed cell proliferation around or slightly above the control line.

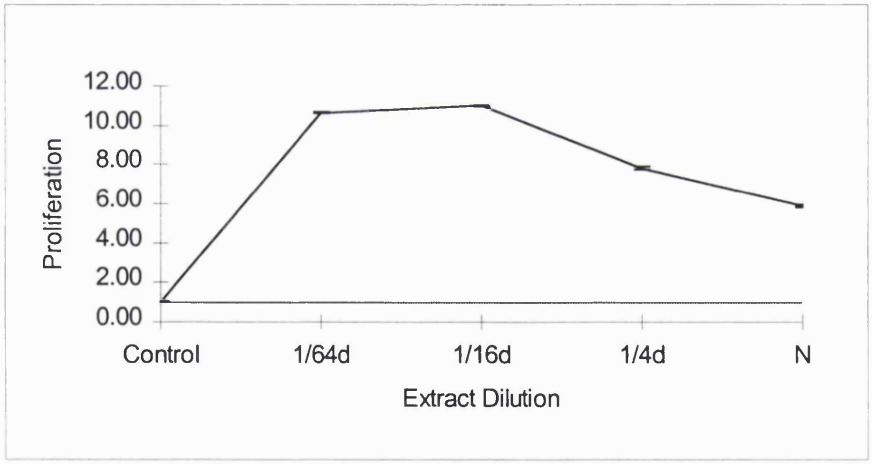

Figure 139: MTT test result for glass $Ca_{40}Na_{15}P_{45}$ (test result after 2 days of incubation)

For the final glass in this ternary system, it has the highest CaO content and hence the lowest solubility. This glass seemed to further enhance the cellular activity compared to the tissue culture plastic. For the undiluted extract, the cellular activity is approximately 6 times higher compared to the tissue culture plastic control. As the solution is diluted, cellular activity further increases.

As it can be seen from these results, cell proliferation can be low or even down regulated for glasses with low CaO content (24 and 28 mol%), cell proliferation become similar in value to the control line for glasses with higher CaO content than 30 mol% . The best proliferation result was achieved for glass $Ca_{40}Na_{15}P_{45}$ with the highest CaO content of the whole glass series. Therefore, the higher the CaO content, the higher the proliferation rate.

12.5 Quaternary system $CaO\text{-}K_2O\text{-}Na_2O\text{-}P_2O_5$

Obviously with a quaternary system, with the number of variables it is not possible to investigate the effect of all variables. Therefore it was decided to fix the CaO content at 28 mol.%, fix the P_2O_5 content at 45mol.% and vary the Na_2O:K_2O. The reason for choosing the CaO content of 28mol.% is because if glasses with very high CaO content were used, the cellular activity may be very high and any effect due to the Na_2O:K_2O ratio may be lost. Therefore it was decided to choose this CaO content as

the cellular activity in the ternary glass is similar to that for the tissue culture plastic. Thus it was hoped that varying the Na_2O:K_2O ratio would give further subtle variations in the solubility which may be detected via the MTT assay.

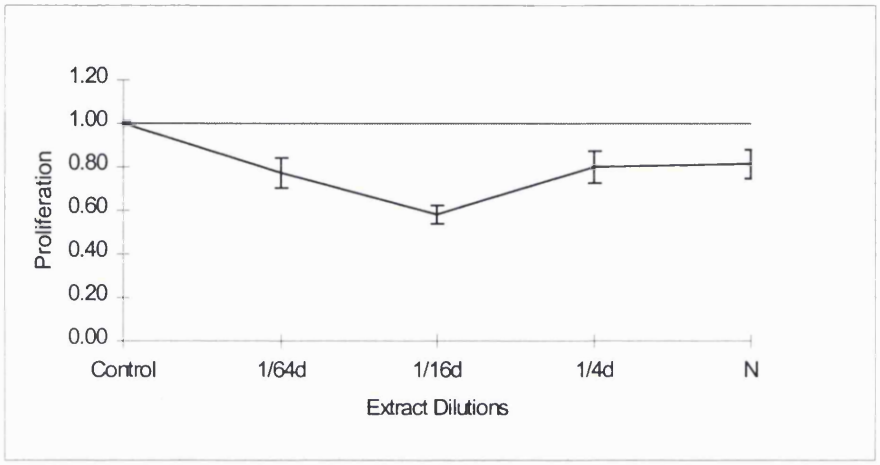

Figure 140: MTT test result for glass $Ca_{28}Na_{22}K_5P_{45}$ (test result after 2 days incubation)

For this first glass, the cellular activity is down regulated even at the very high dilutions. This was not seen in the equivalent ternary glass.

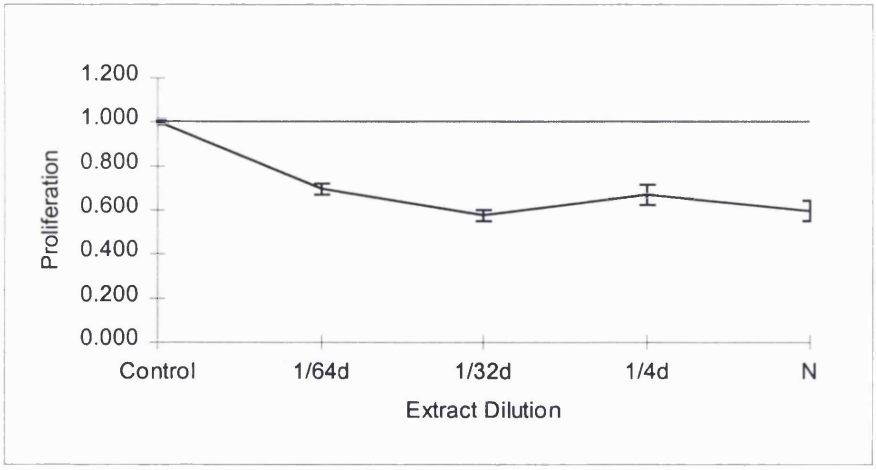

Figure 141: MTT test result for glass $Ca_{28}Na_{17}K_{10}P_{45}$ (test result after 2 days of incubation)

With an increase in the K_2O content, cellular activity is still down regulated relative to the tissue culture plastic for all dilutions. There is some evidence that the K_2O may be further suppressing the cellular activity.

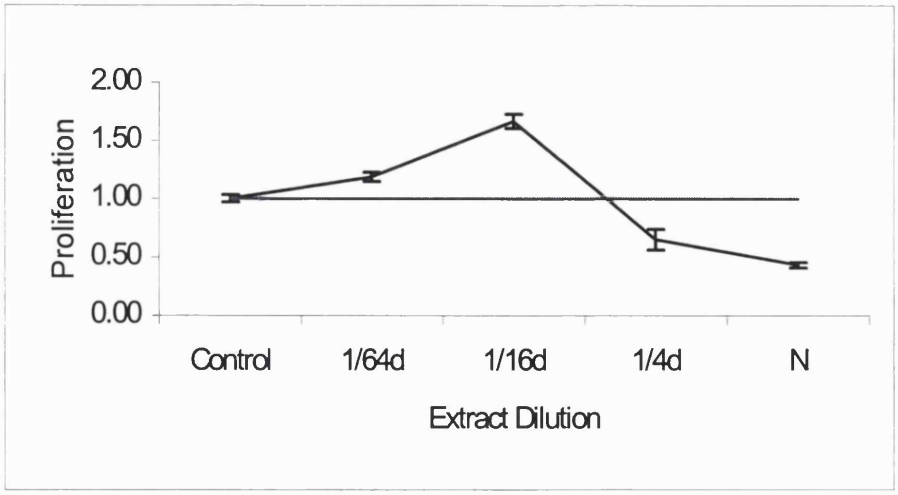

Figure 142: MTT test result for glass $Ca_{28}Na_{12}K_{15}P_{45}$ (test result after 2 days of incubation)

For this next glass, cellular proliferation increased for the higher dilutions and slightly dropping below the control line at the lower dilutions. In general the results were better than the previous glasses in this system.

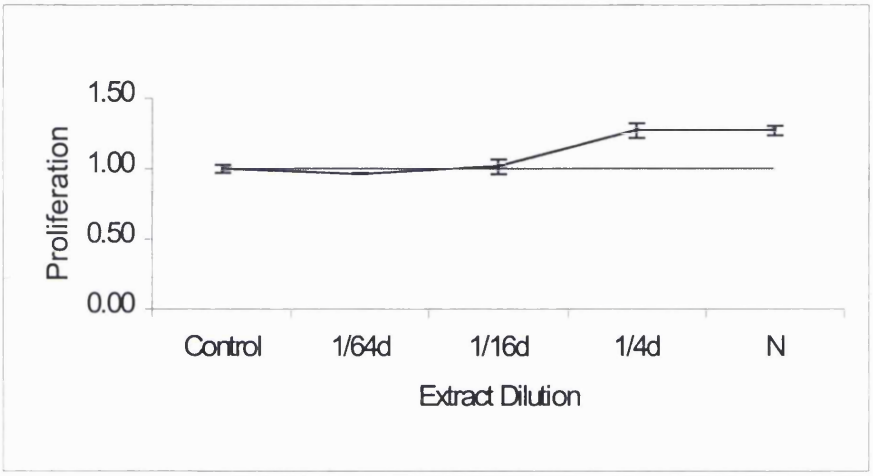

Figure 143: MTT test result for glass $Ca_{28}Na_7K_{20}P_{45}$ (test result after 2 days of incubation)

For this final glass, with the highest K_2O content, the cellular activity seems very similar to the tissue control plastic. There is some evidence for increased cellular activity at the lower dilutions and the neat solution.

12.6 Quaternary system CaO-MgO-Na_2O-P_2O_5

As with the previous quaternary system, a systematic study was performed, but with some variables fixed. The Na_2O content was fixed at 23mol.%, the P_2O_5 content was fixed at 45mol.% and then the CaO was systematically replaced with MgO and this series was examined in vitro using the MTT assay.

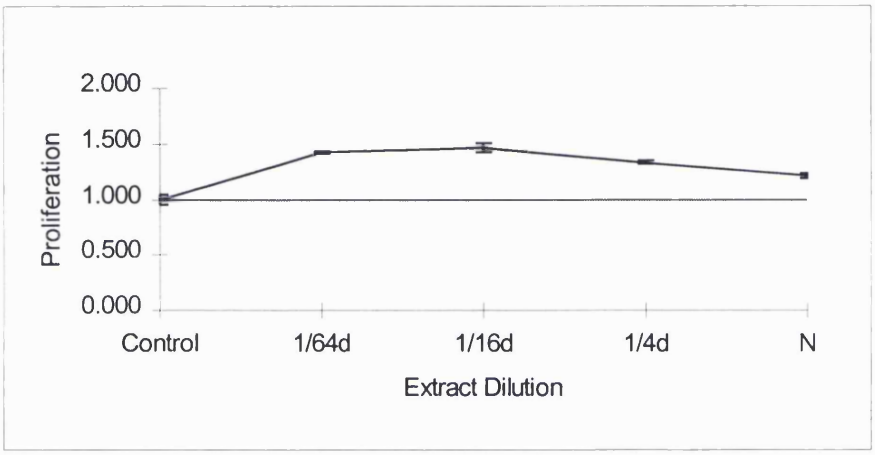

Figure144: MTT test result for glass $Ca_{30}Mg_2Na_{23}P_{45}$ (test result after 2 days incubation)

For this first glass, cellular activity is enhanced for all dilutions. This should be compared with the Na_2O-CaO-P_2O_5 glass equivalent, with 32mol.% CaO. This corresponding ternary system showed cellular proliferation around the control line, here however, with just a small amount of MgO (2 mol.%) proliferation appeared to be enhanced.

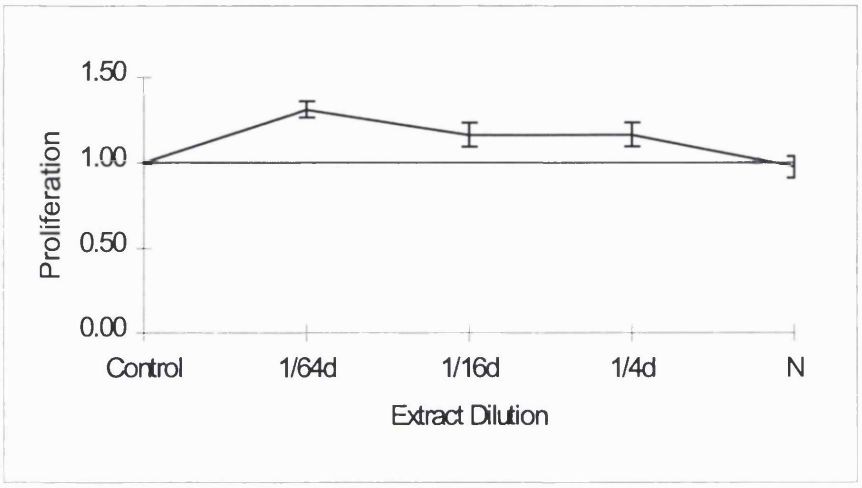

Figure145: MTT test for glass $Ca_{25}Mg_7Na_{23}P_{45}$ (test result after 2 days of incubation)

Further increasing the MgO content appears to have little effect. There is some evidence for down regulation of cellular activity with the higher concentration and neat solutions.

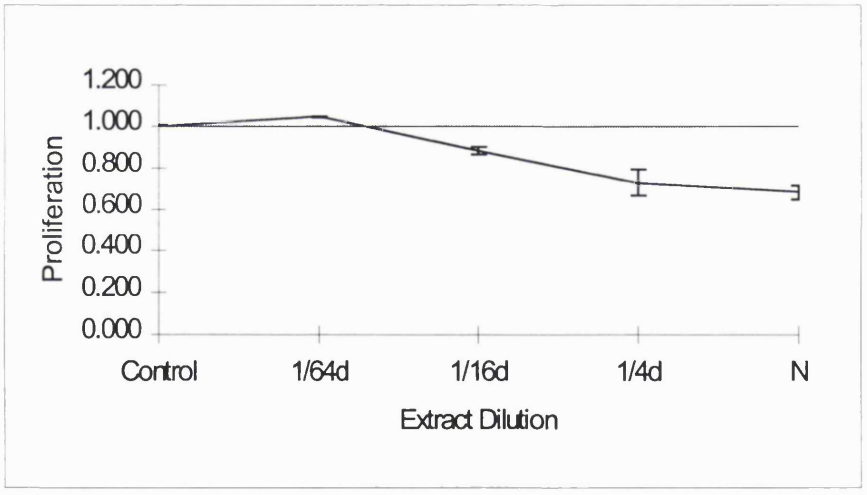

Figure 146: MTT test for glass $Ca_{20}Mg_{12}Na_{23}P_{45}$ (test result after 2 days of incubation)

This plot shows that with increasing MgO content the cellular proliferation is down regulated. Only at a 1 in 64 dilution does cellular activity appear comparable with the tissue culture plastic control.

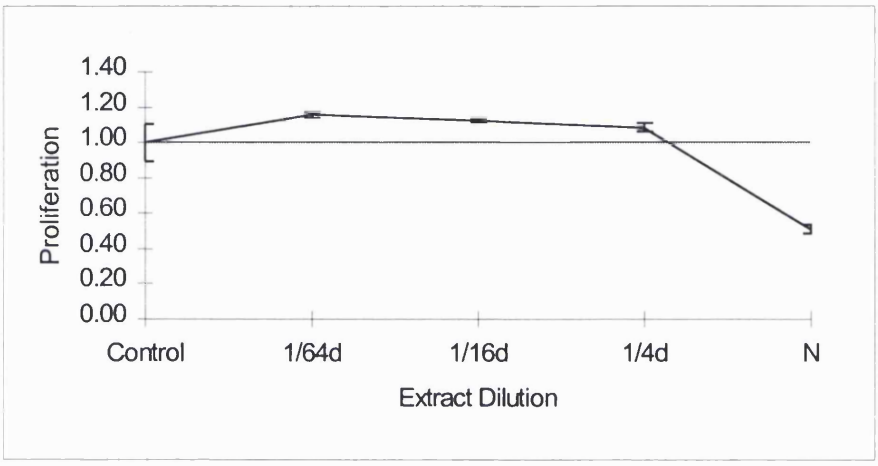

Figure 147: MTT test result for glass $Ca_{15}Mg_{17}Na_{23}P_{45}$ (test result after 2 days of incubation)

Again, with more MgO content proliferation rate is falling particularly at the neat concentration.

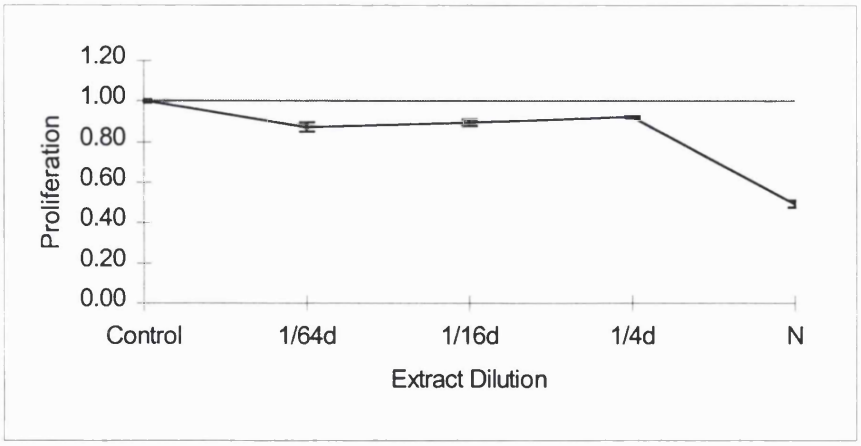

Figure 148: MTT test result for glass $Ca_{10}Mg_{22}Na_{23}P_{45}$ (test result after 2 days of incubation)

At the highest MgO levels, all dilutions and the neat show down regulation of cellular activity.

12.7 Discussion:

The test results for the ternary glass system showed that the higher the CaO content of the glasses, the higher the cell proliferation, the better the cell response. All glasses with CaO contents higher than 24 mol% show cell proliferation around the control line. The rate of proliferation becomes higher with increasing CaO content resulting in one case in an enhanced rate 10 times higher that the control and this was for the glass with the highest CaO content, i.e. $Ca_{40}Na_{15}P_{45}$.

The test results of the CaO-Na_2O-K_2O-P_2O_5 system reveals that potassium only has a positive effect on cell proliferation in higher contents, otherwise cell proliferation gets down regulated. This is a little unusual as the addition of K_2O to the glass appears, as shown in previous chapters, to increase the solubility. Thus, the presence of K_2O appears to be beneficial. In fact it could be postulated that the K_2O is beneficial in these systems, and may be a component that should routinely be used in these glasses.

From the MTT assays for the MgO containing glasses, it can clearly be seen that only small amounts of MgO appear beneficial. This again is unusual in that the MgO

decreases the solubility. Thus it may be concluded that at low levels, the MgO was having a beneficial effect as seen by the increased cellular activity, but at the higher levels, there is evidence for a negative effect due to the MgO.

A preliminary conclusion can be drawn from this study that cell proliferation is very sensitive to the CaO content in soluble phosphate based glasses and that in general, the higher the CaO content the better the cell response. However, it also appears that low levels of MgO and high levels of K_2O may also play a positive role.

Chapter 13

13.1 Conclusions

This study showed that it was possible to

1.) Develop a soluble glass system based on $CaO-Na_2O-P_2O_5$ and extend this basic glass system with the use of different oxides.

2.) Match the chemical composition and solubilities in order to obtain a positive cell response

3.) With structural investigations it was possible to obtain further insights into the glass structure

Conclusion 1. Overall Summary.

Clearly, it was possible to obtain a whole range of compositions within the $Na_2O-CaO-P_2O_5$ ternary glass system. All members are soluble, revealing a continuous degradation process. The higher the CaO content of the glasses, the slower the degradation process and the more the solubility curve becomes non-linear. The degradation process has been investigated, such that prediction of the solubility from composition for any further systems could be made. The degradation process would however benefit from a more precise mathematical approach, which might be established in the future. The pH measurement revealed an ion-exchange process taking place where H_3O^+ ions are exchanging for Na^+/Ca^{2+} ions which accounts for the increase in pH in the preliminary stages of the measurement and is followed by a decrease towards neutral. The results of the ion measurements mirrored the weight loss curves, however it was found that the out-leaching process of Ca^{2+} ions had a bigger impact to the weight loss curves.

Glasses with CaO content around 32 mol% and above showed proliferation rates around the control line or above. Glass $Ca_{40}Na_{15}P_{45}$ was found to have an enhancing proliferation effect, which is a very promising result for future research.

It was found that cell response was best with a high CaO content. It may be of significance that these glasses have non-linear solubility behaviour.

It was also possible to extend the basic Na_2O-CaO-P_2O_5 glass system by substituting either totally Na_2O to give the second ternary K_2O-CaO-P_2O_5 system or substituting parts of the Na_2O content via K_2O giving the first quaternary system Na_2O-K_2O-CaO-P_2O_5. The second quaternary system was achieved by replacing parts of the CaO content with MgO. Further, it was possible to create another system doped with fluoride, which needs to be tested more thoroughly for future research. The weight loss behaviour for the second ternary system K_2O-CaO-P_2O_5 was found to be very similar to the first ternary system, however solubilities were found to be higher, pH and ion measurements however are similar.

The first quaternary system Na_2O-K_2O-CaO-P_2O_5 was found to be similar to both ternary systems, however it was possibly to alter the solubility with addition of K_2O. This was explained by potassium being the heavier ion. No change was seen for pH and ion measurements.

With the second quaternary system it was possible to demonstrate the effect calcium has on both weight loss behaviour and cell proliferation. With increasing MgO content the curves lose their non-linearity/ exponential nature. Again, pH and ion measurements were no different from previous systems with the exception that the Ca^{2+} ion curve becomes less exponential.

Conclusion 2. Overall Summary

It was possible to establish a cell culture test, which allowed a preliminary measure of the level of biocompatibility/ toxicity. Within the ternary system, glasses with a high CaO content initiate a positive cell proliferation result. Especially glasses with extremely high CaO content show an enhanced proliferation rate, 10 times higher in comparison to cell culture tissue plastic.

Both quaternary glass system have been tested in terms of their proliferation rate and the result of these tests show again a positive influence on cells if the CaO content is high.

MgO in small contents can increase proliferation and the same is true for K_2O in high quantities.

The overall positive cell response was found to be due to the chemical composition which is closely related to chemical composition of natural hard tissue.

Conclusion 3. Overall Summary

Q^2 species as $NaPO_3$ and $Na_4Ca(PO_3)_6$ dominating the glass content and Q^1 species as $Ca_3(PO_4)_2$ or $Na_4P_2O_7$ are present in form of minor parts. All isotropic shifts for these species are shifting towards more negative values.

The DTA results supported the NMR results, with varying changes in crystallisation points and corresponding melting points revealing phase changes in addition to phase separation, a common phenomena in silica based glasses.

13.2 Future Work

This work has made a significant contribution to the systematic study of soluble glasses. However there are a number of interesting avenues to be explored in future work:

- Expand the studies in the fluoride systems. Of particular interest the fact that higher CaO contents could be achieved with these systems, opening the way to glasses with Ca:P ratios closer to apatite
- Investigation of the effect of different in vitro media on dissolution rates
- A more rigorous investigation of the kinetics of dissolution in these glass systems
- Studies to determine the effect of dynamic dissolution systems compared to the static system used in this PhD
- Investigation of different cell types and how the glasses affect these different cells
- Performing in vivo studies to correlate in vitro results with a more complex in vivo system

Reference List

1. Hench, L. L. Bioceramcis:From Concept to Clinic. J.Am.Ceram.Soc. 74(7), 1487-1510. 1991.

2. Lendlein, A. Polymere als Implantatwerkstoffe. Chemie in unserer Zeit 5, 279-295. 1999.

3. Boutin, P. M. A view of 15-Years Results Using the Alumina-Alumina Hip Joint Protheses. Ceramics in Clinical Applications, Elsevier, New York , 297. 1987.

4. Hench, L. L. Bioceramics. J.Am.Ceram.Soc. 81(7), 1705-1728. 1998.

5. Ogino, M. Ohuchi F. and Hench L. L. Compositional Dependence of the Formation of Calcium Phosphate Films on Bioglass. J.Biomed.Mater.Res. 14, 55-64. 1980.

6. Clark, A. E. Pantano C. G. and Hench L. L. Auger Spectroscopy Analysis of Bioglass Corrosion Films. J.Am.Ceram.Soc. 59(1-2), 37-39. 1976.

7. Kim, C. Y. Clark A. E. and Hench L. L. Early Stages of Calcium Phosphate Layer Formation in Bioglass. Journal of Non-Crystalline Solids 113, 195-202. 1989.

8. Wang.M., Hench L. L. and Bonfield W. Bioglass/high Density Polyethylene Composite for soft Tissue Applications. J.Biomed.Mater.Res. 42, 577-586. 1998.

9. Kim, C. Y. Clark A. E. and Hench L. L. Compositional Dependence of Calcium Phosphate Layer Formation in Fluoride Bioglass. J.Biomed.Mater.Res. 26, 1147-1161. 1992.

10. Wilson, J. Pigott G. H., Schoen, F. J. and L. L. Hench, and (1981). Toxicology and Biocomoatibility of Bioglass. J.Biomed.Mater.Res. 15, 805-817.

11. Nagase, M. Abe Y. Chigira M. and Udagawa E. Toxicity of Silica-Containing Calcium Phosphate Glasses Demonstrated in Mice. Biomaterials 13(3), 172-175. 1991.

12. Nagase, M. Shimizu T. Chigira M. and Udagawa E. An Analytical Study of the Inflammation induced by a Calcium Phosphate Ceramic. Kitakanto Igaku. 37, 101-106. 1987.

13. Bendall, S. P. Gaies M. Frondoza C. Jinnah R. H. and Hungerford D. S. Effect of Particulate Bioactive Glass on Human Synoviocyte Cultures. J.Biomed.Mater.Res. 41, 392-397. 1998.

14. Vogel, W. und Hoelland W. Zur Entwicklung von Bioglaskeramiken fuer die Medizin. Angew.Chem. 541-558. 1987.

15. Drake, C. F. and Graham M. Inorganic Glasses as Slow Release Herbicides and Fungicides. Standard Telecommunications Laboratories Ltd, London Road, Harlow, Essex, CM17 9NS, 116-121. 1985.

16. Drake, C. F. and Allen M. The Use of Controlled-Release Glass for the Controlled Delivery of Bioactive Materials. Biochem.Soc.Trans. 516-520. 1985.

17. Drake, C. F. Continuous and Pulsed Delivery of Bioactive Materials. Consultation on Immunomodulation, Bellagio, Italy, 1985 , 1-6. 1985.

18. Allen, W. M. Sansom B. F. Drake C. F. and Davis. A new Method for the Prevention of Trace Element Deficientcies. Veterinary Science Communications 2, 73-75. 1978.

19. Allen, W. M. Sansom B. F. Drake C. F. and Moore P. R. Recent Developments in the Treatment of Metabloic Diseases. Veterinary Pharmacology adn Toxicology , 183-191. 1982.

20. Allen, W. M. Sansom Mallinson C. B. Gleed P. T. and Drake C. F. Boluses of Controlled Release Glass for Supplementing Ruminants with Copper. Veterinay Record 115, 55-57. 1984.

21. Allen, W. M. Drake C. F. and Tripp M. Use of Controlled Release Systems for Supplementation During Trace Element Deficiency. TEMA, Aberdeen,1984 , 1-4. 1984.

22. Allen, W. M. Sansom Mallinson C. B. Stebbings R. J. and Drake C. F. Boluses of Controlled Release Glass of Supplementing Ruminants with Cobalt. Veterinay Record 116, 174-177. 1985.

23. McColm, I. J. Ceramic Science for Materials and Technologists. Leonard Hill, New York . 1983.

24. Holleman, A. F. und Wiberg N. Lehrbuch der Anorganischen Chemie. Walter de Gruyter 91-100th edition. 1985.

25. Biscore, A. G. Pincus C. S. and Warren B. E. J.Am.Ceram.Soc. 24, 116-119. 1994.

26. DeDecker, H. Rec.Trav.Chim. 60, 413. 1941.

27. Van Wazer, J. R. Structure and Properties of the Condensed Phospahtes. J.Am.Ceram.Soc. 72, 644-647. 1950.

28. Martin, S. W. Review of the Structure of Phosphate Glasses. Eur.J.Solid State Inorg.Chem. 28, 163-205. 1991.

29. Goldschmitdt. Geochemische Verteilungsgesetze der Elemente VIII. Vid.Akad.Skr.Oslo 8 (132). 1926.

30. Zachariasen, W. H. The Atomic Arrangement in Glass. J.Am.Ceram.Soc. 54, 3841-3851. 1932.

31. Warren, B. E. Z.Kryst. 86, 349. 1933.

32. Haegg, G. J.Chem.Phys. 3, 42. 1935.

33. Grimer, A. R. and Haubenreisser U. High-Field Static and MAS ^{31}P NMR: Chemical Shift Tensors of Polychrystalline Potassium Phosphates. Chem.Phys.Let. 99(5,6), 487-490. 1983.

34. Duncan, T. M. and Douglass. On the ^{31}P Chemical Shift Anisotropy in Condensed Phosphates. Chem.Phys. 87, 339-349. 1984.

35. Mudrakovski, I. L. Shmachkova V. P. Kotsarenko N. S. and Mastikhin V. M. 31P NMR Study of I-IV Group Polycrystalline Phospahtes. J.Phys.Chem.Solids 47, 335-339. 1986.

36. Villa, M. Carduner K. R. and Chiodelli G. A ^{31}P-NMR Study of Binary Borophosphate Glasses. J.Solid State Chem. 69, 19-23. 1987.

37. Prabhakar, S. Rao K. J. and Rao C. N. R. A Magic Angle Spinning ^{31}P NMR Investigation of Crystalline and Glassy Inorganic Phosphate. Chem.Phys.Let. 139, 96-102. 1987.

38. Brow, R. K. Kirkpatrick R. J. and Turner G. L. The Short Range Structure of Sodium Phosphate Glasses. Journal of Non-Crystalline Solids 116, 39-45. 1990.

39. Flechter, J. P. Kirkpatrick J. R. Howell D. and Risbud S. H. ^{31}P Magic Angle Spinning NMR Spectroscopy of Calcium Phosphate Glasses. J.Chem.Soc.Faraday Trans. 89(17), 3297-3299. 1993.

40. Brow, R. K. Phifer C. C. Turner G. L. and Kirkpatrick R. J. Cation Effects on ^{31}P MAS-NMR Chemical Shifts of Metaphosphate Glasses. J.Am.Ceram.Soc. 74(6), 1287-1290. 1991.

41. Kirkpatrick, J. R. and Brow R. K. Nuclear Magnetic Resonance Investigation of the Structure of Phosphate and Phosphate Containing Glasses. Journal of Non-Crystalline Solids 5, 9-21. 1995.

42. Feike, M. Jaeger C. and Spiess H. W. Coonectivities of Coordination Polyhedra in Phosphate Glasses from ^{31}P Double-Quantum NMR-Spectroscopy. Journal of Non-Crystalline Solids 223, 200-206. 1997.

43. Wenslow, R. M. and Mueller K. T. Structure Details of Aqueous Attack on a Phosphate Glass by $^{1}H/^{31}P$ Cross-Polarizatio NMR. J.Phys.Chem.B 102, 9033-9038. 1998.

44. Hartmann, P. Vogel J. and Schnabel B. J.Magn.Reson.Ser.A 111, 110-114. 1994.

45. Haubenreisser, H. Vogel J. Hoeland W. und Vogel W. ^{31}P-Festkoerper-NMR-Untersuchungen zur Struktur einer Phosphateglaskeramik. Wiss.Ztsch.Friedrich-Schiller-Univ.Jena, Naturwiss.R. 36(5/6), 763-776. 1987.

46. Abrahams, I. Franks K. Hawkes G. E. Philippou G. Knowles J. Bodart P. and Nunes T. ^{23}Na, ^{27}Al and ^{31}P NMR and X-ray Powder Diffraction Study of Na/Ca/Al Phosphate Glasses and Ceramics. J.Mater.Chem. 7(8), 1573-1580. 1997.

47. Graham, T. Phil.Trans.Roy.Soc. 123, 253. 1933.

48. Kordes, E. Physicalisch-chemische Untersuchungen ueber den Feinbau von Glaesern. Ztsch.Anor.Allg.Chem. 241, 1-44. 1939.

49. Gresch, R. Mueller-Warmuth W. and Dutz H. X-Ray Photpelectron Spectroscopy of Sodium Phosphate Glasses. Journal of Non-Crystalline Solids 34, 127-136. 1979.

50. Brueckner, R. Chun H. U. Goretzki H. and Sammet M. XPS Measurements and Structural Aspects of Silicate and Phosphate Glasses. Journal of Non-Crystalline Solids 42, 49-60. 1980.

51. Eisenberg, A. Farb H. and Cool L. G. Glass Transition in Inorganic Polymeres. J.Polym.Sci. 4 (PartA-2), 855-868. 1966.

52. Sahar, M. R. and Kamaruddin N. The Phase Equilibrium of Binary MgO- and CaO-Phosphate Glasses. J.Mat.Sc.Let. 15, 1932-1934. 1996.

53. Hudgens, J. J. and Martin S. W. Glass Transition and Infrared Spectra of Low-Alkai, Anhydrous Lithium Phosphate Glasses. J.Am.Ceram.Soc. 76(7),

1691-1696. 1993.

54. Suzuya, K. Price D. L. Loong C. and Martin S. W. Structure of Vitreous P_2O_5 and Alkali Phosphate Glasses. Journal of Non-Crystalline Solids 232-234, 650-657. 1998.

55. Uo, M. Mizuno M. Kuboki Y. Makishima A. and Watari F. Properities and Cytotoxicity of Water soluble Na_2O-CaO-P_2O_5. Biomaterials 19, 2277-2284. 1998.

56. Vasenius, J. Vainionpaeae K. Vihtonen A. Maekelae A. and Rokkanen P. Biomaterials 11, 501. 1990.

57. Pistner, R. Gutwald R. Ordnung J. Reuter R. and Muhling J. ibid 14, 671. 1993.

58. Bos, R. R. M. Rozema F. R. Boering G. Nijenhuis A. J. Pennings A. J. Verwey A. B. Nieuwenhuis P. and Jansen H. W. B. ibid 12, 32. 1991.

59. Morey, I. J. Fournier R. O. and Rowe J. J. Geschim.Cosmochim.Acta 26, 1029. 1962.

60. Enss, J. Experiments on the Relation of the Water Durability of Glasses to Their Chemical Composition. Glastech.Ber. 5, 27. 1928.

61. Charles, R. J. J.Appl.Phys. 11, 1549. 1958.

62. Douglas, R. W. and Isard J. O. J.Soc.Glass Tech. 33, 289. 1949.

63. Dubrovo, S. K. and Shmidt A. Bull.Acad.Sci.USSR, Div.Chem.Sci , 403. 1955.

64. Rana, M. A. and Douglas R. W. Phys.Chem.Glasses 2, 179. 1961.

65. Hlavac, J. and Matej J. Silikaty 1, 261. 1963.

66. Dimbley, V. and Turner W. E. S. J.Soc.Glass Technol. 10, 314. 1926.

67. Shamy, T. M. Ph.D.Thesis, Univeristy of Sheffield . 1966.

68. Strauss, U. P. and Treitler T. L. Chain Branching in Glassy Polyphosphates. Chem.Revs , 1473-1476. 1954.

69. Westerman, A. E. and Crowther J. J.Am.Ceram.Soc. 37, 427-430. 1954.

70. Stevels, J. M. and Trap H. L. Phys.Chem.Glasses 1, 107-116. 1960.

71. Schulz, I. und Hinz W. Ueber die Konstitution des Glases. Silikathechnik 6, 235-241. 1955.

72. Kanazawa, T. Ikeda M. and Kawazoe H. Solubilities and Some Physical Properties of Alkaline Earth Phosphate Glasses. Yogyo-Kyokai-Shi 77, 163-165. 1969.

73. Bunker, B. C. Arnold G. W. and Wilder J. A. Phosphate Glass Dissolution in Aqueous Solutions. Journal of Non-Crystalline Solids , 291-316. 1984.

74. Shih, P. Y. Yung S. W. and Chin T. S. Thermal and Corrosion Beaviour of P_2O_5-Na_2O-CuO Glasses. Journal of Non-Crystalline Solids 224, 143-152. 1997.

75. Bunker, B. C. Arnold G. W. and Wilder J. A. Phosphate Glass Dissolution in Aqueous Solutions. Journal of Non-Crystalline Solids , 291-316. 1984.

76. Delahaye, F. Montagne L. Palavit G. Touray J. C. and Baillif P. Acid Dissolution of Sodium-Calcium Metaphosphate Glasses. Journal of Non-Crystalline Solids 242, 25-32. 1998.

77. Klein, C. P. A. T. de Blieck-Hogervorst Wolke J. G. C. and de Groot K. Studies of the Solubility of Different Calcium Phosphate Ceramic Particles *in Vitro*. Biomaterials 11, 509-512. 1989.

78. Kukobo, T. Kushitani H. Ohtsiki C. Sakka S. and Yamamuro T. Chemical Reaction of Bioactive Glass and Glass-Ceramics with Simulated Body Fluid. J.Mat.Sc.Mat.Med. 3, 79-83. 1992.

79. Knowles, J. C. Rehman I. and Bonfield W. Spectroscopic and Crystallographic Analysis of the Solution Kinetics of a Range of Soluble Phosphate Based Bioactive Glasses. Bioceramcis 7, 85-90. 1994.

80. Kokubo, T. Journal of Non-Crystalline Solids 120, 138-151. 1990.

81. Kumar, M. Xie J. Chittur K. and Riley C. Transformation of Modified Brushite to Hydroxyapatite in Aqueous Solution. Biomaterials 20, 1389-1399. 2000.

82. Roemp Chemielexikon. 9.erweiterte Auflage, Georg Thieme Verlag, Stuttgart, New York.

83. Burnie.J. Controlled Release Glass (C.R.G.) A new Biomaterial. Ph.D.Thesis . 1982.

84. Paul, A. Chemical Durability of glass; A Thermodynamic Approach. J.Mat.Sc. 12, 2246-2267. 1977.

85. Hill, R. personal communication . 1998.

86. Braden, M. personal communication . 1999.

87. McGraw-Hill. Encyclopedia of Science and Technology. 2000.

88. Kreidl N. Phase-separation in glasses. Journal Of Non-Crystalline Solids 1991;129:1-11.

89. Liu W, Liang KM, Zheng YK, Gu SR, Chen H. The effect of an electric field on the phase separation of glasses. Journal Of Physics D-Applied Physics 1997;30:3366-70.

90. Liu W, Gu XM, Liang KM, Chen H, Zheng YK, Gu SR. Controlled phase separation by an electric field in glasses. Materials Science And Engineering A-Structural Materials Properties Microstructure And Processing 1999;265:25-8.

91. Tomozawa M, Mcgahay V, Hyde JM. Phase-separation of glasses. Journal Of Non-Crystalline Solids 1990;123:197-207.

92. Vogel.W. Struktur und Kristallisation der Glaeser. Angew.Chem. 77, 109. 1965.

93. Wood, D. personal communication . 1999.

94. Dietzel, A. Die Kationenfeldstaerken und ihre Beziehungen zu Entglasungsvorgaengen. Ztschr.Elektrochem. 48, 9-23. 1942.

95. Herzfeld, J. and Berger A. E. J.Chem.Phys. 73, 6021. 1980.

96. Haeberlen. High Resolution NMR in Solids - Selective Averaging. Academic Press, New York , 9. 1976.

97. Griffith, E. J. Inorg.Chem. 1, 962. 1962.

98. Cheetham, A. K. Clayden N. J. Dobson C. M. and Jakeman R. J. B. J.Chem.Soc., Chem.Commun. 195. 1986.

99. Dusold, S. Kuemmerlen J. and Sebald A. 31 P NMR Study of Solid Compoounds MxP2O7. J.Phys.Chem.A 101, 5895-5900. 1997.

100. Mosmann, T. Rapid Colorimetric Assay for Cellular Growth and Survival. J.Immunol.Methods 65, 55-63. 1983.

Appendix 1

NMR spectra

Ternary glass system Na_2O-CaO-P_2O_5

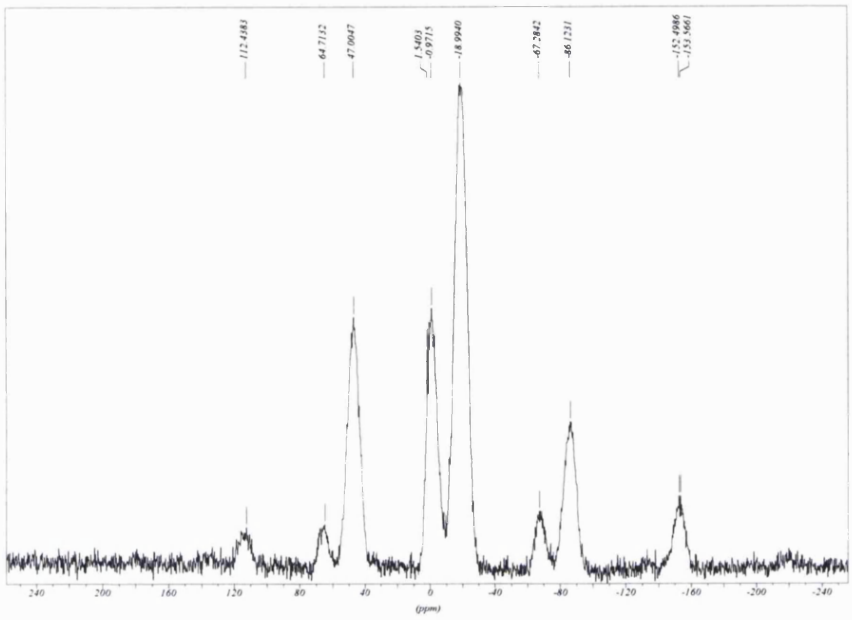

^{31}P MAS-NMR spectra for Glass $Ca_8Na_{47}P_{45}$

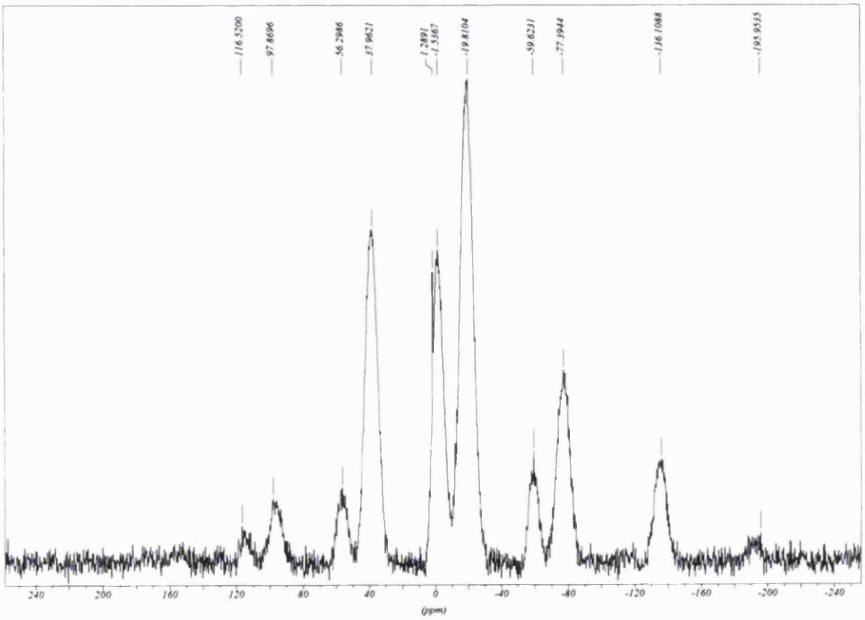

^{31}P MAS-NMR spectra for Glass $Ca_{10}Na_{45}P_{45}$

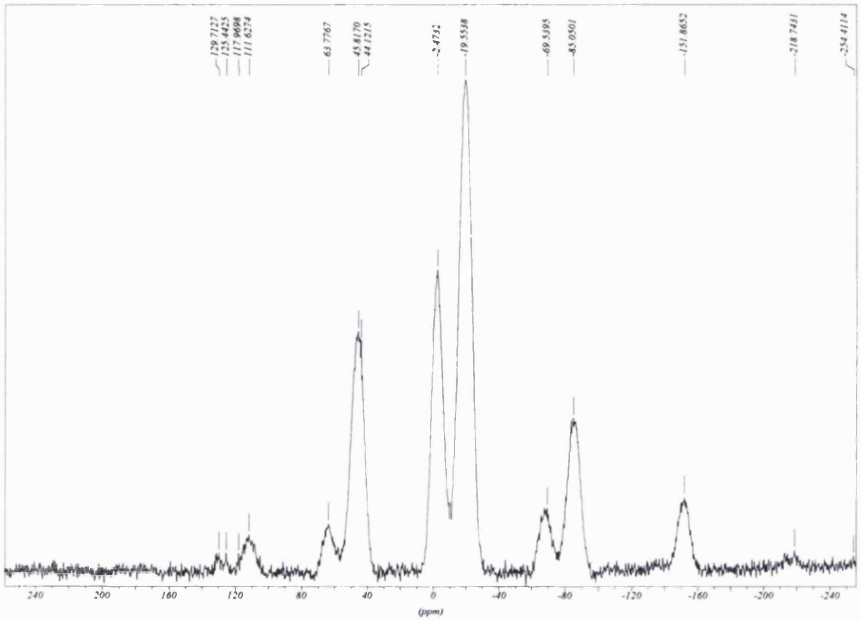

^{31}P MAS-NMR spectra for glass $Ca_{12}Na_{43}P_{45}$

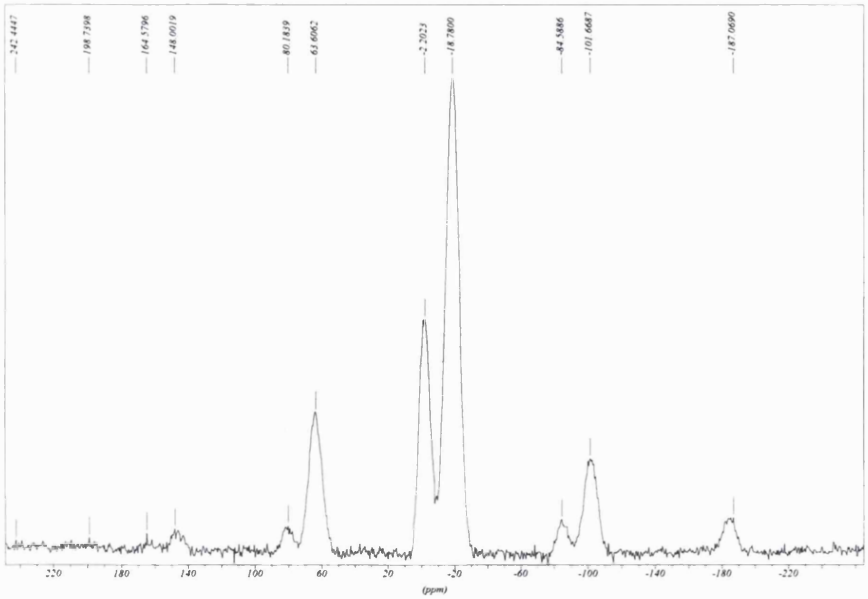

^{31}P MAS-NMR spectra for glass $Ca_{16}Na_{39}P_{45}$

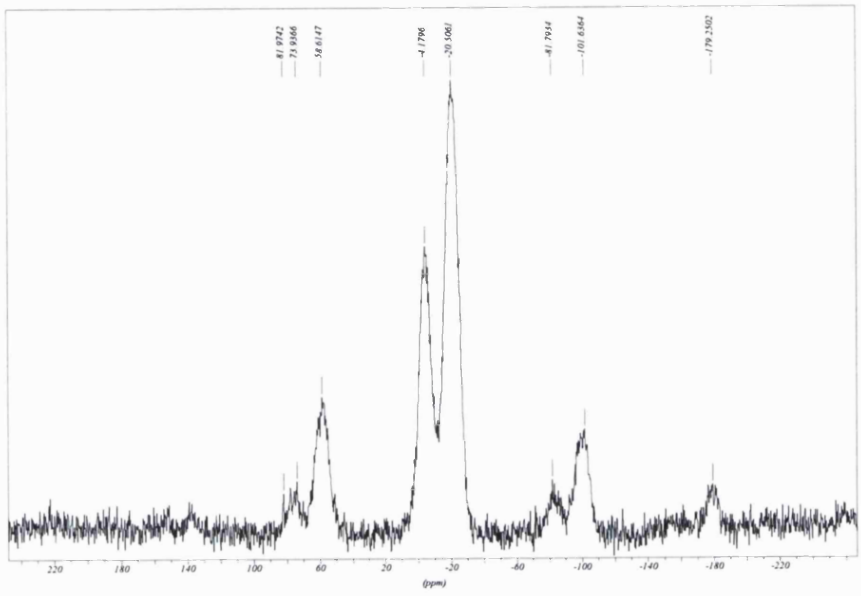

^{31}P MAS-NMR spectra for glass $Ca_{20}Na_{35}P_{45}$

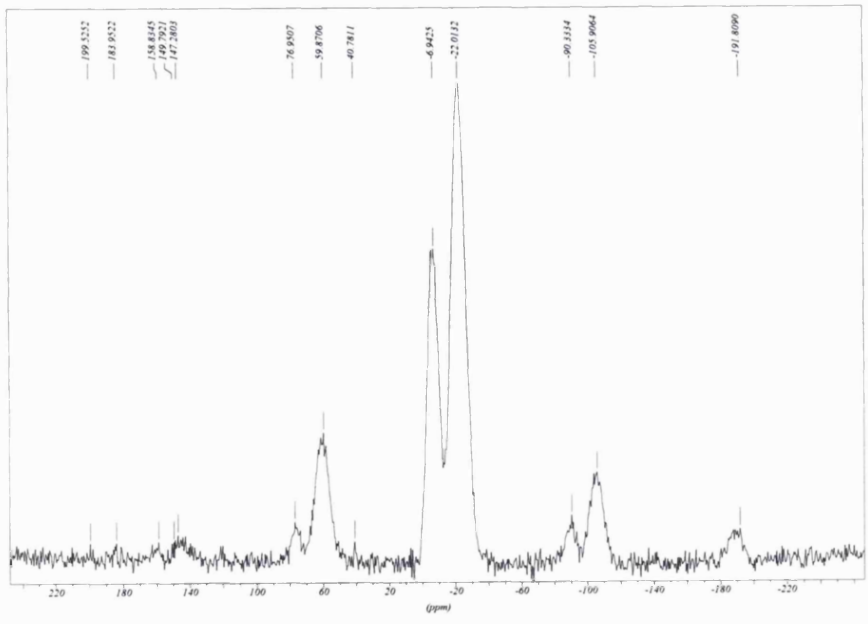

^{31}P MAS-NMR spectra for glass $Ca_{28}Na_{27}P_{45}$

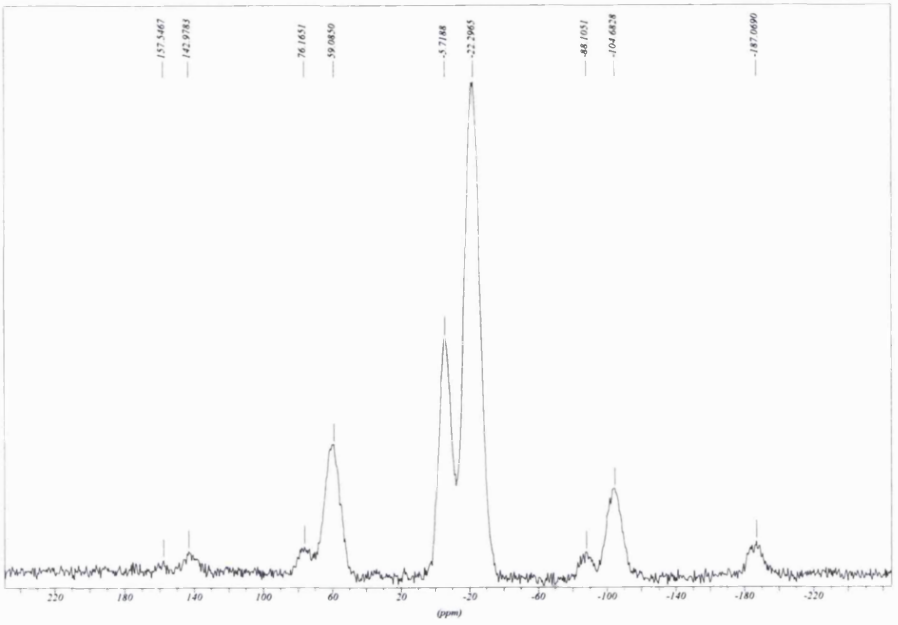

^{31}P MAS-NMR spectra for glass $Ca_{36}Na_{19}P_{45}$

Ternary glass system K_2O-CaO-P_2O_5

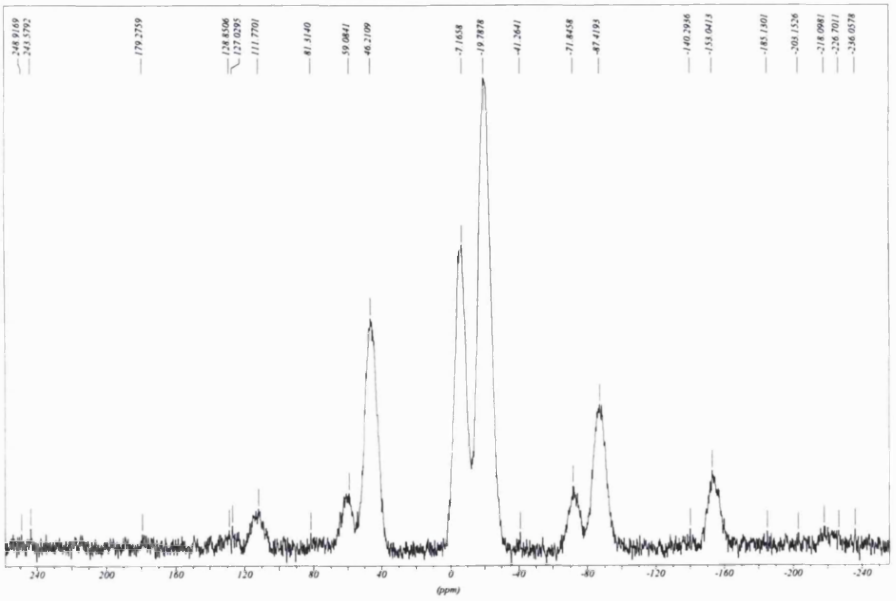

^{31}P MAS-NMR spectra for glass $Ca_{16}K_{39}P_{45}$

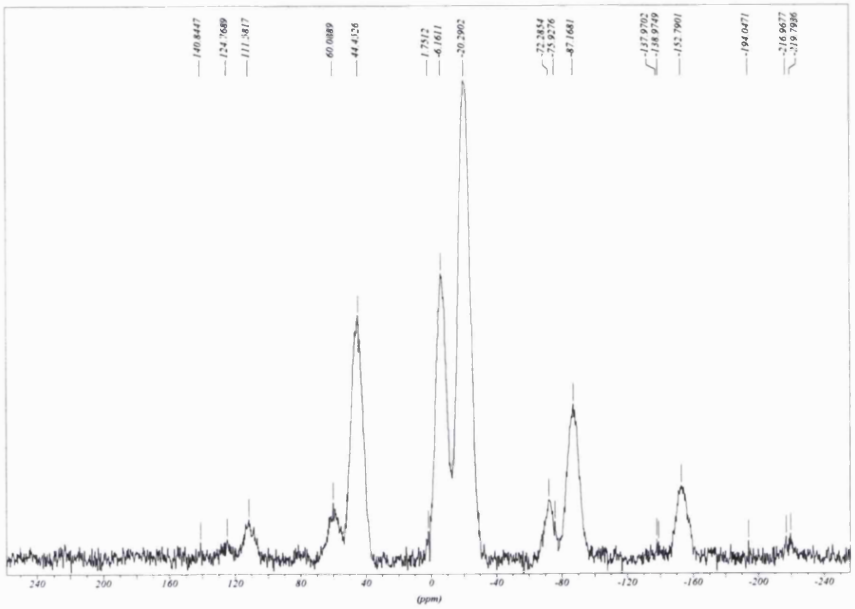

^{31}MAS-NMR spectra for glass $Ca_{20}K_{35}P_{45}$

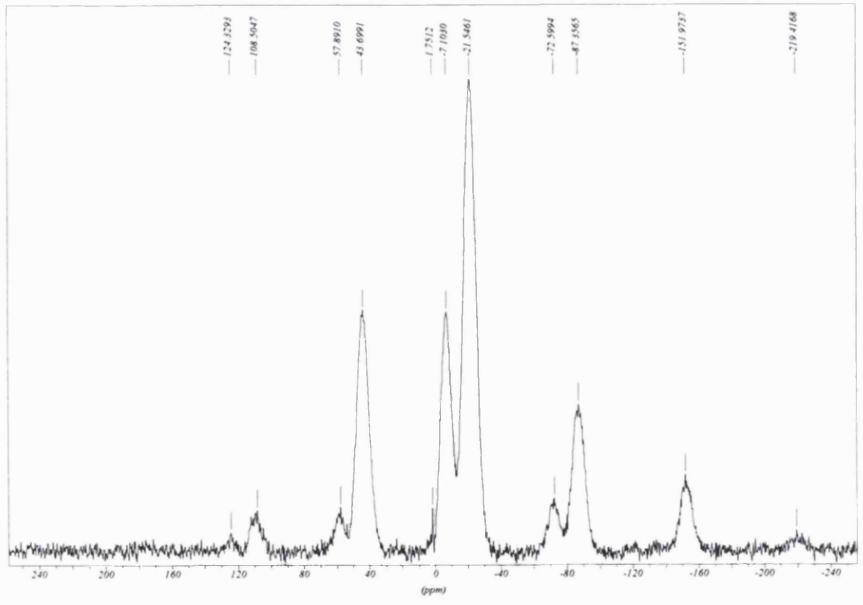

^{31}P MAS-NMR spectra for $Ca_{24}K_{31}P_{45}$

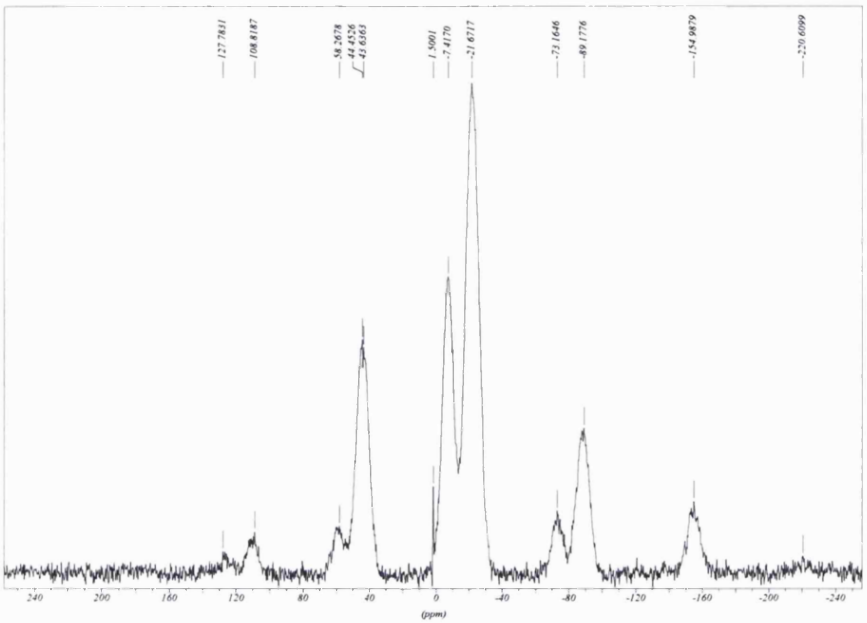

^{31}P MAS-NMR spectra for glass $Ca_{28}K_{27}P_{45}$

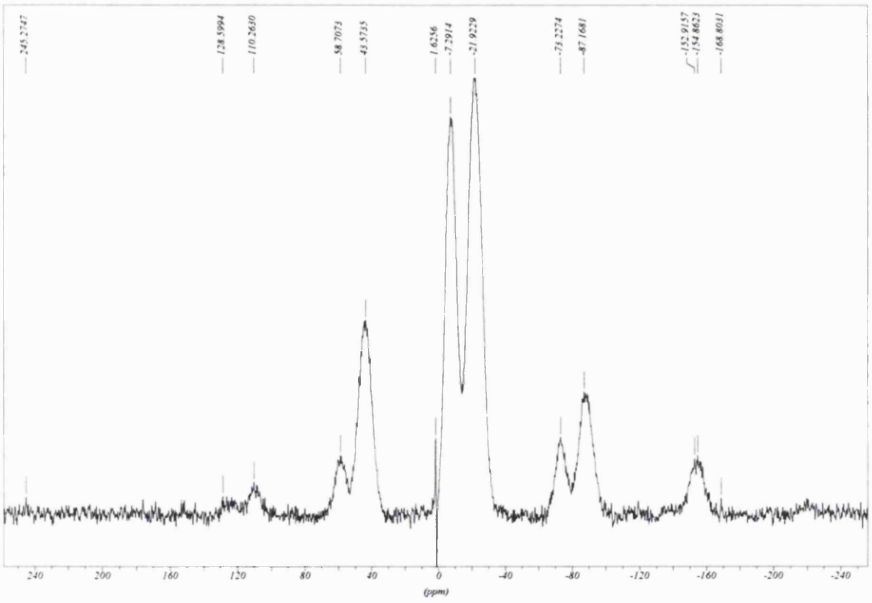

^{31}P MAS-NMR spectra for glass $Ca_{32}K_{23}P_{45}$

Appendix 2

Refereed Papers

I. Abrahams, K. Franks, G.E. Hawkes, G. Philippou, J.C. Knowles, P. Bodart and T. Nunes (1997) " A 23Na, 27Al and 31P NMR and X-ray Powder Diffraction Study of Na/Ca/Al Phosphate Glasses and Ceramics" J. Mat. Chem., Vol.7, No.8, p1573-1580.

V. Salih, I.J. Jalisi, D. Lee, K. Franks, G.W. Hastings, J.C. Knowles and I. Olsen (1998) "The Response of Human Osteoblast Cell Lines to Phosphate-Based Soluble Glasses" Bioceramics Vol.11, p269-272.

Abstracts

K. Franks, J.C. Knowles, G.E. Hawkes, I. Abrahams, I. Jalisi and D. Lee (1998) "Development of Phosphate Based Glasses for Periodontology" J. Dent. Res., Vol.77, No.SIB, p.1047

V. Salih, K. Franks, M. James, G.W. Hastings, J.C. Knowles and I. Olsen (1999) "Biological Response of Human Osteoblasts to Soluble Glasses" J. Dent. Res., Vol.78, No.5, p1075.

K. Franks, I. Abrahams and J.C. Knowles (1999) "Phosphate Based Glasses for Hard Tissue Surgery" In the Proceedings of the 15th European Conference on Biomaterials, Arcachon, France, 8th-12th September.

V. Salih, K. Franks, M. James, G.W. Hastings, J.C. Knowles and I. Olsen (1999) "Biological Response of Human Osteoblasts to Soluble Glasses" In the Proceedings of the 15th European Conference on Biomaterials, Arcachon, France, 8th-12th September.

J.C. Knowles, K. Franks, V. Salih and I. Olsen (1999) "Development of Soluble Glasses for Regeneration of Hard Tissue: A Chemical and Biological Evaluation" in the Proceedings of Conference on Tissue Engineering and Biological Interactions of Materials in Dentistry, Tempe, Arizona, 28th-30th October.

^{23}Na, ^{27}Al and ^{31}P NMR and X-ray powder diffraction study of Na/Ca/Al phosphate glasses and ceramics

Isaac Abrahams,[a] Katrin Franks,[a] Geoffrey E. Hawkes,*[a] George Philippou,[a] Jonathan Knowles,[b] Philippe Bodart[c]† and Teresa Nunes[c]

[a]*Structural Chemistry Group, Department of Chemistry, Queen Mary & Westfield College, University of London, Mile End Road, London, UK E1 4NS*

[b]*Eastman Dental Institute, University of London, 256 Gray's Inn Road, London, UK WC1X 8LD*

[c]*ICTPOL, Av. Prof. Gama Pinto 2, 1699 Lisboa codex, Portugal*

The techniques of X-ray powder diffraction and solid-state magic angle spinning (MAS) ^{23}Na, ^{27}Al, and ^{31}P nuclear magnetic resonance (NMR) spectroscopy have been combined to investigate the speciation in a series of glasses and glass ceramics of general formula $(P_2O_5)_{0.45}(CaO)_{0.24}(Na_2O)_{0.31-x}(Al_2O_3)_x$, $x=0.0$–0.05. The principal phosphate species are shown to be various $P_2O_7^{4-}$ containing phases, and cylic trimetaphosphates bridged by Ca, *i.e.* $Na_4Ca(PO_3)_6$ (instead of open-chain metaphosphates). Higher concentrations of Al_2O_3 result in glass ceramics which are phosphate-depolymerised ($Q^2 \rightarrow Q^1$) with respect to the parent glasses. At a lower level of Al_2O_3 (2%) the aluminium is present in octahedral coordination, while the higher level (5%) results in the formation of tetrahedrally coordinated aluminium. X-Ray powder diffraction of the ceramic with the higher aluminium content indicated the presence of $Na_5Ca_2Al(PO_4)_4$, and the ^{31}P NMR spectrum provides evidence for Q_1^2 species similar to phosphorus in aluminium metaphosphate. The more detailed structural information available from the aluminium-free glass ceramic, and the similarity in the Q^1/Q^2 ratio between the glass and its derived ceramic leads to the thesis that the ceramic structure may, in favourable cases, be used to model phosphate speciation in the glass.

There is a general need for some type of bone replacement for patients who have suffered from trauma, chronic degenerative diseases leading to bone loss, or congenital abnormalities. Some bioactive materials are available, which might potentially be used in this clinical situation and they are based on calcium phosphates,[1] *e.g.* hydroxyapatite (HA), tricalcium phosphate (TCP), fluorapatite (FHA). The bioactivity of these materials is normally attributed to their close chemical relationship to the inorganic phase of bone. Other bioactive materials are also available based on silicates, *e.g.* Bioglass®, and apatite wollastonite glass ceramic (AWGC),[2] which maintain high bioactivity through a dissolution–reprecipitation mechanism as opposed to a close chemical affinity. These materials however, have serious limitations. Firstly, the calcium phosphate based materials are crystalline compounds and their chemistry may not easily be altered, due to their stoichiometry. The second group of materials are hindered in their use by being silicate based and are therefore essentially insoluble and furthermore, their long-term effects are unknown. In this respect soluble phosphate glasses and glass ceramics offer potential advantages, particularly the ability to alter the solubility to a rate suitable for the application. The development of bioactive glass ceramics has been reviewed by Vogel and Höland.[3] Our interest focuses on CaO–Na_2O–P_2O_5 glasses including structure-modifying oxides, and we present here our data on these glasses doped with Al_2O_3.

In order to optimise the glasses, techniques need to be applied to probe their chemistry and currently, because of the non-crystalline nature of glasses, the number of techniques available is few. Solid-state nuclear magnetic resonance (NMR) is one of these few techniques and it can give a wealth of information, which may be used to develop models relating the chemical structure and bonding to the bioactivity of the glass. The application of NMR to the study of phosphate glasses has been recently reviewed by Kirkpatrick and Brow.[4]

† Present address: Department of Chemistry, University of Durham, South Road, Durham, UK DH1 3LE.

^{31}P NMR spectroscopy is particularly useful and can enable the quantification of the relative amounts of Q^n phosphorus species present, $PO_{4-n}(OP)_n$, since in favourable cases resonances due to each of these species are resolved in the magic angle spinning (MAS) spectra. Hartmann *et al.*[5] used ^{31}P NMR in their study on a series of Ca/Na/Al/phosphate glasses and ceramics and found predominantly Q^1 and Q^2 phosphorus units. Their aluminium-free glasses contained 39–53% Q^2 units, and for glasses containing aluminium they found a significant decrease in Q^2 content from 67 to 30% as the Al_2O_3 content increased from 1.1 to 3.1%. In a subsequent investigation on glasses and ceramics of similar composition Hartmann *et al.*[6] used ^{31}P 2D exchange NMR to show the contribution of pyrophosphate to the Q^1 region of the spectrum, and also showed a connectivity between the Q^1 and Q^2 regions indicating the presence of open chain metaphosphate groups. Fletcher *et al.*[7] reported qualitative ^{31}P NMR data on binary calcium phosphate glasses which showed Q^1, Q^2 and Q^3 units. Brow *et al.*[8] quantified Q^1, Q^2 and Q^3 units from binary sodium phosphate glasses, whereas Born and coworkers[9,10] found only Q^2 and Q^3 units in a sodium phosphate glass and from ^{31}P 2D NMR experiments showed connectivity between the two types of unit suggesting an almost regular alternating sequence for the Q^2 and Q^2 units.

For glasses incorporating Al_2O_3, ^{27}Al MAS NMR spectra can be used[4] to quantify relative amounts of four-, five-, or six-coordinate aluminium in the structure. ^{23}Na MAS NMR has been applied in relatively few studies[8,11] of glasses, and the information content from these spectra has been restricted by their relatively poor resolution and the relatively large second-order quadrupole effects which influence the spectra. More recently Koller *et al.*[12] presented a systematic analysis of the ^{23}Na NMR parameters from a series of crystalline sodium compounds, and their data may provide a sound basis for the interpretation of spectra from glasses.

Heating of glasses above the glass transition temperature T_g results in crystallisation within the glass matrix to form a glass ceramic. The phases crystallised in this way can be stoichio-

metric or non-stoichiometric depending on the parent glass. Materials prepared in this way generally contain a mixture of crystalline phases with some residual glass. Whilst the individual phases may not reflect the composition of the original glass the overall composition is the same. The advantage of crystallising glasses is that other techniques such as X-ray powder diffraction can then be used in the study of the material and the results extrapolated to the glass. In addition the NMR linewidths of crystalline phases are much narrower due to the smaller range of chemical environments in ordered crystalline solids when compared to glasses.

We present here our ^{23}Na, ^{27}Al and ^{31}P MAS NMR and X-ray powder diffraction data on a series of glasses and glass ceramics of general formula $(P_2O_5)_{0.45}(CaO)_{0.24}(Na_2O)_{0.31-x}(Al_2O_3)_x$, $x=0.0$–0.05. This composition was chosen because it has an accessible melting point, and glasses with this composition are likely to exhibit a significant bioactivity.[3] The Ca/P ratio was held constant in order to minimise the number of variables across the quaternary glass series.

Experimental

Preparation of glasses and ceramics

Samples of three glass compositions were prepared using appropriate molar quantities of $CaCO_3$, NaH_2PO_4, $CaHPO_4$, P_2O_5 and $AlPO_4$. The mixtures were blended in a Seward 400 stomacher prior to heating, and were then melted at 1200 °C in a platinum crucible for 1 h. Previous work[8,13] has shown that compositional changes due to evaporation of volatile components during glass formation in such materials are negligible especially over short intervals as used in this study. The melt was then poured into a preheated (600 °C) graphite mould and slowly cooled from 600 °C to room temperature at 4 °C min^{-1}. The glass rods produced of approximately 12 mm diameter were cut into discs of approximately 2 mm thickness using a diamond saw.

Investigation of crystallisation and glass transition temperatures was carried out by differential scanning calorimetry using a Perkin Elmer DSC 7, varying the temperature from 25 to 600 °C at a heating rate of 20 °C min^{-1}. Subsequent conversion to ceramic samples was carried out by heating glass discs on gold foil for *ca.* 2–3 h at temperatures just below the crystallisation temperatures. The compositions of the glasses and conditions for crystallisation are summarised in Table 1.

X-Ray crystallography

X-Ray diffraction data were collected on powdered glass ceramic samples on a Siemens D5000 diffractometer in flat-plate mode using graphite-monochromated Cu-Kα radiation ($\lambda=1.5418$ Å). Data were collected in the range 2θ 10–90°, in steps of 0.03°. Data for glass ceramic **3** were collected on an automated Philips PW 1280 diffractometer in flat-plate mode using nickel-filtered Cu-Kα radiation in the range 2θ 5–70°, in steps of 0.02°.

Table 1 Compositions (%) of the glasses and crystallisation conditions

	glass **1**	glass **2**	glass **3**
P_2O_5	45	45	45
Na_2O	31	29	26
CaO	24	24	24
Al_2O_3	0	2	5
T_g^a/°C	250	380	415
T_c^b/°C	478	522	—
ceram.[c]	2 h, 430 °C	2 h, 520 °C	3 h, 539 °C

[a]The glass transition temperature. [b]The crystallisation temperature. [c]The length of time and temperature (°C) for ceramic formation.

NMR spectroscopy

The one-dimensional single-pulse ^{23}Na, ^{27}Al and ^{31}P spectra were measured in London using a Bruker MSL-300 spectrometer operating at 79.4 MHz for ^{23}Na, 78.2 MHz for ^{27}Al and 121.5 MHz for ^{31}P. The samples were contained in 4 mm o.d. rotors and magic angle spinning (MAS) was used at *ca.* 10–11 kHz for ^{23}Na and ^{27}Al, and 7.5 kHz for ^{31}P. Typically 300–1000 transients were acquired for the ^{23}Na spectra using a 2 s relaxation delay, up to 10000 transients for the ^{27}Al spectra with a 0.5 s relaxation delay, and 16 transients for the ^{31}P spectra using a 60 s relaxation delay. The two-dimensional triple-quantum MAS spectrum[14–16] was measured in Lisbon using a Bruker MSL-300 spectrometer. The sample was contained in a 4 mm o.d. rotor and MAS used at 14 kHz; 72 transients were acquired with a 10 s recycling time; 512 and 256 points were acquired in the F1 and F2 dimensions respectively.

NMR spectral simulation

The ^{23}Na MAS NMR spectra were simulated using the program QUASAR.[17] The overlapping resonances in the ^{31}P MAS NMR spectra were deconvoluted using the XEDPLOT routine within the Bruker XWINNMR software.

Results

^{23}Na solid-state NMR spectra

The single-pulse solid-state magic angle spinning (MAS) ^{23}Na NMR spectra of the glass **1** and the corresponding ceramic are shown in Fig. 1. The overall widths of the two spectra are about the same, however it is clear that there is significantly improved resolution of the band shape for the ceramic. It appeared likely that there were two chemical shifts contributing to the spectrum of the ceramic, and to confirm this the two-dimensional triple quantum MAS spectrum[14–16] was acquired.

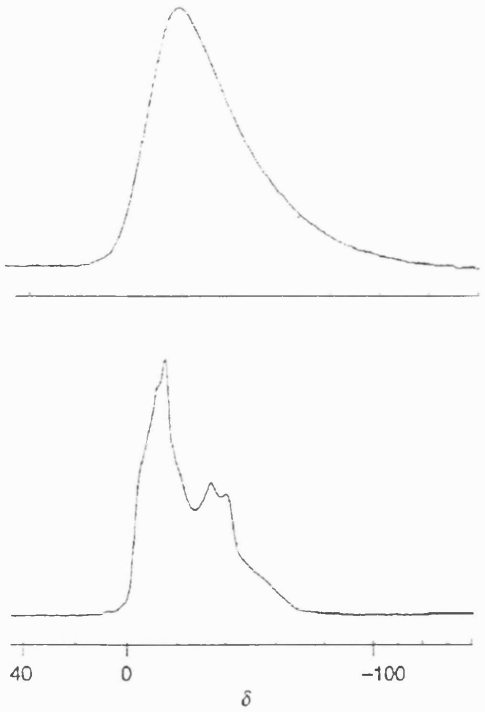

Fig. 1 The 79.4 MHz ^{23}Na MAS NMR spectra of glass **1** (upper) and ceramic **1** (lower). For both spectra the MAS rate was 10.5 kHz.

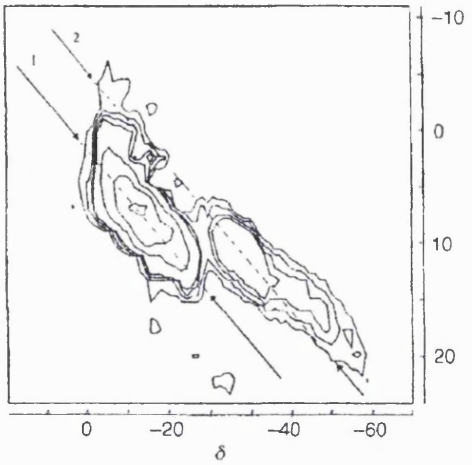

Fig. 2 The 79.4 MHz ^{23}Na triple quantum 2D MAS NMR spectrum of ceramic **1**. The MAS rate was 14 kHz and the diagonal arrows indicate the two distinct sites.

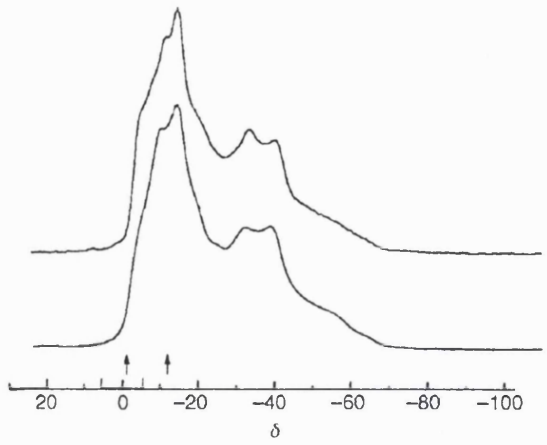

Fig. 3 Experimental (upper) and simulated (lower) 79.4 MHz ^{23}Na MAS NMR spectrum of ceramic **1**. The parameters from the simulation are given in Table 2, and the arrows indicate the isotropic chemical shifts.

The result is shown in Fig. 2, which shows two principal sodium sites. The extractable parameters from the spectrum are the isotropic chemical shifts and the 'second order quadrupole' parameters[15] (SOQE):

$$\mathrm{SOQE} = C_q\left(1+\frac{\eta_q^2}{3}\right)^{1/2} \quad (1)$$

where C_q and η_q are the quadrupole coupling constant and asymmetry parameter respectively, and the values obtained are given in Table 2.

With the information from the 2D-3Q MAS experiment as a starting point the single-pulse ^{23}Na MAS spectrum was simulated. The parameters obtained from this fitting procedure are also collected in Table 2, and the calculated spectrum is shown in Fig. 3. As can be seen there is good agreement between the quadrupole coupling parameters from the two methods, and between the isotropic shifts. There is a small difference (2–3 ppm) in the isotropic shifts from the two experiments, and those values from the single-pulse spectrum are probably the more reliable. The ^{23}Na spectrum of ceramic **3** was similarly fitted as two sodium sites (Table 2) while that for ceramic **2** showed evidence, at the high-frequency edge of the band, for a third site. The spectrum of ceramic **2** was fitted as three sites (Fig. 4) and gave the parameters in Table 2.

^{27}Al solid-state NMR spectra

The ^{27}Al data for the glasses and ceramics **2** and **3** are given in Table 3. The chemical shifts are measured directly from the spectra and so are not corrected for the quadrupolar shift.

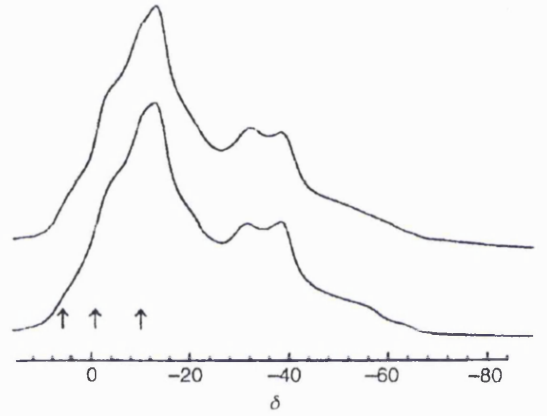

Fig. 4 Experimental (upper) and simulated (lower) 79.4 MHz ^{23}Na MAS NMR spectrum of ceramic **2**. The parameters from the simulation are given in Table 2, and the arrows indicate the isotropic chemical shifts.

^{31}P solid-state NMR spectra

The solid-state ^{31}P MAS spectra of glass **1** and of ceramic **1** are shown in Fig. 5. As with the ^{23}Na spectra (Fig. 1) the spectra are basically similar, but that of the ceramic shows considerably improved resolution, and it is possible to resolve eight resonances in the high-frequency band (band B, δ 0 to −10) and four resonances in the low-frequency band (band A, δ −20 to −23). The integrated intensities of the individual lines were determined by deconvolution of the experimental

Table 2 ^{23}Na NMR parameters for the ceramics

	δ_{iso}[a]	site occupancy (%)	SOQE/MHz	C_q/MHz	η_q
ceramic **1**	−2.7		1.59		
(2D-3Q)	−13.4		2.47		
ceramic **1**	−0.7	45±2	1.62	1.55±0.03	0.53±0.05
(single pulse)	−10.3	55±2	2.45	2.27±0.04	0.69±0.05
ceramic **2**	−2.4	40±2		1.52±0.01	0.68±0.01
(single pulse)	−11.4	48±2		2.26±0.01	0.72±0.01
	5.7	12±2		1.41±0.04	0.50±0.1
ceramic **3**	−1.8	44±2		1.51±0.01	0.60±0.01
(single pulse)	−10.6	56±2		2.36±0.02	0.65±0.02

[a]The chemical shifts are referenced to external NaCl solution. We are unable to estimate the error on the shifts from the 3Q MAS experiment, but the errors are ±0.4 and ±0.8 ppm respectively for the high- and low-frequency signals from the single-pulse experiment.

Table 3 ^{27}Al NMR data for the glasses and ceramics

	δ^a	$\Delta\nu_{1/2}{}^b$/Hz
glass **2**	−15	540
	(10, 37)[c]	(*ca.* 500)[c]
ceramic **2**	−14, −21	130
glass **3**	−16	620
	(8, 33)[c]	(*ca.* 500)[c]
ceramic **3**	−17 (93%)	220
	39 (7%)	150

[a]Chemical shifts in ppm to high frequency of external 1.0 M $AlCl_3$. [b]Full-width at half height. [c]These are minor resonances that constitute < 10% of the total ^{27}Al spectrum.

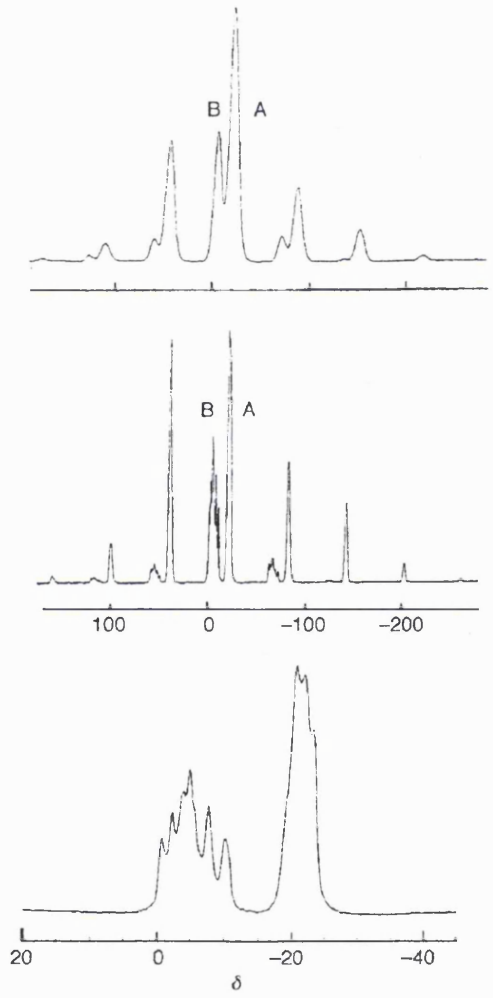

Fig. 5 The 121.5 MHz ^{31}P MAS NMR spectra of: (upper) glass **1** with MAS rate 8.0 kHz, (middle) ceramic **1** with MAS rate 7.4 kHz, (lower) expansion of the centre band region for ceramic **1**

spectrum, as described in the Experimental section, and the total intensity of each band (A and B) was obtained by summation over all spinning side-bands. The result for glass **1** was band B 22% and band A 78%, and for ceramic **1** band B 29% and band A 71%. A similar analysis was performed for glasses and ceramics **2** and **3**, and the results are given in Table 4. For ceramic **2** bands A and B were treated as comprising four and eleven overlapping resonances respectively, and for ceramic **3** these two bands comprised four and ten overlapping resonances. In addition the spectrum of ceramic **3** showed two new bands C (a single resonance) and D (three overlapping resonances). The results of deconvolution of bands B and A are shown schematically in Fig. 6 and 7 respectively. For the ceramic samples the isotropic chemical shift (δ_{iso}, Table 4) for each band is calculated by:

$$\delta_{iso} = \sum_i n_i \delta_i \quad (2)$$

where the index i runs over the number of resonances within that band, δ_i is the shift of each resonance and n_i is the fractional intensity of the ith resonance in that band. The full width at half height ($\Delta\nu_{1/2}$) quoted in Table 4 for each band is the average for the resolved resonances in that band.

The intensities of the spinning side bands were analysed by the method of Herzfeld and Berger,[18] as we have previously described.[19] This analysis yields the principal components (δ_{11}, δ_{22}, δ_{33}) of the chemical shift tensor, for which the isotropic chemical shift (δ_{iso}) is given by:

$$\delta_{iso} = (\delta_{11} + \delta_{22} + \delta_{33})/3 \quad (3)$$

These principal elements were ordered according to the Haeberlen convention:[20] $|\delta_{33} - \delta_{iso}| > |\delta_{11} - \delta_{iso}| > |\delta_{22} - \delta_{iso}|$. The chemical shift anisotropy ($\Delta\delta$) and asymmetry parameter (η) are given by:

$$\Delta\delta = \delta_{33} - (\delta_{11} + \delta_{22})/2 \quad (4)$$

$$\eta = (\delta_{22} - \delta_{11})/(\delta_{33} - \delta_{iso}) \quad (5)$$

These data are reported in Table 4 for each of the bands in the glasses and the ceramics. The analysis was not performed for the individual resonances within band A and within band B because of the large errors in the integrals of these resonances in the weaker side bands.

A selected range of the X-ray patterns for the three glass ceramic samples are shown in Fig. 8. The pattern for ceramic **1** has been successfully indexed[21] with $Na_4Ca(PO_3)_6$ as the major phase. Ceramic **2** has a similar pattern and again indicates that $Na_4Ca(PO_3)_6$ is the major phase present with a slight shift in lattice parameters, indicative of solid-solution formation with aluminium. At 5% Al_2O_3 in ceramic **3** the appearance of a second major phase, which has been indexed as $Na_5Ca_2Al(PO_4)_4$ based on the reported crystal structure,[22] suggests that this phase becomes increasingly more favoured as the Al concentration increases. Again a shift in lattice parameters for $Na_4Ca(PO_3)_6$ is observed. Table 5 summarises the $Na_4Ca(PO_3)_6$ lattice parameter variation with ceramic composition.

Discussion

^{23}Na solid-state NMR spectra

Inspection of the data in Table 2, from the fitting of the single-pulse spectra, shows two principal sodium sites with isotropic chemical shifts δ -1.6 ± 0.9 and -10.7 ± 0.6, and the occupancy of the lower frequency site is slightly greater. The quadrupole coupling constants are consistent over the three ceramics with values 1.4–1.6 MHz and 2.3–2.4 MHz, respectively for the low- and high-frequency sites. There is a paucity of published ^{23}Na solid-state NMR data on sodium phosphate phases, but it is noteworthy that the parameters obtained here are very similar to those measured by Koller *et al.*[12] for the cyclic trimetaphosphate phase $Na_3P_3O_9$, wherein there are[23] two equally populated, five-coordinate sodium sites.

^{27}Al solid-state NMR spectra

The features of the aluminium spectra reported in Table 3 have also been measured by Hartmann *et al.*[5] The lower frequency resonances in the range δ −14 to −21 are due to aluminium octahedrally coordinated by oxygens, $Al(OP)_6$ (see Brow *et al.*[24]), while the higher frequency band (δ 33–39) is most likely[25] arising from four-coordinate aluminium, probably as $AlPO_4$. The signals at intermediate chemical shift, δ 8–10, are

Table 4 ^{31}P chemical shift[a] tensor components for the glasses and the ceramics

	%[b]	δ_{iso}	$\Delta\nu_{1/2}$[c]	δ_{11}	δ_{22}	δ_{33}	$\Delta\delta$	η
glass **1**								
band B (Q^1)	22	−5	940	−80	−22	87	138	0.6_2
band A (Q^2)	78	−21	1190	77	16	−158	−204	0.4_5
ceramic **1**								
band B (Q^1)	29	−5.1	137	−73	−21	80	127	0.6_1
band A (Q^2)	71	−21.1	183	91	25	−181	−239	0.4_2
glass **2**								
band B (Q^1)	27	−7	1360	−88	−15	82	134	0.8_1
band A (Q^2)	73	−21	1430	73	13	−149	−192	0.4_7
ceramic **2**								
band B (Q^1)	49	−10.6	199	−87	−20	75	128	0.7_8
band A (Q^2)	51	−21.1	175	91	26	−179	−238	0.4_1
glass **3**								
band B (Q^1)	25	−9	1313	−86	−27	87	143	0.6_1
band A (Q^2)	75	−21	1729	63	11	−138	−175	0.4_4
ceramic **3**								
band C (Q^1)	4	−0.4	1035	−86	−9	94	141	0.8_3
band B (Q^1)	41	−10.0	204	−87	−16	73	124	0.8_6
band A (Q^2)	44	−20.5	202	74	25	−159	−209	0.3_5
band D (Q_1^2)	11	−28.3	187	−91	−35	41	104	0.8_1

[a] ^{31}P chemical shifts, δ_{iso}, the tensor components δ_{ii}, and the anisotropy, $\Delta\delta$, are in ppm. The chemical shifts are referenced to external 85% aqueous phosphoric acid. Errors on the δ_{ii} values estimated to be *ca.* ±5 ppm for the ceramic bands Q^1 and Q^2 the isotropic chemical shifts are the weighted average of the shifts of the individual resonances within the band. [b] Errors are believed to be <10% of the stated value. [c] Full width at half height of the resonances, obtained from deconvolution of the MAS spectra as described in the Experimental section. For the ceramics the values given are the average of the individual resonances within that band. Errors are *ca.* ±90 Hz for the glasses.

Table 5 Variation of lattice parameters for $Na_4Ca(PO_3)_6$ with ceramic composition

ceramic	*a*/Å	*b*/Å	*c*/Å	*β*/°	*V*/Å^3
1	13.06(13)	8.04(8)	14.46(12)	94.1(3)	1515
2	13.11(9)	8.05(5)	14.32(8)	94.7(2)	1506
3	13.18(8)	7.90(17)	14.03(9)	94.2(4)	1456

more difficult to assign unambiguously. Dupree *et al.*[26] reported octahedral $Al(OAl)_6$ shifts in the range δ 1–12, while Brow *et al.*[24] assign a ^{27}Al peak at δ 15, from a sodium aluminophosphate glass to arise from five-coordinate $Al(OP)_5$ sites. Hartmann *et al.*[5] assigned ^{27}Al peaks at δ *ca.* 11, from Na/Ca/Al/phosphate glasses to $Al(OM)_6$ (M=metal) sites. The linewidths of the intermediate shift ^{27}Al peaks in this study are *ca.* 6 ppm, and therefore we are probably observing signals from the six-coordinate Al sites with metal in the second coordination sphere, but we cannot categorically exclude the five-coordinate Al sites.

^{31}P solid-state NMR spectra

The spectra of both the glasses and the ceramics consist of two principal bands each, with the lower frequency band A assigned to Q^2 phosphate units and band B to Q^1 units (see Table 4). The assignment of these bands respectively to Q^1 and Q^2 phosphate units has recently been discussed by Hartmann *et al.*[5] The isotropic chemical shifts fall within the ranges quoted by Haubenreisser *et al.*[27] for polycrystalline phosphates as δ 4 to −33 for Q^1 units and δ −18 to −53 for Q^2 units. In addition the ^{31}P chemical shift anisotropies for the Q^1 and Q^2 units were originally established[27] to be in the ranges $\Delta\delta$ 14–80 and −160 to −250 respectively. Our values for band B in the glass and ceramic ($\Delta\delta$ 138 and 127) are outside that original range, but in agreement with the subsequent data of Hartmann *et al.*[5] for Q^1 units with sodium and calcium ions in the second coordination sphere ($\Delta\delta$ = 137±6). The values for $\Delta\delta$ reported here for band A in the glass and the ceramic ($\Delta\delta$ −204 and −239) are within the range quoted by Haubenreisser *et al.*[27] (see above) and similar to the values ($\Delta\delta$ −176 and −204) for the Ca/Na/Al/phosphate glasses and ceramics studied by Hartmann *et al.*[5]

The individual chemical shift tensor components determined here for band B (Table 4) in both the glass and ceramic are close to the values indicated by Haubenreisser *et al.*[27] for Q^1 units (δ_{ii} −55, −30 and +75), and similarly the values here for band A are close to the reported values for Q^2 units (δ_{ii} +80, +20 and −155).

When Hartmann *et al.*[5] formed ceramics from their glasses they obtained incomplete crystallisation, but in their ceramic phases there was a clear reduction in the Q^2 content for those samples containing Al_2O_3, whereas they reported no such reduction for the aluminium-free samples. Our ceramic **1** contains no detectable glass contamination, is aluminium free, but does show a slight reduction (*ca.* 7%) in Q^2 content when compared with the glass. However this reduction is not significantly greater than the error limits (*ca.* ±5%) we estimate from the integrations.

Composition of the glasses

A major difference between the data reported here and that of the glasses prepared by Hartmann *et al.*[5] is the relative proportion of the Q^1 and Q^2 units. The aluminium-free $CaO/Na_2O/P_2O_5$ glasses from Hartmann *et al.*[5] contained 39–53% of Q^2 units, and those glasses with low levels of Al_2O_3 contained 67–30% Q^2 units. For all three glasses in this study the Q^2 content is in the range 73–78% and clearly the presence of aluminium in our glass structures, at the expense of sodium, does not significantly change the Q^1/Q^2 ratio. This observation is in contrast to that of Hartmann *et al.*[5] who observed a significant decrease in Q^2 content with increase in Al_2O_3. However in those glasses investigated by Hartmann *et al.*[5] other factors varied, for example they maintained a fairly constant mol% Na_2O (*ca.* 28.4%) whereas the atom ratio P/Ca varied in the range 2.17–2.69. In the glasses reported here the atom ratio P/Ca was constant at 3.75 and the mol% Na_2O varied in the range 26–31%. The preponderance of Q^2 units over Q^1 units in our samples suggests a relatively high proportion of cyclic phosphate structures.

To consider the effect of aluminium content on the glass

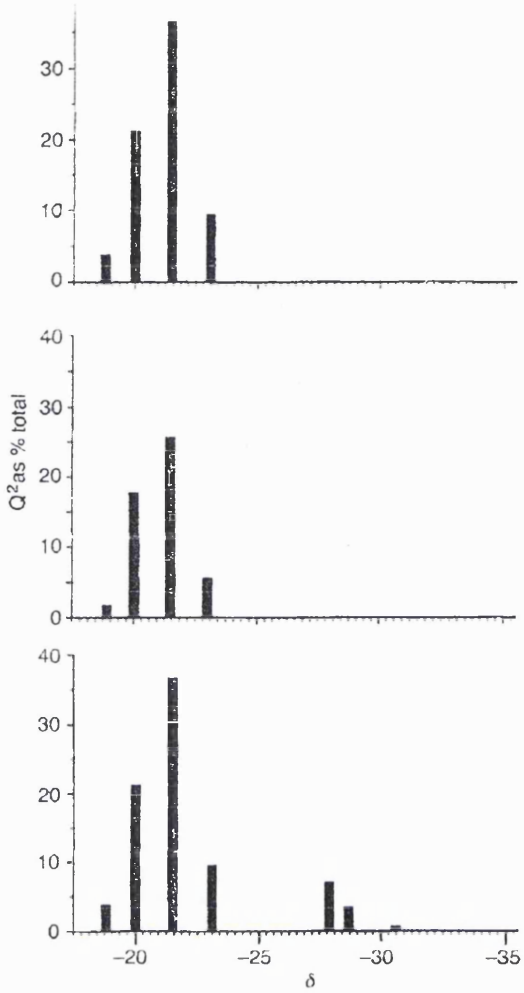

Fig. 6 Schematic presentation of the results of deconvolution of the ^{31}P resonance bands A for the ceramics **1** (upper), **2** (middle), and **3** (lower). The height of the bars indicates the total integrated intensity of each resonance and does not reflect the width of the resonance.

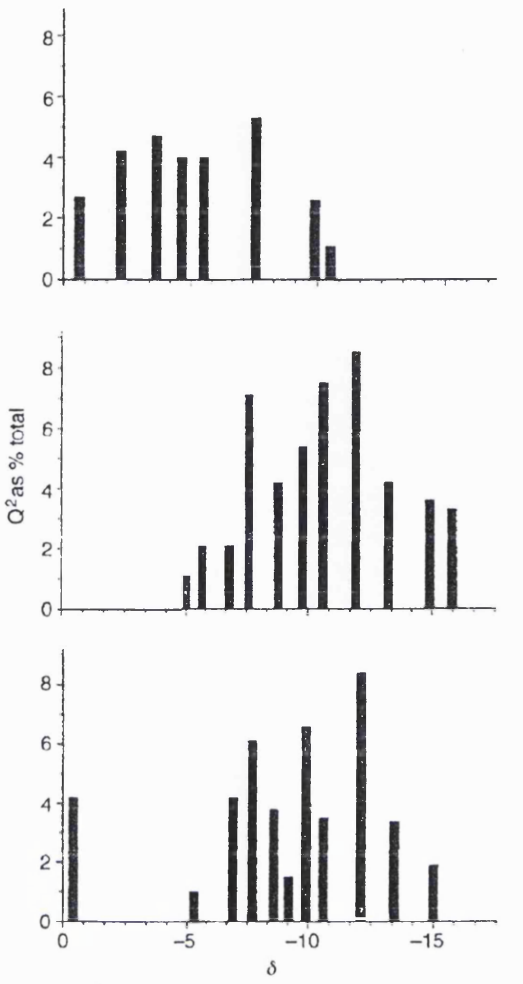

Fig. 7 Schematic presentation of the results of deconvolution of the ^{31}P resonance bands B for the ceramics **1** (upper), **2** (middle), and **3** (lower); this also includes band C at δ −0.7. The height of the bars indicates the total integrated intensity of each resonance and does not reflect the width of the resonance.

structure we note that the glass transition temperature (T_g) increases with increase in the aluminium content (Table 1). This observation is in agreement with that of Brow *et al.*[24,28] who ascribed the effect in sodium aluminophosphate glasses as being due to $Al(OP)_6$ species altering and strengthening the glass network by cross-linking neighbouring phosphate chains. The data in Table 4 for the glasses show that increasing aluminium content results in a slight low-frequency shift for the Q^1 signal without significantly affecting the position of the Q^2 signal. By comparison with the model studies on ^{31}P shifts from crystalline ortho-,[29–31] pyro-[30,31] and meta-phosphates[31] such low-frequency shifts would be expected from replacement of $P-O^-Na^+$ or $P-O^-Ca^{2+}$ by P—O—Al bonds in the structure. We use the 'Q' nomenclature for aluminophosphate species as suggested by Grimmer and Wolf;[32] *i.e.* Q_m^n where as before n is the number of coordinated —OP groups and m is the number of coordinated —OAl groups. Therefore the low-frequency shift is due to the change $Q_0^1 \rightarrow Q_1^1$ (in agreement with the observations of Brow *et al.*[24]). The effect of the low levels of aluminium on the linewidths of the Q^1 and Q^2 resonances is that for 0–2% Al_2O_3 (glass **1** to glass **2**) there is an approximately 45% increase in the width of the Q^1 resonance, while the width of the Q^2 resonance increases by 20%. Such increases in the linewidth can arise from a greater diversity of the metal ions in the second coordination sphere of phosphorus (see above) and a greater spread in P—O—P and O—P—O bond angles.[33] Further increase in the level of Al_2O_3 from 2 to 5% (glass **2** to glass **3**) does not result in an increase of the width of the Q^1 resonance. There is however a further 21% increase in the width of the Q^2 resonance which may be due to the bond angle effect or to the inclusion of lower-frequency, aluminium-containing components (see below the discussion of band D in ceramic **3**).

Composition of the ceramics

A comparison of the schematic ^{31}P spectra (Fig. 6) shows band A in all three ceramics is dominated by the same four isotropic chemical shifts (δ −18.9, −19.9, −21.5 and −23.0), which have approximately the same relative intensities within each spectrum. These four resonances contribute somewhat less to the total ^{31}P spectrum for ceramic **2** than for ceramics **1** and **3**. These isotropic chemical shifts are characteristic of metaphosphate groups (Q^2) with sodium ions in the second coordination sphere of phosphorus; for example, Prabhakar *et al.*[31] reported five resolved resonances in the region δ −15.6 to −26.8 from crystalline $(NaPO_3)_n$, and commented that the number of resonances was not simply related to (being greater than) the number of crystallographically distinguishable phosphorus sites. It is likely that the four component signals of band A observed in this study, which have quite different relative intensities, are due to a mixture of phases. This is consistent with the X-ray data. The predominance of Q^2 units is indicative of cyclic or long-chain phosphates. The crystal

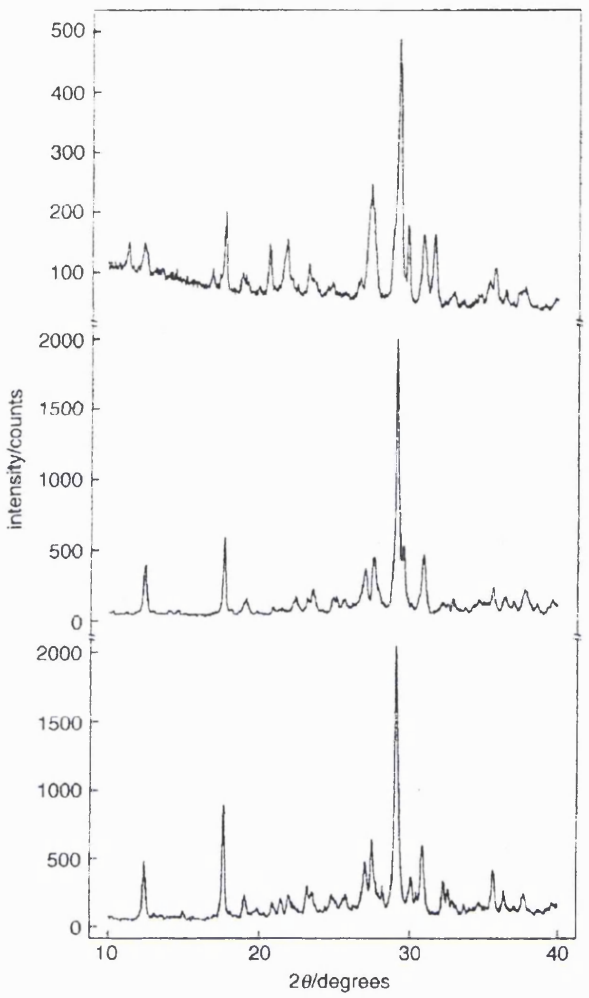

Fig. 8 X-Ray powder diffraction patterns in the range $2\theta = 10$–$40°$ for ceramics **1** (lower), **2** (middle), and **3** (upper)

structure of the major phase present, $Na_4Ca(PO_3)_6$, is unknown, however it has been suggested[34] that the structure is a calcium-bridged trimetaphosphate (Fig. 9). The change in Q^1/Q^2 ratio with Al content can be explained by the replacement of phosphorus atoms in the metaphosphate rings, through solid-solution formation as indicated by the change in lattice parameters. The phosphorus environment thereby changes from Q_0^2 to Q_1^1 which is consistent with the appearance of ^{31}P resonances at the low-frequency edge of band B for ceramics **2** and **3**. The Q^1/Q^2 ratio will also be influenced by ring opening of the cyclic metaphosphates and depolymerisation: a process suggested by Hartmann *et al.*[5] to be catalysed by aluminium. The $Na_5Ca_2Al(PO_4)_4$ structure proposed[22] as a component of ceramic **3** has aluminium tetrahedrally coordinated by four crystallographically distinct Q_1^0 PO_4 groups. The ^{31}P chemical shift for Q_1^0 species has not been reported, but almost certainly it will occur within the range covered by band B. Certainly the observation of a significant tetrahedral

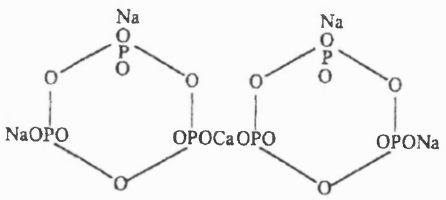

Fig. 9 The suggested[34] structure for $Na_4Ca(PO_3)_6$

^{27}Al signal from ceramic **3** (Table 3) is consistent with the presence of $Na_5Ca_2Al(PO_4)_4$.

On the basis of the NMR data alone the phases in the ceramics could include the distinct[35,36] crystal modifications of sodium metaphosphate, $(NaPO_3)_n$, or cyclic structures as in $Na_3P_3O_9$. From the isotropic chemical shifts it is possible[37] that these Q^2 units have sodium and/or calcium ions in the second coordination sphere of phosphorus although Fletcher *et al.*[7] reported ^{31}P Q^2 shifts from binary calcium phosphate glasses to somewhat lower frequency, in the region δ −25 to −28.

The appearance of band B is different for the three ceramics. The most salient feature (see Fig. 7) is the number of distinct chemical shifts, and this must be due to a complex mixture of phases wherein the Q^1 phosphorus atoms have different combinations of sodium and calcium and aluminium in their second coordination sphere. At the high-frequency edge of the band (δ *ca.* 0) Q^1 phosphorus influenced by sodium is expected, and with substitution by calcium, lower frequency Q^1 shifts occur. The presence of aluminium in the ceramics results in even lower frequency resonances, in the region δ −11 to −16, contributing to band B. This is in accord with the observations of Hartmann *et al.*[5] who assigned resonances in this region to Q^1 (Al, Ca, Na) species. For ceramic **2** these new aluminium-containing species are produced at the expense of species with resonances at the high-frequency edge of the band (sodium-dominated Q^1 units), and arise as described above by the conversions $Q_0^2 \rightarrow Q_1^1$ or $Q_0^1 \rightarrow Q_1^1$.

The patterns of the sharp resonances from ceramics **2** and **3** are similar, with the addition in ceramic **3** of a broad resonance (band C) centred at δ −0.4. The width of band C suggests it is due to an amorphous component in the sample. The isotropic chemical shift is consistent with calcium orthophosphate[31] $[Ca_3(PO_4)_2]$ or sodium pyrophosphate[30] $(Na_4P_2O_7)$. However the chemical shift anisotropy of band C is $\Delta\delta$ 141, which is close to that reported[37] ($\Delta\delta$ 127) for $Na_4P_2O_7$, and very different to that[38] for $Ca_3(PO_4)_2$ ($\Delta\delta$ 0). There is no corroborative evidence for the presence of $Na_4P_2O_7$ from the X-ray data since a low level of an amorphous phase would not give rise to identifiable features in the powder pattern.

With the higher level of aluminium in ceramic **3**, three new ^{31}P resonances appear (band D) at δ −27.9 (7.1%), −28.7 (3.5%) and −30.6 (0.7%). From consideration of the isotropic chemical shift alone these lowest frequency resonances could be due to one or more of the $AlPO_4$ polymorphs which are reported[29,31,33,38] to show resonances in the region δ −24.5 to −29.5. Another possibility for these resonances is Q_1^2 units[37] similar to those from $[Al(PO_3)_3]_n$ which has[32] its ^{31}P resonance at δ −30. The chemical shift tensor components for band D (δ_{ii} −91, −35 and 41) show some similarity with those for $[Al(PO_3)_3]_n$ (δ_{ii} −120, 15 and 15), with the chemical shift anisotropy being somewhat lower for band D ($\Delta\delta$ 104 *vs.* $\Delta\delta$ 135 for aluminium metaphosphate). However the values for the chemical shift tensor components and the chemical shift anisotropy for band D (see Table 4) are effective averages for the three component resonances. Therefore an interpretation of our data is that the major component of band D (δ −27.9) is a Q_1^2 resonance similar to that for aluminium metaphosphate, and either or both of the other two resonances are from $AlPO_4$ for which $\Delta\delta$ is expected[38] to be near zero. The presence of the $AlPO_4$ phase is also supported by the tetrahedral ^{27}Al resonance (see Table 3). The X-ray data do not provide evidence for or against the presence of these phases as such relatively low levels ($\leqslant$7%) would not be detected in the diffraction data.

Conclusion

The solid-state ^{31}P spectra of the glass ceramics show a preponderance of Q^2 units, indicative of long-chain or cyclic

metaphosphates. The ^{23}Na spectral parameters are similar to those reported[12] for the cyclic trimetaphosphate $Na_3(PO_3)_3$, and the X-ray powder diffraction data shows the dominance of $Na_4Ca(PO_3)_6$ for which the structure is thought[34] to consist of bridged trimetaphosphate rings. The presence of the small ring structures, instead of the long-chain polyphosphates has relevance to the long-term solubility of the materials since the alkali-metal polyphosphates are highly insoluble.[39] Because the Q^2 environment dominates the materials, the Q^1 environment must therefore be largely due to pyrophosphate, $P_2O_7^{4-}$, and the various Q^1 resonances from the ceramics are due to the array of different pyrophosphates possible in the presence of the mixed cations. The broad, high-frequency band C in ceramic **3** is probably mostly due to amorphous $Na_4P_2O_7$ in the sample, in spite of the increased time employed for the ceramic formation (Table 1). The higher level of aluminium in this sample may result in less efficient crystallisation of the Q^1 phases through Al cross-linking of the phosphate species. The ^{27}Al spectra of samples **2** and **3** show that the aluminium is predominantly present with octahedral coordination, and at the higher concentration (5% in sample **3**) there is additionally four-coordinate aluminium. The X-ray powder pattern for ceramic **3** indicates the presence of $Na_5Ca_2Al(PO_4)_4$ for which the Q_1^0 ^{31}P resonances would fall within band B. The lowest frequency band D in the ^{31}P spectrum of ceramic **3** could be due to Q_1^2 phosphorus similar to that in aluminium metaphosphate, but we cannot exclude the possibility of contributions from Q_4^0 sites from one or more of the polymorphs of $AlPO_4$.

The Q^1/Q^2 ratio for both samples **2** and **3** shows a significant increase upon ceramic formation, which does not occur for sample **1**. Hartmann *et al.*[5] have made a similar observation for Na/Ca/Al/phosphate glasses and ceramics and have speculated that the aluminium in some way catalyses the depolymerisation of the metaphosphate during ceramic formation. It is noteworthy that the Q^1/Q^2 ratios for the glasses in this study did not vary significantly with Al_2O_3 content, and this effect certainly merits further study. Our observation that the Q^1/Q^2 ratio in the aluminium-free sample **1** is not significantly different between the glass and the ceramic raises the possibility of using the more detailed structural information from aluminium-free ceramics to model the phosphate structures in glasses.

We wish to thank the University of London Intercollegiate Research Service in Solid State NMR at University College for the provision of the MSL-300 NMR spectrometer, and Dr. P. J. Barrie, Dr. A. E. Aliev and Mr. D. Butler for measuring the one-dimensional spectra. We also thank the IRC in Biomedical Materials at QMW for use of a diffractometer and thermal analysis equipment. G. P. acknowledges the receipt of a studentship from the EPSRC, and K. F. received support from the EC ERASMUS programme.

References

1 H. Aoki, *Science and Medical Applications of Hydroxyapatite*, Takayama Press Syste, Centre Co. Inc., Tokyo, JAAS, 1991.
2 K. Kawanabe, T. Yamamuro, T. Nakamura and S. Kotani, *Bioceramics*, ed. G. Heimke, Deutsche Keramische Geselleschaft, Köln, 1990, vol. 2, p. 121, and references therein.
3 W. Vogel and W. Höland, *Angew. Chem., Int. Ed. Engl.*, 1987, **26**, 527.
4 R. J. Kirkpatrick and R. K. Brow, *Solid State NMR*, 1995, **5**, 9.
5 P. Hartmann, J. Vogel and B. Schnabel, *J. Non-Cryst. Solids*, 1994, **176**, 157.
6 P. Hartmann, J. Vogel and C. Jäger, *Ber. Bunsenges. Phys. Chem.*, 1996, **100**, 1658.
7 J. P. Fletcher, R. J. Kirkpatrick, D. Howell and S. H. Rishbud, *J. Chem. Soc. Faraday Trans.*, 1993, **89**, 3297.
8 R. K. Brow, R. J. Kirkpatrick and G. L. Turner, *J. Non-Cryst. Solids*, 1990, **116**, 39.
9 C. Jäger, M. Feike, R. Born and H. W. Spiess, *J. Non-Cryst. Solids*, 1994, **180**, 91.
10 R. Born, M. Feike, C. Jäger and H. W. Spiess, *Z. Naturforsch. A*, 1995, **50**, 169.
11 R. K. Sato, R. J. Kirkpatrick and R. K. Brow, *J. Non-Cryst. Solids*, 1992, **143**, 257.
12 H. Koller, G. Engelhardt, A. P. M. Kentgens and J. Sauer, *J. Phys. Chem.*, 1994, **98**, 1544.
13 J. Burnie, PhD Thesis, University of Strathclyde, 1982.
14 L. Frydman and J. S. Harwood, *J. Am. Chem. Soc.*, 1995, **117**, 5367.
15 C. Fernandez and J. P. Amoureux, *Chem. Phys. Letts.*, 1995, **242**, 449.
16 C. Fernandez and J. P. Amoureux, *Solid State NMR*, 1996, **6**, 315.
17 J. P. Amoureux, C. Fernandez, L. Carpentier and F. Cochon, *Phys. Status Solidi A*, 1992, **132**, 461.
18 J. Herzfeld and A. E. Berger, *J. Chem. Phys.*, 1980, **73**, 6021.
19 G. E. Hawkes, K. D. Sales, L. Y. Lian and R. Gobetto, *Proc. R. Soc. London, Ser. A*, 1989, **424**, 93; G. E. Hawkes, K. D. Sales, S. Aime, R. Gobetto and L. Y. Lian, *Inorg. Chem.*, 1991, **30**, 1489.
20 U. Haeberlen, *High Resolution NMR in Solids—Selective Averaging*, Academic Press, New York, 1976, p. 9.
21 J-C. Grenier, C. Martin and A. Durif, *Bull. Soc. Fr. Mineral. Cristalogr.*, 1970, **93**, 52.
22 J. Alkemper, H. Paulus and H. Fuess, *Z. Kristallogr.*, 1994, **209**, 76.
23 H. M. Ondik, *Acta Crystallogr.*, 1965, **18**, 226.
24 R. K. Brow, R. J. Kirkpatrick and G. L. Turner, *J. Am. Ceram. Soc.*, 1993, **76**, 919.
25 D. Müller, G. Berger, I. Grunze, G. Ladwig, E. Hallas and U. Haubenreisser, *Phys. Chem. Glasses*, 1983, **24**, 37.
26 R. Dupree, I. Farnan, A. J. Forty, S. El-Mashri and L. Bottyan, *J. Phys.*, 1985, **46**, C8.
27 H. Haubenreisser, J. Vogel, W. Höland and W. Vogel, *Wiss. Ztschr. Friedrich-Schiller-Univ. Jena, Naturwiss. R.*, 1987, **36**, 763.
28 R. K. Brow, R. J. Kirkpatrick and G. L. Turner, *J. Am. Ceram. Soc.*, 1990, **73**, 2293.
29 G. L. Turner, K. A. Smith, R. J. Kirkpatrick and E. Oldfield, *J. Magn. Reson.*, 1986, **70**, 408.
30 A. K. Cheetham, N. J. Clayden, C. M. Dobson and R. J. B. Jakeman, *J. Chem. Soc., Chem. Commun.*, 1986, 195.
31 S. Prabhakar, K. J. Rao and C. N. Rao, *Chem. Phys. Lett.*, 1987, **139**, 96.
32 A. R. Grimmer and G. U. Wolf, *Eur. J. Solid State Inorg. Chem.*, 1991, **28**, 221.
33 D. Müller, E. Jahn, G. Ladwig and U. Haubenreisser, *Chem. Phys. Lett.*, 1984, **109**, 332.
34 E. J. Griffith, *Inorg. Chem.*, 1962, **1**, 962.
35 K. H. Jost, *Acta Crystallogr.*, 1961, **14**, 844.
36 K. H. Jost, *Acta Crystallogr.*, 1963, **16**, 640.
37 T. M. Duncan and D. C. Douglass, *Chem. Phys.*, 1984, **87**, 339.
38 I. L. Mudrakovskii, V. P. Shmachkova, N. S. Kotsarenko and V. M. Mastikhin, *J. Phys. Chem. Solids*, 1986, **47**, 335.
39 D. E. C. Corbridge, *The Structural Chemistry of Phosphorus*, Elsevier, Amsterdam, 1974, ch. 6.

Paper 6/08325K; *Received* 10*th December*, 1996

THE RESPONSE OF HUMAN OSTEOBLAST CELL LINES TO PHOSPHATE-BASED SOLUBLE GLASSES

V. Salih[1], I.J.Jalisi[2], D.Lee[2], K.Franks[1], G. W. Hastings[3], J.C. Knowles[1], I. Olsen[4]

Departments of Biomaterials[1] and Periodontology[4], Eastman Dental Institute, University of London, 256 Gray's Inn Road, London WC1 8LD, U.K.; [2]IRC in Biomedical Materials, Institute of Orthopaedics, Royal National Orthopaedic Hospital, Brockley Hill, Middlesex HA7 4LP, U.K.; [3]Institute of Materials Research & Engineering, The National University of Singapore, Kent Ridge, Singapore 119260.

ABSTRACT

Two human osteoblast cell lines, MG63 and HOS (TE85), were incubated *in vitro* in culture medium containing increasing concentrations of extracts of phosphate-based glasses. The effects of the extracts on the proliferation of the cells were measured using the MTT assay. A cell ELISA assay was used to measure fibronectin (FN), osteonectin (ON) and bone sialoprotein (BSP), antigens which play a fundamental part in connective tissue integrity and function. The results indicated that, over a period of 5 days, the glass extracts did not adversely affect the growth of the cells compared with control cultures. However, the expression of FN and especially ON, but not BSP, was found to be down-regulated, especially when cells were cultured in the presence of the more soluble glass extracts. These findings suggest that these glasses are not cytotoxic and could be effective for use in bone repair systems after their composition is modified to elicit an optimal biological response from the host tissue.

KEYWORDS: soluble glasses, osteoblasts, proliferation, extracellular matrix.

INTRODUCTION

A novel group of glasses has recently been developed that are phosphate-based, the solubility of which is directly related to their chemical composition[1]. Such biomaterials could promote the growth of soft and hard connective tissue cells as occurs, for example, in the repair of periodontal defects and bone[2]. The purpose of this study was to determine the biocompatibility of these soluble glasses by examining certain key features of the cellular response of two human osteoblast-like cell lines *in vitro*.

MATERIALS AND METHODS

Glass Formulations

The glasses were composed of calcium oxide (CaO), sodium oxide (Na_2O) and phosphorous pentoxide (P_2O_5). They were prepared in the form of rods, approximately 70mm long. Individual discs, of total surface area approximately 5cm^2, were cut from each rod using a diamond rotary saw. All discs had a smooth finish and appeared opaque. The P_2O_5 mol.% weight was kept constant at 45%. The solubility of the glasses is related to the proportion of CaO present, glasses containing lee than approximately 20% CaO being very soluble, whereas those containing more than approximately 20% are much less soluble. The composition of the glasses used in the present experiments is shown in Table 1, which also indicates their solubility.

Preparation of Glass Extracts

Glass discs were sterilised by dry heat at 180°C for 2 h. They were placed into 50 ml Falcon tubes containing 10 ml of cell culture medium. This latter volume was chosen in accordance with BS-EN 30993-5 (1994), which recommends that the ratio between the surface area of the test material and the volume of the extraction vehicle is equal to or greater than 0.5cm^2/ml. A volume of 5 ml of each extract was collected for each glass, after 1 day and after 5 days of incubation at

37°C, with occasional agitation. Because of precipitation of the more soluble glasses, extracts of all the glasses were passed through a 0.22μm Millipore filter and then stored at –20°C.

Table 1 – Composition and relative solubility of phosphate-glass preparations.

Glass No.	Solubility	Composition (mol. %)		
		CaO	Na_2O	P_2O_5
44	+++	8	47	45
47	+++	16	39	45
51	+	28	27	45
54	+	40	15	45

Cell Culture

Two human osteosarcoma cell lines, HOS (TE85) and MG63, were used in this study. Both show osteoblast-like characteristics and are often used as experimental models for investigating aspects of osteoblast function[3]. The cells were cultured at 37°C in a humidified atmosphere of 5% CO_2 in air, in flasks containing 10 ml of DMEM supplemented with 10% (v/v) foetal calf serum, 2 mM L-glutamine, 50 IU/ml of penicillin and 50 μg/ml of streptomycin. The culture media were changed twice weekly and for sub-culture the monolayers were rinsed with phosphate-buffered saline (PBS) and incubated with trypsin-EDTA for 5 min at 37°C, prior to reculturing in 96-well microtitre plates. Dilutions of 1:100 (1%) and 1:2 (50%) of the glass extracts were prepared using DMEM culture medium. HOS and MG63 cells were incubated with the 1% and 50% dilutions of the glass extracts in 96-well microtitre plates as described below.

MTT Assay for Cell Proliferation

MTT is a substrate that is converted by a mitochondrial enzyme, which is active in living cells, to yield a dark blue formazan product. The intensity of the colour produced is directly related to the number of viable cells, and thus their proliferation *in vitro*. Cells were plated at a density of 2000 cells/well in replicate 96 well culture plates and allowed to attach overnight at 37°C, after which the media were removed and replaced by the diluted extracts. Cells maintained in normal culture medium were used as controls. The cells were then incubated for a further 5 days. Cell proliferation was measured after 1, 3 and 5 days using the MTT test (Chemicon, Temecula Ca., USA). Absorbance was measured at 560nm using a Titertek Multiskan Spectrophotometer. The results are expressed as the average absorbance of 6 replicate wells.

ELISA for Expression of Tissue-Specific Antigens

The enzyme-linked immunosorbent assay (ELISA) requires few cells and can measure large numbers of samples simultaneously. 2000 cells/well were seeded into 96-well microtitre plates and incubated for 2 days at 37°C, after which the medium was removed and replaced by either 100 μl of fresh DMEM (controls) or the respective diluted extracts. After a further 5 days of incubation the medium was removed and the cells fixed and permeabilised with 3% paraformaldehyde/0.1% saponin in PBS. The cells were then washed with PBS containing 0.05% Tween. Non-specific binding was inhibited by adding 200 μl of PBS-Tween containing 1% milk to each well and incubating for 1 h. After washing, the cells were reacted with rabbit antibodies against FN, ON and BSP (1:1000 dilution) for 1 h. After washing, horseradish peroxidase (HRP)-conjugated goat anti-rabbit antibody (1:5000 dilution) was applied for 30 min. After further washing, the enzyme substrate, o-phenylenediamine dihydrochloride was added for 10 min. The reaction was stopped by adding 25 μl of 2 M H_2SO_4. The absorbance was measured at 450nm.

RESULTS AND DISCUSSION

Cell proliferation

Fig. 1 shows the proliferation of MG63 cells cultured in the presence of the glasses extracted for 1 day (a, b) and 5 days (c, d).

Fig. 1a - 1 day extract, 1% dilution

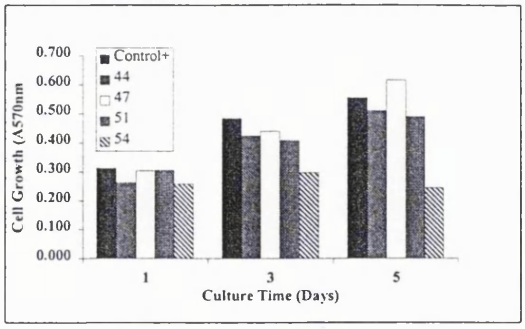

Fig. 1b – 1 day extract, 50% dilution

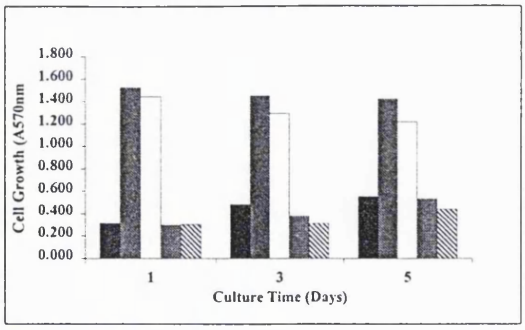

Fig. 1c - 5 day extract, 1% dilution

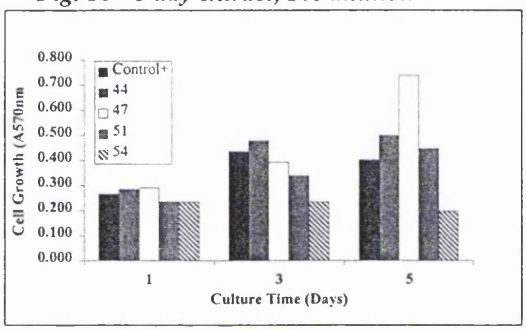

Fig. 1d - 5 day extract, 50% dilution

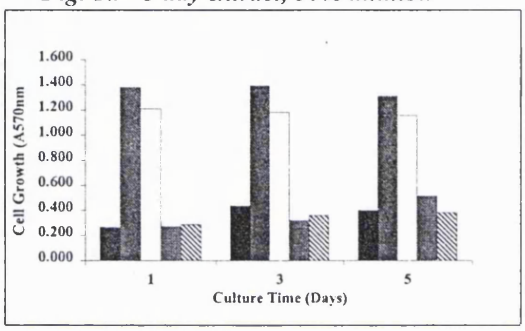

Fig. 1. – The effects of glass extracts on the growth of MG63 cells at 1, 3 and 5 days.

There is a marked difference in the growth of the MG63 cells depending on the concentration and composition of extract used. Extracts obtained after 1 day and diluted 1:100 had little effect on cell proliferation, except for the glass with the highest CaO concentration (No. 54), which resulted in a decrease in cell number (Fig. 1a). In contrast, when higher concentrations (50%) of extracts of the more insoluble glasses (Nos. 51 & 54) were added, they did not affect cell growth compared with the control cells, whereas the low CaO glasses (Nos. 44 & 47) increased the apparent cell numbers (Fig. 1b). Similar results were obtained when the 5-day extracts were added to the cells either dilute (Fig. 1c) or highly concentrated (Fig. 1d). However, the apparent increases in proliferation caused by the very soluble glasses (Nos. 44 & 47; Fig. 1b, 1d) may not have been due to an actual change in cell numbers, but rather to an absorbance effect caused by precipitation of these glasses in solution. This caused turbidity in the media, which interfered with the absorbance measurements and the cells in these cultures were found not to be viable and became detached. The results for HOS cells were very similar (data not shown). These results suggest that at low concentrations (1%) of glass extracts, there are no obvious deleterious effects on the viability and proliferation of MG63 cells even in the presence of the very soluble glass extracts. However, at higher

concentrations (50%), the more soluble glasses (CaO content <20%) appeared to inhibit proliferation, even when extracted for only 1 day.

Antigen expression

The expression of FN, ON and BSP was measured by ELISA as described. Table 2 shows the levels of these antigens expressed by MG63 and HOS cells incubated with the concentrated (50%) extracts obtained on days 1 and 5 of a soluble (No. 44) glass and less soluble (No. 54) glass.

Table 2 – Expression of connective tissue antigens in MG63 and HOS cells

Cell Type	Glass No.	Days of Extract	Relative Antigen Expression (% of control)		
			FN	**ON**	**BSP**
MG63	44	1	41	31	59
	44	5	51	36	86
	54	1	79	33	131
	54	5	59	34	93
HOS	44	1	44	44	68
	44	5	46	38	62
	54	1	50	41	61
	54	5	61	33	60

The results show that, in the presence of the concentrated extracts, both cell types expressed all three antigens, although at reduced levels compared to the controls. The more soluble glass (No. 44) appeared to inhibit expression of all 3 antigens more than the less soluble glass extract (No. 54), for both cell types. Thus, in MG63 cells, while FN levels were only 41 and 51% of the control in the presence of the more soluble glass, they were 79 and 59% of control with the less soluble glass (day 1 and day 5 extracts respectively). Similar differences were found for HOS cells. ON was the most severely affected antigen being only 31 to 44% of control levels under all conditions. In contrast, while BSP was 59 and 86% of controls in the presence of the soluble glass, this antigen was unaffected by the low solubility glass (131 and 93% of control levels). In HOS cells, however, BSP expression reached only 68% of that in control cells. The apparent down-regulation of expression of some of these proteins by the presence of soluble glass products may be due to direct effects on protein synthesis or to the different turnover rates of the proteins.

CONCLUSION

These studies have shown that human osteoblast cell lines can proliferate and express several antigens even in the presence of highly concentrated (50%) extracts of phosphate-based soluble glasses. However, while the expression of BSP was largely unaffected by the extracts and remained near control levels, particularly in the MG63 cells, the expression of FN and especially ON were considerably reduced compared to controls. Further chemical modification of these glasses is now in progress in order to elicit a more optimal biological response for potential clinical application.

REFERENCES

1. Burnie J. Controlled Release Glass (CRG) – A New Biomaterial (1982) PhD Thesis.
2. Videau JJ & Dupuis V. *Eur. J. Solid State Inorg. Chem.* 1991; **28**: 303-343.
3. Clover J & Gowen M. *Bone* 1994; **15**: 585-591.

Development of Phosphate Based Glasses for Periodontology.

K. Franks*, J.C. Knowles, G.E. Hawkes, I. Abrahams, I. Jalisi and D. Lee
Department of Biomaterials, Eastman Dental Institute, London. UK.

Soluble phosphate based glasses show great potential for use in hard tissue surgery due to their chemical relationship to bone. Variation in composition allows alteration of the solubility rate of the glasses. However, no systematic study in the literature has been carried out to investigate the relationship between composition and solubility and extend this to *in vitro* or *in vivo* results. The aim of this work was to characterise the glasses by SS-NMR and X-ray diffraction and also measure the solubility and solution pH change of a range of glasses. This work was then extended to characterise the cellular reaction to the extracts from these materials using the MTT assay. Ten glasses were made in the ternary phase diagram Na_2O-CaO-P_2O_5. The P_2O_5 content was kept constant at 45mol.% and with CaO varying between 8 and 40mol.% and the remainder being made up with Na_2O. Disks were placed in either distilled water or Hanks Buffered Saline Solution (HBSS) and the weight change measured at various time periods. Any solution pH changes were also recorded. For the MTT assay, the glasses were extracted in culture medium for 24 hours and the effect of these extracts on cell proliferation was measured by MTT die uptake. From X-ray diffraction and SS-NMR, the glasses were consisted of a mixture of pyrophosphate and trimetaphosphate groups. As expected the glasses showed a strong relationship between composition and solubility. With increasing CaO content, the solubility rapidly decreased. Solubility was also higher in the HBSS. For the MTT assay, again a very strong correlation between composition and cellular proliferation was seen. Furthermore, evidence for increasing the cellular activity above normal levels was seen.

We conclude that due to the ease with which the solubility of these materials may be altered, will allow optimal properties to be obtained, to combine slow resorption with enhanced tissue activity.

This study was supported by Colebrand Inc.

Biological response of human osteoblasts to soluble glasses

V. SALIH*[1], K. FRANKS[1], M. JAMES[1], G. W. HASTINGS[2], J.C. KNOWLES[1] AND I. OLSEN[3] (Departments of Biomaterials[1] and Periodontology[3], Eastman Dental Institute, University of London, U.K.; [2]IMRE, National University of Singapore)

A group of novel glasses has recently been developed that are phosphate-based, the solubility of which is directly related to their chemical composition. Such biomaterials could be useful for promoting the growth of soft and hard connective tissue cells as occurs, for example, in the repair of periodontal defects. This study has assessed the biocompatibility of the soluble glasses by examining certain key features of the cellular response of two human osteoblast-like cell lines, MG63 and HOS (TE85), incubated *in vitro* in culture medium containing increasing concentrations of extracts of these glasses. The effects of the extracts on the proliferation of the cells were measured using the MTT assay and flow cytometry was used to measure expression of fibronectin (FN), osteonectin (ON) and bone sialoprotein (BSP), antigens which play an important role in connective tissue integrity and function. The results indicated that, over a period of 5 days, the glass extracts did not adversely affect the growth of the cells compared with control cultures. Similarly, the expression of extracellular matrix proteins was comparable to that of control cultures. These findings suggest that the phosphate glasses are not cytotoxic and do not adversely affect connective tissue production. Further chemical modifications are now in progress in order to develop formulations, which promote an optimal biological response and could be clinically effective for the repair of periodontal effects.

PHOSPHATE BASED GLASSES FOR HARD TISSUE SURGERY

K. Franks, I. Abrahams* and J.C. Knowles

Department of Biomaterials, Eastman Dental Institute, University of London, 256 Gray's Inn Road, London WC1X 8LD UK. *Department of Chemistry, Queen Mary and Westfield College, Mile End Road, London E1 4NS UK.

Introduction Phosphate based glasses are soluble and their solubility in aqueous solutions can be used to develop implant materials, which are used as temporary devices. Two major benefits of soluble phosphate based glasses are (1) their chemical similarity to the inorganic phase of bone which indicates biocompatibility and (2) as a temporary device, a second device removing operation is no longer of need. The out-leaching ions are beneficial for the surrounding tissue and the cells can use these ions to rebuild their own inorganic matrix. To develop these materials for implant use, it is essential to understand simple phosphate glass system in terms of their *in vitro* solubility.

Materials and Methods.. A ternary system based on Na_2O-CaO-P_2O_5 has been developed (with fixed P_2O_5 content of 45mol.%). To monitor the dissolution process the weight loss has been recorded in both distilled water and Hanks Buffered Saline Solution (HBSS). The pH values and ion measurements such as Ca^{2+} and Na^+ have been monitored. The bulk glasses were characterised using DTA, MAS-NMR and XRD. A quaternary system K_2O-Na_2O-CaO-P_2O_5 has been prepared for comparison to the ternary system and the same tests as above carried out on this system. In addition, preliminary cell culture tests have been performed on both glass systems to evaluate biocompatibility.

Results. The solubility of the ternary system is very sensitive to the glass composition. It shows an inverse exponential relationship between solubility and CaO content as seen in Figure 1.

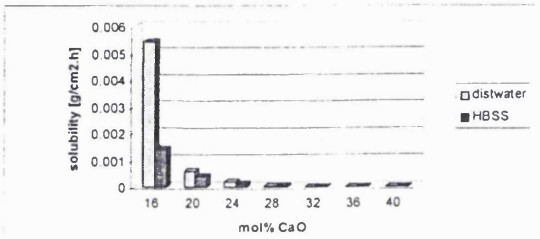

Figure 1. Solubility of ternary glass system in distilled water and HBSS.

With increasing CaO content, the pH of the test solution changes less dramatically with time. For the quaternary system, the substitution of Na_2O with K_2O gives an increase in solubility as seen in Figure 2.

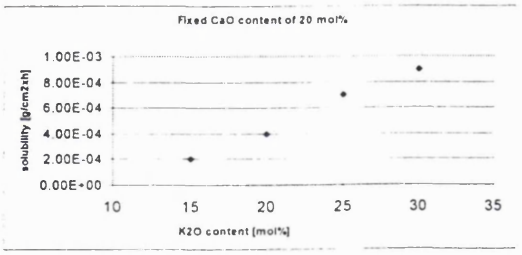

Figure 2. Effect of K_2O addition on solubility in distilled water.

The ion measurements for the quaternary system are similar to the ternary system.

Cell culture tests show enhanced cellular activity of cells placed in extracts from the quaternary system compared to the ternary system.

Conclusion. The solubility of the glasses may be easily varied and a number of different ions substituted. The ternary system shows bioactivity and this has been further enhanced by development of a quaternary system. Thus, these materials have great potential for hard tissue surgery.

BIOLOGICAL RESPONSE OF HUMAN OSTEOBLASTS TO SOLUBLE GLASSES

V. Salih[1], K. Franks[1], M. James[1], G. W. Hastings[2], J.C. Knowles[1], I. Olsen[3]
(Departments of Biomaterials[1] and Periodontology[3], Eastman Dental Institute, University of London, U.K.; [2]IMRE, National University of Singapore)

Introduction

A novel group of glasses has recently been developed that are phosphate-based, the solubilities of which are directly related to their chemical composition. Such soluble glasses are considered to be of potential clinical value in orthopaedic and dental surgery, for promoting the growth of soft and hard connective tissue cells as occurs, for example, in the repair of periodontal defects. However, the biological response of human cells to these materials is not well known. This study has therefore assessed the biocompatibility of the soluble glasses by examining the effects of increasing concentrations of extracts of these glasses on cell proliferation and the expression of extracellular matrix proteins in two human osteoblast-like cell lines, MG63 and HOS (TE85).

Materials and Methods

A number of different compositions of a quarternary glass system, K_2O-Na_2O-CaO-P_2O_5, were prepared. The relative amounts of P_2O_5 and CaO were kept constant at 45 mol% and 28 mol%, respectively. The effects of various dilutions of extracts of the glasses on the proliferation of cells were measured over a period of 5 days using the MTT assay, in which the intensity of the colour produced is directly related to the number of viable cells and thus their proliferation *in vitro*. Flow cytometry (FCM) was used to measure the size and granularity of the cells and the expression of bone sialoprotein (BSP), osteonectin (ON) and fibronectin (FN), antigens which play important roles in connective tissue repair, integrity and function.

Results

The MTT results showed that, over a period of 5 days, the glass extracts did not adversely affect the overall growth of the cells compared with that of control cultures. Thus, while there was some inhibition of cell proliferation at the early time period (2 days), the proliferation rates became similar to control cells by the end of the culture period (5 days). The FCM results showed that, even in the presence of the undiluted extracts, both cell types expressed all three antigens, although at 2 days the levels were reduced compared to the controls, particularly of BSP, which was only 60% of control cultures. However, as with the growth of the cells, expression of all three antigens by 5 days had recovered to levels that were similar or higher than control cells. Thus, while the expression of some of these proteins appeared initially to be down-regulated by the presence of soluble glass products, possibly as a result of a direct inhibition of protein synthesis or acceleration of protein turnover, these apparently deleterious effects were only transient. Both cell function as well as growth returned to control levels on prolonged culture.

Conclusion

These findings suggest that the phosphate glasses are not cytotoxic and do not adversely affect connective tissue production over an extended period *in vitro*. Further chemical modifications are now in progress in order to develop material formulations which promote an enhanced biological response and thereby clinically improve the repair of both orthopaedic and dental defects.

Development of Soluble Glasses for Regeneration of Hard Tissue: A Chemical and Biological Evaluation. J.C. KNOWLES, K. FRANKS, V. SALIH and I. OLSEN. (Eastman Dental Institute, University of London, 256 Gray's Inn Road, London WC1X 8LD, UK)

Soluble glasses are a unique group of materials, which offer great potential for hard tissue surgery. These glass based on an Na_2O-CaO-P_2O_5 system, may potentially release ions which help to stimulate osteoblast activity. The aim of this work was firstly to characterise the glasses in terms of their solubility and then to carry out an *in vitro* cell culture study to determine optimal compositional ranges for further study.

Glasses were made with fixed P2O5 content and varying CaO content (glass code 44: 8mol.% CaO, 47: 16mol.%, 51: 28mol.%, 52: 32mol.%, 54: 40mol.%) between 8 and 32mol.%. These glasses were cast into rods and then annealed to remove residual stress. The rods were cut into discs solubility assessed in distilled water at 37°C. For the cellular activity assays, certain key features of the cellular response of two human osteoblast-like cell lines, MG63 and HOS (TE85), incubated *in vitro* in culture medium containing increasing concentrations of extracts of these glasses. The effects of the extracts on the proliferation of the cells were measured using the MTT assay and flow cytometry was used to measure expression of fibronectin (FN), osteonectin (ON) and bone sialoprotein (BSP), antigens which play an important role in connective tissue integrity and function. For the solubility studies, it was seen that as the Na_2O content was decreased, the solubility decreased. Furthermore, as the solubility decreased the graphs became more non-linear. This non-linearity was attributed to differences in the H+ and OH- attack, dependant on glass composition. A precipitate formation was also seen which X-ray diffraction revealed to be brushite, a precursor of apatite formation.

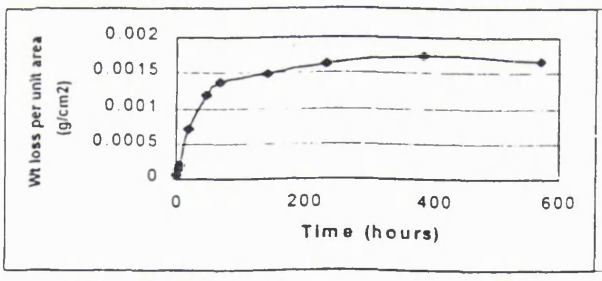

Figure 1. Solubility curve for glass 54

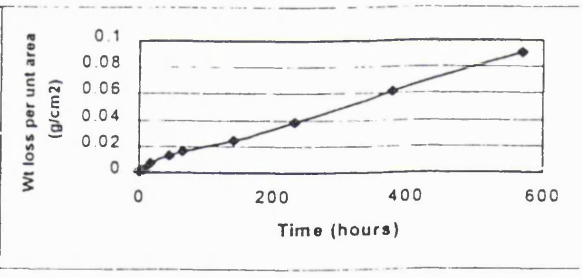

Figure 2. Solubility curve for glass 52

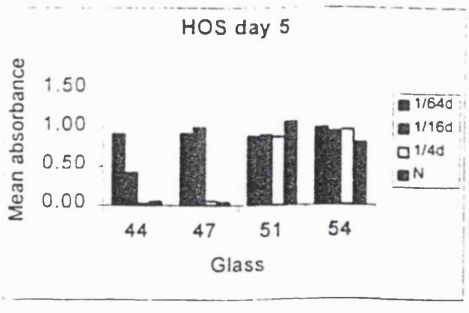

Figure 3. MTT assay of HOS cells.

For the MTT assays, using HOS cells, after 5 days there is a strong correlation between both glass solubility and dilution of the extracts. As the glass becomes more soluble (glasses 44 and 47), this affects the proliferation of the cells and as would be expected, if this is diluted with normal medium, cellular proliferation returns to normal values. The low solubility glasses appear relatively unaffected and there is evidence for the glasses increasing cellular activity even when the cells were cultured in the neat extracts. In conclusion, these glasses may promote enhanced cellular activity, dependant on the composition. Further development may be undertaken to examine other glass systems and also more complex quaternary systems.